METABOLITE PROFILING FOR NEW ADVANCES IN BIOMARKER DISCOVERY, CYSTIC FIBROSIS SCREENING AND DRUG SURVEILLANCE

METABOLITE PROFILING FOR NEW ADVANCES IN BIOMARKER DISCOVERY, CYSTIC FIBROSIS SCREENING AND DRUG SURVEILLANCE

By ALICIA DIBATTISTA, M.Sc.

A Thesis Submitted to the School of Graduate Studies in Partial Fulfillment of the Requirements for the Degree

Doctor of Philosophy

October 2017

DOCTOR OF PHILOSOPHY (2017) McMaster University

(Chemistry and Chemical Biology) Hamilton, ON

TITLE: Metabolite Profiling for New Advances in Biomarker Discovery, Cystic Fibrosis Screening and Drug Surveillance

AUTHOR: Alicia DiBattista, M.Sc. (McMaster University)

SUPERVISOR: Professor Philip Britz-McKibbin

PAGES: xxi, 234

Abstract

The role of biological markers (biomarkers) in public health, pediatric medicine and clinical toxicology cannot be understated. Clinically validated biomarkers used in newborn screening (NBS) serve to detect individuals at risk for a disease in the population, pre-symptomatically diagnose affected neonates early in life and/or accurately predict disease progression and treatment responses to therapy. However, there is urgent need for the discovery of more specific biomarkers that can improve screening accuracy in a high throughput, cost-effective yet ethical manner. The major objectives of this thesis were to develop innovative nontargeted metabolite profiling methodologies based on multisegment injection-capillary electrophoresis-mass spectrometry (MSI-CE-MS) for early detection of treatable genetic diseases, as well as comprehensive surveillance of drugs of abuse (DoA) in high risk subjects. *Chapter II* introduces a multiplexed MSI-CE-MS strategy for confirmatory testing of known biomarkers for various inborn errors of metabolism from a dried blood spot (DBS) that was rigorously validated using proficiency test specimens from Centres for Disease Control and Prevention (CDC) and authentic neonatal samples from Newborn Screening Ontario (NSO) with quality assurance. Additionally, MSI-CE-MS together with temporal signal pattern recognition revealed for the first time a novel class of pathognomonic marker elevated in galactosemia, namely *N*-galactated amino acids. *Chapter III* describes an untargeted metabolomic study to discover biomarkers of cystic fibrosis (CF) to reduce the high false positive rate and

widespread carrier identification by current two-tiered NBS algorithms that rely on genetic testing. A panel of metabolites from retrospective DBS specimens, including several amino acids, ophthalmic acid and an unknown peptide, allowed for differentiation of asymptomatic CF neonates from screen-positive yet unaffected carriers and transient hypertrypsinogenemic cases. *Chapter IV* develops and validates a high throughput MSI-CE-MS assay for rapid screening for DoA and their metabolites in human urine with improved specificity and broad spectrum coverage as compared to classic targeted immunoassays. This method can also applied to ensure compliance, drug efficacy and patient safety while detecting for potential substitution or adulteration when using high resolution MS/MS. In summary, this thesis contributes an innovative methodology and data workflow for biomarker discovery for improved neonatal screening of rare genetic diseases in the population, which was also applied for more effective drug surveillance strategies in public health given the alarming worldwide opioid crisis.

Acknowledgements

I would like to begin by thanking my supervisor Dr. Philip Britz-McKibbin. When I joined his lab, I was a plant biologist who decided to learn mass spectrometry. He was willing to take a chance on me and that speaks volumes about his confidence and optimism. His refusal to get discouraged is one of his finest qualities, and it is what helped me get through some of the lowest points in my research. I was able to develop into an independent researcher as I was given the support I needed to explore and tinker. However, his door was always cracked open and he always had time to talk about my project, my goals and what was important to me. I would like to offer sincere thanks to my committee member, Dr. Fred Capretta for his feedback and encouragement during my committee meetings. His willingness to ask direct questions kept me on track and ensured I didn't miss the forest for the trees. I would also like to thank my other committee member, Dr. Murray Potter. His passion for clinical research led me to realize why this degree is so important to me and his support and knowledge has helped me to achieve it. I am also indebted to Dr. Pranesh Chakraborty for his openness and candor, Dr. Osama Al-Dirbashi for his feedback, Nathan McIntosh for his technical expertise in newborn screening and Monica Lamoureux for ensuring we always had the highest quality samples and seamless data transfer.

The Britz lab members, both past and present, have made my time in this lab not only bearable, but wonderful. I could always rely on my labmates to

answer questions, brainstorm with me, repair instruments with me, support me and be a (literal) shoulder to cry on. Nadine Wellington, Michelle Saoi, Mai Yamamoto, Stellena Mathiaparanam, Ritchie Ly, Sandi Azab and Biban Gill you have all been such wonderful sources of support for me. I would also like to thank Karen Lam, Jennifer Wild and Dr. Meera Shanmuganathan for always being there for me and for going far beyond your roles as colleagues. You are dear friends and you have helped me to accomplish my personal and academic goals, and I am forever grateful and fortunate to have you in my life.

I would not have the level of mass spectrometry experience without the patience, expertise and kindness of Paul Campanelli and Marcus Kim. Paul allowed me to assist with instrument repairs and troubleshooting and answered every question I could think to ask. Marcus provided me with many opportunities to present my work and meet other researchers within the field and gave me much support and guidance on surviving graduate school.

I would also like to offer my deepest gratitude to my parents, Roger and Eveline. They have always supported my academic endeavours and had faith that I could be successful, even when I did not. They were understanding when I cancelled plans and missed family events and never made me feel guilty for focusing on school. I was, and am, able to succeed because of them and I love them dearly. Finally, I would like to thank Peter for believing that I was capable. You loved me during the best times and somehow even more during the worst.

Table of Contents

List of Figures

Supporting Figures

List of Tables

Supporting Tables

List of Abbreviations and Symbols

$[M+H]^+$	Protonated molecular ion
$[M+Na]^+$	Sodiated molecular ion
2MBG	2-methylbutyrylglycinuria
ACMG	American College of Medical Geneticists
ADA	Adenosine deaminase deficiency
Adn	Adenosine
AECOPD	Acute exacerbations of chronic obstructive pulmonary disease
AJS	Agilent JetStream
Ala	*L*-alanine
Arg	*L*-arginine
AUC	Area under the curve
Bet	Glycine betaine
BGE	Background electrolyte
BIA	Bacterial inhibition assay
C0	*L*-carnitine
C10	Decanoyl-*L*-carnitine
C2	*O*-acetyl-*L*-carnitine
C3	Propionyl-*L*-carnitine
C3DC	Malonyl-*L*-carnitine
C4DC	Methylmalonyl-*L*-carnitine
C5DC	*O*-glutaryl-*L*-carnitine
C6	Hexanoyl-*L*-carnitine
C8	*O*-octanoyl-*L*-carnitine
CBL	Cobalamin deficiencies
CBS	Cystathione beta-synthase deficiency
CDC	Centres for Disease Control and Prevention
CE	Collision energy
CE-MS	Capillary electrophoresis-mass spectrometry
CF	Cystic fibrosis
CF-SPID	CF screen-positive inconclusive diagnosis
CFTR	Cystic fibrosis transmembrane conductance regulator gene
CFTR	Cystic fibrosis transmembrane conductance regulator
CHEO	Children's Hospital of Eastern Ontario
CI	Confidence interval
Cit	*L*-citrulline
CIT I	Citrullinemia Type I
CIT II	Citrullinemia Type II
Cl-Tyr	3-chloro-*L*-tyrosine
CPT I	Carnitine palmitoyltransferase type I deficiency
CRMS	*CFTR*-related metabolic syndrome
CUD	Carnitine uptake deficiency

CV	Coefficient of variation
dAdn	2-deoxyadenosine
DBS	Dried blood spot
DE-RED	4-dienoyl-coA reductase deficiency
DI-MS	Direct infusion-mass spectrometry
DI-MS/MS	Direct infusion-tandem mass spectrometry
D-IS	Deuterated internal standard
DoA	Drugs of Abuse
EIE	Extracted ion electropherogram
EI-MS	Electron impact- mass spectrometry
EMA	European Medicines Agency
EOF	Electroosmotic flow
ESI	Electrospray ionization
ESI+	Positive electrospray ionization
FC	Fold-change
FC	Fold-change
FDA	Food and Drug Administration
FDR	False discovery rate
FIA-MS/MS	Flow injection analysis-tandem mass spectrometry
F-Phe	4-fluoro-*L*-phenylalanine
FWER	Family-wise error rate
GA I	Glutatric acidemia type I
GA II	Glutaric acidemia type II
Gal	Galactose
Gal-1P	Galactose-1-phosphate
GALT	Galactose-1-phosphate uridylyltransferase enzyme
GC	Gas chromatography
GC	Galactonic acid
GC-MS	Gas chromatography-mass spectrometry
Glc-1P	Glucose-1-phophate
Glc-Gln	*N*-glycated glutamine
Glc-Glu	*N*-glycated glutamic acid
Glc-Gly	*N*-glycated glycine
Glc-GSSG	*N*-glycated oxidized glutathione
Glc-Leu/Ille	*N*-glycated leucine/isoleucine
Gln	*L*-glutamine
Glu	*L*-glutamic acid
Gly	Glycine
GSD	Glutathione synthetase deficiency
GSH	Reduced glutathione
GSSG	Oxidized glutathione
HCY	Homocystinuria
HEPES	2-[4-(2-hydroxyethyl)piperazin-1-yl]ethanesulfonic
HHH	Hyperornithinemia hyperammonemia hypercitrullinemia

H-LYS	Alpha-aminoadipic semialdehyde synthase deficiency
HMDB	Human Metabolome Database
HP-321	Hexamethoxyphosphazine
HP-922	Hexakis(2,2,3,3-tetraflurorpropoxy) phosphazine
HPRBIL	Hyperbilirubinemia
IBG	Isobutyrylglycinuria
IEM	Inborn errors of metabolism
Ile	*L*-Isoleucine
IRT	Immunoreactive trypsinogen
IS	Internal standard
isoC4	Isobutyryl-*L*-carnitine
isoC5	Isovaleryl-*L*-carnitine
IVA	Isovaleric acidemia
KNN	K-nearest neighbour
K-S	Kolmogorov-Smirnov test
LA	Lactic acidemia
LC	Liquid chromatography
LC-MS	Liquid chromatography-mass spectrometry
LLOQ	Lower limit of quantification
LOD	Limit of detection
Lys	*L*-lysine
m/z	Mass-to-charge ratio
m/z:RMT	Mass-to-charge : relative migration time ratio
MADD	Multiple acyl-coA dehydrogenase deficiency
MALDI-MS	Matrix-assisted laser desorption/ionization mass spectrometry
MAT	Methionine adenosyltransferase deficiency
MCADD	Medium chain acyl-coA dehydrogenase deficiency
MCD	Multiple carboxylase deficiency
Met	*L*-Methionine
MFE	Molecular feature extractor
MM2	Molecular mechanisms 2
MMA	Methylmalonic aciduria
MRI	Magnetic resonance imaging
MS	Mass spectrometry
MS/MS	Tandem mass spectrometry
MSUD	Maple syrup urine disease
MT	Migration time
NA	1-methylnictotininc acid
NASH	Non-alcoholic steatohepatitis
NKHG	Non-ketotic hyperglycemia
NMS	Naphthalene monosulfonic acid
NPV	Negative predictive value
NSB	Newborn screening
NSO	Newborn Screening Ontario

OPA	Ophthalmic acid
OQN	Probabilistic quotient normalization
Orn	*L*-ornithine
PA	Propionic acidemia
PAH	Phenylalanine hydroxylase enzyme
PAP	Pancreatitis-associated protein
PCA	Principal component analysis
PCDL	Personal compound library database
Phe	*L*-phenylalanine
PKU	Phenylketonuria
PLS-DA	Partial least squares-discriminant analysis
POC	Point of Care
PPV	Positive predictive value
Pro	*L*-proline
PT	Proficiency testing
QC	Quality control
REB	Research ethics board
RMT	Relative migration time
ROC	Receiver operating characteristic
RSD	Relative standard deviation
RT	Retention time
S/N	Signal-to-noise ratio
SAMHSA	Substance Abuse and Mental Health Services Administration
SCAD	Short-chain acyl-coA dehydrogenase deficiency
SCID	Severe combined immunodeficiency
Ser	*L*-serine
SP/non-CF	Screen-positive CF-negative
SVM	Support vector machines
S-W	Shapiro-Wilk test
Thr	*L*-threonine
TIE	Total ion electropherogram
TNM	Tumour Node Metastasis cancer staging system
TOF	Time-of-flight
TREC	T-cell receptor excision circle
Tyr	*L*-tyrosine
UA	Urocanic acid
Val	*L*-valine
Xle	Total leucines
z	Charge state
z_{eff}	Effective charge

Declaration of Academic Achievement

The following material has been previously published and has been reprinted with written permission:

Chapter II. Reprinted and adapted from DiBattista, A.; McIntosh, N.; Lamoureux, M.; Al-Dirbashi, O.Y.; Chakraborty, P.; Britz-McKibbin, P. Temporal Signal Pattern Recognition in Mass Spectrometry: A Method for Rapid Identification and Accurate Quantification of Biomarkers for Inborn Errors of Metabolism with Quality Assurance. *Anal Chem.* **89**, 8112-812. Copyright (2017) American Chemical Society.

Chapter IV. Reprinted and adapted from DiBattista, A.; Rampersaud, D.; Lee, H.; Kim, M.; Britz-McKibbin, P. A High Throughput Screening Method for Systematic Surveillance of Drugs of Abuse by Multisegment Injection-Capillary Electrospray Electrophoresis-Mass Spectrometry. *Anal Chem*. **89**, 11853-11861, Copyright (2017) American Chemical Society.

The following material is in preparation for submission:

Chapter III. DiBattista, A.; DiBattista, A.; McIntosh, N.; Lamoureux, M.; Al-Dirbashi, O.Y.; Chakraborty, P.; Britz-McKibbin, P. Metabolic Signatures of Cystic Fibrosis in Dried Blood Spots from Asymptomatic Neonates: Reducing False Positives and Carrier Identification for Newborn Screening.

Chapter I

Introduction to Biomarker Discovery and Method Validation For Population-based Screening

Chapter I: Introduction to Biomarker Discovery and Method Validation For Population-based Screening

1.1 Biomarkers in a clinical context

Clinically relevant biological markers (biomarkers) are objective and measurable attributes that indicate a biological state or condition.[1] They can be used as barometers of underlying biological processes, both normal and pathogenic, or to indicate pharmacological responses to therapy or intervention.[2] Biomarkers can also be used as *surrogate* end points for clinical risk assessment;[3] for instance routine point-of-care (POC) measurements like blood pressure can be used to assess the risk of cardiovascular disease before the onset of the symptoms, such as stroke or myocardial infarction.[4] In this case, blood pressure is serving as an *antecedent* biomarker by identifying susceptible individuals at risk of developing a future atherosclerotic cardiovascular event that is dependent on various confounding factors such as genetics, diet, lifestyle and lifelong environmental exposures.[5] *Screening* or *diagnostic* biomarkers are those that indicate the presence of a disease, either pre-symptomatically as in the case of blood-based biomarkers used in universal newborn screening programs (NBS) for inborn errors of metabolism (IEM)[6] or in the presence of clear symptoms, such as invasive biopsy and histopathology for assessing liver damage and fibrosis associated with non-alcoholic steatohepatitis (NASH).[7] Biomarkers can also be used in *staging*, as in the case of the "TNM" staging system for cancer, which uses tumour size or depth (T), number of lymph nodes with cancer (N) and

metastasis (M) to classify cancer into four stages (I-IV).[8] Finally, *prognostic* biomarkers are clinically to anticipate the course of a disease, such as therapeutic monitoring of elevated plasma copeptin, which is a stress hormone used to predict the length of hospitalization, the need for ICU care or subsequent hospitalizations or death in those with acute exacerbations of chronic obstructive pulmonary disease.[9]

Biomarkers can be, and traditionally were, anatomical or physiological measurements, such as using regional cortical thickness as measured by magnetic resonance imaging (MRI) to predict those at risk for Alzheimer's disease[10] or using urine output volume to monitor changes in kidney function after injury.[11] However, clinical biomarkers increasingly signify distinct molecular markers that can be reliably and quantitatively measured in human biofluids or tissue specimens, including DNA/RNA, proteins/peptides, metabolites or electrolytes.[12] Genetic biomarkers can be whole genes, segments of DNA, or RNA (*e.g.* microRNAs). Genetic markers have been used with some success in screening for autosomal recessive diseases such as cystic fibrosis (CF). For instance, the presence of two known mutations in the cystic fibrosis transmembrane conductance regulator (*CFTR*) is presumptive for CF for infants who are at high risk of being affected by the disease.[13] However the utility of genetic or genomic biomarkers have demonstrated limited applicability in polygenic or chronic human diseases such as cancer, where there is great phenotypic heterogeneity as a result of complex interactions of genetic and environmental factors.[13]

Furthermore, invasive sampling of localized tumour tissue is often needed for early detection of many cancers as germline DNA does not contain the mutations of interest.[14] As a result, the focus has shifted to non-invasive monitoring of biomarkers in circulation (*e.g.* plasma or serum) such as protein markers of cancers.[14] However, the discovery and development of screening biomarkers for early detection of cancer remains elusive. Cancer is often defined as a disorder of cellular proliferation, but growing evidence suggests that it may also be considered a metabolic disease reflected by aberrant protein expression (*i.e.* C-reactive protein or serum amyloid A), which may not be specific to a particular type of tumour or tissue.[15] Despite billions of dollars of investment into cancer biomarkers in proteomics research, few candidates have been successfully translated for routine use in clinical practice.[16,17] Proteins may still have some clinical utility however, as prognostic biomarkers for predicting clinical progression and treatment responses to pharmacological therapy, such as prostate-specific antigen nadir for prostate cancer-specific mortality.[18] For example, a panel of protein features detected by matrix-assisted laser desorption/ionization mass spectrometry (MALDI-MS) has demonstrated the ability to predict which patients with non-small-cell lung cancer will show positive clinical outcomes (*i.e.* increased survival and a longer time to progression) after treatment with epidermal growth factor receptor tyrosine kinase inhibitors.[19] This suggests a burgeoning role for biomarkers in precision medicine, which seeks to tailor treatment plans to an individual based on their unique "omics profile."[20]

In light of the limited clinical performance of genomic and proteomic biomarkers, there is a push towards the discovery of metabolite-based biomarkers. Metabolites are low molecular weight (< 1.5 kDa) compounds present in human organs, tissues, cells and/or fluids, such as urine and plasma.[21,22] They can be endogenous (*i.e.* produced and consumed within the organism itself) or exogenous (*i.e.* taken up from external sources and metabolized within the organism, either by host metabolism or by gut microflora).[23] Metabolites represent "real-world" endpoints, reflective of the underlying changes in genomic, transcriptomic and proteomic expression, and are more closely associated with clinical outcomes and phenotypes.[21,24] However, metabolites are also subjected to the effects of external factors, including dietary intake, lifestyle choices (*e.g.* physical activity, psychosocial stress) and the influence of the microbiome.[25] **Figure 1.1** illustrates the relationship between the metabolome and the other "omes" while highlighting its unique role as an indicator of both intrinsic and extrinsic status.

1.2 Metabolomics for biomarker discovery

Metabolomics involves the comprehensive profiling of metabolites within a given biological sample under defined physiological conditions.[21,26] Broadly, metabolomics studies can be targeted and/or untargeted in scope; targeted metabolomics is hypothesis-driven and limits analysis to a defined number of known metabolites and well-characterized metabolic pathways. In contrast, untargeted metabolomics is hypothesis-generating and aims to measure a large number of metabolites with little *a priori* information on the number or identity of

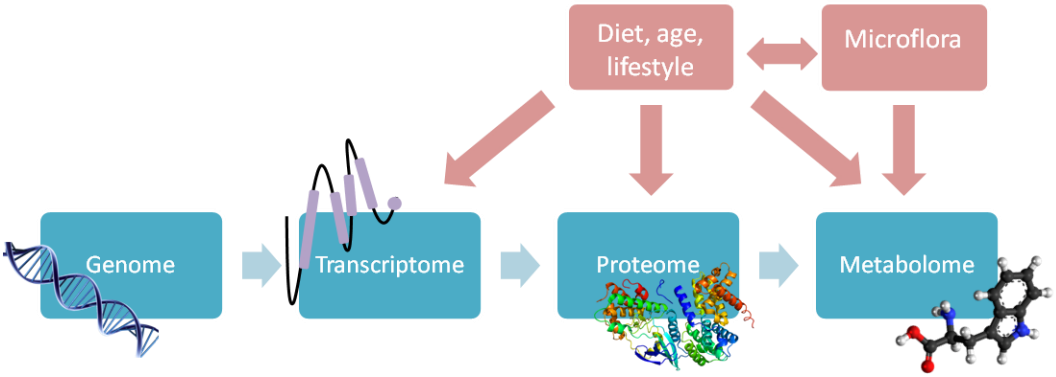

Figure 1.1. Scheme illustrating the "omics" cascade. Metabolites are the end result of a complex set of interactions between internal factors (blue boxes) and external factors (peach boxes).

detectable features.[27] Despite the aforementioned advantages of using metabolites as biomarkers rather than genes or proteins, similar challenges remains in metabolomics related to biomarker discovery and clinical validation. Indeed, although metabolomics may represent the "apogee of the –omics trilogy"[24] it also can learn from the failures and pitfalls that have plagued earlier genomic and proteomic-based biomarker discovery initiatives.

1.2.1 Challenges in biomarker discovery

Most (protein) biomarkers have failed to reach the clinic despite robust discovery and validation protocols because of poor performance in terms of improving patient outcomes, such as reducing mortality, morbidity, hospitalizations and/or enhancing quality of life. In other words, these biomarkers are true discoveries that may provide insights into biological mechanisms, but they ultimately have low sensitivity (*i.e.* a positive test result in the presence of disease), specificity (*i.e.* a negative result in the absence of disease) and/or poor positive predictive value (*i.e.* the proportion of screen positive results that are true

positives, PPV); thus, they do not contribute to new clinical information for improving patient care to justify additional costs and changes to existing paradigms.[28] For instance, CA125 antigen is a glycoprotein that is expressed in many epithelial ovarian cancers,[29] however it is not specific to ovarian cancer and is, in fact, elevated in several other malignant and benign conditions.[30] The PPV for serum CA125 is only 3.7%, and a retrospective case study from 2000-2002 showed that only 20% of positive screens were actually caused by an ovarian malignancy; it is therefore recommended that CA125 measurements should not be used alone and must be taken in conjunction with other tests (*e.g.* transvaginal ultrasonography) to reduce the number of invasive and potentially harmful follow-up procedures, such a bilateral salpingo-oophorectomy.[29,30] Visitin *et al.* proposed the use of an additional five biomarkers, including prolactin, leptin, and osteopontin, for highly specific (99.4%) and sensitive (95.3%) ovarian cancer screening and reported a PPV of 99.3%.[31] However, this assumed an incidence rate of ovarian cancer of 50% in a screening population, which is a gross overestimation; when using a more realistic incidence rate of 0.04%, the PPV dropped to 6.5% and the authors retracted their support for the test as a screening tool for ovarian cancer.[31,32] Perhaps the best known and most widely reported failure of biomarker discovery was that of a serum proteomic pattern for early detection of ovarian cancer by Petricoin *et al.* in the prestigious journal *The Lancet*.[33] The authors reported perfect sensitivity (100%) and near-perfect specificity (94%) and a PPV of 94%. This represented a substantial increase in

PPV over CA125 (*i.e.* 35%) as measured on the same samples. However, it was later determined that some of the reported discriminatory peaks were actually matrix-derived noise and not biologically relevant.[34] Additionally, other biomarkers are not adopted for clinical practice due to bias, inadequate study power and many other shortcomings as depicted in the data workflow in the discovery pipeline of "-omics" sciences **(Figure 1.2)**.[35,36] These are false discoveries, as further validation studies fail to substantiate the claims made in the original report.[28] Remarkably, it has been estimated that while there are 150,000 papers claiming to document biomarkers, less than 100 markers are currently used in the clinic.[37]

1.2.2 Pre-analytical considerations for biomarker discovery

Failures can occur in the pre-analytical phase, which involves patient recruitment, study design, sample collection and transportation, and sample storage and workup.[38] Metabolic changes are often subtle and there is a high degree of inherent biological variability in human populations so care must be taken in the pre-analytical stages to ensure the study findings are not biased.[39] **Table 1.1** summarizes potential issues that contribute to false discoveries and ways to circumvent this by careful consideration of pre-analytical factors. It should be noted that sample size calculations are challenging, and traditional power analyses are not appropriate for large and untargeted multivariate studies,[40] where *a priori* information about the number of metabolites and concentrations is limited or lacking, as in the case of unknown metabolic features.

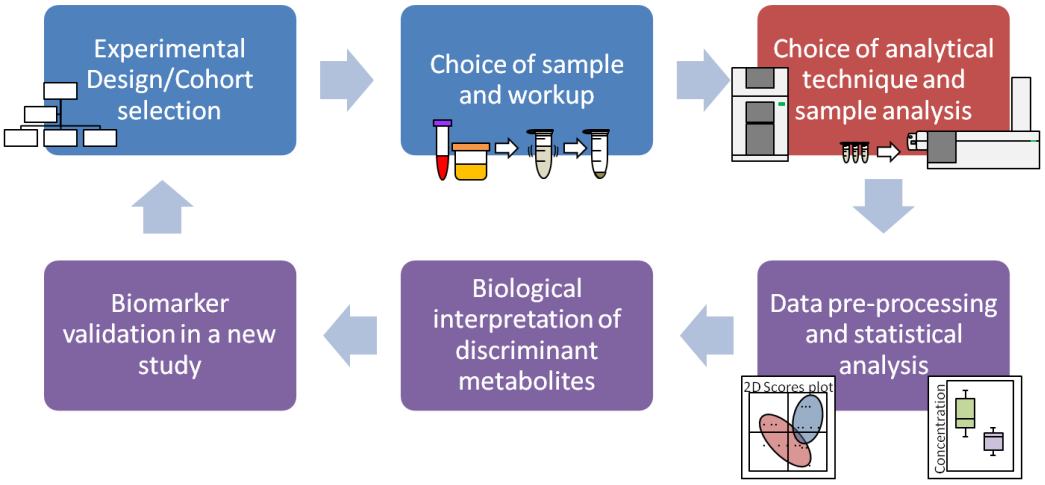

Figure 1.2. Scheme describing the biomarker discovery process. Blue boxes represent steps in the pre-analytical stage, red boxes indicate analytical steps and purple boxes represent the post-analytical stage of the pipeline.

1.2.3 Analytical considerations for biomarker discovery

Care must be taken to choose an analytical platform that will best suit the study objectives. The sheer chemical diversity of metabolites, in terms of both physicochemical properties (*e.g.* molecular weight, polarity, volatility, stability, etc.) and concentration ranges (10^7 to 10^9-fold)[41] coupled to a large fraction of unknown metabolites that comprise the human serum metabolome[42] or urine metabolome[43] suggests that a single, holistic platform for global metabolomics does not exist. As a result, cross-platform metabolomic studies are needed to attain broader metabolite coverage. However, the strengths and limitations of each methodology must be understood within the context of the study objectives and practical constraints (*e.g.* budget, sample volume, time). Results from complementary metabolomic platforms or multiple targeted metabolite studies can

Table 1.1. Common causes and potential solutions to false discoveries in metabolomics-based biomarker studies. Adapted from Dunn et al.,[39] Dunn et al.,[23] and Broadhurst and Kell.[44]

Potential Failures in Biomarker Discovery	Result	Suggestions for avoiding these problems
Inadequate sample sizes	Reduced statistical power and increased likelihood of false discoveries	Well controlled observational studies can be performed prior to large-scale clinical studies
Large studies require samples to be analyzed across multiple batches	Instrument drift can lead to differences in analyte responses	Identical QC samples should be analyzed at regular intervals with instrument cleaning
Control and case groups are not drawn from the same population	Bias in the study means that detected differences cannot be confidently assigned to the disease or treatment	Consider nested case-control or cross-over study, if possible, or population-based matching of all reasonable parameters (*i.e.* gender, age, diet)
Improper or inconsistent biofluid choice (e.g. serum vs. plasma)	Results obtained using one fluid cannot be directly compared to results from another	Be consistent and consider handling requirements. *e.g.* Serum requires no refrigeration and is easier to collect in a large study
Improper sample collection, handling or storage	Artifacts and bias can be introduced into the results by consumables, failure to quench enzymatic reactions, cross-contamination, non-random processing, differences in storage/transport	Adhere to standardized operating protocols. Keep samples on ice while processing and thawing, randomize samples, maintain consistent storage and transportation conditions

and should be combined to converge on true global metabolome analysis.[42,45] In fact, metabolomics is often used as an umbrella term to describe a range of scopes in the context of metabolite analysis, including: metabolic fingerprinting or footprinting, targeted metabolic profiling, and untargeted metabolomics.[21] Metabolic fingerprinting refers to the analysis of the intracellular metabolome by holistic methods.[23] It is typically rapid, can be quantitative (*i.e.* NMR) but is often

qualitative, and it provides a temporal snapshot or "fingerprint" of the metabolome. A metabolic footprint is the extra-cellular equivalent of the fingerprint, and measures metabolite uptake and/or secretion.[23] Targeted profiling is the hypothesis-driven quantitative study of a limited portion of the metabolome, which focuses on a few specific metabolites of interest, typically related in chemical class and/or function, with available reference standards.[23,45] Finally, untargeted (*i.e.* nontargeted) metabolomics, or untargeted profiling, is the hypothesis-generating global analysis of a wide range of metabolites within the metabolome. These studies are performed with minimal *a priori* information regarding metabolites and of interest and are therefore often followed by targeted, reductionist studies.[23] **Table 1.2** summarizes the strengths and limitations of common analytical techniques in targeted and nontargeted metabolomics. The inappropriate selection of instrumental methods can preclude the analysis of certain compounds or classes, whereas a lack of fundamental understanding of mechanisms of separation, ionization and chemical stability can lead to inaccuracies in terms of quantification and subsequent identification. For example, matrix effects can alter the ion response of a given metabolite, particularly when using electrospray ionization (ESI) that is coupled to liquid chromatography-mass spectrometry (LC-MS) or capillary electrophoresis-MS (CE-MS).[23] The use of stable-isotope internal standards can correct for ionization suppression or enhancement effects[46] whereas standard calibrant solutions are

Table 1.2. Strengths and limitations of various analytical platforms used to conduct metabolomic analyses.

Analysis Type	Platform	Strengths	Limitations
Metabolic fingerprinting	Nuclear Magnetic Resonance (NMR)[36,47,48]	-Universal detector -Quantitative -Stable and robust -Rapid data acquisition -Minimal sample workup -Non destructive -Structural information	-Low sensitivity -Expensive infrastructure -Large sample volume requirements -Inadequate spectral resolution (^{1}H NMR)
	Direct infusion mass Spectrometry (DI-MS)[23,41,49]	-High-throughput/ rapid -Multiplexed screening -Greater sensitivity and coverage than NMR -Low sample volumes -Low operating and infrastructure cost -No separation and minimal carry over	-No resolution of isomers or isobars -Lower specificity -Ion suppression and matrix effects -Stable-isotope IS for quantification -Complicated data processing
Metabolic profiling/ metabolomics	Gas chromatography-mass spectrometry (GC-MS)[36,45,49]	-High separation efficiency/resolution -Reproducible elution times -High specificity -Low sample volumes -Extensive EI-MS databases for identification	-Limited to thermally stable metabolites -Long analysis times -Expensive reagents -Multiple labeling and sampling artifacts
	Liquid chromatography-mass spectrometry (LC-MS)[36,41,49]	-Diverse column types -Broad metabolome coverage/wide selectivity -Simple sample workup -High sensitivity -High resolution with UPLC or core-shell LC -Different ion sources and mass analyzers for qualitative identification	-Need for complex elution programs -Mobile phase compatibility with ESI -Large sample volumes -High solvent consumption/waste -Prone to sample carry-over
	Capillary electrophoresis-mass spectrometry (CE-MS)[23,49,50]	-Small sample volumes -Low cost aqueous buffers -High separation efficiency/resolution -Ideal for polar/ionic metabolites -Effective desalter to reduce ion suppression -Accurate prediction of ion migration behaviour	-Poor migration time reproducibility -Low sensitivity with sheath-liquid interfaces -Poor robustness for large-scale studies -Not applicable to neutral compounds

required for absolute quantification due to differences in solute ionization efficiency.[51] Some a *priori* knowledge of the sample composition (*i.e.* blood or urine) and the desired metabolomic approach (fingerprinting, targeted or nontargeted) can help with selection of optimal analytical technique. To avoid any bias in the results, regardless of the analytical platform, sample run order and batch number should be fully randomized,[52] and a representative sample to serve as a quality control (QC) should be integrated periodically every fifth or tenth run.[52,53] This QC allows for the downstream assessment of instrumental system drift and stability during large-scale metabolomic studies that also enables for correction of within- and between-batch effects.[54]

1.2.4 Post-analytical considerations for biomarker discovery

The first step in the post-analytical stage of biomarker discovery involves pre-processing of data following acquisition. This involves several operations, including peak picking or binning, spectral deconvolution, filtering/smoothing, time alignment, normalization, and/or appropriate data transformation and scaling.[26,27,55] Depending on the instrumental platform, the dataset and the population from which the samples were drawn, not all of the aforementioned steps are necessary. In MS-based metabolomic studies, signal conversion refers to the transformation of the detector output of continuous data (*e.g.* a chromatogram or electropherogram of retention/migration time *vs.* ion counts *vs. m/z*) to a smaller dataset consisting of discrete molecular features defined by information such as accurate mass, retention/migration time and/or fragmentation pattern

(MS/MS) whose responses are determined by their integrated peak area often normalized to an internal standard.[23] Data filtering can now occur, where signals that correspond to random or instrumental noise are removed from the data. One method is called matched filtration which removes all chromatographic peaks that do not match the shape parameters of an authentic peak (*i.e.* are Gaussian).[56] Another powerful way to eliminate spurious signals in electrophoretic separations is dilution trend filtering based on the pooled QC sample.[57] This method exploits the unique capabilities of multisegment injection (MSI)-CE-MS by performing a series of injections of a QC sample which include a set of triplicate injections, a blank and three injections that serially dilute. An authentic yet reliably measurable metabolite is one with acceptable precision (CV < 30%, n=3), no detectable signal in the blank and adequate linearity upon serial dilution. The filtered data set can then be time-aligned to account for instrumental drift that occurs in separations coupled to MS. Alignment ensures that a feature will be correctly and consistently identified across multiple samples (*i.e.* peak 12 in one file is peak 12 in all files).[39] Various algorithms for alignment are available (*e.g.* mapping of time axes of raw chromatograms, clustering detected features to correct for drift, or time-warping) and either proprietary vendor (*e.g.* Agilent MassHunter, Waters MassLynx) or open-access software (*e.g.* XCMS,[56] MZmine,[58] metAlign[59]) can be used.[60] Electrospray ionization (ESI), a common soft ionization technique used in LC- and CE-MS-based metabolomic studies, is prone to adduct formation, leading one compound to form multiple different ion types (*e.g.* $[M+H]^+$and $[M+Na]^+$),

including multiple charge states ($[MH_2]^{2+}$).[61,62] Adducts, along with fragments, dimers and isotopes, are considered secondary signals and should be removed to eliminate data redundancy and expedite statistical analysis downstream.[63] This can be automated and performed along with peak detection and filtering, as in the case of Agilent's Molecular Feature Extractor (MFE) algorithm which combines related ions together (*i.e.* multiple charge states, isotopes, or common fragments and/or adducts) into a single feature.[64] However, not all commercial software is capable of this and care must be taken to manually inspect the data to determine the presence of these redundancies that contribute to bias and data overfitting. Features that are not consistently detected above a user-defined threshold (*e.g.* >50% or 80%) in either the QCs or the individual samples can be discarded to avoid an abundance of missing values; for those metabolites that remain undetectable, missing value imputation can be performed.[65] These zero values can be replaced with a small residual value (*i.e.* lower limit of detection or minimum response measured for a specific metabolite within the study)[66,67] or they can be estimated by statistical methods such as K-nearest-neighbour (KNN) method.[68]

If samples are run across multiple batches, a necessity in large-scale metabolomic studies when access to infrastructure is limited, batch effects can be seen in peak responses when plotting intermittent QC runs on a control chart. Changes in instrument response and signal intensity can result from interaction of the sample with the instrument, as in the case of coupling LC, GC and CE separations to MS,[39] or differences in solvent composition, reagent lots, and/or

laboratory conditions.[52,69] Furthermore, columns and capillaries must be changed, and routine cleaning and maintenance must be performed on the instrument, all of which can contribute to variability and potential bias.[70] Here, the inclusion of the QC samples within the injection and/or run sequence is crucial to identify system instability and drift (**Figure 1.3**). There are numerous approaches and algorithms to normalize or correct for batch effects and these commonly employ empirical Bayes methods (*e.g.* ComBat[71]) or regression models (linear or nonlinear).[70] These methods can perform the correction using the regularly included QC runs,[72] and/or the sample injection or run order.[54] Normalization can also be performed to account for variations in sample injection volume or sample dilution. It is well known that the concentration of metabolites in urine varies due to hydration status, so samples can be normalized to an endogenous metabolite excreted at a constant rate (*i.e.* creatinine) or bulk physical properties (*i.e.* specific gravity)[73] or by methods such as probabilistic quotient normalization (PQN) which calculates the most probable dilution by scaling to a reference profile.[48,74] The end result is the replacement of peak area for a metabolite with a relative peak area ratio that may reduce biological variation within a data matrix. Furthermore, for CE-based separations, apparent migration times can be normalized to an internal standard in terms of a relative migration time (RMT) to correct for run-to-run variations in the electroosmotic flow (EOF).[75] Metabolites that fail to meet set criteria for QC precision for each feature after batch correction and normalization are recommended to be removed prior to multivariate or univariate statistical analyses

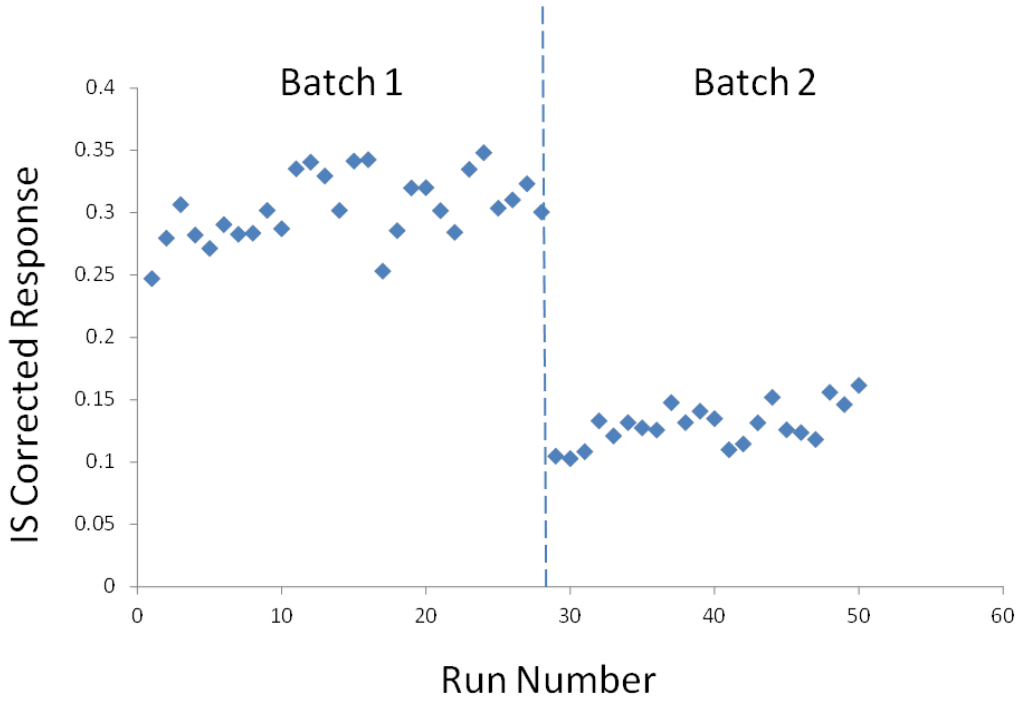

Figure 1.3. Control chart showing differences in internal standard corrected responses for periodic QC samples run in two separate batches.

to prevent false discoveries. FDA guidelines require a coefficient of variation (*CV*) <20% for QC runs for a biomarker,[76] however *CV* cutoffs of 30% are frequently applied in discovery-based nontargeted metabolomics studies.[77,78]

1.2.5 Statistical Analysis and Machine Learning in Metabolomics

Once the peak matrix is finalized (*i.e. m/z*:RMT *vs.* normalized relative peak area) statistical analyses can be performed and predictive models can be created for application to clinical laboratories.[26] It is worth noting that at the time of writing (August 2017) a PubMed search using metabolom* in any search field returned 23270 references, while also including statistic* only returned 2814 results. This suggests that only about 12% of references appear to emphasize the

statistical methods applied; this is consistent with Broadhurst and Kell[44] who reported that as of 2006, only 10% of papers mentioned statistical treatment. However, even when statistical methods are described, it is estimated that about 50% of published articles have at least one statistical error.[79] Many issues arise from not testing for normality prior to using parametric tests, as this can lead to decreased robustness, inaccurate *p*-values and false inferences.[40,65,79] Metabolomics data is often heavily skewed and non-normally distributed,[27] thus it is important to apply a Shapiro-Wilk (S-W) or Kolmogorov-Smirnov (K-S) test for normality in order to select the appropriate statistical model.[80] A *log* transformation may permit the use of classic univariate parametric tests such as Student's *t*-test or ANOVA.[40] However, if a transformation fails to normalize the data to a Gaussian distribution, non-parametric statistical tests are preferred, such as a Mann-Whitney *U* test or a Kruskal-Wallis test.[40,44] These univariate tests are frequently used to compare disease *vs.* non-disease classes or the effect of some treatment or intervention by assessing the significance of each metabolite separately allowing for more facile biological interpretation.[81] However, the probability of finding a random relationship between the dependent and independent variables increases with each additional univariate test performed, so a multiple hypothesis testing correction must be applied to avoid potential false discoveries (*i.e.* Type I errors).[65] For example, a Bonferroni adjustment controls the family-wise error rate (FWER) by lowering the significance level to α/n;[82] this ensures that the probability of at least one false positive test is, at most, 5%.[83]

However, this correction is extremely conservative and can lead to a high risk for of false-negatives (*i.e.* Type II errors), particularly when the number of measured metabolites is large. Alternatively, a false discovery rate (FDR) correction can be used, such as the Benjamini-Hochberg procedure, which controls the fraction of significant results that are false positives.[83] The decision to use either a FWER or FDR correction depends on what must be controlled (Type I or Type II errors) and whether or not a high level of confidence is required at a given stage in the study.[26] For instance, in early exploratory studies where follow-up tests are expected and the cost of a false-discovery is therefore low, FDR correction is a valid and prudent choice.

When a broad spectrum of metabolites are being measured, as is the case in nontargeted metabolomic studies, multivariate statistics can be used to assess the relationship amongst all variables *simultaneously*.[81] Even if none of the univariate tests reveal any significant effects, it is possible that independent variables may have a synergistic effect (*i.e.* within a common metabolic pathway), or that multiple testing correction unavoidably introduced false negatives into the data set.[81] Principal component analysis (PCA) is an unsupervised multivariate statistical method that is widely used for exploratory data analysis in metabolomics to visualize overall trends in the data structure (*i.e.* group clustering).[36] This is achieved by reducing the dimensionality of the data by creating a set of new, uncorrelated latent variables, or principle components, that are linear combinations of the original features and maximize data variance.[84]

Data preprocessing, such as *log* transformation and centering or scaling (*e.g.* autoscaling, Pareto scaling, range scaling, etc.) should be performed to ensure that highly abundant variables, often with high levels of variation, do not exert undue influence on the PCA model.[48,85] PCA does not require *a priori* class membership information and is useful for identifying outliers and the major sources of variation in the data.[27,63] If class information is known, partial least squares-discriminant analysis (PLS-DA) can be used to identify variation that is explicitly related to the classification samples in the training set (*e.g.* disease *vs*. control) and predict class membership of new data, often referred to as a hold-out or validation data set.[86] Alternatively, data ensemble or machine learning algorithms can also be used for multivariate data modelling in metabolomics, including artificial neural networks, random forests and support vector machines (SVM). The latter algorithm seeks to define a hyperplane that maximizes the distance between the two data sets (*i.e.* between disease and control) and then assign class membership to new data.[87,88] Care must be taken, however, to validate the results, ideally using an independent data set or, if that is not feasible, cross-validation or permutation testing or the original training set, since PLS-DA and SVM are prone to overfitting.[65]

Receiver operating characteristic (ROC) curves are widely used in metabolomics to assess the diagnostic performance of the putative biomarkers for binary classification of health outcome or disease status (*e.g.* disease *vs*. healthy).[89] An ROC curve is created by plotting the sensitivity of the test (*i.e.* the

proportion of people with the disease that give a positive test result) at all possible false positive rates (*i.e.* the number of positive tests in the absence of disease).[90] ROC curves are based on non-parametric statistics (*i.e.* no underlying assumption of data distribution) and are independent of the prevalence of the disease in the population, so ROC curves for various tests or methods can be compared to one another.[65,89] The area under the curve (AUC) is then a major criterion reflecting the diagnostic accuracy of the biomarker(s) as it incorporates both sensitivity and specificity (*i.e.* the proportion of people without a disease that give a negative result) into a single value.[89] The AUC as the indicates the probability that a randomly selected patient with the condition will have a test result more indicative of disease than a patient without the disease.[91] An AUC of 1.0 indicates that the test is a perfect classifier, while an AUC of 0.5 indicates that the test is no better than chance at predicting disease.[65] While the nature of the disease and its clinical applicability for routine analysis of a biomarker factors into the acceptability of a test, generally speaking, an AUC > 0.9 is considered excellent, an AUC from 0.8 – 0.9 is good, an AUC from 0.7 – 0.8 is fair, an AUC of 0.6 – 0.7 is poor, whereas if the AUC < 0.6, the test should be discarded.[65] It is crucial that the 95% confidence interval (CI) is reported for any AUC, as the AUC is a value calculated from a sample and thus has a statistical error associated with it; reporting the AUC with a 95% CI permits the comparison of various tests and/or a comparison against pure chance (AUC = 0.5) for more meaningful clinical decision making.[92] The total AUC is useful in the discovery stages of biomarker

evaluation and can be used to determine if the metabolite(s) perform better than chance and thus warrant further investigation (*i.e.* AUC > 0.80) within a larger cohort and/or across multiple population centres.[89,91] **Figure 1.4** illustrates potential steps taken to analyze a pre-processed data set by both univariate and multivariate statistical methods to determine the diagnostic performance of putative biomarkers.

1.2.6 Identification of unknown biomarkers by mass spectrometry

The number of metabolites comprising the human metabolome is not known, owing to the fact that metabolites are not strictly dictated by genomic and transcriptomic information. Indeed, the metabolome is the sum total of endogenous and exogenous compounds, and encompasses a diverse range of chemical structures and physicochemical properties (*e.g.* amino acids, nucleotides, phospholipids, toxins, drugs).[20,93] Currently, there are > 74,000 metabolite entries in the Human Metabolome Database (HMDB), with > 4,200 of them classified as "detected" in human samples and >70,000 classified as "expected but not quantified." Despite these significant efforts at curation, identification and quantification of metabolites and their isomers that comprise the entire human metabolome remains elusive.[62] As a result, structural elucidation of detected, yet unknown, metabolites by high resolution accurate MS or MS/MS is a considerable challenge. For instance, each metabolite detected in a complex biological sample generates a number confounding signals in ESI-MS that

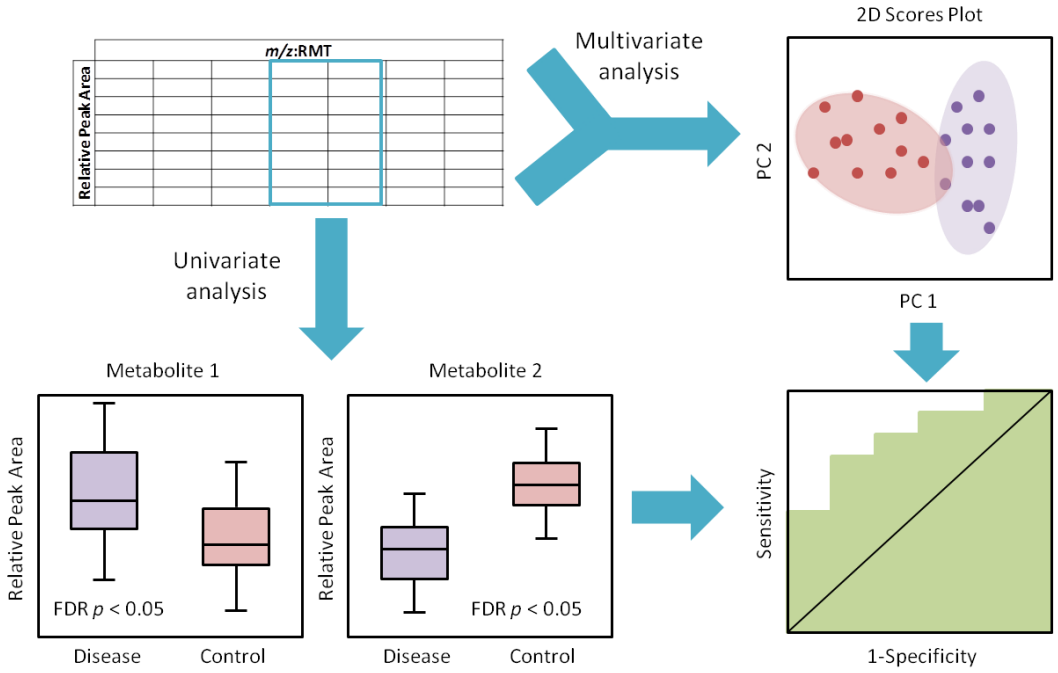

Figure 1.4. Workflow for the univariate and multivariate statistical analysis of individual metabolites or the sum metabolome, respectively. Significant features can be tested for diagnostic performance by ROC curve.

complicates data processing, including in-source fragments, adducts, multiple charge states and/or multiple derivatives.[60] Depending on the ionization mode, it is likely that the number of detectable features will exceed the number of samples, and it is estimated that upwards of 90% of these features will be redundant, spurious and/or unreliable signals.[94,95] However, this peak degeneracy can be exploited to identify or annotate metabolites by hinting at functional groups or molecular structure. Identification of unknown and low abundance compounds in MS remains a mostly manual undertaking and is therefore typically reserved for those metabolites that show significant effects. To facilitate data sharing and the development of best practices, the Chemical Analysis Working Group of the

Metabolomics Standards Initiative has described four levels of metabolite identification as follows:[62,96] *Level 1* consists of confidently *identified* metabolites and requires the comparison of at least two orthogonal properties, such as *m/z* and RT or MT, accurate mass and fragmentation spectrum, or accurate mass and isotope pattern, with authentic chemical standards under identical analytical conditions. *Level 2* consists of putatively *annotated* compounds and this is based on comparisons of *m/z*, RT or MT, and/or fragmentation spectra to publically or commercially available libraries or databases. Here, it is worthwhile to note that absolute retention times are variable and rely heavily on column/stationary phase type and elution conditions. In GC-MS applications, only a limited number of column types are used and a normalized retention index is widely reported in databases (*e.g.* NIST, NIH or EPA).[23] Furthermore, extensive and consistent fragmentation under standard ionization conditions (*e.g.* 70 eV in EI-MS) permits structural elucidation and facilitates database matching.[23,41] For LC and CE-based separations, no standardized retention or migration index exists and MS/MS spectral quality and reproducibility is dependent on the specific mass analyzer and MS vendor used to acquire data, resulting in non-trivial database matching.[97,98] *Level 3* comprises the putatively annotated compound classes, which relies on comparisons of measured properties or obtained spectra to other compounds of the same chemical class (*e.g.* searching for product ions or neutral losses common to amino acids from the METLIN database). Finally, *Level 4* consists of metabolites that do not have any good quality acquired MS/MS spectra (*e.g.,* low

abundance precursor ion) or database matches, but can still be defined by an accurate mass (*m/z*), as well as RT or MT. While these four classes provide reporting standards to the metabolomics community so that data can be shared and reused, they are only the first step towards a biochemical understanding of the role or function of identified metabolites of clinical significance.[99] For instance, it is recommended that researchers note the level of identification (*i.e.* 1-4) in addition to common names and structural codes (*e.g.* SMILES or InChI), if possible.[100]

Advances in the development and accessibility of high resolution mass spectrometers permit accurate mass measurements (< 5 ppm)[41] and molecular formula generation to facilitate database matching and reduce bias when standards are not commercially available.[23] However, it is common that one accurate mass is equivalent to multiple formulae and numerous potential chemical structures (*i.e.* isobars) and stereoisomers;[63] it is therefore suggested that top-ranked molecular formulae derived for a molecular ion be carefully inspected and to reduce the sheer number of possible chemical structures. Kind and Fiehn[101] proposed seven "golden rules" to reduce the number of molecular formulae in order to converge on the most likely candidate. These include restricting the maximum number of each possible element, using LEWIS and SENIOR rules for valences, filtering based on isotopic pattern, restricting the ratio of hydrogen/carbon ratio to 0.2-3.1, setting appropriate heteroatom numbers, and checking ratios of nitrogen, oxygen, phosphorus and sulfur to carbon.[101] Additionally, other complementary approaches could be used to facilitate compound identification or rule out possible

candidates, such as chemical reactivity, transformation by enzymatic reaction, and/or isolation for NMR or MS/MS analyses.

1.3 Clinical validation and population-based newborn screening

1.3.1 The shift to expanded newborn screening

Newborn screening (NBS) is widely regarded as one of the ten greatest achievements in public health of the early 21st century.[102,103] Universal NBS programs aim to pre-symptomatically identify neonates with treatable genetic diseases to ensure early treatment to prevent death, disability and/or poor quality of life.[104] NBS as a tool for population-based screening was first implemented in 1963, with the introduction of an elegant and simple bacterial inhibition assay (BIA) and filter paper card for collecting dried blood spots (DBS) to test for phenylketonuria (PKU) by Dr. Robert Guthrie and Ada Susi.[105] Classical PKU is caused by a mutation on chromosome 12 at the locus for phenylalanine hydroxylase (PAH), whereas mutations loci that code for tetrahydrobiopterin (BH_4) synthesis and/or regeneration are associated with hyperphenylalaninemia/non-PKU that typically result in milder symptoms.[106] The result is a lack of conversion of phenylalanine (Phe) to tyrosine (Tyr), and a toxic accumulation in Phe concentrations in blood (>120 μM) which represents a biomarker for screening for PKU.[107] Untreated PKU can lead to severe cognitive impairment and/or mental retardation. Excess Phe can also be converted to phenylketones, including phenylpyruvate, phenyllactate and phenylacetate which represent secondary biomarkers that are readily measured in urine (**Figure 1.5**).

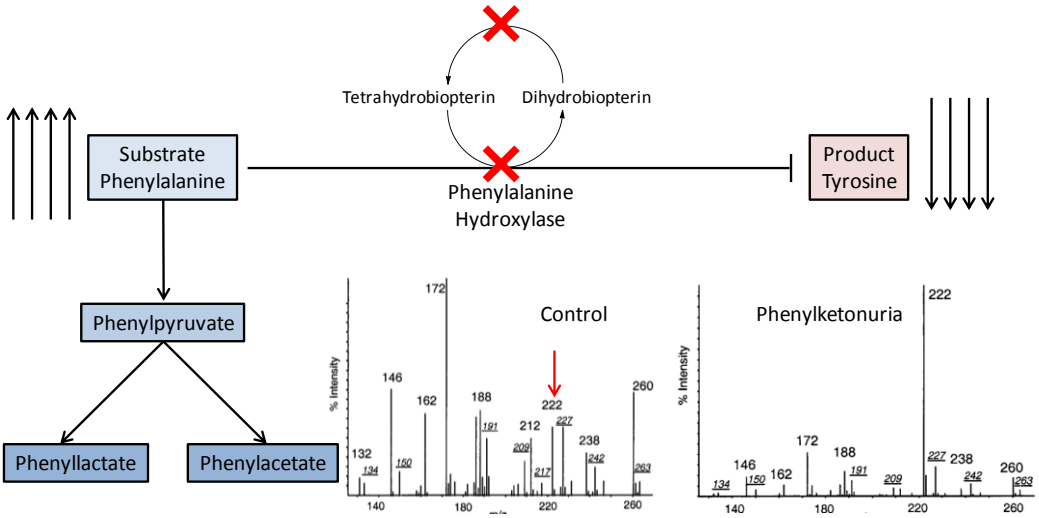

Figure 1.5. Biochemical pathway illustrating the impact of a mutation, as indicated by the "x", that affects phenylalanine hydroxylase or tetrahydrobiopterin recycling. Accumulated Phe can be converted to phenyllactate and phenylacetate via phenylpyruvate. DBS are derivatized to butylesters for enhanced sensitivity in NBS programs and Phe is detected by a neutral loss scan of 102 in MS/MS.

Bioassays (*i.e.* immunoassays or enzyme kinetic assays) were the gold standard for biomarker screening in NBS programs, including galactosemia,[108] congenital hypothyroidism[109] and congenital adrenal hyperplasia.[110] Population-based screening for IEM and other rare genetic diseases, however, was reserved for a limited number of diseases with elevated local prevalence and early onset that demonstrated clear clinical benefits from early intervention as compared to symptomatic intervention.[104] However, consensus was often difficult to reach and external factors such as politics and economics often dictated the exact panel of diseases in regional NBS programs.[111]

In 1968 Wilson and Jungner introduced a framework of criteria within which decisions on screening for human diseases could be evaluated (**Table 1.3**).

Table 1.3. Criteria for screening by Wilson and Junger.[112]

Wilson and Jungner Principles
The condition should be an important health concern
There should be an accepted treatment for affected individuals
Facilities and resources for diagnosis and treatment should be in place
The natural history of the disorder must be understood
There should be a latent or early symptomatic stage
There should be a suitable test
The test should be acceptable to the population being screened
There should be an agreed upon policy on whom to treat
The cost of screening, diagnosis and treatment should be balanced in relation to medical expenses
Screening should be a continual process

However, the advent of high throughput commercial instrumentation based on direct infusion-tandem mass spectrometry (DI-MS/MS) revolutionized NBS and challenged the principles of Wilson and Jungner.[113] In this case, a wide range of metabolites as specific biomarkers for IEM can be analyzed simultaneously by DI-MS/MS in a multiplexed manner at incremental costs, which has led to the development of expanded NBS programs[114] to screen for fatty acid oxidation disorders, organic acidurias, amino acidemias and others.[115] Despite a significant initial infrastructure cost (typically estimated at ~$500,000), ongoing analysis costs are low (~$19 per infant).[116] Furthermore, the addition of new biomarkers for IEM to the MS/MS panel occurs at less than $1 per disorder.[117] However, this has led to discussions about including diseases that do not meet the Wilson and

Jungner criteria, such as those with extremely low incidence rates and unknown or underreported natural histories without available treatment options.[6] It is worth nothing that many families are comforted by a definitive diagnosis, even in the absence of effective treatments, and a diagnosis can empower families to make decisions on future pregnancies.[118]

As there is no national newborn screening policy in Canada, provinces and territories decide autonomously to screen for certain genetic diseases based on good medical practice. As a result, some jurisdictions screen for many diseases, while others screen for only a few.[111] To combat disparities between NBS programs the American College of Medical Geneticists (ACMG) was commissioned to develop recommendations for a uniform panel of conditions for state NBS programs.[119] A total of 84 conditions were evaluated, chosen based on current inclusion in NBS programs, accidental discovery by current screening, identification by expert groups, identification by advocacy groups and/or current use in differential diagnosis for another condition.[119] Conditions were given scores in three areas (*i.e.* Condition/disorder, Screening test, and Treatment and Management), for a total score of 2100. Criteria included prevalence rate, whether signs or symptoms are early onset and thus likely detectable within 48 hours of life, analytical cost, efficacy of treatment and availability of acute management.[120] A combined score of > 1200 was considered appropriate for inclusion in the "core" panel (**Figure 1.5**). It should be noted that for some disorders, such as

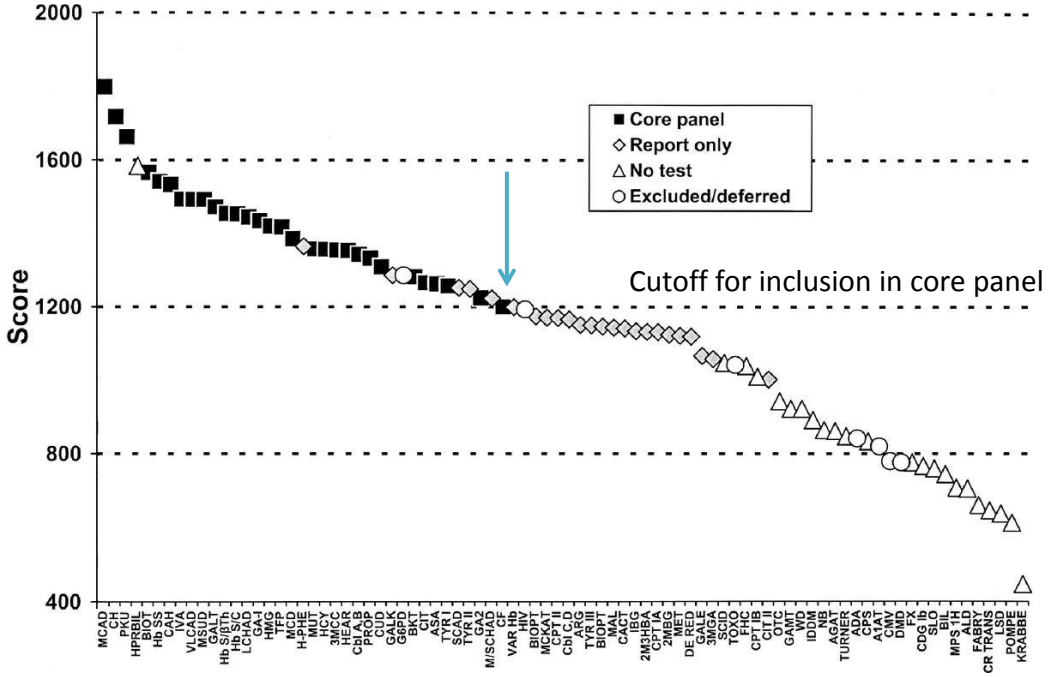

Figure 1.6. Cumulative scores for 84 inborn errors of metabolism assessed for suitability in a recommended panel of diseases to be included in NBS programs. A score of > 1200 was considered appropriate for inclusion in screening, with a few exceptions for those diseases with no approved test or those that are reported on the basis of being a secondary target.[120] CF lies right on the cutoff for inclusion (blue arrow).

hyperbilirubinemia (HPRBIL), while the cumulative score is high (1584), no validated test currently exists and it thus excluded from the panel. Cystic fibrosis (CF), which lay exactly on the boundary of inclusion (score of 1200), was included on the basis that there is a high incidence rate and a screening/diagnostic test available, despite a lack of consensus on the availability and efficacy of treatment at the time.[120] However, it is now widely understood that early intervention in CF has clear benefits for the patient, and children diagnosed by NBS have better health outcomes than those diagnosed symptomatically.[121] In total, the ACMG supports a core panel of 29 disorders, in addition to 25 secondary targets that may be diagnosed or revealed when screening for the core

conditions.[119] However, it must be noted that many jurisdictions still deviate from this panel, such as Alberta, which currently screens for only 17 disorders.[122]

1.3.2 The need for biomarker discovery in expanded newborn screening

While many genetic diseases can be screened for using MS/MS, which offers a cost-effective and highly sensitive yet specific platform for high throughput screening,[117] not all disorders have MS-compatible biomarkers. Of the 29 disorders on the ACMG recommended panel, approximately one-third of them are detected by other methods, such as enzymatic assays, immunoassays or a combination of methods.[117] Approximately two-thirds (~66%) of all screen-positive NBS results are from those disorders that are not detected by MS/MS.[123] For example, classical galactosemia is caused by a deficiency in the galactose-1-phosphate uridylyltransferase (GALT) enzyme and is potentially fatal if not detected and treated early.[124] Screening is currently done by enzymatic kinetic assay for GALT deficiency, however, it is prone to false-positive results due to enzyme denaturation during transportation, particularly during summer months.[6] Another example is cystic fibrosis (CF), which has an incidence rate of about 1 in 3600 in Canada.[125] It is the most common fatal genetic disease in Caucasian populations and Cystic Fibrosis Canada estimates that approximately 1 in 25 individuals in Canada is a carrier. It is caused by mutations in the CF transmembrane conductance regulator gene (*CFTR*), a chloride channel present on apical membrane surfaces in epithelial cells.[126] CF is a multi-organ disease that affects the lungs, pancreas, intestines and sweat glands.[127] However the

pulmonary effects are usually the most severe, as impaired chloride conduction leads to the buildup of thick, sticky mucus which results in ciliary collapse and persistent lung infections and inflammation.[22,126] Screening for CF is a two-step algorithm composed of an immunoassay for elevated levels of the pancreatic zymogen, immunoreactive trypsinogen (IRT)[128] followed by a DNA mutation analysis that tests for common *CFTR* mutations.[129] However, this algorithm is prone to false-positive results, as IRT can be elevated for a variety of non-CF reasons, including meconium contamination of the dried blood spot (DBS) card, hypoglycemia and certain trisomies.[130] In fact, CF alone accounts for over one-third of all screen-positive results in Ontario.[123] It is clear that more specific biomarkers that can be measured by MS/MS have the potential to improve screening accuracy for diseases such as galactosemia and CF, and that biomarker discovery studies using metabolomics are a worthwhile undertaking in support of NBS programs.

1.3.3 Stages of Clinical Validation for Biomarkers

Once a metabolite or panel of metabolites has been shown to differentiate controls and cases (*e.g.* CF *vs.* non-CF), validation or "qualification" studies are required are required.[131] Publication alone does not qualify a biomarker within its intended context, and detection of an interesting metabolite should be clinically interpreted.[131] Biomarker qualification is a complex process that should involve stringent standards, clear guidelines and multidisciplinary teams of researchers, clinicians, regulators, and industry to prevent the uncoordinated approach that has

failed to produce viable biomarkers in earlier genomic and proteomic initiatives.[132] Koulman *et al.*[133] have proposed a pathway to qualification to increase the chance that differentiating metabolites are properly validated as clinically relevant biomarkers that are associated with improved patient outcomes as summarized in **Table 1.4**.

1.3.4 Determination of clinical parameters for biomarker translation

Once a differentiating metabolite has satisfied several stages to become a candidate biomarker that is subsequently replicated within a larger multi-centre cohort, the clinical performance or diagnostic properties of the biomarker must be calculated and compared to the currently accepted or "gold-standard" method.[134] **Table 1.5** summarizes clinical parameters and how they are calculated from the data. At this stage, ROC curves can be created once again, based on the sensitivity and specificity calculated from a clinical population and not simply from a discovery sample cohort, which have an abundance of easily diagnosed patients as a result of the study sampling and therefore tend to overestimate accuracy.[89,90]

Here, calculating partial AUC may be more informative than total AUC.[92] The clinical landscape in which the test will be applied must be taken into consideration; for example the optimal cutoff concentration range for NBS must be set to minimize false negative results (*i.e.* maximize sensitivity) as the implications of not treating IEM are often fatal.[135] In this case, it is prudent to calculate the partial AUC at a given and acceptable level of sensitivity to ensure that a fair comparison is being made between the proposed biomarker and the

Table 1.4. Steps to clinical validation of a biomarker, from discovery to application in the population. Adapted from Koulman *et al*.[133]

Clinical Validation Stage	Requirements	Suggested Terminology
Discovery	***Metabolite(s) that can differentiate between case and control:*** Experimental design, sample analysis and statistical tests	Differentiating Metabolite
Qualification 1	***Identification of the biomarker:*** Unknown metabolites have limited use as they cannot be connected to underlying biological pathways and/or other studies ***Analytical Validation:*** The method must be validated for use in a clinical laboratory ***Repeat study:*** Testing the biomarker in a new sample set from a wider population to eliminate the possibility that the changes are from sample bias in discovery	Candidate biomarker
Qualification 2	***Assay for specificity:*** Test on a large and elaborate sample set that reflects the expected population while controlling for biases. Comparison to controls with related pathophysiologies is useful (*e.g.* non-CF lung exacerbations *vs.* CF) ***Assay for robustness:*** Test the biomarker on a large, but minimally controlled population (*e.g.* CF *vs.* non-CF across various ages and severities) ***Assay for limitations:*** Test the biomarker in healthy populations to determine the likelihood of a false-positive based on biological variability ***Test in wider population:*** Test the performance of the candidate biomarker(s) alongside the current, conventional methods	Candidate biomarker
Application	***Use and documentation of the biomarker:*** Impact of the use of the biomarker on the screened population	Biomarker

current one.[89,92] In NBS programs, it is helpful to monitor and report sensitivity, specificity and PPV.[6] Low population prevalence of most IEM means there are few true positive results and the PPV in NBS programs is often low. For instance, in Ontario in 2012, the reported PPV for PKU was 36% while the PPV for CF was only 9.3%.[123] However, the use of secondary markers (*e.g.* Phe/Tyr ratio for PKU

Table 1.5. Summary of clinical parameters their formulae used to determine the diagnostic potential of a biomarker.

Parameter and description	Formula
Sensitivity: The proportion of people with a given condition that test positive. Also called true positive rate.	$Sensitivity = \frac{\#\ true\ positive\ results}{Total\ \#\ with\ disease}$
***Specificity*:** The proportion of people without a given condition that test negative. 1-specificity is the also called the false positive rate	$Specificity = \frac{\#\ true\ negative\ results}{Total\ \#\ without\ disease}$
Positive predictive value (PPV): The proportion of those with a positive test result that have the disease. Population prevalence rate is factored into this calculation	$PPV = \frac{\#\ true\ positive\ results}{Total\ \#\ positive\ results}$
Negative predictive value (NPV): The proportion of those with a negative test result that do not have the disease. Population prevalence rate is factored into this calculation	$NPV = \frac{\#\ true\ negative\ results}{Total\ \#\ negative\ results}$

or succinylacetone for Tyrosinemia Type I)[136] or second-tier tests (*e.g.* LC-MS/MS for branched chain amino acids in maple syrup urine disease, MSUD)[6] can reduce the number of false positive results thereby increasing the overall PPV for the population-based screen.

To facilitate successful biomarker discovery, the Food and Drug Administration (FDA) and the European Medicines Agency (EMA) have created a voluntary exploratory data submission strategy to promote scientific, statistical and clinical discussions to assist in navigating the complexities of qualification of biomarkers and clinical decision making.[137,138] As part of the qualification process, the analytical performance of the method must be demonstrated and the

FDA has released a seminal document "FDA Guidance for Industry-Bioanalytical Method Validation" which is widely used in both the pharmaceutical industry and elsewhere as the standard reference for method validation.[134]

1.4 Analytical validation for drug of abuse screening

1.4.1 The need for improved drug screening methodology

While universal screening of newborns for IEM is a successful public health policy in preventative medicine with direct benefits to affected patients and their families, the merits of universal population-based screening for drugs of abuse (DoA) are perhaps less obvious.[139] As a result, screening for DoA is usually performed for defined occupations or high-risk populations in the context of pre-employment screening and workplace monitoring, pain management and compliance, substance abuse testing, therapeutic drug monitoring and forensic toxicology.[140] However, there has been a staggering increase in the prevalence of prescribed drug abuse due to over-prescription of opioids, including an alarming number of deaths attributed to drug poisoning (*i.e.* overdose). Since 2000, the US has witnessed a 137% increase in overdose deaths and a 200% increase in opioid-induced deaths.[141] There has been a shift towards the illicit use of synthetic, non-methadone, opioids such as fentanyl.[141] In 2016 the government of Canada reported almost 2600 deaths from opioids (not including data from Quebec), and in Ontario alone, deaths from opioids have increased two-fold from 2003 to 2015.[142] The socioeconomic impact of widespread drug addiction/abuse not only

directly impact public healthcare in Canada, but also workplace productivity, substance abuse treatment and criminal justice.

Current drug screening is done by colourimetric immunoassay, which is a rapid screening method routinely employed in clinical settings as it allows for point-of-care testing.[140] However, immunoassays display poor screening performance, particularly with opioids, as antibodies raised against the natural opioids (*e.g.* morphine and codeine) show limited affinity for semi-synthetic or synthetic opioids (*i.e.* oxycodone or fentanyl).[143] Furthermore, some antibodies show cross-reactivity with non-target drugs, such as over-the-counter or prescribed drugs. For example, certain decongestants and some Parkinson's drugs can give positive results on amphetamine assays.[144] All screening results are therefore considered presumptive until more sensitive and selective confirmatory testing based on GC-MS and increasingly LC-MS/MS.[145] However, there is a trend towards replacing the primary screens based on immunoassay with LC-MS to reduce false-positive and false-negative results.[145] Traditionally, these exploited the LC-MS/MS confirmatory platform, which relies on *a priori* information on drugs of interest.[146] However, as newer designer and synthetic drugs (*e.g.* Spice/K2 or bath salts) become more prevalent, it became clear that nontargeted methods or broad spectrum screening using full scan using time-of-flight (TOF) instruments were a more prudent choice.[147] In many ways, the screening approach and analytical challenges associated with DoA testing is similar to NBS programs, such as neonatal CF screening that is prone to false positives and thus requires

more specific follow-up confirmatory test for diagnosis of presumptive CF neonates, such as sweat chloride.

1.4.2 Stages of analytical validation in accredited laboratories

Bioanalytical method validation is used to *"test whether methods for measuring concentrations of measurands in biological matrices are accurate and fit for the intended purpose"* while verification is performed to ensure that data obtained by manufacturers during validation can be reproduced in the user's lab.[134] Typically, a verification of an already-established and validated method involves determining accuracy, precision, linearity, reportable range and reference intervals,[134] however, in some instances a full validation may still be performed.[76] A full validation is required for a newly developed method, or when new analytes are being added to an existing assay.[76] A full validation occurs in two parts: establishing the analytical performance characteristics (*i.e.* technical performance) and establishing if the method is fit for purpose (*i.e.* clinical performance). **Table 1.6** summarizes the figures of merit for a validation of an analytical method, while **Table 1.4** summarized the requirements of a clinical validation. Once a method has been validated, the results can be compared to current or standard methods to determine the degree of agreement between the measurements. A Bland-Altman plot constructs limits of agreement between two methods by plotting the differences of the two measurements against the mean of the measurements and calculating the 95% CI of the mean difference.[80] However, acceptable bias must be defined in the context of the biological or clinical applications of the test. For

Table 1.6. Summary of figures of merit for validation of an analytical method. From the FDA Bioanalytical Method Validation.[76]

Validation Parameters	Requirements	Acceptable Criteria
Precision: closeness of individual measures when the procedure is applied repeatedly to multiple aliquots of a single sample	A minimum of 5 measurements at a minimum of 3 concentration levels for within-run intra-batch and between-run, inter-batch	CV ≤ 15% or ≤ 20% at the lower limit of quantification (LLOQ)
Accuracy: closeness of mean test results obtained by the method to the true value (concentration) when analyzing replicates	A minimum of 5 measurements at a minimum of 3 concentration levels	Mean value must be within 15% of the actual value, or within 20% of the value at the LLOQ
Selectivity: ability to differentiate and quantify the analyte in the presence of the matrix	Analysis of blank matrix from a minimum of 6 sources to test for interference.	Response of interference < 20% of the LLOQ of the analyte.[148]
Recovery: response obtained after addition and extraction of analyte in the matrix, compared to the response obtained for the pure authentic standard	Analysis at 3 concentration levels compared to an unextracted standard at 100% recovery.	Extent of recovery must be precise and reproducible
Calibration Curve: the relationship between instrument response and known concentrations of the analyte	Analysis of 6-8 non-zero samples, a blank sample and a zero sample in the biological matrix of interest	LLOQ response is 5 times the blank with a precision ≤ 20% and accuracy of 80-100% CV of other levels ≤ 15%
Stability: evaluate and report the stability of the analytes under various conditions that represent situations likely to be encountered during handling and analysis	*Freeze-thaw*: 3 aliquots analyzed after 3 freeze-thaw cycles *Short-term temperature*: 3 aliquots thawed and kept at room temperature for 4-24 h *Long-term*: Store 3 aliquots of high and low concentration under same conditions as study samples and analyze 3 times *Stock solution*: Analysis following room temperature storage of stocks for 6 h *Post-preparative:* Stability of processed samples held over the anticipated run time compared to a fresh sample	Statistical methods can be used to compare calculated concentrations to original concentrations. Various statistical methods can be used (*e.g.* 95% CI), as long as they are defined.

example, in DoA screening, accuracy of the analytical method is determined not by closeness of the concentration to the true value, but by the ability of the method to correctly detect the presence of a drug above a defined cutoff (*i.e.* as defined by the Substance Abuse and Mental Health Services Administration).[149]

1.5 Thesis motivations and objectives: New biomarkers for screening

Population-based screening programs exist to promote and protect the health and well-being of individuals within a population. Whether universal (*i.e.* newborn screening for IEM) or tailored for a specific population or purpose (*i.e.* screening for DoA), screening relies on rapid yet reliable measurements of one more biomarkers associated with disease risk. It is imperative, therefore, that these biomarkers are rigorously validated and tested in both an analytical and clinical context. Missteps along the long and arduous path from discovery to application are unintentional and often reflect common failures or weaknesses perpetrated by well-meaning researchers. However, it is often said that "the road to hell is paved with good intentions" and a lack of decisive action in the face of poor candidate biomarker performance is not acceptable given its direct impact on patient well-being and clinical decision making. For instance, misuse of common biomarkers can inadvertently contribute to higher costs and adverse health outcomes, such as unnecessary follow-up clinical testing and treatments based on invasive surgical procedures or drug prescriptions. Researchers must be consistent and thorough at all stages of discovery to ensure that the scientific community is truly poised to take full advantage of the power of metabolomics for new advances in precision

medicine and population health. The work in this thesis, therefore, stands to demonstrate the development and validation of MSI-CE-MS with temporal signal pattern recognition as an improved approach for confirmatory testing of known biomarkers for IEM from DBS extracts, which can also be applied to the discovery of unanticipated biomarkers for genetic disorders not screened by MS/MS (*Chapter II*). Furthermore, nontargeted metabolite profiling approaches using MSI-CE-MS were then applied for the discovery of novel metabolic signatures in asymptomatic CF neonates as compared to screen-negatives and importantly screen-positive yet unaffected carriers as a way to reduce the false positive rate of current IRT/DNA screening algorithms (*Chapter III*). Finally, the development and validation of a high throughput method based on MSI-CE-MS for broad spectrum screening of DoA and their metabolites in urine was also demonstrated, which offers a cost-effective, specific and reliable method for screening and confirmatory testing as compared to immunoassays, that can also detect novel designer drugs not part of targeted/known drug panels (*Chapter IV*).

1.5.1 Multiplexed confirmatory testing of inborn errors of metabolism

Current newborn screening programs primarily rely on DI-MS/MS for high-throughput and multiplexed screening of a panel of IEM within 2-3 minutes.[150] Depending on the province or territory, upwards of 30 diseases can be screened using DI-MS/MS based on elevated levels of amino acids and/or acylcarnitines.[108] However, screening for IEM favours sensitivity over specificity, as many IEM are fatal if not detected and treated pre-symptomatically; this leads

to an increased number of false-positive results that can lead to familial stress and anxiety.[151] Second-tier or confirmatory tests with high levels of specificity are therefore required for a definitive diagnosis.[152] These tests require chromatographic separation to resolve isomers or isobars, such as the differentiation of the pathognomonic marker of MSUD *allo*-isoleucine from its isomers and the benign isobar hydroxyproline.[153,154] However, LC-MS/MS analyses are low-throughput and time consuming and represent a return to the "one test-one disorder" paradigm of conventional bioassay-based screening.[135] *Chapter II* presents a novel method for higher-throughput yet unambiguous confirmation of IEM based on MSI-CE-MS using an asymmetric injection sequence for temporal signal pattern recognition in MS with quality assurance.[155] This method was validated on proficiency-testing samples and authentic neonatal dried blood spots from Newborn Screening Ontario (NSO), which showed clinically acceptable levels of precision and accuracy. Furthermore, previously unreported metabolites, putatively identified as *N*-galactated amino acids by MS/MS (level 2), were found to be highly elevated in a neonate with classic galactosemia (type 1). If successful, the process of validation can begin to determine if such biomarkers can be implemented using existing MS/MS infrastructure with improved PPV, thus eliminating the need for a stand-alone enzyme kinetic assay for galactosemia which is prone to false positives.

1.5.2 Biomarker discovery for improved screening for cystic fibrosis

Current screening for CF is based on a two-stage IRT/DNA algorithm, which has a low PPV (*i.e.* < 10%[123,156]) despite a high incidence rate in the population.[123,157] This is because the IRT/DNA algorithm is prone to false-positive results (*e.g.* elevated Apgar scores can elevate IRT in the absence of CF)[157] and carrier identification (*i.e.* infants with a single disease-causing *CFTR* mutation are considered screen-positive), which can complicate genetic counselling and clinical decision making during follow-up sweat chloride testing.[129,158] While there is no shortage of metabolomics investigations for CF, these have been focused on understanding the pathophysiology[159,160] or severity[161] of CF or to predict the onset of pulmonary exacerbation[162] in previously-diagnosed adults. However, there is sparse research on the development of metabolite-based *screening* assays for pre-symptomatic diagnosis of CF in neonatal populations. Thus, *Chapter III* details a nontargeted metabolomics approach for biomarker discovery in CF that is the culmination of research efforts over five years in collaboration with colleagues at NSO at the Children's Hospital of Eastern Ontario (CHEO). Nontargeted MSI-CE-MS was performed on retrospective DBS collected from confirmed CF neonates, as well as screen-negative controls and screen-positive yet unaffected carriers or transient hypertrypsinogenemic cases – the latter group are consider presumptive CF prior to sweat chloride testing and are the major reason for the unacceptably high false positive rate in neonatal CF screening. A total of 70 cationic metabolites were

detected consistently in DBS extracts after applying a rigorous data filtering approach to reject spurious, redundant, background and irreproducible signals, with selected metabolites showing good agreement with measurements performed independently by DI-MS/MS at NSO. To the best of our knowledge, this work represents the first report of measurable metabolic phenotype differences between asymptomatic CF and unaffected/screen-positive neonates that can be acquired from an original DBS specimen using a single 3.2 mm diameter hole-punched cut-out. Preliminary analyses suggest that, when combined with initial IRT results, these metabolites could significantly reduce false-positive results for improved PPV of the CF screen when using MS/MS infrastructure at incremental costs. Most importantly, this can reduce healthcare costs by limiting the number of unnecessary genetic and sweat chloride tests and reduce the number of families that must endure under anxiety with follow-up testing on their newborn baby.

1.5.3 Systematic screening for substance abuse surveillance

Alcohol and drug abuse represent a serious public health issue. In 2012, approximately 10% of Canadians over the age of 15 used cannabis in the past year, while 11.3% used another illicit drug such as cocaine or methamphetamine.[163] While these numbers remain unchanged from previous years, there were increases in abuse among prescription pharmaceutical users, particularly for opioid drugs such as heroin and fentanyl.[141] Sensitive and specific tools for screening are therefore required as test results can have far-reaching implications including criminal prosecution, medical treatment decisions and

surgical eligibility. However, current immunoassay-based screens are not specific due to cross-reactivity with over-the-counter medications (*i.e.* false-positives) or a lack of affinity of the antibodies for chemically diverse drug classes (*i.e.* false-negatives).[139] All screening results are therefore presumptive and require confirmation by more specific yet lower throughput LC-MS/MS methods. *Chapter IV* details the development and validation of a multiplexed CE-MS method to increase screening throughput by an order of magnitude without added infrastructure costs while providing the specificity typically reserved for confirmatory assays. Separations were optimized to obtain a runtime of < 3 min/sample and the method was demonstrated to have acceptable accuracy and long-term precision with minimal carry-over effects when analyzing large numbers of samples. Furthermore, untargeted analysis of both human urine and a synthetic urine matrix revealed signatures of authentic urine, both endogenous and exogenous, that can be used for specimen verification or sample adulteration without the need for additional testing (*i.e*. pH or specific gravity). This work has been part of an exciting industrial collaboration with colleagues at Seroclinix Inc., a laboratory diagnostic company with core interests in translating novel MS-based technologies for forensic toxicology, human health and wellness and veterinary medicine applications, which has two locations based in Mississauga (ON, Canada) and Amherst (NY, USA).

1.6 References

(1) Strimbu, K.; Tavel, J. A. *Curr Opin HIV AIDS* **2011**, *5*, 463–466.

(2) Group, B. D. W. *Clin. Pharmacol. Ther.* **2001**, *69*, 89–95.

(3) Puntmann, V. O. *Postgrad. Med. J.* **2009**, *85*, 538–545.

(4) Kannel W. B. *Jama* **1996**, *275*, 1571–1576.

(5) Mayeux, R. *NeuroRx* **2004**, *1*, 182–188.

(6) Lehotay, D. C.; Hall, P.; Lepage, J.; Eichhorst, J. C.; Etter, M. L.; Greenberg, C. R. *Clin. Biochem.* **2011**, *44*, 21–31.

(7) Wieckowska, A.; McCullough, A. J.; Feldstein, A. E. *Hepatology* **2007**, *46*, 582–589.

(8) Ludwig, J. A; Weinstein, J. N. *Nat. Rev. Cancer* **2005**, *5*, 845–856.

(9) Stolz, D.; Christ-Crain, M.; Morgenthaler, N. G.; Leuppi, J.; Miedinger, D.; Bingisser, R.; Müller, C.; Struck, J.; Müller, B.; Tamm, M. *Chest* **2007**, *131*, 1058–1067.

(10) Liu, C. H. *Future Neurol.* **2015**, *10*, 49–65.

(11) Okusa, M. D.; Jaber, B. L.; Doran, P.; Duranteau, J.; Yang, L.; Murray, P. T.; Mehta, R. L.; Ince, C. *Contrib. Nephrol.* **2013**, *182*, 65–81.

(12) Rifai, N.; Gillette, M. A; Carr, S. A. *Nat. Biotechnol.* **2006**, *24*, 971–983.

(13) Novelli, G.; Ciccacci, C.; Borgiani, P.; Amati, M. P.; Abadie, E. *Clin. Cases Miner. Bone Metab.* **2008**, *5*, 149–154.

(14) Sawyers, C. L. *Nature* **2008**, *452*, 548–552.

(15) Hanash, S. M.; Pitteri, S. J.; Faca, V. M. *Nature* **2008**, *452*, 571–579.

(16) Gutman, S.; Kessler, L. G. *Nat. Rev. Cancer* **2006**, *6*, 565–571.

(17) Füzéry, A. K.; Levin, J.; Chan, M. M.; Chan, D. W. *Clin. Proteomics* **2013**, *10*, 1.

(18) Scholz, M.; Lam, R.; Strum, S.; Jennrich, R.; Johnson, H.; Trilling, T. *Urology* **2007**, *70*, 506–510.

(19) Taguchi, F.; Solomon, B.; Gregorc, V.; Roder, H.; Gray, R.; Kasahara, K.; Nishio, M.; Brahmer, J.; Spreafico, A.; Ludovini, V.; Massion, P. P.; Dziadziuszko, R.; Schiller, J.; Grigorieva, J.; Tsypin, M.; Hunsucker, S.

W.; Caprioli, R.; Duncan, M. W.; Hirsch, F. R.; Bunn, P. A.; Carbone, D. P. *J. Natl. Cancer Inst.* **2007**, *99*, 838–846.

(20) Wishart, D. S. *Nat. Rev. Drug Discov.* **2016**, *15*, 473–484.

(21) Serkova, N. J.; Standiford, T. J.; Stringer, K. A. *Am. J. Respir. Crit. Care Med.* **2011**, *184*, 647–655.

(22) Jain, K. K. *The handbook of biomarkers*; Humana Press, 2010.

(23) Dunn, W. B.; Broadhurst, D. I.; Atherton, H. J.; Goodacre, R.; Griffin, J. L. *Chem. Soc. Rev.* **2011**, *40*, 387–426.

(24) Patti, G. J.; Yanes, O.; Siuzdak, G. *Nat. Rev. Mol. Cell Biol.* **2012**, *13*, 263–269.

(25) Walsh, M. C.; Nugent, A.; Brennan, L.; Gibney, M. J. *Nutr. Bull.* **2008**, *33*, 316–323.

(26) Griffiths, W. J.; Koal, T.; Wang, Y.; Kohl, M.; Enot, D. P.; Deigner, H. P. *Angew. Chemie - Int. Ed.* **2010**, *49*, 5426–5445.

(27) Tzoulaki, I.; Ebbels, T. M. D.; Valdes, A.; Elliott, P.; Ioannidis, J. P. A. *Am. J. Epidemiol.* **2014**, *180*, 129–139.

(28) Diamandis, E. P. *BMC Med.* **2012**, *10*, 87.

(29) Moss, E. L.; Hollingworth, J.; Reynolds, T. M. *J. Clin. Pathol.* **2005**, *58*, 308–312.

(30) Mai, P. L.; Wentzensen, N.; Greene, M. H. *Cancer Prev. Res.* **2011**, *4*, 303–306.

(31) Visintin, I.; Feng, Z.; Longton, G.; Ward, D. C.; Alvero, A. B.; Lai, Y.; Tenthorey, J.; Leiser, A.; Flores-Saaib, R.; Yu, H.; Azori, M.; Rutherford, T.; Schwartz, P. E.; Mor, G. *Clin. Cancer Res.* **2008**, *14*, 1065–1072.

(32) Greene, M. H.; Feng, Z.; Gail, M. H. *Clin. Cancer Res.* **2008**, *14*, 7574–7574.

(33) Petricoin, E. F.; Ardekani, A. M.; Hitt, B. A.; Levine, P. J.; Fusaro, V. A.; Steinberg, S. M.; Mills, G. B.; Simone, C.; Fishman, D. A.; Kohn, E. C.; Liotta, L. A. *Lancet* **2002**, *359*, 572–577.

(34) Diamandis, E. P. *Mol. Cell. Proteomics* **2004**, *3*, 367–378.

(35) Diamandis, E. P. *J. Natl. Cancer Inst.* **2010**, *102*, 1462–1467.

(36) Mussap, M.; Antonucci, R.; Noto, A.; Fanos, V. *Clin. Chim. Acta* **2013**,

426, 127–138.

(37) Poste, G. *Nature* **2011**, *469*, 156–157.

(38) Plebani, M. *Clin. Biochem. Rev.* **2012**, *33*, 85–88.

(39) Dunn, W. B.; Broadhurst, D.; Begley, P.; Zelena, E.; Francis-McIntyre, S.; Anderson, N.; Brown, M.; Knowles, J. D.; Halsall, A.; Haselden, J. N.; Nicholls, A. W.; Wilson, I. D.; Kell, D. B.; Goodacre, R. *Nat Protoc* **2011**, *6*, 1060–1083.

(40) Vinaixa, M.; Samino, S.; Saez, I.; Duran, J.; Guinovart, J. J.; Yanes, O. *Metabolites* **2012**, *2*, 775–795.

(41) Dunn, W. B.; Ellis, D. I. *TrAC - Trends Anal. Chem.* **2005**, *24*, 285–294.

(42) Psychogios, N.; Hau, D. D.; Peng, J.; Guo, A. C.; Mandal, R.; Bouatra, S.; Sinelnikov, I.; Krishnamurthy, R.; Eisner, R.; Gautam, B.; Young, N.; Xia, J.; Knox, C.; Dong, E.; Huang, P.; Hollander, Z.; Pedersen, T. L.; Smith, S. R.; Bamforth, F.; Greiner, R.; McManus, B.; Newman, J. W.; Goodfriend, T.; Wishart, D. S. *PLoS One* **2011**, *6*, 1-23.

(43) Bouatra, S.; Aziat, F.; Mandal, R.; Guo, A. C.; Wilson, M. R.; Knox, C.; Bjorndahl, T. C.; Krishnamurthy, R.; Saleem, F.; Liu, P.; Dame, Z. T.; Poelzer, J.; Huynh, J.; Yallou, F. S.; Psychogios, N.; Dong, E.; Bogumil, R.; Roehring, C.; Wishart, D. S. *PLoS One* **2013**, *8*, 1-28.

(44) Broadhurst, D. I.; Kell, D. B. *Metabolomics* **2006**, *2*, 171–196.

(45) Dettmer, K.; Aronov, P. A.; Hammock, B. *Indian J. Exp. Biol.* **2009**, *47*, 987–992.

(46) Wieling, J. *Chromatographia* **2002**, *55*, S107–S113.

(47) Fillet, M.; Frédérich, M. *Drug Discov. Today Technol.* **2015**, *13*, 19–24.

(48) Smolinska, A.; Blanchet, L.; Buydens, L. M. C.; Wijmenga, S. S. *Anal. Chim. Acta* **2012**, *750*, 82–97.

(49) Holmes, E.; Wijeyesekera, A.; Taylor-Robinson, S. D.; Nicholson, J. K. *Nat. Rev. Gastroenterol. Hepatol.* **2015**, *12*, 458–471.

(50) Ramautar, R.; Somsen, G. W.; de Jong, G. J. *Electrophoresis* **2013**, *34*, 86–98.

(51) Chalcraft, K. R.; Lee, R.; Mills, C.; Britz-McKibbin, P. *Anal. Chem.* **2009**, *81*, 2506–2515.

(52) Want, E. J.; Masson, P.; Michopoulos, F.; Wilson, I. D.; Theodoridis, G.; Plumb, R. S.; Shockcor, J.; Loftus, N.; Holmes, E.; Nicholson, J. K. *Nat. Protoc.* **2012**, *8*, 17–32.

(53) Luo, P.; Yin, P.; Zhang, W.; Zhou, L.; Lu, X.; Lin, X.; Xu, G. *J. Chromatogr. A* **2016**, *1437*, 127–136.

(54) Wehrens, R.; Hageman, J. A.; van Eeuwijk, F.; Kooke, R.; Flood, P. J.; Wijnker, E.; Keurentjes, J. J. B.; Lommen, A.; van Eekelen, H. D. L. M.; Hall, R. D.; Mumm, R.; de Vos, R. C. H. *Metabolomics* **2016**, *12*, 1–12.

(55) Bijlsma, S.; Bobeldijk, I.; Verheij, E. R.; Ramaker, R.; Kochhar, S.; Macdonald, I. A.; Van Ommen, B.; Smilde, A. K. *Anal. Chem.* **2006**, *78*, 567–574.

(56) Smith, C. A.; Want, E. J.; O'Maille, G.; Abagyan, R.; Siuzdak, G. *Anal. Chem.* **2006**, *78*, 779–787.

(57) Kuehnbaum, N. L.; Kormendi, A.; Britz-McKibbin, P. *Anal. Chem.* **2013**, *85*, 10664–10669.

(58) Katajamaa, M.; Miettinen, J.; Orešič, M. *Bioinformatics* **2006**, *22*, 634–636.

(59) Lommen, A. *Anal. Chem.* **2009**, *81*, 3079–3086.

(60) Katajamaa, M.; Orešič, M. *J. Chromatogr. A* **2007**, *1158*, 318–328.

(61) Cech, N. B.; Enke, C. G. *Mass Spectrom. Rev.* **2002**, *20*, 362–387.

(62) Dunn, W. B.; Erban, A.; Weber, R. J. M.; Creek, D. J.; Brown, M.; Breitling, R.; Hankemeier, T.; Goodacre, R.; Neumann, S.; Kopka, J.; Viant, M. R. *Metabolomics* **2013**, *9*, 44–66.

(63) Courant, F.; Antignac, J. P.; Dervilly-Pinel, G.; Le Bizec, B. *Proteomics* **2014**, *14*, 2369–2388.

(64) Sana, T. R.; Roark, J. C.; Li, X.; Waddell, K.; Fischer, S. M. *J. Biomol. Tech.* **2008**, *19*, 258–266.

(65) Xia, J.; Broadhurst, D. I.; Wilson, M.; Wishart, D. S. *Metabolomics* **2013**, *9*, 280–299.

(66) Arrieta, M.-C.; Stiemsma, L. T. L. T.; Dimitriu, P. A. P. A.; Thorson, L.; Russell, S.; Yurist-Doutsch, S.; Kuzeljevic, B.; Gold, M. J. M. J.; Britton, H. M. H. M.; Lefebvre, D. L. D. L.; Subbarao, P.; Mandhane, P.; Becker, A.; McNagny, K. M. K. M.; Sears, M. R. M. R.; Kollmann, T.; Mohn, W. W. W.; Turvey, S. E. S. E.; Finlay, B. B.; Brett Finlay, B. *Sci. Transl. Med.*

2015, *7*, 1-14.

(67) Miller, M. J.; Kennedy, A. D.; Eckhart, A. D.; Burrage, L. C.; Wulff, J. E.; Miller, L. A. D.; Milburn, M. V.; Ryals, J. A.; Beaudet, A. L.; Sun, Q.; Sutton, V. R.; Elsea, S. H. *J. Inherit. Metab. Dis.* **2015**, *38*, 1029–1039.

(68) Southam, A. D.; Weber, R. J. M.; Engel, J.; Jones, M. R.; Viant, M. R. *Nat. Protoc.* **2017**, *12*, 255–273.

(69) Wang, S. Y.; Kuo, C. H.; Tseng, Y. J. *Anal. Chem.* **2013**, *85*, 1037–1046.

(70) Kirwan, J. A.; Broadhurst, D. I.; Davidson, R. L.; Viant, M. R. *Anal. Bioanal. Chem.* **2013**, *405*, 5147–5157.

(71) Johnson, W. E.; Li, C.; Rabinovic, A. *Biostatistics* **2007**, *8*, 118–127.

(72) Zhao, Y.; Hao, Z.; Zhao, C.; Zhao, J.; Zhang, J.; Li, Y.; Li, L.; Huang, X.; Lin, X.; Zeng, Z.; Lu, X.; Xu, G. *Anal. Chem.* **2016**, *88*, 2234–2242.

(73) Dasgupta, A. *Beating Drug Tests and and Defending Positive Results: A Toxicologist 's Perspective*; Dasgupta, A., Ed.; Humama Press, **2010**.

(74) Dieterle, F.; Ross, A.; Schlotterbeck, G.; Senn, H. *Anal. Chem.* **2006**, *78*, 4281–4290.

(75) Robledo, V. R.; Smyth, W. F. *Electrophoresis* **2014**, *35*, 2292–2308.

(76) Food and Drug Administration (FDA). *Guidance for industry. Bioanalytical Method validation.*; **2001**.

(77) Kamleh, M. A.; Ebbels, T. M. D.; Spagou, K.; Masson, P.; Want, E. J. *Anal. Chem.* **2012**, *84*, 2670–2677.

(78) Cajka, T.; Fiehn, O. *Anal. Chem.* **2016**, *88*, 524–545.

(79) Ghasemi, A.; Zahediasl, S. *Int. J. Endocrinol. Metab.* **2012**, *10*, 486–489.

(80) Giavarina, D. *Biochem. Medica* **2015**, *25*, 141–151.

(81) Saccenti, E.; Hoefsloot, H. C. J.; Smilde, A. K.; Westerhuis, J. A.; Hendriks, M. M. W. B. *Metabolomics* **2014**, *10*, 361–374.

(82) Noble, W. S. *Nat. Biotechnol.* **2009**, *27*, 1135–1137.

(83) Glickman, M. E.; Rao, S. R.; Schultz, M. R. *J. Clin. Epidemiol.* **2014**, *67*, 850–857.

(84) Jolliffe, I. T.; Cadima, J.; Cadima, J. *Philos. Trans. A* **2016**, *374*, 1–16.

(85) van den Berg, R. a; Hoefsloot, H. C. J.; Westerhuis, J. a; Smilde, A. K.; van der Werf, M. J. *BMC Genomics* **2006**, *7*, 142.

(86) Muhlebach, M. S.; Sha, W. *Mol. Cell. Pediatr.* **2015**, *2*, 1–7.

(87) Baumgartner, C.; Baumgartner, D. *J. Biomol. Screen.* **2006**, *11*, 90–99.

(88) Li, L.; Tang, H.; Wu, Z.; Gong, J.; Gruidl, M.; Zou, J.; Tockman, M.; Clark, R. A. *Artif. Intell. Med.* **2004**, *32*, 71–83.

(89) Obuchowski, N. A.; Lieber, M. L.; Wians, F. H. *Clin. Chem.* **2004**, *50*, 1118–1125.

(90) Florkowski, C. M. *Clin. Biochem. Rev.* **2008**, *29*, S83-7.

(91) Zhou, X.-H.; Obuchowski, N. A.; McClish, D. K. In *Statistical Methods in Diagnostic Medicine*; John Wiley & Sons: Hoboken, NJ, 2011.

(92) Park, S. H.; Goo, J. M.; Jo, C.-H. *Korean J. Radiol.* **2004**, *5*, 11–18.

(93) Wishart, D. S.; Jewison, T.; Guo, A. C.; Wilson, M.; Knox, C.; Liu, Y.; Djoumbou, Y.; Mandal, R.; Aziat, F.; Dong, E.; Bouatra, S.; Sinelnikov, I.; Arndt, D.; Xia, J.; Liu, P.; Yallou, F.; Bjorndahl, T.; Perez-Pineiro, R.; Eisner, R.; Allen, F.; Neveu, V.; Greiner, R.; Scalbert, A. *Nucleic Acids Res.* **2013**, *41*, 801–807.

(94) Tikunov, Y. M.; Laptenok, S.; Hall, R. D.; Bovy, A.; de Vos, R. C. H. *Metabolomics* **2012**, *8*, 714–718.

(95) Mahieu, N. G.; Patti, G. J. *Anal. Chem.* **2017**, *89*, 10397-10406.

(96) Sumner, L. W.; Amberg, A.; Barrett, D.; Beale, M. H.; Beger, R.; Daykin, C. A.; Fan, T. W.-M.; Fiehn, O.; Goodacre, R.; Griffin, J. L.; Hankemeier, T.; Hardy, N.; Harnly, J. *Metabolomics* **2007**, *3*, 211–221.

(97) Kind, T.; Tsugawa, H.; Cajka, T.; Ma, Y.; Lai, Z.; Mehta, S. S.; Wohlgemuth, G.; Barupal, D. K.; Showalter, M. R.; Arita, M.; Fiehn, O. *Mass Spectrom. Rev.* **2017**, *9999*, 1–20.

(98) Bristow, A. W. T.; Webb, K. S.; Lubben, A. T.; Halket, J. *Rapid Commun. Mass Spectrom.* **2004**, *18*, 1447–1454.

(99) Creek, D. J.; Dunn, W. B.; Fiehn, O.; Griffin, J. L.; Hall, R. D.; Lei, Z.; Mistrik, R.; Neumann, S.; Schymanski, E. L.; Sumner, L. W.; Trengove, R.; Wolfender, J. L. *Metabolomics* **2014**, *10*, 350–353.

(100) Salek, R. M.; Steinbeck, C.; Viant, M. R.; Goodacre, R.; Dunn, W. B. *Gigascience* **2013**, *2*, 13.

(101) Kind, T.; Fiehn, O. *BMC Bioinformatics* **2007**, *8*, 105.

(102) De Jesús, V.; Mei, J.; Cordovado, S.; Cuthbert, C. *Int. J. Neonatal Screen.* **2015**, *1*, 13–26.

(103) US Centres for Disease Control and Prevention. *MMWR* **2011**, *60*, 619–623.

(104) Pitt, J. J. *Clin. Biochem. Rev.* **2010**, *31*, 57–68.

(105) Guthrie, R.; Susi, A. *Pediatrics* **1963**, *32*, 338–343.

(106) Williams, R. A; Mamotte, C. D. S.; Burnett, J. R. *Clin. Biochem. Rev.* **2008**, *29*, 31–41.

(107) van Calcar, S. C.; Ney, D. M. *J. Acad. Nutr. Diet.* **2012**, *112*, 1201–1210.

(108) Marsden, D.; Larson, C.; Levy, H. L. *J. Pediatr.* **2006**, *148*, 577–584.e5.

(109) Dussault, J. H.; Coulombe, P.; Laberge, C.; Letarte, J.; Guyda, H.; Khoury, K. *J. Pediatr.* **1975**, *86*, 670–674.

(110) Pang S, Hotchkiss J, Drash AL, Levine LS, N. M. *J Clin Endocrinol Metab* **1977**, *5*, 1003–1008.

(111) Therrell, B. L.; Adams, J. *J. Inherit. Metab. Dis.* **2007**, *30*, 447–465.

(112) Wilson, J. M.; Jungner, Y. G. *Principles and practice of screening for disease*; World Health Organization: Geneva, **1968**.

(113) Rousseau, F.; Giguère, Y.; Berthier, M. T. In *Tandem Mass Spectrometry-Applications and Principles*; Prasain, J., Ed.; InTech, **2012**; pp 751–776.

(114) Lanpher, B.; Brunetti-Pierri, N.; Lee, B. *Nat. Rev. Genet.* **2006**, *7*, 449–460.

(115) Schulze, A.; Lindner, M.; Kohlmüller, D.; Olgemöller, K.; Hoffmann, G. F.; Olgemo, K. *Pediatrics* **2003**, *111*, 1399–1406.

(116) Cipriano, L. E.; Rupar, C. A.; Zaric, G. S. *Value Heal.* **2007**, *10*, 83–97.

(117) Garg, U.; Dasouki, M. *Clin. Biochem.* **2006**, *39*, 315–332.

(118) Pollitt, R. J.; Green, A.; McCabe, C. J. *Health Technol. Assess. (Rockv).* **1998**, *2*.

(119) Watson, M. S.; Mann, M. Y.; Lloyd-Puryear, M. A.; Rinaldo, P.; Howell, R. R. *Genet. Med.* **2006**, *8*, 1S–11S.

(120) Watson, M. S.; Lloyd-Puryear, M. A.; Mann, M. Y.; Rinaldo, P.; Howell,

R. R. *Genet. Med.* **2006**, *8*, 12S–252S.

(121) Accurso, F. J.; Sontag, M. K.; Wagener, J. S. *J. Pediatr.* **2005**, *147*, 37–41.

(122) Program, N. M. S. *Screened Conditions Quick Reference*; **2013**.

(123) NSO. *Newborn Screening Ontario Annual Public Report*. **2012**

(124) Wilcken, B.; Wiley, V. *Pathology* **2008**, *40*, 104–115.

(125) Farrell, P. M. P.; Rosenstein, B. J. B.; White, T. T. B.; Accurso, F. J.; Castellani, C.; Cutting, G. R.; Durie, P. R.; Legrys, V. a; Massie, J.; Parad, R. B.; Rock, M. J.; Campbell, P. W.; Fibrosis, C.; Health, C.; Hospital, M.; Children, S.; Hill, C.; Foundation, C. F. *J. Pediatr.* **2008**, *153*, S4–S14.

(126) Ratjen, F. a. *Respir. Care* **2009**, *54*, 595–605.

(127) Mishra, A.; Greaves, R.; Massie, J. *Clin. Biochem. Rev.* **2005**, *26*, 135–153.

(128) Lindau-Shepard, B. A.; Pass, K. A. *Clin. Che* **2010**, *56* (3), 445–450.

(129) Castellani, C.; Massie, J.; Sontag, M.; Southern, K. W. *Lancet Respir. Med.* **2016**, *4*, 653–661.

(130) Massie, J.; Curnow, L.; Tzanakos, N.; Francis, I.; Robertson, C. F. *Arch. Dis. Child.* **2006**, *91*, 222–225.

(131) Goodsaid, F. M.; Frueh, F. W.; Mattes, W. *Toxicology* **2008**, *245*, 219–223.

(132) Poste, G. *Trends Mol. Med.* **2012**, *18*, 717–722.

(133) Koulman, A.; Lane, G. A.; Harrison, S. J.; Volmer, D. A. *Anal. Bioanal. Chem.* **2009**, *394*, 663–670.

(134) Theodorsson, E. *Bioanalysis* **2012**, *4*, 305–320.

(135) Ozben, T. *Clin. Chem. Lab. Med.* **2013**, *51*, 157–176.

(136) Sahai, I.; Marsden, D. *Crit. Rev. Clin. Lab. Sci.* **2009**, *46*, 55–82.

(137) Goodsaid, F. M.; Amur, S.; Aubrecht, J.; Burczynski, M. E.; Carl, K.; Catalano, J.; Charlab, R.; Close, S.; Cornu-Artis, C.; Essioux, L.; Fornace, A. J.; Hinman, L.; Hong, H.; Hunt, I.; Jacobson-Kram, D.; Jawaid, A.; Laurie, D.; Lesko, L. J.; Li, H.-H.; Lindpaintner, K.; Mayne, J.; Morrow, P.; Papaluca-Amati, M.; Robison, T. W.; Roth, J.; Schuppe-Koistinen, I.; Shi, L.; Spleiss, O.; Tong, W.; Truter, S. L.; Vonderscher, J.; Westelinck, A.; Zhang, L.; Zineh, I. *Nat. Rev. Drug Discov.* **2010**, *9*, 435–445.

(138) Drucker, E.; Krapfenbauer, K. *EPMA J.* **2013**, *4*, 7.

(139) Hammett-Stabler, C. A.; Pesce, A. J.; Cannon, D. J. *Clin. Chim. Acta* **2002**, *215*, 125–135.

(140) Rentsch, K. M. *TrAC - Trends Anal. Chem.* **2016**, *84*, 88–93.

(141) Rudd, R. A.; Aleshire, N.; Zibbell, J. E.; Gladden, R. M. *Increases in Drug and Opioid Deaths - United States, 2000-2014*; 2016; Vol. 64.

(142) Ontario, P. H. Interactive Opioid Tool https://www.publichealthontario.ca/en/dataandanalytics/pages/opioid.aspx (accessed Aug 30, 2017).

(143) Milone, M. C. *J. Med. Toxicol.* **2012**, *8*, 408–416.

(144) Freye, E.; Levy, J. V. In *Pharmacology and Abuse of Cocaine, Amphetamines, Ecstasy and Related Designer Drugs: A Comprehensive Review on their Mode of Action, Treatment of Abuse and Intoxication*; Springer: Dordrecht Heidelberg London New York, 2009; pp 1–300.

(145) Marin, S. J.; Hughes, J. M.; Lawlor, B. G.; Clark, C. J.; McMillin, G. A. *J. Anal. Toxicol.* **2012**, *36*, 477–486.

(146) Tsai, I. L.; Weng, T. I.; Tseng, Y. J.; Tan, H. K. L.; Sun, H. J.; Kuo, C. H. *J. Anal. Toxicol.* **2013**, *37*, 642–651.

(147) Guale, F.; Shahreza, S.; Walterscheid, J. P.; Chen, H. H.; Arndt, C.; Kelly, A. T.; Mozayani, A. *J. Anal. Toxicol.* **2013**, *37*, 17–24.

(148) EMA. *Guideline on bioanalytical method validation*; 2012; Vol. 44.

(149) SAMHSA. Analytes and Their Cutoffs https://www.samhsa.gov/sites/default/files/workplace/2010GuidelinesAnalytesCutoffs.pdf (accessed Aug 30, 2017).

(150) Chace, D. H. *J. Mass Spectrom.* **2009**, *44*, 163–170.

(151) Chace, D. H.; Hannon, W. H. *Clin. Chem.* **2010**, *56*, 1653–1655.

(152) Chace, D. H.; Kalas, T. A; Naylor, E. W. *Annu. Rev. Genomics Hum. Genet.* **2002**, *3*, 17–45.

(153) Dietzen, D. J.; Weindel, A. L.; Carayannopoulos, M. O.; Landt, M.; Normansell, E. T.; Reimschisel, T. E.; Smither, C. H. *Rapid Commun. mass Spectrom.* **2008**, *22*, 3481–3488.

(154) Whitley, R. J.; Hannon, W. H.; Dietzen, D. J.; Rinaldo, P. In *Follow-up Testing for Metabolic Diseases Identified by Expanded Newborn Screening Using Tandem Mass Spectrometry*; **2009**; pp 9–29.

(155) DiBattista, A.; McIntosh, N.; Lamoureux, M.; Al-Dirbashi, O.; Chakraborty, P.; Britz-McKibbin, P. *Anal. Chem.* **2017**, *89*, 8112–8121.

(156) Sontag, M. K.; Lee, R.; Wright, D.; Freedenberg, D.; Sagel, S. D. *J. Pediatr.* **2016**, *175*, 150–158.e1.

(157) Gregg, R.; Simantel, A.; Farrell, P.; Koscik, R.; Kosorok, M.; Laxova, A.; Laessig, R.; Hoffman, G.; Hassemer, D.; Mischler, E.; Splaingard, M. *Pediatrics* **1997**, *99*, 819–824.

(158) Wilcken, B.; Wiley, V. *Paediatr. Respir. Rev.* **2003**, *4*, 272–277.

(159) Wetmore, D. R.; Joseloff, E.; Pilewski, J.; Lee, D. P.; Lawton, K. a; Mitchell, M. W.; Milburn, M. V; Ryals, J. A; Guo, L. *J. Biol. Chem.* **2010**, *285*, 30516–30522.

(160) Laguna, T. A.; Reilly, C. S.; Williams, C. B.; Welchlin, C.; Wendt, C. H. *Pediatr. Pulmonol.* **2015**, *50*, 869–877.

(161) Joseloff, E.; Sha, W.; Bell, S. C.; Wetmore, D. R.; Lawton, K. a; Milburn, M. V; Ryals, J. a; Guo, L.; Muhlebach, M. S. *Pediatr. Pulmonol.* **2014**, *49*, 463–472.

(162) Quinn, R. A.; Lim, Y. W.; Mak, T. D.; Whiteson, K.; Furlan, M.; Conrad, D.; Rohwer, F.; Dorrestein, P. *PeerJ* **2016**, *4*, 1–21.

(163) Canada, H. Canadian Alcohol and Drug Use Monitoring Survey https://www.canada.ca/en/health-canada/services/health-concerns/drug-prevention-treatment/drug-alcohol-use-statistics/canadian-alcohol-drug-use-monitoring-survey-summary-results-2012.html (accessed Aug 30, 2017).

Chapter II

Temporal Signal Pattern Recognition in Mass Spectrometry: A Method for Rapid Identification and Accurate Quantification of Biomarkers for Inborn Errors of Metabolism with Quality Assurance

Authors of this work are Alicia DiBattista, Nathan McIntosh, Monica Lamoureux, Osama Y. Al-Dirbashi, Pranesh Chakraborty, and Philip Britz-McKibbin

Anal. Chem. **2017** *89*, 8112-8121

A.D conducted all of the experiments for optimization and validation of the MSI-CE-MS method. A.D performed most of the data analysis and wrote the initial draft for publication. Co-authors obtained ethics approval for the study, selected the sample cohort, shipped all specimens, provided all data regarding the results of newborn screening performed at the regional screening centre and provided valuable feedback on the manuscript drafts.

Chapter II: Temporal Signal Pattern Recognition in Mass Spectrometry: A Method for Rapid Identification and Accurate Quantification of Biomarkers for Inborn Errors of Metabolism with Quality Assurance

2.1 Abstract

Mass spectrometry (MS)-based metabolomic initiatives that use conventional separation techniques are limited by low sample throughput and complicated data processing that contribute to false discoveries. Herein, we introduce a new strategy for unambiguous identification and accurate quantification of biomarkers for inborn errors of metabolism (IEM) from dried blood spots (DBS) with quality assurance. A multiplexed separation platform based on multisegment injection-capillary electrophoresis-mass spectrometry (MSI-CE-MS) was developed to provide comparable sample throughput to flow injection analysis-tandem MS (FIA-MS/MS), but with greater selectivity as required for confirmatory testing and discovery-based metabolite profiling of volume-restricted biospecimens. Mass spectral information is encoded temporally within a separation by serial injection of three or more sample pairs, each having a unique dilution pattern, alongside a quality control (QC) that serves as a reference in every run to facilitate between-sample comparisons and/or batch correction due to system drift. Optimization of whole blood extraction conditions on DBS filter paper cut outs was first achieved to maximize recovery of a wide range of polar metabolites from DBS extracts. An inter-laboratory comparison study was also conducted using proficiency test and retrospective neonatal DBS that demonstrated good agreement between MSI-CE-MS and validated FIA-MS/MS

methods within an accredited facility. Our work demonstrated accurate identification of various IEM based on reliable measurement of a panel of primary or secondary biomarkers above an upper cutoff concentration limit for presumptive screen-positive cases without stable-isotope labeled reagents. Additionally, nontargeted metabolite profiling by MSI-CE-MS with temporal signal pattern recognition revealed new biomarkers for early detection of galactosemia, such as *N*-galactated amino acids that are a novel class of pathognomonic marker due to galactose stress in affected neonates.

2.2 Introduction

Metabolomics offers a revolutionary approach for phenotyping individuals at a molecular level that is needed for new advances in precision medicine.[1,2] However, the chemical diversity of metabolites, in terms of the range of chemical structures, physicochemical properties and stereochemistry, presents immense challenges for their quantitative and qualitative analyses in complex biological mixtures.[3] As a result, complementary separation techniques based on chromatography, electrophoresis and ion mobility play critical roles in expanding the performance of MS for resolution and identification of thousands of metabolites and their isomers, a large fraction of which remain unknown.[4] Due to the lack of standardized methods used in MS-based metabolomics research, conventional separations are typically slow and vary substantially in duty cycle (ranging from 10 to over 70 min) depending on metabolome coverage required, as well as sample matrix, column type, and separation mode.[5-7] For instance,

optimized gradient elution programs in reversed-phase UPLC-MS enable fast profiling of a broad range of targeted metabolites within 5 min,[8] but suffer from less comprehensive coverage, greater ion suppression effects and solute co-elution that hinder identification of unknown metabolites of clinical significance. Moreover, complicated time alignment and peak picking algorithms are required for data pre-processing when performing nontargeted metabolite profiling that reduces overall throughput and reproducibility when pooling data across multiple batches of runs and/or instrumental platforms.[9] Metabolomic initiatives thus face similar challenges as protein cancer biomarker discoveries that have largely failed to reach the clinic.[10] Sources of bias have been attributed either to false discoveries due to inadequate method validation and/or technical artifacts, or to true discoveries that ultimately lack demonstrable socioeconomic value in terms of improved clinical outcomes for patients at reduced costs.[11] However, bias can be minimized with a carefully planned study design with adequate statistical power, including knowledge of a biomarker's variability in the population and intrinsic chemical stability.[12] Also, standardization of the pre-analytics of sample collection, storage and pretreatment,[13] as well as implementation of stringent quality assurance protocols in large-scale clinical or epidemiological studies[14] are essential to validate clinically relevant biomarkers from merely differentiating metabolites.[15]

Universal newborn screening (NBS) programs for pre-symptomatic identification of inborn errors of metabolism (IEM) represent one of the most

successful preventative and cost-saving initiatives in public health care over the past fifty years.[16] Several criteria have evolved for selecting genetic diseases suitable for NBS, including access to high throughput methods for screening on a population level, and effective treatment strategies that benefit from prompt intervention to prevent critical illness, death, and/or lifelong disabilities as compared to symptomatic diagnosis.[17] NBS has historically relied on metabolites as clinically relevant biomarkers for IEM since the introduction of Guthrie cards for routine collection of small volumes of capillary blood on filter paper, and an inexpensive bacterial inhibition assay to measure hyperphenylalaninemia for early detection of phenylketonuria (PKU).[18, 19] With the advent of commercial flow injection analysis-tandem MS (FIA-MS/MS), most developed countries have expanded NBS programs for multi-analyte screening of more than twenty IEM, at minimal incremental costs, based on targeted analysis of amino acids, acylcarnitines and other classes of metabolites from a neonatal dried blood spot (DBS).[20] However, second-tier tests with greater specificity are often required for confirmatory testing of screen-positive cases with a presumptive diagnosis, such as *allo*-isoleucine that is a stereospecific and pathognomonic marker of maple syrup urine disease (MSUD).[21] Nevertheless, NBS programs continue to rely on "single analyte" biochemical assays for several classes of IEM (*e.g.*, cystic fibrosis, congenital hypothyroidism, biotinidase deficiency) due to the lack of viable biomarkers that can be routinely analyzed by FIA-MS/MS.[22] Indeed, some metabolites present diagnostic dilemmas in NBS since they are biomarkers for

more than one disorder and/or have poor positive predictive value (PPV) by identifying non-affected infants, as well as mild/benign disease variants in the population who do not require treatment. In this context, metabolomics offers the advantage of profiling a wider range of metabolites that are closely associated with phenotype, while providing new mechanistic insights into disease progression and treatment responses to therapy on an individual level.[23]

Herein, we introduce a multiplexed separation platform for high throughput metabolite profiling that allows for rapid identification and accurate quantification of biomarkers based on temporal signal pattern recognition when using multisegment injection-capillary electrophoresis-mass spectrometry (MSI-CE-MS).[24, 25] We apply this strategy for second-tier or confirmatory testing of IEM from neonatal DBS extracts and proficiency test specimens based on quantification of a panel of known biomarkers that exceed upper cutoff limits, while rigorously validating our method relative to stable-isotope dilution FIA-MS/MS. Importantly, we report for the first time a new class of biomarker for early detection of galactosemia, which currently relies on a stand-alone fluorescence-based enzyme activity assay yet is sub-optimal for screening due to protein instability and interferences from exogenous reagents in blood.[26]

2.3 Experimental Section

2.3.1 Blood Spot Collection and Sample Preparation

Proficiency test (PT) samples of DBS cut-outs used for method validation were provided by the Newborn Screening Quality Assurance Program at the

Centers for Disease Control (CDC).[22] Duplicate punches (technical replicates) of PT samples that mimic metabolite profiles of phenylketonuria (PKU), maple syrup urine disease (MSUD), citrullinemia type 1 (CIT I), medium chain acyl-coA dehydrogenase deficiency (MCADD) and glutaric acidemia type 1 (GA I) were created at the CDC by spiking in known amounts of primary biomarkers of IEM to pooled blood from consenting adult donors.[22] Also, authentic neonatal DBS filter paper cut-outs collected by Newborn Screening Ontario (NSO) at the Children's Hospital of Eastern Ontario (CHEO) were collected and stored at -80°C as retrospective specimens over a two year period from 2013-2015. This study involving secondary use of de-identified DBS specimens was approved by the CHEO Research Ethics Board and the Hamilton Integrated Research Ethnic Board (REB#: 14-669-T). Four replicate punches of sex-balanced and normal birth weight screen-negative neonate controls (n=30) and duplicate punches of cases with a confirmed IEM diagnosis (n=10) were transferred to McMaster University and stored frozen at -80°C. The ten presumptive/confirmed IEM cases included medium-chain CoA dehydrogenase deficiency (MCADD), phenylketonuria (PKU), tyrosinemia type I (TYR I, two cases), glutaric acidemia type I and type II (GA I and II), severe combined immune deficiency (SCID) caused by adenosine deaminase deficiency (ADA), hypermethionemia caused by methionine adenosyltransferase deficiency (MAT), propionic academia (PA) subsequently confirmed as methylmalonic aciduria (MMA), and citrullinemia (CIT) later diagnosed as galactosemia (type I) due to galactose 1-phosphate

uridylyltransferase (GALT) deficiency. An internal quality control (QC) and reference sample was prepared in-house by pooling together DBS extracts from screen-negative infants (*n*=30) from NSO. Separate QC aliquots were stored at -80°C and thawed once prior to each analysis. In all cases, DBS were comprised of hole-punched 3.2 mm diameter disks of filter paper equivalent to about 3.4 µL of whole blood.[27] High cut-off concentration limits for amino acids, acylcarnitines and purines were based on 99th percentile of a multi-centre cumulative healthy neonatal population,[28] and internal cut-off limits applied at NSO. All DBS materials were collected and handled according to WHO standards for testing using DBS specimens.[29] Disks were placed in 0.5 mL centrifuge tubes containing 100 µL of methanolic extraction solvent with 10 µM of 4-fluoro-*L*-phenylalanine (F-Phe) as recovery standard. Analytes were extracted from the disk via sonication for 15 min and the DBS extract was filtered through a Nanosep 3K Omega (3kDa MWCO) ultracentrifugation tube (Pall Life Sciences, MI, USA) at 14,000 *g* for 15 min to remove protein. The resulting filtrate was dried down in a Vacufuge vacuum concentrator at room temperature (Eppendorf Inc., New York, USA). DBS extracts were then dissolved in 30 µL of reconstitution solvent comprising 200 mM ammonium acetate, 15% *v* acetonitrile, 10 µM 4-chloro-*L*-tyrosine (Cl-Tyr), and 10 µM naphthalene monosulfonic acid (NMS), pH 5.0 unless otherwise noted.

2.3.2 MSI-CE-MS with Temporal Signal Pattern Recognition

A seven-segment serial injection format was used in MSI-CE-MS to maximize sample throughput while ensuring quality assurance for confirmatory testing of DBS extracts from screen-positive IEM cases, as well as identifying new biomarkers for genetic diseases not currently screened by MS/MS. In this case, duplicate injections of three presumptive IEM cases were analyzed along with a QC sample, which represents a pooled healthy neonate control. Validation studies were performed independently on two different mass analyzers with high mass resolution/accuracy and fast data acquisition (TOF and QTOF) to demonstrate cross-platform applicability that differ in analytical performance and infrastructure costs. All analyses by MSI-CE-MS involving PT specimens from the CDC were performed on an Agilent G7100A CE system (Agilent Technologies Inc., Mississauga, ON, Canada) with a coaxial sheath liquid dual Agilent Jet Stream (AJS) electrospray ion source interface to an Agilent 6230 TOF-MS. Confirmatory testing of retrospective neonatal DBS specimens and MS/MS experiments (*i.e.*, product ion scan) for biomarker identification were performed on an Agilent 6550 QTOF-MS that is equipped with an iFunnel for improved ion transmission and better sensitivity. Acquisition was performed using Agilent MassHunter Workstation LC/MS Data Acquisition Software version B.05.01 and all data processing was performed using MassHunter Qualitative Analysis Software version B.06.00. CE separations were performed using uncoated fused-silica capillaries (Polymicro Technologies, AZ, USA) with

50 µM ID and 110 cm total length capillary. All separations were performed with an applied voltage of 30 kV at 25°C. The background electrolyte (BGE) was 1 M formic acid, 15% *v* acetonitrile, pH 1.8. The injection sequence used in MSI-CE-MS on the TOF was a series of hydrodynamic injections at 100 mbar, alternating between a 5 s injection of sample and a 40 s injection of BGE for a total of seven discrete sample injections within a single run.[24] For QTOF analyses, the pressure used for hydrodynamic injection was 50 mbar. The same injection configuration was used when using 50 mM ammonium bicarbonate, pH 8.5 as the BGE for resolving acidic metabolites with negative ion mode[25] on the QTOF. Alternatively, on-line sample preconcentration in CE-MS was also performed via transient isotachophoresis[30] by injecting 90 s of sample followed by 60 s of BGE when improved concentration sensitivity was needed for confirmatory testing. Between runs, the capillary was flushed with BGE at 950 mbar for 15 min. The sheath liquid was 60:40 MeOH:H_2O with 0.1% formic acid supplied at a flow rate of 10 µL/min by an Agilent 1260 Infinity isocratic pump for positive ion mode detection, whereas 50:50 MeOH:H_2O was used for negative ion mode conditions.

2.4 Results

2.4.1 DBS Extraction Optimization and Temporal Signal Pattern Recognition in MS

MSI-CE-MS is a multiplexed separation technique whereby multiple injections of discrete sample plugs are introduced into the same capillary in series, separated by segments of BGE.[24] In this way, mass spectral information is encoded temporally within the separation as ions from the different samples

migrate with a steady-state electrophoretic mobility in solution, and thus remain offset in time prior to ionization (*i.e.*, 3-5 min). This method is also tunable, in that different serial injection configurations and/or dilution patterning can be used to reflect the experimental design. For example, seven discrete sample plugs were analyzed in MSI-CE-MS within a single run in order to first assess the impact of organic solvent composition (50%, 75%, 100% methanol) and temperature (4°C or 25°C) on metabolite recovery during DBS extraction in a single run. A blank is also included within the serial injection format in order to confirm the lack of sample carry-over effects (**Figure S2.1A**). Overall, maximal recovery of DBS extracts for a series of known biomarkers for IEM was optimal when using 75:25 (methanol:water) at room temperature (**Figures S2.1B** and **S2.1C**). The presence of water was important for efficient cell lysis and whole blood extraction of polar/ionic metabolites from a DBS absorbed onto filter paper **(Table S2.1**). External calibration and validation studies also confirmed good linearity (R^2 > 0.999) with low nanomolar (*O*-octanoyl-*L*-carnitine, C8) to low micromolar (glycine, Gly) detection limits ($S/N \approx 3$) reflecting differences in their physicochemical properties that impact solute ionization efficiency.[31] Moreover, inter-day precision and recovery studies at three concentration levels in DBS extracts demonstrated good reproducibility (average *RSD*=11%, *n*=14) and excellent accuracy (average recovery of 97%, *n*=9) when using MSI-CE-MS together with a single non-isotope internal standard for data normalization (**Table S2.2**).

2.4.2 External Method Validation of Known Biomarkers of IEM in Proficiency Test Samples

Figure 2.1A shows the serial injection configuration in MSI-CE-MS developed for rapid confirmatory testing of IEM using PT samples from the CDC, which are used for external validation of accredited clinical laboratories.[22] In this case, three pairs of DBS extracts are injected serially in duplicate by MSI-CE-MS, including a singly injected reference sample derived from screen-negative infants that were pooled together as a healthy control. This sample also serves as a QC for monitoring system drift in every run that also allows for batch correction as required in large-scale metabolomic studies.[5,6] As a result, the specific dilution pattern for each pair of DBS extracts (*i.e.*, 1:2, 1:1 or 2:1) provides a simple visual cue for identifying the sample, while duplicate injections provide greater confidence for confirmatory testing of IEM based on measuring one or more biomarkers above an accepted critical threshold limit. **Figure 2.1B** shows an extracted ion electropherogram (EIE) for *L*-citrulline (Cit, *m/z* 176.103 as MH^+), which demonstrates no evidence of hypercitrullinemia among the three presumptive IEM cases analyzed as related to early onset urea cycle disorders, such as CIT I and argininosuccinic aciduria.[16] As a result, there were no significant differences ($p > 0.05$) in ion responses measured for Cit among the three pairs of DBS extracts analyzed within the run relative to the QC after normalization of integrated peak areas relative to an internal standard. Thus, differences in measured ion response ratios reflect normal biological variation in metabolite concentrations between-subjects ($CV < 50\%$) that does not exceed the

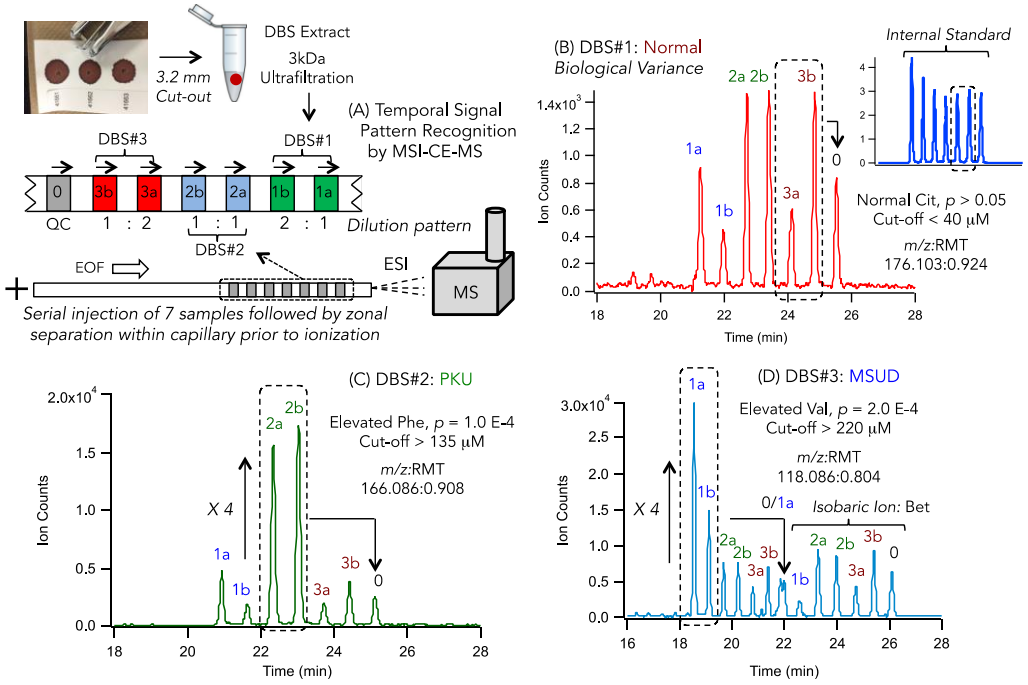

Figure 2.1. (A) Design of a 7-sample plug injection series in MSI-CE-MS with temporal signal pattern recognition for confirmatory testing of IEM using PT specimens from the CDC. Duplicate injection of three pairs of DBS samples together with a single pooled QC enables unambiguous identification of IEM cases with high selectivity, sample throughput and quality assurance. Three representative extracted ion electropherograms are depicted, including (B) a screen-negative case showing a signal pattern without statistically significant elevation in Cit ($p > 0.05$) in all sample pairs relative to QC as healthy reference, (C) a PKU case reflected by a 4-fold elevation in Phe, and (D) a MSUD case characterized by elevation in branched-chain amino acids, such as Val unlike its isobar, glycine betaine (Bet). An internal standard is included in all DBS extracts, which allows for correction for differences in injection volume between-samples during peak integration while correcting for changes in EOF for RMT determination.

high cut-off target range for Cit (< 40 μM).[28] In contrast, **Figure 2.1C** highlights that the middle pair of DBS extracts with an elevated 1:1 signal pattern was consistent with PKU based on a 4-fold elevation (p = 1.0 E-4) in *L*-phenylalanine (Phe, *m/z* 166.086 as MH^+) that exceeds the high cut-off target range for Phe (> 135 μM). **Figure 2.1D** also shows that the first pair of samples for the branched-chain amino acid *L*-valine (Val, *m/z* 118.086 as MH^+) with a distinctive 1:2 signal pattern, confirming the detection of MSUD due to its 4-fold higher concentration

exceeding the high cut-off target range for Val (> 220 μM).[28] In this case, resolution of the slower migrating structural isomer/isobaric interference in DBS extract, glycine betaine (Bet) was critical for method specificity.

Table 2.1 summarizes the performance of MSI-CE-MS when analyzing IEM using PT samples from the CDC based on absolute quantification of single or ratiometric biomarkers associated with CIT 1, PKU, MSUD, MCADD and GA I. In the latter case, GA I is marked by elevated *O*-glutaryl-*L*-carnitine (C5DC, *m/z* 276.144 as MH^+), which was below the method detection limit in all DBS extracts analyzed. As a result, on-line sample preconcentration in CE-MS[30] was performed to boost concentration sensitivity prior to ionization. Qualitative identification of C5DC was confirmed by high resolution MS/MS and accurate prediction of relative migration time (RMT)[30] with a bias under 1.5% (**Figure S2.2**). In order to estimate its concentration, the ion response ratio for C5DC was predicted *in silico* based on a linear regression model that relates solute ionization efficiency to ion molecular volume[31] using a homologous series of acylcarnitines. **Table 2.1** confirms there was good overall precision (average *RSD* = 11%) and acceptable accuracy (average bias = -34%) for measured concentrations of fourteen single or ratiometric biomarkers when comparing MSI-CE-MS with expected concentrations from the CDC. Importantly, all measured biomarker concentrations were also above the high cut-off target range established by the Region 4 Stork collaborative project[28] with exception of Arg since it was not spiked in DBS to mimic CIT I.

Table 2.1. Summary of the performance of MSI-CE-MS to confirm detection of IEM based on elevated concentrations of biomarkers and their ratios from DBS extracts using PT specimens from the CDC.

Presumptive Diagnosis	Single or Ratiometric Biomarker	High Cut-off Target Range (μM)[a]	CDC Expected Conc. (μM)[b]	Average Measured Conc. (μM)[b]	Precision (%RSD)	Bias (%)
CIT	Arg	32-40	11	8.8 ± 0.6	6.8	-20
CIT	Cit	28-40	165	110 ± 7	6.4	-33
GA I	C5DC[c]	--	1.05	0.27 ± 0.06	22	-74
MCADD	C2	7.0-10	12.5	14 ± 1	7.1	-11
MCADD	C6	0.18-0.24	1.03	0.78 ± 0.02	2.6	-57
MCADD	C8	0.21-0.71	1.08	1.3 ± 0.3	23	+20
MCADD	C8/C2	0.011-0.030	0.0864	0.0928	--	+7.4
MCADD	C10	0.26-0.30	1.09	0.60 ± 0.05	8.3	-45
MSUD	Val	180-220	592	397 ± 72	18	-33
MSUD	Val/Phe	3.0-3.5	--	8.9	--	--
MSUD	Xle[d]	235-260	891	520 ± 52	10	-42
MSUD	Xle/Phe	3.5-3.8	--	11.7	--	--
PKU	Phe	97-135	268	157 ± 6	3.8	-41
PKU	Phe/Tyr	1.6-2.5	1.7	2.8	--	-39

[a] *High cut-off target range of recommended for amino acids and acylcarnitines in newborn screening based on 99th percentile of a cumulative infant control population from ref [23].*
[b] *Estimated whole blood extract concentration after correction for dilution based on a 3.2 mm diameter cut-out of DBS with approximate volume of 3.4 µL, which was measured in duplicate using two different extracts (n=4).*
[c] *Estimated concentration for C5DC based on predictive modeling of ion responses of a homologous series of acylcarnitines.*
[d] *Xle represents total Leu and Ile as they are not resolved by FIA-MS/MS*

2.4.3 Confirmatory Testing of Screen-positive Neonates for Unambiguous IEM Identification and Inter-laboratory Method Comparison

Table 2.2 summarizes results comparing measured biomarkers and their ratios in ten retrospective DBS specimens from NSO involving screen-positive IEM cases from affected neonates. In this case, DBS extracts were analyzed by MSI-CE-MS using a similar injection configuration as **Figure 2.1**. Early detection of MCADD by FIA-MS/MS is primarily based on elevated C8 (> 0.4 µmol/L), however secondary analytes such as other medium-chain acylcarnitines (C6, C10) or their ratios (C8:C2, C8:C10) are also used to confirm borderline C8 results in

order to reduce false-negatives.[32] **Figure 2.2A** highlights that confirmatory testing of MCADD is based on detection of elevated levels of all three medium-chain acylcarnitines, most strikingly for C8 (17.2 μM). The distinctive 1:1 signal pattern clearly indicates that it was derived from the second sample pair injected within the serial injection sequence. However, no signals were measured for medium-chain acylcarnitines for the pooled QC sample (*i.e.*, screen-negative), as well as most other disease controls. **Figure 2.2A** shows a comparison of EIE traces for two separate runs where C5DC is used as a screening biomarker for both GA I (type I) and GA II (type II). Elevated C5DC was only detected in GA I (1.04 μM) in a characteristic 1:1 signal pattern in this run, but was not detected in GA II. Indeed, presumptive GA II cases caused by multiple acyl-CoA dehydrogenase deficiency (MADD) can have mildly elevated C5DC levels near cut-off limits (> 0.21 μM)[33] as shown in **Table 2.2**. As a result, differential identification of GA II from GA I was realized based on detection of elevated levels of medium-chain acylcarnitines (C6, C8, and notably C10) as secondary biomarkers (**Figure S3**). Also, **Figure 2A** demonstrates unambiguous identification of SCID due to adenosine deaminase deficiency (ADA) based on accumulation of two purine substrates, namely adenosine (Adn) and 2-deoxyadenosine (dAdn). In fact, Adn concentration levels are over 25-fold higher in ADA relative to other controls. Population-based screening of SCID relies on a high throughput T-cell receptor excision circle (TREC) assay using real-time qPCR for early detection of the absence of functional T cells.[34] However, it cannot distinguish ADA from other

Table 2.2. MSI-CE-MS for confirmatory testing of 10 confirmed IEM cases based on elevated concentrations of primary biomarkers using retrospective screen-positive DBS specimens from neonates.

Presumptive/ Confirmed Diagnosis	Single or Ratiometric Biomarker	High Cut-off Target Range (μM)[a]	NSO Cutoff (μM)[b]	MS/MS Conc. (μM)[b]	MSI-CE-MS Conc. (μM)[b]	Bias (%)
SCID/ADA	dA	--	1.0	33.7	8.76	-118
SCID/ADA	A	--	5.0	51.0	42.5	-18
CIT/GALT	Cit	28-40	70	71	56.2	-23
GA/GA I	C5DC[c]	0.10-0.21	0.37	3.13	1.04	-67
GA/GA II	C5DC[c]	0.10-0.21	0.37	0.37	nd	--
HCY/MUT	Met	44-48	100	121	94.1	-25
HCY/MUT	Met/Phe	0.74-0.99	1.34	2.34	1.94	-18
MCAD	C6	0.18-0.24	0.24	2.23	1.31	-52
MCAD	C8	0.21-0.71	0.40	17.17	17.40	+1.3
MCAD	C8/C2	0.011-0.030	0.01	0.55	0.47	-15
MCAD	C8/C10	2.3-3.0	2.5	10.45	9.88	-5.6
MCAD	C10	0.26-0.30	0.30	1.64	1.76	+7.4
PA/MMA	C3	4.7-5.5	4.0 or 5.5	8.47	8.31	-1.9
PA/MMA	C3/C2	0.18-0.20	0.23	0.37	0.47	+24
PKU	Phe	97-135	160 or 130	463	401	-14
PKU	Phe/Tyr	1.6-2.5	1.72	8.1	8.7	+6.4
TYR/TYR I[d]	Tyr	207-226	600	112	91	-20
TYR/TYR I[d]	Tyr	207-226	600	327	300	-8.7

[a] *High cut-off target range of recommended for amino acids and acylcarnitines in newborn screening based on 99th percentile of cumulative healthy infant control population from Genet. Med.* ***2011*** *13: 230-54.*

[b] *Estimated whole blood extract concentration after correction for dilution based on a 3.2 mm id cut-out of DBS specimen with approximate volume of 3.4 µL, which was measured once by MS/MS and in duplicate by MSI-CE-MS.*

[c] *Estimated concentration based on predictive modeling of ion responses of a homologous series of acylcarnitines, which is screened as C5DC/C10OH or C5DC+C10OH – the latter acylcarnitine was not detected by MSI-CE-MS.*

[d] *Two cases of TYR I, where succinylacetone is used as primary marker for TYR screening due to poor sensitivity of Tyr; however, chemical derivatization is required with hydrazine for its detection by MS/MS with positive ion mode.*

genetic causes of SCID, demonstrating the potential of MSI-CE-MS as a reliable tool for confirmatory testing.

Table 2.2 summarizes measured concentrations for primary/secondary biomarkers and their ratios from ten screen-positive IEM samples, including a

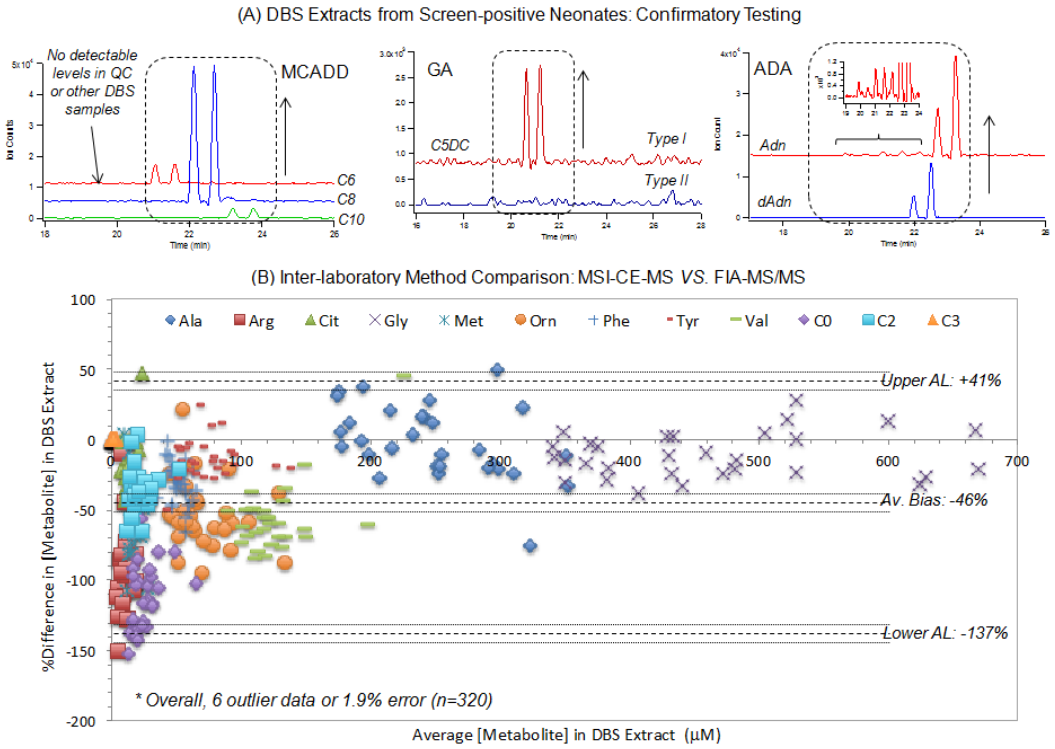

Figure 2.2. (A) Confirmatory testing of screen-positive IEM cases from retrospective neonatal DBS specimens is demonstrated by MSI-CE-MS for low abundance biomarkers that are not detected in normal/healthy infants and other disease controls under full-scan TOF-MS, but are elevated in specific IEM, including MCADD (*e.g.*, medium-chain acylcarnitines, C6, C8 and C10), GA (*e.g.*, *O*-glutaryl-*L*-carnitine, C5DC for GA type I case only), and ADA (*e.g.*, adenosine, A and 2-deoxyadenosine, dA). (B) Inter-method comparison using a Bland-Altman %difference plot (n=320) of DBS extracts from screen-negative infants (n=30) measured by stable-isotope dilution FIA-MS/MS and MSI-CE-MS for twelve primary biomarkers of IEM. The average bias and upper/lower agreement limits are represented as dashed lines while their 95% CI are indicated by dotted lines.

case tentatively identified as CIT, but subsequently confirmed as galactosemia (type I) due to GALT deficiency. Overall, there was good agreement in measured concentrations for biomarkers with an average negative bias of -22%, which were performed independently on different DBS cut-outs from the same filter card when using FIA-MS/MS and MSI-CE-MS. In all cases, measured biomarker concentrations exceed the high cut-off target range for a large multi-centre

population,[27] as well as the NSO cut-off derived from the provincial population with the exception of GA II and one case of TYR I. The latter outcome is due to the poor sensitivity of *L*-tyrosine (Tyr) for screening of TYR I, which is optimally detected by measuring succinylacetone following chemical derivatization with hydrazine to enhance its detectability when using MS/MS in positive ion mode.[35] **Figure 2.2B** summarizes the inter-laboratory comparison between FIA-MS/MS and MSI-CE-MS methods for twelve amino acids and acylcarnitines consistently measured in a cohort of screen-negative neonates (*n*=30), which further demonstrates an acceptable extent of bias (-46%, *n* =320) for retrospective DBS specimens that is analyte and concentration dependent. Indeed, the Bland-Altman %difference plot demonstrates that 314 of 320 biomarkers (1.9% error with 6 outliers) measured from DBS extracts were distributed randomly within agreement limits, where the magnitude of bias for biomarkers ranged from -1.3% for *L*-alanine (Ala) to –117% for *L*-carnitine (C0) (**Table S2.3**).

2.4.4 Nontargeted Metabolite Profiling Reveals New Biomarkers for Early Detection of Galactosemia by MS/MS

The validated MSI-CE-MS method was next applied for the discovery of new classes of biomarkers for IEM, such as galactosemia. In this case, full-scan data acquisition by TOF-MS allowed for non-targeted metabolite profiling of DBS extracts beyond the targeted panel of biomarkers used in NBS programs. A total of 85 unique molecular features were annotated based on their unique mass-to-charge-ratio and relative migration time (*m/z*:RMT) after filtering out spurious, irreproducible and artifact signals generated during spray formation.[24] **Figure**

2.3A demonstrates that this approach re-confirmed the incidental finding of hypercitrullinemia reported by NSO, as well as detecting other metabolites significantly elevated in galactosemia relative to screen-negative and disease controls (*i.e.*, average fold-change or FC), including *L*-arginine (Arg, FC = 3.8), 1-methylnicotinamide (NA, FC = 3.6) and urocanic acid (UA, FC = 5.5) as summarized in **Table S2.4**. Importantly, a series of unknown late migrating cations with a distinctive 1:2 signal pattern were also found to be elevated in galactosemia relative to controls (up to 40-fold), including an unknown isobar of Adn (*m/z* 268.104). These ions were tentatively classified as a group of *N*-galactated amino acid adducts following acquisition of MS/MS spectra, such as the non-proteinogenic amino acid, Cit, as shown in **Figure 2.3B**. Also, **Figure 2.3C** highlights that the neonate with galactosemia had a distinctive metabolic phenotype relative to other IEM (n=9) and healthy controls (n=30) as depicted in a 2D scores plot when using principal component analysis (PCA). This difference was largely attributed to a series of *N*-galactated amino acids, notably Gal-Gly (*m/z* 238.092) and Gal-Glu (*m/z* 310.115) as summarized in **Table S2.4**. All tentatively identified *N*-galactated amino acids were found to undergo a characteristic neutral loss of a hexose (*m/z* 162) and a product ion in their MS/MS spectra corresponding to the free amino acid, such as Val (**Figure S2.4B**). These compounds were also highly correlated to each other as a distinct group (R^2 > 0.800) (**Figure S2.4A**). Similarly, **Figure 2.3D** shows a heat map with hierarchical cluster analysis (HCA) for the nine most discriminating metabolites

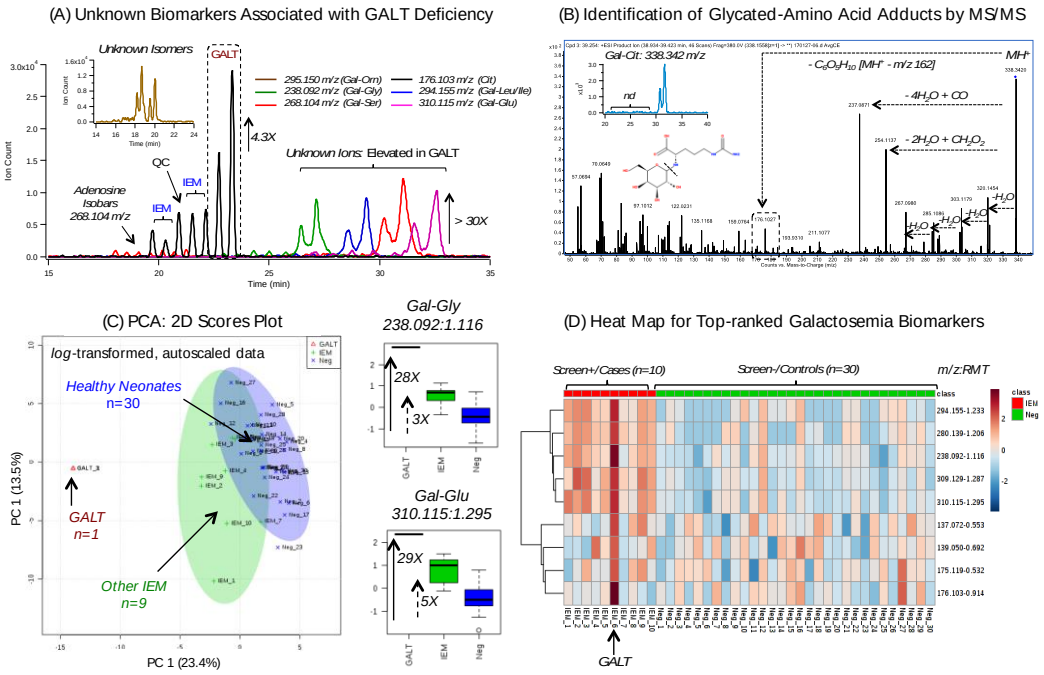

Figure 2.3. (A) Non-targeted metabolite profiling of DBS extracts by MSI-CE-MS using temporal signal pattern recognition reveals a series of unknown metabolites significantly elevated in galactosemia, including independent confirmation of hypercitrullinemia. (B) Unknown metabolites associated with galactosemia migrate with a slow positive electrophoretic mobility with a doublet (1:2) signal pattern (*i.e.*, non-detected or present at low levels in IEM and QC) while having a MS/MS spectra indicative of a *N*-galactated amino acid adduct with neutral loss of a hexose (*m/z* 162) under positive ion mode. (C) 2D scores plot from PCA of 85 polar/ionic metabolites consistently detected in majority of DBS extracts confirmed that the metabolic phenotype of the infant with galactosemia was distinct relative to other IEM (*n*=9) and healthy controls (*n*=30), with (D) nine lead metabolites strikingly elevated in GALT (FC > 3.0), including five different *N*-galactated amino acid adducts, such as Gal-Gly and Gal-Glu.

in galactosemia, including a series of *N*-galactated amino acids that were also detected at much lower levels in most healthy neonates. Confirmation of aberrant galactose metabolism was performed by analysis of the same DBS extract using MSI-CE-MS under alkaline conditions and negative ion mode detection for acidic metabolites.[25] For instance, accumulation of galactose-1-phosphate (Gal-1P, *m/z* 259.022) and galactonic acid (GA, *m/z* 195.051) along with a modest attenuation

in UDP-Gal (*m/z* 565.048) was confirmed by MSI-CE-MS (**Figure S2.5A**). These data are consistent with low residual GALT activity that is associated with classic galactosemia (type I). Moreover, the stereochemistry of the hexose monosaccharide likely conjugated to amino acids was deduced to be *L*-galactose (Gal). This was confirmed by acquisition of MS/MS spectra at a low collisional energy and comparing the relative intensity of a common product ion (*m/z* 241.012) generated by both Gal-1P and Glc-1P corresponding to a neutral water loss (**Figure S2.5B**).

2.5 Discussion

Confirmatory testing of screen-positive cases is critical for timely yet accurate diagnosis of affected infants in NBS programs due to potential isobaric/isomeric interferences in FIA-MS/MS, as well as biochemical screens with poor PPV.[16] False-positives, in the absence of additional clinical information, contribute to increased healthcare costs due to unnecessary follow-up diagnostic testing, as well as undue parental stress.[36] To reduce false positives as well as false negatives, secondary biomarkers are often included in a screening algorithm for certain IEM that share the same primary biomarker, such as C5DC which is used for screening both GA I and GA II. The latter IEM is often confirmed by a measuring a medium-chain acylcarnitine profile characteristic to GA II[33] (**Figure S2.3**). Similarly, specialized LC-MS/MS methods are also required as a second-tier test for biochemical assays in NBS that lack specificity, such as ADA deficiency that is associated with about 15% of all SCID patients (**Figure 2.2**).[37]

In this context, MSI-CE-MS offers a rapid multiplexed platform for second tier or confirmatory testing of presumptive IEM cases given the diverse chemical properties of metabolites that vary widely in their polarity. This is unlike most LC-MS assays that require different column types, retention mechanisms and/or elution conditions when resolving highly ionic amino acids and surface-active long-chain acylcarnitines under a single condition.[21] Indeed, this problem has contributed to variable NBS coverage of IEM between states and provinces across North America due to the additional costs required for both chromatographic method development and decision algorithms for confirmatory tests that can delay reporting results.[38] Thus, MSI-CE-MS greatly facilitates data interpretation and decision-making given the distinctive temporal signal pattern encoded by MS with quality assurance. Additionally, no stable-isotope internal standards or reagents are needed for absolute quantification due to effective in-column desalting and post-column ionization under steady-state conditions when using a isocratic sheath liquid solution as make-up flow in the CE-MS interface.[24] Overall, internal validation of MSI-CE-MS based on spike/recovery studies (**Table S2.2**), external validation based on analysis of PT specimens from the CDC **(Table 2.2)**, as well as inter-laboratory comparisons of both screen-positive and screen-negative neonates using stable-isotope dilution-FIA-MS/MS at an accredited laboratory at NSO, confirm good accuracy with an average negative bias ranging from -22 to -46% (**Figure 2.2, Table S2.3**). This magnitude of bias for MSI-CE-MS is acceptable when using DBS cut outs as biospecimens due to variations in total

spot blood volume and hematocrit on filter cards that only permit semi-quantitative analysis of biomarkers of IEM for population-based screening.[20] Also, the consistent negative bias of MSI-CE-MS relative to FIA-MS/MS was likely attributed to differences in extraction conditions (**Table S2.1**) and the impact of long-term storage when analyzing retrospective DBS specimens (up to 2 years at -80°C) since intrinsic chemical stability varies widely for different amino acids and acylcarnitines prone to hydrolysis.[12]

The discovery of new biomarkers for early detection and prevention of human diseases represents the "holy grail" of clinical metabolomics, a goal not easily realized in other -omics fields.[39, 40] In this work, MSI-CE-MS with temporal signal pattern recognition was developed to accelerate the discovery of novel biomarkers associated with galactosemia when using nontargeted metabolite profiling of DBS extracts in comparison to healthy and disease controls. High efficiency CE separations not only provide effective desalting of major electrolytes in biofluids while resolving isobaric interferences (**Figure 2.1**), but also facilitates identification of unknown metabolites of clinical significance in cases when authentic standards or MS spectral libraries are incomplete, such as prediction of RMT (**Figure S2.2**). In this work, we report for the first time a significant elevation of a series of *N*-galactated amino acids in DBS extracts collected from a neonate diagnosed with galactosemia, which were likely formed *in vivo* by non-enzymatic galactation (*i.e.,* Maillard reaction) of free amino acids with elevated galactose as the reducing sugar. Similar to protein glycation and

advanced glycan end-product formation in type 2 diabetes and other chronic diseases,[41] galactation of protein occurs in classical galactosemia (type I) on reactive Lys residues[42] that contribute to endoplasmic reticulum stress due to accumulation of misfolded protein.[43] However, our data supports that, along with Gal-1-P and GA accumulation in response to galactose stress, *N*-galactation of several free amino acids (*e.g.,* Gly, Leu/Ile, Val, Glu, Gln, Tyr, Phe, Arg), including non-proteinogenic amino acids (*e.g.,* Cit, Orn), is a hallmark of galactosemia in asymptomatic neonates, where DBS specimens are collected within 48 hr after birth (**Figure S2.5**). We propose that *N*-galactated amino acids represent promising biomarkers for early detection of galactosemia, which are amenable to multi-analyte screening by MS/MS under positive ion mode detection. This approach would provide significant cost savings concurrent with improved PPV since enzyme activity assays for galactosemia are prone to false positives due to heat-induced enzyme denaturation during transport of DBS specimens or contamination with EDTA.[44] Also, false negative test results would be avoided for identification of other variants of galactosemia, including Duarte galactosemia that is more prevalent in the population, as well as rarer cases of type II (galactokinase), and type III (UDP galactose 4-epimerase) which are not detected by GALT screening when used as the first tier test.[45] Future work will further validate the screening performance of *N*-galactated amino acids as biomarkers for galactosemia within a larger cohort, as well as extending this approach to other genetic diseases that do not employ MS/MS technology for

screening yet suffer from poor specificity and carrier identification, such as cystic fibrosis.

2.6 Conclusion

Despite the success of expanded NBS programs, selective and rapid confirmatory tests are needed to ensure timely yet accurate diagnosis of fatal or debilitating genetic diseases among affected infants that ultimately guides treatment decisions. For the first time, we have demonstrated that serial sample injections enables the encoding of mass spectral information temporally within a separation in order to accelerate biomarker discovery while reliably quantifying biomarkers from presumptive IEM cases with quality assurance. The inclusion of QC samples, as well as healthy or disease controls within a single run increases sample throughput while allowing for multiple comparisons or batch correction for unambiguous IEM confirmation. Extensive validation studies were performed using PT samples and retrospective DBS specimens from healthy neonates, as well as screen-positive cases associated with impaired amino acid, fatty acid, organic acid or purine metabolism, which demonstrated good precision and acceptable accuracy when comparing MSI-CE-MS with stable-isotope dilution FIA-MS/MS. This strategy was also used to identify a series of *N*-galactated amino acids as novel pathognomonic markers for early detection of galactosemia, which offer the potential to replace single-purpose biochemical assays with multi-analyte screening using existing MS/MS infrastructure at incremental costs. Further work is needed to evaluate the robustness of MSI-CE-MS technology as

applied to large-scale clinical and epidemiological studies together with more sensitive sheathless/low flow CE-MS interface designs, and automated software processing tools optimized for multiplexed electrophoretic separations..

2.7 Acknowledgements

P.B.M. wishes to acknowledge funding support from the Natural Sciences and Engineering Research Council of Canada, Canada Foundation for Innovation, and Cystic Fibrosis Canada. Further thanks are directed to Marcus Kim at Agilent Technologies Inc. and to CDC's Newborn Screening Quality Assurance Program.

2.8 References

(1) Beger, R. D.; Dunn, W.; Schmidt, M. A.; Gross, S. S.; Kirwan, J. A. *et al. Metabolomics* **2016**, *12*, 149.

(2) Wishart, D. S. *Nat. Rev. Drug Disc.* **2016**, *15*, 473–484.

(3) Kuehnbaum, N. L.; Britz-McKibbin, P. *Chem. Rev.* **2013**, *113*, 2437–2468.

(4) Bowen, B. P.; Northen, T. R. *J. Am. Soc. Mass Spectrom.* **2010**, *21*, 1471–1476.

(5) Want, E. J.; Wilson, I. D.; Gika, H.; Theodoridis, G.; Plumb, R. S.; Shockcor, J.; Loftus, N.; Holmes, E.; Nicholson, J. K. *Nat. Protoc.* **2010**, *5*, 1005-1018.

(6) Want, E. J.; Masson, P.; Michopoulos, F.; Wilson, I. D.; Theodoridis, G.; Plumb, R. S.; Shockcor, J.; Holmes E.; Nicholson, J. K. *Nat. Protoc.* **2013**, *8*, 17-32.

(7) Ivanisevic, J.; Zhu, Z.-J.; Plate, L.; Tautenhahn, R.; Chen, S.; O'Brien, P. J.; Johnson, C. H.; Marletta, M. A.; Patti, G. J.; Siuzdak, G. *Anal. Chem.* **2013**, *85*, 6876-6884.

(8) Guo, L.; Milburn, M.V.; Ryals, J. A; Lonergan, S. C.; Mitchell, M. W.; Wulff, J. E.; Alexander, D. C.; Evans, A. M., Bridgewater, B.; Miller, L., Gonzalez-Garay, M. L.; Caskey, C. T. *Proc. Nat Acad. Sci.* **2015**, *112*,

E4901-E4910.

(9) Brunius, C.; Shi, L.; Landberg, R. *Metabolomics* **2016**, *12*, 1–13.

(10) Diamandis, E. P. *BMC Med.* **2012**, *10*, 87.

(11) Ioannidis, J. P. A. *PLoS Med.* **2005**, *2*, e124.

(12) Strnadová, K. A.; Holub, M.; Mühl, A.; Heinze, G.; Ratschmann, R.; Mascher, H.; Stöckler-Ipsiroglu, S.; Waldhauser, F.; Votava, F.; Lebl, J.; Bodamer, O. A. *Clin. Chem.* **2007**, *53*, 717–722.

(13) Yin, P.; Lehmann, R.; Xu, G. *Anal. Bioanal. Chem.* **2015**, *407*, 4879–4892.

(14) Dunn, W. B.; Lin, W.; Broadhurst, D.; Begley, P.; Brown, M. *et al. Metabolomics* **2014**, *11*, 9–26.

(15) Koulman, A.; Lane, G. A; Harrison, S. J.; Volmer, D. A. *Anal. Bioanal. Chem.* **2009**, *394*, 663–670.

(16) Sahai, I.; Marsden, D. *Crit. Rev. Clin. Lab. Sci.* **2009**, *23*, 326–334.

(17) Fernhoff, P. M. *Pediatr. Clin. North Am.* **2009**, *56*, 505–513.

(18) Guthrie, R.; Susi, A. *Pediatrics* **1963**, *32*, 338–343.

(19) Ombrone, D.; Giocaliere, E.; Forni, G.; Malvagia, S.; La Marca, G. *Mass Spectrom Rev.* **2016**, *35*, 71-84.

(20) Chace, D. H. *J. Mass Spectrom.* **2009**, *44*, 163–170.

(21) Chalcraft, K. R.; Britz-McKibbin, P. *Anal. Chem.* **2009**, *81*, 307–314.

(22) De Jesús, V. R.; Mei, J. V.; Cordovado, S. K.; Cuthbert, C. D. *Int. J. Neonatal Screen.* **2015** *1*, 13-26.

(23) Miller, M. J.; Kennedy, A. D.; Eckhart, A. D.; Burrage, L. C.; Wulff, J. E.; Miller, L. A. D.; Milburn, M. V.; Ryals, J. A.; Beaudet, A. L.; Sun, Q.; Sutton, V. R.; Elsea, S. H. *J. Inherit. Metab. Dis.* **2015**, *38*, 1029–1039.

(24) Kuehnbaum, N. L.; Kormendi, A.; Britz-McKibbin, P. *Anal. Chem.* **2013**, *85*, 10664–10669.

(25) Yamamoto, M.; Ly, R.; Gill, B.; Zhu, Y.; Moran-Mirabal, J.; Britz-McKibbin, P. *Anal. Chem.* **2016**, *88*, 10710–10719.

(26) Pitt, J. J. *Clin. Biochem. Rev.* **2010**, 31, 57-68.

(27) Chace, D. H.; Kalas, T. A; Naylor, E. W. *Clin. Chem.* **2003**, *49*, 1797–1817.

(28) McHugh, D. M. S.; Cameron, C. A; Abdenur, J. E.; Abdulrahman, M.; Adair, O.; Al Nuaimi, S. A. et al. *Genet. Med.* **2011**, *13*, 230–254.

(29) World Health Organization. *WHO Manual for HIV Drug Resistance Testing using Dried Blood Spot Specimens*; WHO, 2012.

(30) Lee, R.; Ptolemy, A. S.; Niewczas, L.; Britz-McKibbin, P. *Anal. Chem.* **2007**, *79*, 403–415.

(31) Chalcraft, K. R.; Lee, R.; Mills, C.; Britz-McKibbin, P. *Anal. Chem.* **2009**, *81*, 2506–2515.

(32) Kennedy, S.; Potter, B. K.; Wilson, K.; Fisher, L.; Geraghty, M.; Milburn, J.; Chakraborty, P. *BMC Pediatr.* **2010**, *10*, 82.

(33) Sahai, I.; Garganta, C. L.; Bailey, J.; James, P.; Levy, H. L.; Martin, M.; Neilan, E.; Phornphutkul, C.; Sweetser, D. A.; Zytkovicz, T. H.; Eaton, R. B. *JIMD Rep.* **2013**, *13*, 1–14.

(34) Gerstel-Thompson, J. L.; Wilkey, J. F.; Baptiste, J. C.; Navas, J. S.; Pai, S. Y.; Pass, K. A.; Eaton, R. B.; Comeau, A. M. *Clin. Chem.* **2010**, *56*, 1466–1474.

(35) Al-Dirbashi, O. Y.; Fisher, L.; McRoberts, C.; Siriwardena, K.; Geraghty, M.; Chakraborty, P. *Clin. Biochem.* **2010**, *43*, 691–693.

(36) Schmidt, J. L.; Castellanos-Brown, K.; Childress, S.; Bonhomme, N.; Oktay, J. S.; Terry, S. F.; Kyler, P.; Davidoff, A.; Greene, C. *Genet. Med.* **2012**, *14*, 76–80.

(37) Kelly, B. T.; Tam, J. S.; Verbsky, J. W.; Routes, J. M. *Clin. Epidemiol.* **2013**, *5*, 363–369.

(38) Hall, P. L.; Marquardt, G.; McHugh, D. M. S.; Currier, R. J.; Tang, H.; Stoway, S. D.; Rinaldo, P. *Genet. Med.* **2014**, *16*, 889-895.

(39) Rifai, N.; Gillette, M. A; Carr, S. A. *Nat. Biotechnol.* **2006**, *24*, 971–983.

(40) Crutchfield, C. A.; Thomas, S. N.; Sokoll, L. J.; Chan, D. W. *Clin.*

Proteomics **2016**, *13*, 1.

(41) Zhang, Q.; Ames, J. M.; Smith, R. D.; Baynes, J. W.; Metz, T. O. *J. Proteome Res.* **2008**, *8*, 754–769.

(42) Frost, L.; Chaudhry, M.; Bell, T.; Cohenford, M. *Anal. Biochem.* **2011**, *410*, 248–256.

(43) Staubach, S.; Müller, S.; Pekmez, M.; Hanisch, F.-G. *J. Proteome Res.* **2017**, *16*, 516-527.

(44) Ohlsson, A.; Guthenberg, C.; von Döbeln, U. *JIMD Rep.* **2012**, *2*, 113–117.

(45) Pyhtila, B. M.; Shaw, K. A.; Neumann, S. E.; Fridovich-Keil, J. L. *JIMD Rep.* **2015**, *15*, 79–93.

2.9 Supplemental Experimental

2.9.1 Chemicals and Reagents

Deionized water used for aqueous buffer and stock preparations was obtained from a Thermo Scientific Barnstead EasyPure II ultrapure water system (Cole Parmer, Vernon Hills, IL, USA). Ammonium acetate, formic acid, acetic acid, 3-chloro-*L*-tyrosine (Cl-Tyr), 2-[4-(2-hydroxyethyl)piperazin-1-yl]ethanesulfonic acid (HEPES), 4-fluoro-*L*-phenylalanine (F-Phe), 2-napthalenesulfonic acid (NMS) and other chemical standards were purchased from Sigma-Aldrich (St. Louis, MO, USA). HPLC-grade methanol (Caledon, Georgetown, ON, Canada) and HPLC-grade acetonitrile (Honeywell, Muskegon, MI, USA) were used to prepare sheath liquid and background electrolyte (BGE), respectively. Acylcarnitine standards were kindly provided by Dr. Murray Potter at McMaster University. Polar standards were prepared in water and stored at

+4°C, whereas acylcarnitine standards were prepared in methanol and stored at -20°C.

2.9.2 Newborn Screening of IEM by Stable-isotope Dilution FIA-MS/MS and LC-MS/MS

All analyses of DBS specimens from healthy neonates and IEM cases were performed using standard operating procedures within an accredited laboratory at Newborn Screening Ontario (NSO). Briefly, 3.2 mm diameter punches from newborn DBS specimens were placed into 96 well plates. These samples were extracted and derivatized using the PerkinElmer Neogram kit. This involved a methanol-based extraction, followed by transfer of the extract to a new 96 well plate for butylation under acidic conditions together with stable-isotope internal standards for corresponding amino acids and acylcarnitines. The residual dry DBS was re-extracted using acetonitrile:water (8:2 *v/v*) containing hydrazine hydrate (15 mM) and formic acid (0.1%) to measure succinylacetone as a biomarker of Tyrosinemia type 1. The contents of the two 96-well plates were combined and analyzed using a Waters 2777c autosampler, 1525u binary HPLC pump and TQD Tandem Mass Spectrometer in positive electrospray (ESI+) mode. 10 µL was injected sample with 80% acetonitrile mobile phase in isocratic mode with an initial flow rate of 0.140 mL/min and a run time of 1.50 min. Amino acids were quantified using scanning for neutral losses of 102 Da, whereas parent ion scan for *m/z* 85 and/or multiple reaction monitoring (MRM) were used for butylated acylcarnitines; a source temperature of 120°C, capillary voltage of 3.5

kV, desolvation gas flow of 600 L/h and desolvation temperature of 250°C that were implemented at NSO. MassLynx v4.1 and NeoLynx was used to acquire, analyze and manage the analytical data. For confirmatory testing of screen-positive adenosine deaminase deficiency (ADA) cases, adenosine (Ado) and 2'-deoxyadenosine (dAdo) were analyzed using stable-isotope internal standards 13C10 15N5 Ado and 15N5 dAdo, following a simple methanol:water (2:1) extraction of a 3.2 mm DBS cut-out. The final contents of the 96-well plates, evaporated to dryness with nitrogen gas, were reconstituted with the mobile phase, 70% acetonitrile with 0.1% formic acid and analyzed using a LC-MS/MS in positive electrospray (ESI+) mode. A 10 µL sample was injected with mobile phase in isocratic mode with an initial flow rate of 0.140 mL/min and a run time of 1.60 min. Purines were quantified by MRM and compound specific cone voltage (CV) (Adn =26/dAdn=22) and collision energy (CE) (Adn =15/dAdn=13), whereas all other ion source and data acquisition parameters for MS/MS were similar to conditions described for amino acids and acylcarnitines.

2.9.3 MS/MS Spectral Acquisition for Unknown Metabolite Identification

Unknown metabolites from DBS extracts were fragmented at three fixed collision energies of 10, 20 and 40 V using collision-induced dissociation (CID) of precursor ions by QTOF-MS in cases when authentic chemical standards were unavailable for unambiguous identification by comparing with in-house MS/MS spectra and co-migration of spiked samples. For identification, either an averaged product ion spectrum or a product ion spectrum that ensured near complete

fragmentation of the precursor ion (*i.e.*, molecular ion with about 10% of base peak intensity) was used at an optimum collisional energy. Compounds were picked by the Find by Targeted MS/MS algorithm in MassHunter and subsequent structural elucidation was performed by searching the METLIN database via the MassHunter Personal Compound Database and Library (PCDL) manager with a minimum forward search score of 25 and a minimum reverse score of 80. For putative galactated-amino acids detected under positive ion mode, which had no entries in the local METLIN PCDL, neutral loss searches were performed using the METLIN online database neutral loss search tool (http://metlin.scripps.edu), as well as an independent search on the Human Metabolome Database (http://hmdb.ca). Additionally, for galactose-1-phopshate and glucose-1-phosphate without product ion spectra in the PCDL, fragmentation of neat standards was performed at 10, 20 and 40 V under negative ion mode conditions and product ion spectra were uploaded to the PDCL prior to a library search. In this case, the experimental product ion spectra of DBS extracts were compared with standard spectra and a match was made if both the fragments and intensity ratios were in mutual agreement.

2.9.4 Calibration and Method Validation

Calibration curves for metabolite standards on the TOF were performed and analyzed in triplicate (n = 9) by serial dilution in 200 mM ammonium acetate, 25% *v* acetonitrile, pH 5.0 with 25 µM Cl-Tyr as the internal standard. Linearity was measured over a 400-fold range for polar metabolites and over a 200-fold

range for medium and long-chain acylcarnitines. Spike-recovery studies into a pooled QC sample were performed for representative biomarkers for IEM at three levels: approximately at 50% of normal concentration, 75% of elevated disease concentration and the midpoint. Concentrations of spikes were adjusted slightly for each metabolite to ensure that a significant response change relative to non-spiked DBS extract was detected. Instrumental triplicate analyses of the spike and recovery solutions were performed in a four injection format using MSI-CE-MS, namely (1) unspiked DBS extract (2) low-spike (3) mid-spike and (4) high-spike. Percent recovery was calculated as [(*measured concentration - endogenous concentration)/added concentration* x 100]. Intraday precision was determined by triplicate analysis of pooled QC extracts by MSI-CE-MS using seven sample injection series run before and after analysis (n=14). Calibration standards were prepared for the QTOF in duplicate by diluting standards in water with 15% *v* acetonitrile and 10 µM Cl-Tyr and 10 µM F-Phe as internal standards, and linearity was measured over a 400-fold range for polar metabolites and a 200-fold range for medium and long-chain acylcarnitines. For experiments on the TOF, purine and hexakis(2,2,3,3-tetraflurorpropoxy) phosphazine (HP-921) were spiked into the sheath liquid at 0.02% *v* as reference ions at *m/z* 121.0509 and *m/z* 922.0098 for internal mass calibration, whereas the QTOF used an additional reference mass, hexamethoxyphosphazine (HP-321) at *m/z* 322.0481. The TOF-MS was operated in positive ion mode with a mass range of *m/z* 50-1700 in 2GHz Extended Dynamic Range mode with an acquisition rate of 2 Hz and acquisition

time of 500 ms. The dual AJS ESI settings were as follows: dry gas = 8 L/min at 300°C, nebulizer = 10 psi, sheath gas = 3.5 L/min @ 195°C, VCap = 2000 V, Nozzle voltage = 2000 V. The TOF-MS settings were: fragmentor = 120 V, skimmer = 65 V, Oct 1 RF = 750 V. The QTOF-MS was operated in full scan MS positive or negative ion mode with a mass range of *m/z* 50-1700 in 4GHz HiRes acquisition mode with a scan rate of 1 Hz. The dual AJS ESI settings were as follows: dry gas = 16 L/min at 200°C, nebulizer = 8 psi, sheath gas = 3.5 L/min @ 199°C, VCap = 2000 V, Nozzle voltage = 2000 V. The QTOF-MS settings were: fragmentor = 380 V, skimmer = 65 V, Oct 1 RF = 750 V.

2.9.5 Nontargeted Metabolite Profiling of DBS Extracts

Data from targeted analysis of known biomarkers of IEM was combined with results from nontargeted metabolite profiling when using molecular feature extractor (MFE) on the Q-TOF. MFE was performed with a migration time window in CE that spans the region between the salt front and the neutral migration zone (*i.e.,* neutral species that co-migrate with the EOF) where ion suppression is greatest. A minimum of 300 counts was used as a threshold for a molecular feature to be extracted. Positive ion species of +H and +Na and neutral loss of H_2O were considered. Further manual filtering of known in-source fragments and adducts was also performed to avoid inclusion of redundant signals generated by the same metabolite. A molecular feature was then considered to be a definitive and sample-derived metabolite if it was not present in a blank extract and the signal is adequately reproducible (*RSD* < 40%) in MSI-CE-MS.[1] Overall,

all filtered metabolites from DBS extracts were defined by their characteristic mass-to-charge ratio and relative migration time (*m/*z:RMT) as a paired variable and was included in the final data matrix if it was present in > 75% of samples detected in DBS extracts from healthy neonates, and had a precision with a RSD < 40% on all QC samples.

2.9.6 Statistical and Computational Analysis

All electropherograms were processed using Igor Pro 5.0 software (Wavemetric Inc., Lake Oswego, OR, USA). Statistical analyses included linear regression were performed using Excel 2007 (Microsoft Inc., Redmond WA, USA), which was used to predict the RMT [2] and relative ion response (*i.e.*, sensitivity)[3] of an ion based on a training set derived from a homologous series of acylcarnitines. Chem3D Professional software, version 12 (CambridgeSoft Inc., Cambridge, MA.) was used to calculate the Connolly solvent-excluded volume of acylcarnitines following an energy minimization using molecular mechanisms 2 (MM2) algorithm with molecular dynamics and 10,000 iterations. This approach was used to tentatively identify *O*-glutaryl-*L*-carnitine (C5DC) based on its characteristic *m/z*:RMT, as well as estimate the concentration of C5DC from a DBS extract in a presumptive GA I case since a commercial standard was not available. Additionally, unsupervised (PCA, HCA) and supervised (OPLS-DA) multivariate statistical analysis was performed on *log*-transformed and autoscaled data using Metaboanalyst 3.0,[4] in order to identify and rank metabolites associated with galactosemia relative to healthy neonates and IEM controls.

2.10 Supplemental References

(1) Kuehnbaum, N. L.; Kormendi, A.; Britz-McKibbin, P. *Anal. Chem.* **2013**, *85*, 10664–10669.

(2) Lee, R.; Ptolemy, A. S.; Niewczas, L.; Britz-McKibbin, P. *Anal. Chem.* **2007**, *79*, 403–415.

(3) Chalcraft, K. R.; Lee, R.; Mills, C.; Britz-Mckibbin, P. *Anal. Chem.* **2009**, *81*, 2506–2515.

(4) Xia, J.; Sinelnikov, I. V.; Han, B.; Wishart, D. S. *Nucleic Acids Res.* **2015**, *43*, W251–W257.

Table S2.1. Differential extraction efficiency of metabolites from DBS extracts as a function of solvent composition (MeOH:H_2O) and solvent temperature under standard conditions when using MSI-CE-MS.

	Metabolite Recovery Based on Mean Ion Response Ratio by Extraction Solvent					
	MeOH[a]		**MeOH:H_2O (75:25)[b]**		**MeOH:H_2O (50:50)**	
Compound	***Room Temp***	***Ice Cold***	***Room Temp***	***Ice Cold***	***Room Temp***	***Ice Cold***
Glycine	0.19 ± 0.04	0.11 ± 0.02	0.21 ± 0.07	0.16 ± 0.01	0.11 ± 0.02	0.08 ± 0.02
Alanine	0.80 ± 0.15	0.38 ± 0.07	0.73 ± 0.18	0.54 ± 0.05	0.38 ± 0.07	0.30 ± 0.07
Arginine	0.034 ± 0.004	0.028 ± 0.005	0.064 ± 0.010	0.048 ± 0.004	0.053 ± 0.007	0.039 ± 0.008
Ornithine	0.10 ± 0.04	0.12 ± 0.03	0.23 ± 0.07	0.18 ± 0.03	0.12 ± 0.03	0.10 ± 0.007
Methionine	0.09 ± 0.01	0.050 ± 0.006	0.09 ± 0.02	0.07 ± 0.01	0.05 ± 0.006	0.04 ± 0.01
C0	0.47 ± 0.18	0.27 ± 0.12	0.46 ± 0.22	0.32 ± 0.11	0.27 ± 0.12	0.19 ± 0.04
Phenylalanine	0.48 ± 0.06	0.27 ± 0.01	0.47 ± 0.08	0.39 ± 0.05	0.27 ± 0.01	0.23 ± 0.04
Citrulline	0.06 ± 0.01	0.05 ± 0.008	0.09 ± 0.005	0.08 ± 0.01	0.05 ± 0.008	0.05 ± 0.01
C2	0.32 ± 0.12	0.13 ± 0.03	0.29 ± 0.13	0.24 ± 0.05	0.13 ± 0.03	0.13 ± 0.01
C3	0.048 ± 0.020	0.040 ± 0.010	0.045 ± 0.020	0.033 ± 0.008	0.020 ± 0.007	0.018 ± 0.002
Adenosine	0.002 ± 0.0005	0.002 ± 0.0003	0.003 ± 0.0008	0.002 ± 0.0008	0.002 ± 0.0003	0.003 ± 0.0009
GSSG	0.020 ± 0.005	0.26 ± 0.02	1.48 ± 0.51	0.88 ± 0.27	0.26 ± 0.02	0.28 ± 0.06

[a] *Expanded NBS programs typically perform DBS extracts using 100% MeOH together with hydrazine chemical derivatization for detection of succinylacetone for early detection of TYR I.*
[b] *Significantly higher recovery ($p < 0.05$) for polar metabolites when performing extraction using MeOH:H_2O (75:25) at ambient condition notably Arg, Orn, Cit and GSSG.*

Table S2.2. Figures of merit based on method calibration and validation of MSI-CE-MS for reliable quantification of 22 biomarkers used for population-based screening of IEMs associated with impaired amino acid, acylcarnitine/fatty acid, thiol and purine metabolism

Biomarkers (IEM)[a]	***m/z*:RMT**	**Linearity (R^2)** [b]	**Sensitivity (µmol/L^{-1})**	**LOD (nmol/L)**	**Precision (*%CV*, *n*=14)**[c]	**%Recovery (3 Levels, *n*=9)**[d]
Gly (NKHG)	77.039:0.643	0.9641	0.00707	2700	8.7	--
Ala (LA)	90.055:0.703	0.9995	0.0192	321	9.3	--
Val (MSUD)	118.086:0.804	0.9997	0.0752	390	6.9	93
Leu (MSUD)	132.102:0.830	0.9997	0.112	190	2.5	97
Orn (HHH)	133.097:0.509	0.9995	0.0747	420	12	109
Lys (DE-RED, H-LYS)	147.113:0.830	0.9999	0.0811	65	9.0	--
Met (HCY/CBS, MAT, TYR)	150.058:0.875	0.9997	0.0829	120	8.0	--
Phe (PKU)	166.086:0.908	0.9999	0.141	150	5.5	91
Arg (ARG, CIT II)	175.119:0.533	0.9999	0.150	70	5.9	100
Cit (CIT I/II, HHH)	176.103:0.924	0.9998	0.0817	140	7.6	101
Tyr (TYR I)	182.081:0.948	0.9999	0.106	110	4.7	91
C0 (CUD, CPT I)	204.123:0.732	0.9850	0.272	480	9.5	--
C2 (CUD)	204.123:0.738	0.9981	0.309	80	13	--
C3 (PA, MMA MUT, MCD, CBL)	218.139:0.781	0.9990	0.320	50	9.0	--
isoC4 (SCAD, IBG, GA II)	232.154:0.804	0.9996	0.436	18	5.2	--
isoC5 (IVA, GA II, 2MBG)	246.171:0.823	0.9996	0.436	40	14	--
C6 (MCADD)	260.186:0.845	0.9959	0.442	6.0	28	93
C8 (MCADD)	288.217:0.882	0.9998	0.411	10	34	100
C10 (MCADD)	316.249:0.919	0.9996	0.470	12	25	97
dA (ADA)	252.109:0.864	0.9997	0.165	260	10	--
A (ADA)	268.104:0.884	0.9998	0.0744	250	8.0	--
GSSG (GSD)	307.083:1.046	0.9916	0.0977	310	6.7	--

[a] *IEM abbreviations represent adenine deaminase deficiency (ADA), arginase deficiency (ARG), citrullinemia type I or II (CIT I, II), cystathione beta-synthase deficiency (CBS), carnitine palmitoyltransferase type I deficiency (CPT I), carnitine uptake defect (CUD), 4-dienoyl-CoA reductase deficiency (DE-RED), glutathione synthetase deificiency (GSD), homocystinuria (HCY), hyperonrithinemia, hyperammonemia, hypercitrullinemia (HHH), alpha-aminoadipic semialdehyde synthase deficiency, (H-LYS), lactic acidemia (LA), 2-methylbutyrylglycinuria (2MBG), medium-chain acyl-CoA dehydrogenase deficiency (MCADD), multiple carboxylase deficiency (MCD), methionine adenosyltransferase (MAT), methylmalonic acidemia (MMA), maple syrup urine disease, (MSUD), non-ketotic hyperglycinemia (NKHG), phenylketonuria (PKU), short-chain acyl-CoA dehydrogenase deficiency (SCAD).*

[b] *Linear range for external calibration curves were 0.50-200 µM for amino acids and nucleosides, and 0.10-20 µM for acylcarnitines using Q-TOF-MS, respectively normalized to 25 µM 3-chlorotyrosine as internal standard.*

[c] *Intra-day precision based on sets of replicate injection of DBS extract from healthy control by MSI-CE-MS*

[d] *Accuracy based on spike-recovery studies performed on DBS extracts (n=3) from healthy control following addition of low (50% level), mid (62.5% level) and high (75% level) concentration levels of calibrant standards*

Table S2.3. Bland-Altman (%difference) plots derived for 12 metabolites measured consistently by MSI-CE-MS and FIA-MS/MS platforms in DBS specimens from screen-negative infants (*n*=30) at NSO.

Screening Biomarker	Mean %Difference[a] *[MSI-CE-MS – MS/MS]/Average*	Standard Deviation	Limits of Agreement		%Within Limits of Agreement
			Lower	*Upper*	
Alanine	-1.6	26.0	-52.5	49.4	96.7
Glycine	-11.5	14.5	-43.4	20.4	96.7
Tyrosine	-14.9	15.6	-42.5	12.8	93.3
Citrulline	-19.9	23.6	-55.1	15.2	96.7
Phenylalanine	-31.7	29.2	-60.2	-3.3	93.3
C2	-37.7	16.3	-68.4	-7.1	93.3
Methionine	-54.3	14.1	-102.9	-5.7	90.0
Ornithine	-54.8	24.3	-101.1	-8.6	96.7
Valine	-56.6	76.7	-104.1	-9.0	96.7
Arginine	-92.9	27.7	-147.1	-38.6	93.3
C3	-84.3	24.8	-234.7	66.0	96.7
C0	-116.8	17.9	-174	-59.5	93.3

[a] *An overall mean %difference of -43% for all 12 metabolites measured in DBS extracts from 30 screen-negative infants (n=320) when comparing data derived from MSI-CE-MS and MS/MS platforms with average of 5.3% of data outside agreement limits.*

Table S2.4. A panel of nine top-ranked putative markers (*FC* > 3.0) identified in DBS extracts by MSI-CE-MS for pre-symptomatic diagnosis of classic galactosemia in neonates, including 99th percentile cut-off limits as determined for a cohort of age-matched healthy/screen-negative infants (*n*=30).

Metabolite (*m/z*:RMT)	**Molecular Formula/ID[a]**	**RPA (Screen +)**	**RPA ± 1s (Screen -)**	**Biological Variance (RSD)**	**Fold-change**	**99th % Cutoff[b]**	**Above Cut-off**
137.072:0.553	1-Methyl Nicotinamide	0.281	0.078 ± 0.036	46%	3.62	0.166	*Yes*
139.050:0.692	Urocanic Acid	1.326	0.24 ± 0.19	79%	5.52	0.707	*Yes*
175.119:0.533	Arginine	0.416	0.110 ± 0.062	56%	3.78	0.262	*Yes*
176.103:0.924	Citrulline	0.519	0.120 ± 0.043	36%	4.33	0.227	*Yes*
238.092:1.116	$C_8H_{15}NO_7$ Gal-Gly[c]	0.337	0.0120 ± 0.0066	55%	28.1	0.0280	*Yes*
280.139:1.206	$C_{10}H_{21}NO_7$ Gal-Val[c]	0.341	0.0084 ± 0.0084	100%	40.8	0.0290	*Yes*
294.155:1.233	$C_{12}H_{23}NO_7$ Gal-Leu/Ile[c]	0.351	0.0098 ± 0.0090	92%	35.8	0.320	*Yes*
309.129:1.287	$C_{11}H_{20}N_2O_8$ Gal-Gln[c]	0.744	0.059 ± 0.034	58%	12.7	0.141	*Yes*
310.115:1.295	$C_{11}H_{19}NO_9$ Gal-Glu[c]	0.419	0.015 ± 0.011	73%	28.9	0.041	*Yes*

[a] *Most likely molecular formula as determined by molecular ion [MH+] with mass error < 3.0 ppm*

[b] *99th percentile cut-off based on 99% upper confidence interval of the mean (t = 2.457, n = 30) using normal birth weight screen-negative infants as healthy control population*

[c] *Tentative level 2 identification of a series of N-glycated amino acid conjugates elevated in GALT yet also detected in screen-negative DBS extracts and other IEMs at lower levels based on their MS/MS spectra*

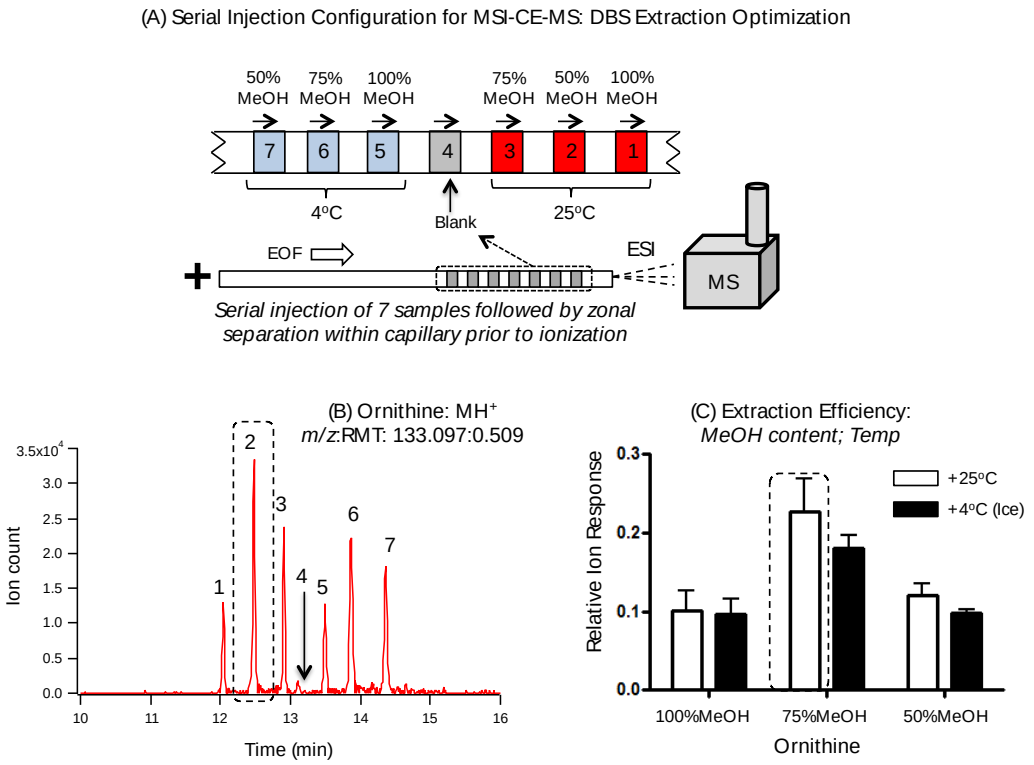

Figure S2.1. (A) Serial injection configuration in MSI-CE-MS for optimization of DBS extraction conditions to maximize recovery of metabolites based on changes in solvent composition (MeOH:H_2O) and solvent temperature. All DBS extracts were consistently sonicated for 15 min after addition of 100 µL of solvent, ultrafiltered using a 3kDa MWCO at 14,000 *g* for 15 min to remove protein and then the filtrate of the DBS extract was vacuum evaporated and reconstituted in 30 µL of 200 mM ammonium acetate and 25% *v* acetonitrile with internal standard prior to duplicate injection by MSI-CE-MS using a distinct dilution pattern for each sample. (B) A representative extracted ion electropherogram (EIE) for *L*-ornithine (Orn) highlights that a single experiment is able to clearly demonstrate that optimal recovery is realized when 75:25 MeOH:H_2O is used at room temperature without sample carry-over by as shown by including a blank extract as control (4) in the same run. (C) A significant enhancement in extraction efficiency was found for Orn and most other metabolites examined as summarized in **Table S1**, notably highly polar/ionic metabolites, such as *L*-arginine (Arg) and *L*-citrulline (Cit), as well as intracellular metabolites, such as reduced glutathione (GSH). It is important to note that sample carry-over effects (as determined in blank sample injected) between injections are minimized by removing a 5 mm section of the outer polyimide coating notably when injecting samples containing residual organic solvent. Also, small differences in apparent migration time can be corrected by normalization to an internal standard (*i.e.*, relative migration time or RMT) to correct for changes in electroosmotic flow (EOF).

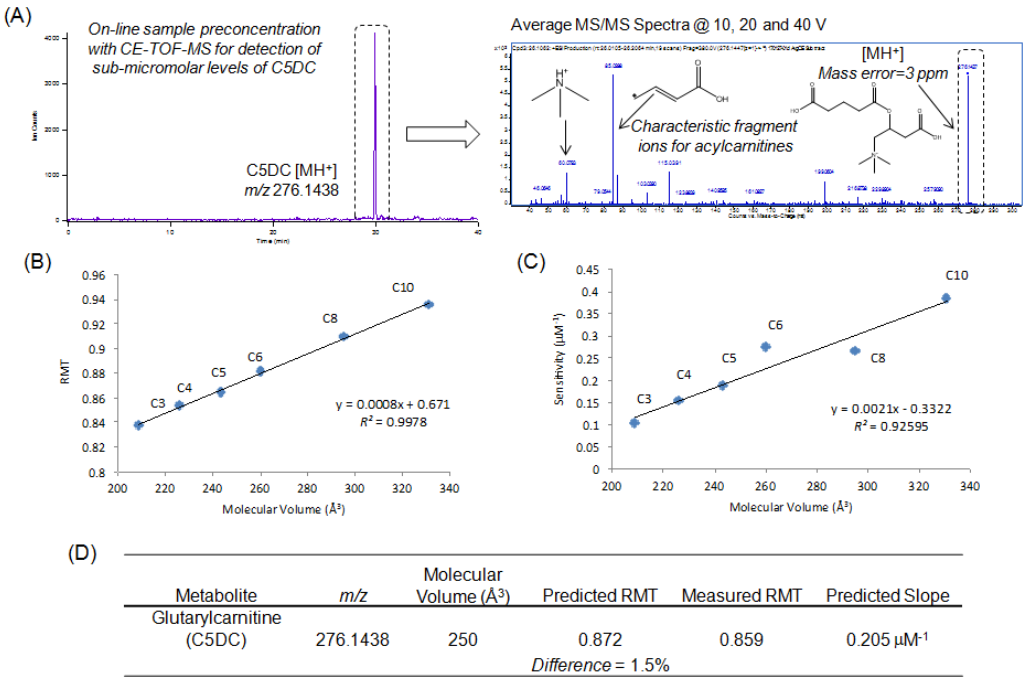

(D)

Metabolite	*m/z*	Molecular Volume (Å³)	Predicted RMT	Measured RMT	Predicted Slope
Glutarylcarnitine (C5DC)	276.1438	250	0.872	0.859	0.205 µM^{-1}
			Difference = 1.5%		

Figure S2.2. (a) On-line preconcentration of DBS extract derived from a presumptive GA I case using a single long injection in CE-MS in order to boost concentration sensitivity by about 50-fold, which shows a large signal corresponding to elevated levels of *O*-glutaryl-*L*-carnitine (C5DC), which is a biomarker of GA I. Sample enrichment of the precursor ion, C5DC allows for acquisition of a better quality MS/MS spectra based on collisional-induced dissociation at different collisional energies (10, 20 and 40 V), which confirm the detection of product ions characteristic of an acylcarnitine, namely *m/z* 85.0288 and *m/z* 60.0793. (b) A linear regression model that is used to predict the relative migration time (RMT) of C5DC in CE based on its intrinsic physicochemical properties (*i.e.*, molecular volume, *MV*) using a homologous series of short-chain and medium-chain acylcarnitines as a training set. (c) Similarly, a linear regression model is also applied to estimate the relative response factor (RRF) or sensitivity (µM^{-1}) for C5DC since a chemical standard was not available for spiking to confirm identity and establish an external calibration curve for quantification. In all cases, RMT and RRF were normalized to an internal standard, 25 µM 3-chloro-*L*-tyrosine that was included in all DBS extracts and calibrants to correct for changes in spray stability. (d) Summary of linear regression models for predicting RMT relative to measured RMT experimentally, as well as predicted RRF used for estimation of C5DC concentration in DBS extract.

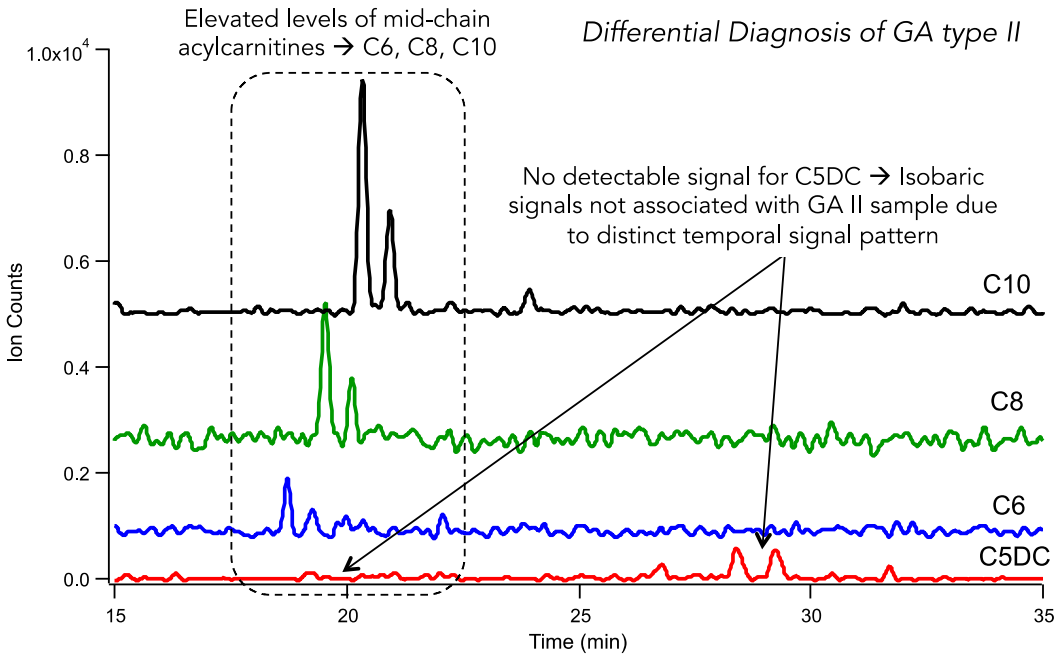

Figure S2.3. Confirmatory testing and differential diagnosis of glutaric acidemia type II (GA II) that is associated with multiple acyl-CoA dehydrogenase deficiency (MADD) from glutaric acidemia type I (GA I), which is associated with mutations of the *GCDH* gene that encodes the enzyme glutaryl-CoA-dehydrogenase. Both distinct inherited metabolic disorders rely on detection of C5DC as the primary biomarker for screening, however GA II cases can be only mildly elevated near the 99th percentile cut-off level, and it was below the detection limit for MSI-CE-MS. However, GA II was confirmed and differentiated from GA I based on elevated levels of medium-chain acylcarnitines (2:1 dilution signal pattern for DBS extract derived from GA II) that is most pronounced for C10. This profile of abnormally elevated medium-chain acylcarnitines is distinct from MCADD (C8 is most elevated), as well as most other IEM and healthy controls.

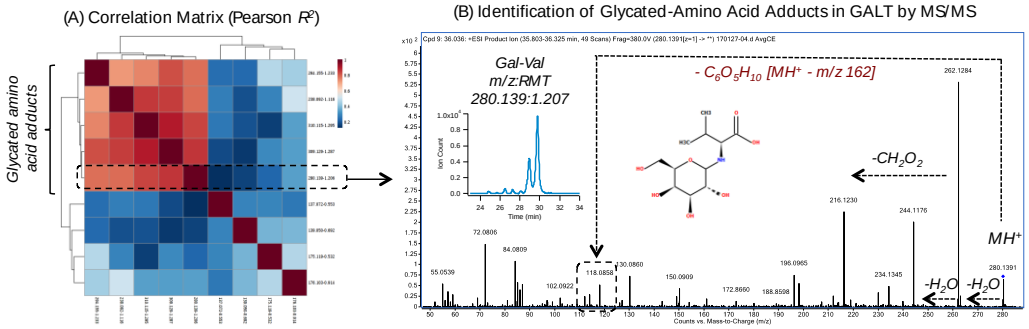

Figure S2.4. (A) A correlation matrix for the top nine most discriminating metabolites for classic galactosemia (type I) relative to healthy and disease controls that highlights the high degree of correlation (R^2 > 0.800) among five *N*-galactated amino acid adducts that were also consistently detected in most DBS extracts in healthy infant population. (B) High resolution, accurate MS/MS spectra (average) of the precursor ion, Val-Gal (*m/z* 280.139 as MH^+), which highlights the characteristic neutral loss of hexose moiety (*m/z* 162) upon fragmentation and detection of free amino acid, Val as product ion (*m/z* 118.086). This was a common MS/MS fragmentation pathway observed for all other *N*-galactated amino acid adducts identified in this work along with two or more neutral water loses for the precursor ion at lower collisional energies (+10 V).

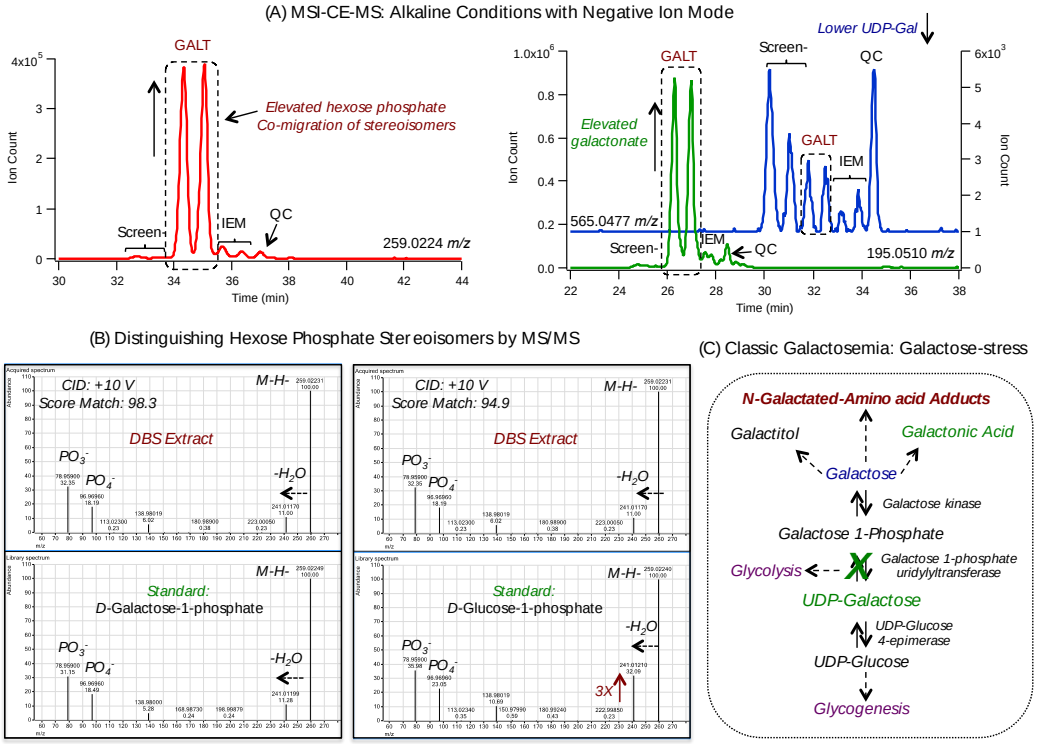

Figure S2.5. Confirmatory testing of classic galactosemia (type I) by MSI-CE-MS via temporal signal pattern recognition under alkaline buffer conditions with negative ion mode detection for acidic metabolites in DBS extracts. (A) An extracted ion electropherogram (EIE) confirms substrate accumulation of galactose 1-phosphate (Gal-1P, 1:1 doublet pattern derived from DBS#2a/b) due to GALT deficiency that is present at much lower levels in both screen-negative and other IEM controls, including the pooled QC reference. Similarly, a pronounced accumulation in the down-stream oxidized by-product of galactose, galactonic acid (GA, *m/z* 195.051) was also detected in DBS extract from galactosemia infant together with a mild attenuation in the product of GALT activity, UDP-galactose (UDP-Gal, *m/z* 565.048). (B) Comparison of MS/MS fragmentation spectra of standards of the two major hexose 1-phosphate stereoisomers at low collisional energy (+10 V), confirms that the precursor ion (MH^+) measured in galactosemia was due to Gal-1-P as a result of the lower relative intensity of the product ion (*m/z* 241.012) corresponding to neutral water loss. (C) An overview of the impacts of aberrant galactose metabolism due to GALT deficiency, which results in Gal-1-P and galactose (Gal) accumulation, as well as down-stream products, such as galactonic acid (GA), galactitol and various *N*-galactated amino acids as determined in this study.

Chapter III

Metabolic Signatures of Cystic Fibrosis in Dried Blood Spots from Asymptomatic Neonates: Reducing False Positives and Carrier Identification for Newborn Screening

Authors of this work are Alicia DiBattista, Nathan McIntosh, Monica Lamoureux, Osama Y. Al-Dirbashi, Pranesh Chakraborty, and Philip Britz-McKibbin

* manuscript in preparation

A.D. performed all of the sample workup and conducted all of the MSI-CE-MS-based metabolomic studies. A.D. performed most of the data analysis and wrote the initial draft for publication. Co-authors obtained ethics approval for the study, selected the sample cohort, shipped all specimens, provided all data regarding the results of newborn screening performed at the regional screening centre and provided valuable feedback on manuscript drafts

Chapter III: Metabolic Signatures of Cystic Fibrosis in Dried Blood Spots from Asymptomatic Neonates: Reducing False Positives and Carrier Identification for Newborn Screening

3.1 Abstract

Cystic fibrosis (CF) is a complex multi-organ disease that is among the most common life-shortening genetic disorders in North America, which benefits from early detection with therapeutic interventions initiated during infancy. Most newborn screening (NBS) programs for CF rely on a two-stage immunoreactive trypsinogen and cystic fibrosis transmembrane conductance regulator (*CFTR*) mutation panel (IRT/DNA) algorithm that is sensitive, but not specific for detecting affected CF neonates in the population. We hypothesize that metabolic phenotyping of dried blood spot (DBS) specimens may allow for improved discrimination of true CF neonates from unaffected carriers and transient hypertrypinsogenmic cases as confirmed by low sweat chloride (< 29 mM). For the first time, we report the discovery of a panel of CF-specific metabolites from DBS extracts when using multisegment injection-capillary electrophoresis-mass spectrometry (MSI-CE-MS) as a high throughput metabolomics platform for nontargeted metabolite profiling of volume-restricted biospecimens with quality assurance. This retrospective case-control study design identified 29 metabolites from a single 3.2 mm diameter DBS cut-out that were differentially expressed in asymptomatic yet normal birthweight CF neonates without meconium ileus (n=34) as compared to age/sex-matched screen-negative controls (n=40) after a false discovery rate (FDR) adjustment (q < 0.05), including *N*-glycated amino

acids, oxidized glutathione, and nicotinamide indicative of oxidative/redox stress and dysregulated glucose metabolism in CF. Importantly, 16 metabolites from DBS extracts ($q < 0.05$, FDR) also allowed for discrimination of true CF neonates from screen-positive yet unaffected carriers and hypertrypsinogenemic cases (n=60) identified by IRT/DNA screening. Notably, 6 CF-specific biomarker candidates satisfying a Bonferroni adjustment (p < 7.25 E-5) included several amino acids (Thr, Ser, Pro, Tyr) reflecting protein maldigestion/maladsorption, ophthalmic acid as an indicator of severe glutathione depletion, as well as an unknown trivalent peptide that was the only metabolite directly correlated with IRT (ρ = 0.420, p = 2.57 E-5). These biomarker candidates offer an intriguing way to improve the specificity of neonatal CF screening using existing MS/MS infrastructure by reducing false-positives, unaffected carrier identification and parental anxiety as a result of unnecessary follow-up testing of presumptive CF with *CFTR* mutations of unknown or variable consequence.

3.2 Introduction

Cystic fibrosis (CF) is one of the most common autosomal recessive disorders prevalent among Caucasian populations, which is caused by mutations to the gene encoding the cystic fibrosis transmembrane conductance regulator (*CFTR*).[1] More than 2,000 different mutations of *CFTR* comprising six broad mutation classes have been identified with a majority of CF patients classified as homozygous or heterozygous for an in-frame deletion of Phe at the 508 position (F508del).[2] Disease-causing mutations in *CFTR* lead to severe gene product

deficiency or loss/impaired chloride transport function causing the formation of thick mucus at the surface of exocrine epithelial cells,[3] contributing to pancreatic insufficiency, recurrent lung infections and progressive respiratory dysfunction.[4] Although often considered a classic monogenic disease, there is great clinical heterogeneity in CF phenotypes as influenced by non-*CFTR* gene modifiers and environmental factors whose complex interactions with *CFTR* genotypes remain poorly understood.[5] This results in variable symptom severity and disease progression among CF patients with early stages of lung disease and bronchiectasis evident in a third of infants within the first few months.[6] Nevertheless, life expectancy and quality of life has significantly improved with early diagnosis since its inclusion within newborn screening (NBS) programs[7] as it allows for therapeutic interventions to be initiated before the onset of the first debilitating symptoms. Growing evidence has demonstrated the cost-effectiveness and efficacy of dietary management on later growth, lung function and survival for individuals diagnosed by NBS as compared to symptomatically for most infants without meconium ileus or a family history of CF.[8,9] Although a cure for CF still does not exist, early detection of CF by NBS together with standard CF management practices[10] and new targeted CFTR modulator therapies to restore chloride transport function[11,12] represent major milestones to prevent chronic lung disease later in life. Additional benefits in overall survivorship and quality of life are still expected with patient access to healthcare due to the recent advent of NBS for CF in North America.[13]

A "two-tiered" strategy is most widely used for universal CF screening based on detection of elevated immunoreactive trypsinogen (IRT) followed by a DNA mutation panel from a neonatal dried blood spot (DBS) collected around 2 days of age.[14–16] Since elevated IRT levels are sensitive, but not specific for CF detection,[17–19] a second-tier *CFTR* mutation panel was promoted to reduce false-positives when relying on an original DBS specimen[20,21] following the discovery of the *CFTR* gene.[22] However, the exact IRT threshold and total number of *CFTR* mutations included in panels varies widely by jurisdiction, which has contributed to diagnostic dilemmas in CF.[23,24] Even when a floating cut-off is used for IRT due to reagent lot and seasonal variations, the overall positive predictive value (*PPV* ≈ 4.5%) for CF screening by optimal IRT/DNA algorithms is low[25] as compared to NBS for most genetic diseases by tandem mass spectrometry (MS/MS), such as phenylketonuria.[26] Limitations of CF screening include poor specificity due to transient neonatal hypertrypsinogenemia, the identification of unaffected carriers with *CFTR* allele variants who do not express the disease, and potential false-negatives for ethnic groups with mutations not included within panels.[27,28] Alternative strategies have been proposed to improve *PPV*, including a repeat IRT[29,30] or a pancreatitis-associated protein (PAP)[31,32] plus DNA screen performed on a second DBS specimen collected from 7-10 days. NBS for CF have also proposed a repeat IRT/PAP without a third-tier DNA screen given ethical concerns about widespread genetic testing of *CFTR* variants of unknown or variable consequence.[33] However, this adds to screening costs while relying on

a repeat DBS specimen that can further delay CF diagnosis and treatment. As a result, the pilocarpine-stimulated iontophoresis sweat test remains the "gold standard" for confirmatory diagnosis of all presumptive CF infants based on functional assessment of CFTR activity since sweat ducts display impermeability to chloride.[34–36] IRT and/or mutation screens provide only probable information regarding disease risk; only about 5.6% of screen-positive CF infants having elevated sweat chloride (≥ 60 mM) while the majority of infants (> 90%) are likely unaffected with low/normal chloride (< 29 mM).[37] A direct consequence of CF screening with extended genetic sequencing[38] is the identification of asymptomatic neonates with intermediate sweat chloride (30-59 mM) and unclear prognosis corresponding to an equivocal diagnosis.[39] The frequency of these CF-screen positive inconclusive diagnosis or *CFTR*-related metabolic syndrome (CF-SPID/CRMS) cases are higher than desired based on evolving diagnostic and screening consensus guidelines,[18] a sub-set of whom may be at risk at being later diagnosed with CF (*i.e.*, delayed CF) with follow-up monitoring.[37] This raises the question - is there is a better way to screen for CF that is ethical, cost-effective yet accurate to better inform clinical decision-making without undue parental anxiety?

Recent advances in nontargeted metabolite profiling (*i.e.*, metabolomics) offers a revolutionary approach for phenotyping individuals at a molecular level that is needed for new breakthroughs in precision medicine.[40] Since metabolites are "real-world" end-products of gene expression and environmental exposures,

metabolomics offers a promising approach for biomarker discovery.[41] Metabolomics not only serves to identify and validate clinically relevant biomarkers of disease at early stages of latency,[42] but also can provide new insights of the mechanisms of disease pathophysiology,[43] predict disease risk outcomes in critically ill patients,[44] and reveal the phenotype of "silent" genetic mutations.[45] As a result, there is growing interest in applying metabolomics for characterizing the metabolic phenotype of CF.[46] For instance, serum metabolomic studies using LC-MS and GC-MS revealed altered energetic metabolism in children with CF reflected by abnormal central energy metabolism, oxidative stress, and microflora activity.[47] Similarly, metabolomic profiling of cultured human airway epithelial cells from CF and non-CF patients[48] confirmed known perturbations in oxidative and osmotic stress, as well as other metabolic pathways, including altered purine nucleoside degradation, tryptophan catabolism and glucose metabolism. Volatile metabolites indicative of lung inflammation were identified by GC-MS based analysis of exhaled breath of CF children with and without positive cultures for *P. aeruginosa*.[49] Also, metabolomic analysis of bronchoalveolar lavage (BAL) fluids using NMR demonstrated that branched-chain amino acids and lactate were associated with CF patients having airway inflammation.[50] Similarly, metabolomic profiling on BAL fluids using LC-MS have demonstrated that purines and amino acids were strongly correlated with neutrophil counts and lung function,[51] which also served as predictive biomarkers of future lung disease.[52] Recently, metabolomic studies of longitudinal sputum

samples from adult CF patients revealed that platelet activating factor and related inflammatory lipids were elevated during active pulmonary exacerbations.[53] Thus, unique metabolite signatures and aberrant metabolic pathways exist in CF that reflect the complex interactions between host, diet, environment and microbes for individual patients. However, metabolomic studies to date have largely focused on a mechanistic understanding of CF pathophysiology in children or adult patients with a confirmed diagnosis. Herein, we apply multi-segment injection-capillary electrophoresis-mass spectrometry (MSI-CE-MS) as a high throughput platform in metabolomics for biomarker discovery,[54,55] which revealed for the first time a panel of CF-specific metabolites measured from DBS extracts of asymptomatic neonates as compared to healthy controls/screen-negatives, as well as screen-positive yet unaffected carriers and hypertrypsinogenemic cases. We anticipate that this work may improve the cost-effectiveness and specificity of neonatal CF screening following an initial elevated IRT test result when measuring CF-specific metabolites from an original DBS specimen using existing MS/MS infrastructure at NBS facilities. Major benefits include reducing the false positive rates of CF screening and unnecessary molecular diagnostic (genetic) and physiological testing (sweat chloride) that also contributes to parental anxiety notably for screen-positive infants with an inconclusive diagnosis. Additionally, metabolic phenotyping of CF neonates will provide deeper insights into functional significance of novel *CFTR* mutations of unknown consequence and unknown reported clinical histories.

3.3 Experimental Section

3.3.1 Chemicals and Reagents

Ultra LC-MS grade methanol (Caledon, Georgetown, ON, Canada) and Ultra LC-MS grade acetonitrile (Honeywell, Muskegon, MI, USA) were used to prepare sheath liquid and BGE, respectively. Ammonium acetate, formic acid, 3-chloro-*L*-tyrosine (Cl-Tyr), 2-[4-(2-hydroxyethyl)piperazin-1-yl]ethanesulfonic acid (HEPES), 4-fluoro-*L*-phenylalanine (F-Phe), 2-napthalenesulfonic acid (NMS) and all other chemical standards were purchased from Sigma-Aldrich (St. Louis, MO, USA). All stock solutions were made in distilled, deionized water and stored at 4°C, unless otherwise stated.

3.3.2 Patient and Sample Selection

All samples consisted of authentic neonatal dried blood spot (DBS) filter paper punches which are 3.2 mm-diameter disks equivalent to approximately 3.4 µL of whole blood.[56] DBS specimens were collected by Newborn Screening Ontario (NSO) at the Children's Hospital of Eastern Ontario (CHEO) and analyzed as part of their expanded newborn screening (NBS) mandate with residual spots for all screen-positive samples stored frozen at -80°C. All samples were sex-matched and normal birth weight/gestational age unless otherwise stated. Samples were excluded from the study if they had meconium ileus at birth, were twins, had a DBS collection date > 7 days or were being fed other than by breast or formula. This study was approved by the CHEO Research Ethics Board

and the Hamilton Integrated Research Ethnic Board (REB#: 14-669-T) as a study involving the secondary use of biobanked and de-identified specimens.

For the initial study, duplicate punches of all CF-affected neonates (*n*=24) and four replicate punches of all screen-negative neonates (*n*=30) were transferred from Newborn Screening Ontario (NSO) to McMaster University and stored at -80°C upon receipt. Affected CF neonates were confirmed by detection of an elevated IRT (IRT > 96thcentile), two disease-causing *CFTR* mutations, and a sweat chloride concentration > 60 mM with most CF infants also having pancreatic insufficiency as measured by fecal elastase-1 assay at NSO. Age-matched and normal birthweight screen-negative/healthy neonates (*n*=30) had normal IRT levels and were also screen-negative for all other IEM in the expanded NBS panel at NSO. Stored DBS cut-out specimens from CF neonates were collected between January 2013 and December 2014, whereas screen-negative DBS samples were collected in October 2014 and frozen at -80°C since they are not routinely stored at NSO.

For the second stage of the work, duplicate punches of CF-affected neonates (*n* = 10) were selected using the aforementioned criteria and collected between December 2013 and September 2015. Duplicate punches of screen-positive/presumptive CF neonates, who were confirmed as unaffected carriers (*n*=30) were selected based on IRT > 96thcentile, one *CFTR* mutation (*n* = 20 with one ΔF508 mutation and *n* = 10 with one non-ΔF508 mutation), and a sweat chloride < 29 mM. These samples were collected between July 2013 and July

2015. Additionally, a set of screen-positive/presumptive CF cases (*n*=30) but confirmed as unaffected hypertrypsinogenics (IRT > 99.9thcentile, but 0 *CFTR* mutations detected within 39+4 panel and a sweat chloride < 29 mM) were collected between August 2013 and October 2015. Duplicate punches of screen-negative DBS samples (*n* = 10) were also collected in October 2014 as previously mentioned were also included in this cohort. A third batch of samples (*n*=18), collected between August 2013 and October 2015 contained CF-positive (*n*=2), unaffected carriers (*n*=7), hypertrypsinogenics (*n*=5), screen-negatives (*n*=4) were analyzed and will be included with the training set data at a later date.

3.3.3 Blood Spot Collection and Sample Workup

Metabolites were extracted from the filter paper disks by solvent extraction. Disks were placed in 0.5 mL centrifuge tubes containing 100 µL of a 75% *v* methanol solution containing 10 µM of 4-fluoro-*L*-phenylalanine (F-Phe) as an internal standard. Disks were sonicated for 15 min and the extraction solution was then filtered through a Nanosep 3K Omega (3kDa MWCO) ultracentrifugation tube (Pall Life Sciences, MI, USA) at 14,000 *g* for 15 min to deproteinize the samples. The filtrate was evaporated to dryness at room temperature in a Vacufuge vacuum concentrator (Eppendorf Inc., New York, USA). DBS extracts were then reconstituted in 30 µL of distilled, deionized water containing 15% *v* acetonitrile, 10 µM 3-chloro-*L*-tyrosine (Cl-Tyr) as a backup internal standard. An internal quality control (QC) and reference sample was prepared in-house by pooling together DBS extracts from one disk of each screen-

negative pediatric sample (n = 30) from the initial study. Separate QC aliquots were stored at -80°C and each aliquot was thawed once prior to each analysis.

3.3.4 MSI-CE-MS with Temporal Signal Pattern Recognition

The seven-segment MSI-CE-MS serial injection format[57] was used to discover metabolites of interest in cystic fibrosis. Asymmetric pattern recognition was used to unambiguously identify differentiating metabolites with a high degree of confidence, as previously described. [54] Briefly, duplicate injections (or pairs) of three distinct samples were analyzed alongside the screen-negative QC control. The first sample pair was injected in a 1:2 pattern, the second sample was injected in a 1:1 pattern, and the final sample was injected on a 2:1 pattern. The QC is assigned to position 1, 3, 5 or 7 so as to not interfere with a sample pair. The asymmetric pattern of dilutions used for each pair of samples encodes sample information within the resulting data, permitting facile and unambiguous localization of elevated and/or unique metabolites to a particular sample. Samples were randomized to a particular run and, within each run, both the injection position and the position of the QC control were randomized to prevent any positional bias. This method was previously validated on both proficiency testing DBS from the Centres for Disease Control and Prevention's Newborn Screening Quality Assurance Program and authentic neonatal DBS collected and analyzed by DI-MS/MS at NSO. Acceptable precision and accuracy were obtained for quantification by MSI-CE-MS.[54]

3.3.5 Separations and Instrumentation

All runs, including MS/MS analyses, were performed on an Agilent 6550 QTOF-MS running Agilent MassHunter Workstation LC/MS Data Acquisition Software version B.05.01. All data processing was performed using MassHunter Qualitative Analysis Software version B.06.00. All CE separations were performed with 30kV of applied voltage at 25°C using uncoated fused-silica capillaries (Polymicro Technologies, AZ, USA) with 50 μM ID and a total length 110 cm. A BGE consisting of 1 M formic acid, 15% *v* acetonitrile, pH 1.8 was used. A series of 50 mbar hydrodynamic injections was used, alternating between a 5 s injection of sample and a 40 s injection of BGE for a total of seven discrete sample injections within a single run.[57] The capillary was flushed with BGE at 950 mbar for 15 min between each run. An Agilent 1260 Infinity isocratic pump was used to deliver a sheath liquid consisting of 60:40 MeOH:H_2O with 0.1% formic acid supplied at a rate of 10 μL/min. For real-time internal reference mass correction, the reference masses purine, hexamethoxyphosphazine and hexakis(2,2,3,3-tetraflurorpropoxy) phosphazine (HP-921) were spiked into the sheath liquid at 0.02% *v* to provide reference ions at *m/z* 121.0509 and *m/z* 922.0098. For analysis of all individual DBS samples, the QTOF-MS was operated as a full scan MS in 4GHz HiRes acquisition mode with a mass range of *m/z* 50-1700 and a scan rate of 1 Hz. The source parameters for the dual AJS ESI were as follows: dry gas = 16 L/min at 200°C, nebulizer = 8 psi, sheath gas = 3.5 L/min @ 199°C, VCap = 2000 V, Nozzle voltage = 2000 V, fragmentor = 380 V,

skimmer = 65 V, Oct 1 RF = 750 V. At the start of each day, the QTOF was mass calibrated in positive ion mode and the spray chamber of the ion source and CE inlet electode were cleaned with isopropanol:water (50:50) to prevent sample carryover and salt buildup. As part of quality assurance practices, each day of sample analysis began with one run of a seven serial injections of an amino acid standard mixture followed by one run of seven serial pooled QC injections to ensure instrumental performance was satisfactory.

3.3.6 Nontargeted Metabolomics of DBS Extracts

Data from targeted analysis of metabolites previously determined to be detectable in DBS extracts[54] were combined with results from untargeted metabolite profiling using the MassHunter Molecular Feature Extractor (MFE) algorithm. A migration time window was set to avoid picking peaks in the salt front and the electroosmotic flow/neutral zone (EOF) as ion suppression is great in these regions. A minimum of 300 counts was used as a threshold for a molecular feature to be extracted to ensure that low abundance features were included and +H, +Na -H_2O species were included. Manual filtering of known in-source fragments and adducts from a curated in-house list and was also performed to avoid inclusion of redundant signals. A molecular feature was then considered to be a definitive and sample-derived metabolite if it was not present in a blank extract, if it showed the appropriate asymmetric dilution (i.e. is sample- and not matrix-derived) and the signal is adequately reproducible in the QC samples (*CV* < 40%) in MSI-CE-MS. [57] All resultant compounds from DBS extracts were

defined by their characteristic mass-to-charge ratio and migration time relative to F-Phe (*m/*z:RMT) as a paired variable and were included in the final data matrix if present in > 75% of runs. All peaks were normalized to 10 µM F-phe and reported as relative peak areas (RPA). RPA for the duplicate injections were averaged to give a single measurement for each metabolite in every sample. Non-detectable peaks (*i.e.* < LOD) were replaced with half of the minimum value for that metabolite. The original data derived from three separate batches of runs was then batch-corrected using the BatchCorrMetabolomics package[58] in R-Studio (R-Studio) which corrects for between-batch variation using the randomized QC injection included in every run in MSI-CE-MS, which was critical when adjusting for long-term system drift even when applying daily preventative maintenance and mass tuning procedures

3.3.7 MS/MS for Unknown Identification

Unknown metabolites of significance were fragmented using high resolution, accurate tandem mass spectrometry (MS/MS) in order to facilitate structural identification. To ensure a strong precursor ion signal, CE-MS with on-line sample preconcentration by transient isotachophoresis was performed by injecting a single plug of DBS extract for 90 s followed by 60 s of background electrolyte (BGE). Prior to the injection, samples were diluted 2-fold in 400 mM ammonium acetate at pH 5.0. Precursor ions were fragmented by collision induced dissociation (CID) at three fixed collision energies of 10, 20 and 40 V. Either a CID-averaged product ion spectrum or a product ion spectrum at an

optimal voltage that resulted in near-complete fragmentation of the molecular ion was used for spectral interpretation. The Find by Targeted MS/MS algorithm in MassHunter was used to find compounds and subsequent structural elucidation was performed by searching the METLIN database via the MassHunter Personal Compound Database and Library (PCDL) manager with a minimum forward search score of 25 and a minimum reverse score of 80. If no database match existed in the METLIN PCDL, the compound was manually annotated using the fragment similarity and neutral loss search tools from the METLIN online database (http://metlin.scripps.edu).

3.3.8 Quantification of IRT and Mutational Analysis for CF Screening

All samples sent to Newborn Screening Ontario (NSO) as part of routine newborn screening (NBS) for CF were analyzed by a 1235 AutoDELFIA automatic immunoreactive assay (Perkin Elmer) containing two monoclonal antibodies, one of which is labelled with europium. Briefly, each DBS is placed in a well containing immobilized antibodies which are directed against specific antigen sites on the IRT molecule. The Enhancement Solution is added to each well to dissociate the europium and form fluorescent chelates. The fluorescence is measured and is proportional to IRT concentration. Mutations in the *CFTR* gene are assayed by the xTag Cystic Fibrosis Kit v2.0 and a Luminex 200 xMAP instrument (Luminex Corp). Briefly, a DBS punch is extracted in PCR buffer and 16 regions of the *CFTR* gene are amplified. A total of 86 universally-tagged primers are added to allow for allele specific primer extension (ASPE) and

incorporation of biotin-labeled dCTP nucleotides. Fluorescent beads, each spectrally corresponding to each of the 39 pathogenic alleles + 4 variants are added and bind to complementary sequences on the ASPE products. The addition of Streptavidin-R-Phycoerythrin causes the phycoerythrin moieties to fluoresce which can identify the presence or absence of wild-type and/or mutant alleles.

3.3.9 Quantification of Metabolites by Stable-Isotope Dilution FIA-MS/MS and LC-MS/MS

All DBS specimens sent to Newborn Screening Ontario (NSO) as part of routine newborn screening (NBS) were extracted and analyzed by FIA-MS/MS according to standard operating procedures in an accredited laboratory as previously described.[54] Briefly, 3.2 mm diameter punches from newborn DBS specimens were placed into 96 well plates and, following a methanol-based extraction, the solution is transferred to a new plate and derivatized by butylation under acidic conditions along with stable-isotope internal standards for all relevant amino acids and acylcarnitines using the PerkinElmer Neogram kit. Extracts were analyzed in positive ion mode using a Waters 2777c autosampler, 1525u binary HPLC pump and TQD Tandem Mass Spectrometer with ESI. A 10 µL sample was injected using an 80% acetonitrile mobile phase with an initial isocratic flow rate of 0.140 mL/min for a total runtime of 1.50 min. All amino acids were quantified using neutral loss scanning of 102 Da, whereas butylated acylcarnitines were quantified using a parent ion scan for *m/z* 85 and/or multiple reaction monitoring (MRM). The source temperature was 120°C, capillary voltage was 3.5 kV, desolvation gas flow was 600 L/h and desolvation temperature was

250°C. Data was acquired and analyzed using MassLynx v4.1 and NeoLynx. In total, 44 metabolites were analyzed at NSO as outlined in **Table S3.4.**

3.3.10 Statistical and Computational Analysis

All electropherograms were processed using Igor Pro 5.0 software (Wavemetric Inc., Lake Oswego, OR, USA). All analyte peak areas were normalized to the internal standard F-Phe prior to statistical analysis. Data from all stages were combined and subjected to batch correction based on QCs using the BatchCorrMetabolomics package[58] in R-Studio (R-Studio). Data was *log*-transformed and autoscaled prior to multivariate statistical analysis, including unsupervised principal component analysis (PCA) and supervised partial least squares-discriminant analysis (PLS-DA) using Metaboanalyst 3.0.[59] Non-parametric tests Mann-Whitney *U* test and Kruskal-Wallis tests, as well as Spearman rank correlation analysis were performed in SPSS/PASW 18 (SPSS Inc. Released 2009. PASW Statistics for Windows, Version 18.0. Chicago: SPSS Inc.) as data was not normally distributed. Also, receiver operating characteristic (ROC) curves were performed using MedCalc for Windows, version 12.5.0.0 (MedCalc Software, Ostend, Belgium) for evaluating the predictive accuracy of top-ranked single or ratiometric metabolites when classifying CF cases from screen-negative/healthy or screen-positive yet unaffected neonates.

3.4 Results

3.4.1 Study Design, Metabolite Profiling of DBS Extracts and Batch Correction

Metabolomic studies were conducted using a validated MSI-CE-MS protocol and accelerated data workflow for biomarker discovery based on a single 3.2 mm diameter DBS cut-out specimen[54] stored frozen (-80°C) at Newborn Screening Ontario (NSO) from 2012-2014. A retrospective case-control study was performed by analysis of DBS filtrate extracts (75% *v/v* MeOH) at three stages over a period of two years (2015-2016) from a cohort of normal birthweight/gestational age CF infants without meconium ileus (*n*=34) relative to screen-negative/healthy infants (*n*=40), and screen-positive yet unaffected infants (*n*=60) defined by a two-tiered IRT/DNA algorithm, and later confirmed by sweat chloride testing at CF clinics at regional pediatric hospitals. In the province of Ontario, which has a CF incidence of about 1:3600, screen-positive infants with presumptive CF are classified within three categories according to both IRT levels and mutational status (a 39 *CFTR* mutation panel, including 3 variants are used at NSO), namely category A (IRT > 96th percentile + 2 mutations) category B (IRT > 96th percentile + 1 mutation) and category C (IRT > 99.9th percentile + 0 mutations).[60] **Table 3.1** summarizes the characteristics of a cohort of sex-balanced and normal birth weight neonates, with CF infants confirmed with two disease-causing *CFTR* mutations (majority were homozygous or compound heterozygous for delF508; 32 of 34), high sweat chloride (> 60 mM) and pancreatic insufficient

Table 3.1. Study cohort information for metabolomics study of CF screen-positive and screen-negative neonates based on a "two-tiered" IRT/DNA algorithm followed by sweat chloride.

Variable[a]	**True CF (*n*=34)**	**Carriers (*n*=30)**	**Hyper-trypsinogenic (*n*=30)**	**Screen negative (*n*=40)**
Sex				
Female (#)	17	15	19	20
Male (#)	17	15	11	20
Birth weight (g) mean ± SD	3220 ± 490	3460 ± 430	3620 ± 360	3460 ± 450
IRT (ng/mL) median ± IQR	179 ± 140	59 ± 29	175 ± 63	16.2 ± 9.6
Sweat Cl^- (mmol/L)[b] median ± IQR	87 ± 10	13 ± 5	10 ± 2	*n/a*
CFTR genotype[c]				
0 mutations	--	--	30	40
1 mutation: ΔF508/-	--	20	--	--
1 mutation: other/-	--	10	--	--
2 mutations: ΔF508/ΔF508	23	--	--	--
2 mutations: ΔF508/other	9	--	--	--
2 mutations: other/other	2	--	--	--
Pancreatic Status[d]				
Sufficient	1	*n/a*	*n/a*	*n/a*
Insufficient	33			

[a] *All major variables were tested for normality using a Shapiro-Wilks test and only birthweight was significant ($p < 0.05$)*
[b] *Standardized pilocarpine-stimulated iontophoresis using macrobore collectors were used for confirmatory diagnosis of all presumptive CF cases at regional CF clinics in the province of Ontario.*
[c] *NSO uses a 39 CFTR mutation panel, including 4 variants in a two-tier IRT/DNA algorithm for CF detection in the population.*
[d] *Fecal elastase-1 measurements performed to assess pancreas status of confirmed CF cases with high sweat chloride at regional CF clinics in the province of Ontario using a cut-off of 100 µg/g for pancreatic insufficiency.*

33 of 34) based on fecal elastase-1 below cut-off levels (< 100 µg/g). In contrast, other CF presumptive neonates who were unlikely unaffected (*i.e.* carriers and

hypertrypsinogenics, collectively referred to as SP/non-CF) had sweat chloride well below cut-off levels (< 29 mM), whereas screen-negative/healthy neonate controls had IRT concentrations within normal reference ranges. Most carriers were identified with one delF508 mutation (20 out of 30) or another less prevalent mutation of variable consequence. The first stage for metabolomic studies of DBS extracts were performed on confirmed CF cases and screen-negative controls (May 2015) followed by a second (June 2016) and a third (October 2016) batch of runs involving the analysis of confirmed CF cases, screen-negatives and SP/non-CF controls. To ensure that runs from each stage of this study could be directly compared despite the potential for long-term system drift in MS-based metabolomic studies,[58] additional DBS cut-outs from a cohort of screen-negative controls (*n*=30) were used to create a series of pooled quality control (QC) aliquots that was included in all batches of runs analyzed throughout this study. In this case, MSI-CE-MS with temporal signal pattern recognition was used as the primary discovery-based platform for metabolomics as it offers higher sample throughput with quality assurance when analyzing volume-restricted biospecimens, such as 3.2 mm diameter DBS extracts comprising about 3.4 μL of dried whole blood.[54] A major advantage of this multiplexed separation platform is that unique data workflows can be applied involving a serial injection of seven or more sample plugs for unambiguous identification of putative biomarkers since disease controls and healthy references (*i.e.,* pooled QC) are analyzed within the same run.[54] In this case all DBS extracts were analyzed in duplicate and randomly

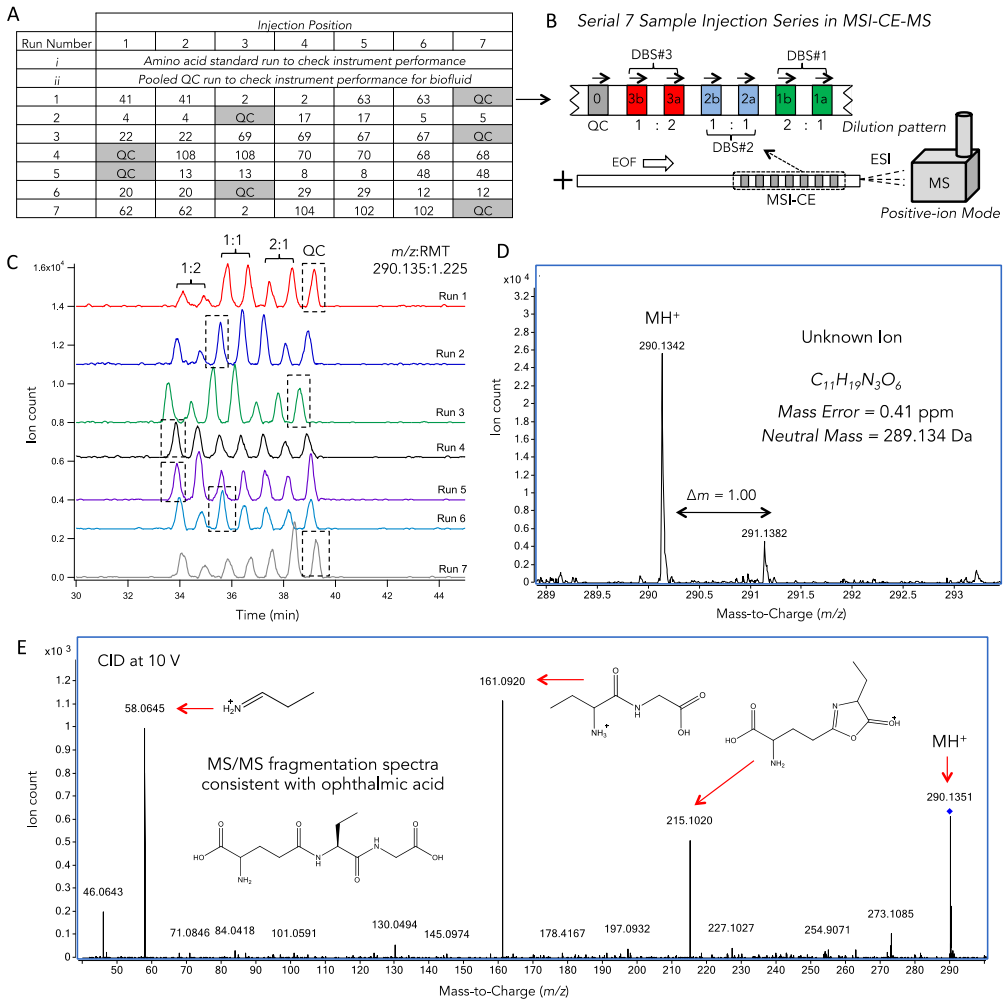

Figure 3.1. (A) A representative data workflow when using MSI-CE-MS with temporal signal pattern recognition based on a randomized injection series of three pairs of DBS extracts together with a pooled QC with each run. (B) A schematic depicting the 7 plug serial injection series used in MSI-CE-MS (*e.g.*, shown for run 1), where each pair of DBS extract is injected in duplicate, but encoded by a unique dilution pattern to facilitate peak assignment with quality assurance. (C) A series of extracted ion electropherograms for a batch of runs by MSI-CE-MS under positive ion mode detection for an unknown ion annotated by its characteristic *m/z*:RMT that was selected after a dilution trend filter and QC check. (D) A full-scan high resolution mass spectrum for the single charged protonated molecule (MH^+) with low mass error (< 1 ppm) and most likely molecular formula. (E) Structural elucidation of unknown ion after collision-induced dissociation (CID) of precursor ion resulting in formation of three characteristic product ions that was consistent with ophthalmic acid.[62]

assigned to both an injection position and a run number with a QC also randomly included within each run (**Fig. 3.1A**) with all experiments performed under full-

scan mass spectral acquisition under positive ion mode detection (**Fig. 3.1B**). A series of extracted ion electropherograms (EIE) for an unknown ion denoted by its characteristic mass-to-charge and relative migration time (*m/z*:RMT) are depicted in **Fig. 3.1C** over a full day of data acquisition involving a block of seven runs prior to running of daily standard metabolite mixture and a QC run with blank to confirm system performance. Overall, a total of 70 cationic metabolites were detected reliably (*CV* < 40%) in majority of DBS extracts (> 75%) after performing a dilution trend filter in MSI-CE-MS[57,61] to rigorously eliminate redundant fragments/adducts, spurious peaks and/or background signals. This conservative approach to peak selection and data filtering in metabolomics was used to minimize false discoveries and data overfitting by focusing on consistently measurable yet authentic metabolites detected from a majority of neonatal DBS extracts. All known metabolites were identified by spiking with authentic standards (if available), whereas unknown metabolites of significance were characterized by high resolution, accurate MS (*i.e.*, charge state and most likely molecular formula) and MS/MS (*i.e.*, structural elucidation of characteristic product ions and neutral losses) as shown for ophthalmic acid in **Fig. 3.1D** and **E**.

During the time period between completing data acquisition of all three batches of retrospective DBS specimens by MSI-CE-MS, the quadrupole-time-of-flight (QTOF) mass spectrometer underwent a full preventative maintenance service and a detector replacement, which likely contributed to long-term system drift as evident in a control chart profile of QC runs (*n*=54). For instance, a 2D

scores plot of a principal component analysis (PCA) of original datasets highlighted three distinct clusters of QC from each batch of run with poor technical precision as reflected by a median *CV* = 21% for 70 metabolites as compared to overall biological variance for screen-positive CF and screen-negative neonates of about *CV* = 40% (**Fig. S3.1A**). Upon further investigation, it was apparent that the extent of system drift was metabolite dependent as shown by representative control charts for glycine (Gly), carnitine (C0) and *N*-glycated glutamic acid (Glc-Glu) plotted as a function of batch/date and injection number (**Fig. S3.1B**). However, the batch-to-batch variability for both Gly and C0 were both reduced significantly with a median *CV* < 10% following application of an optimal QC-based batch correction algorithm while the random/non-systemic variation shown for Glc-Glu was maintained (**Fig. S3.2C**). Overall, the experimental/batch-related variability in the repeat QC samples was reduced by 66%, whereas the natural biological/non-batch variation in the original data set was largely preserved (**Fig. S3.1D**).

3.4.2 Metabolic Phenotype of True CF Neonates as Compared to Screen-negative Controls

A 2D scores plot from PCA of the batch-corrected data is depicted in **Fig. 3.2A** which provides an overview of the improved data structure following batch correction as reflected by a single tight cluster of QC samples (*n*=54) analyzed over a two year period with a median *CV* = 11% as a measure of long-term technical precision. In contrast, individual DBS extracts from a cohort of screen-positive (SP)/presumptive CF (*n*=94) and screen-negative (SN)/healthy neonates

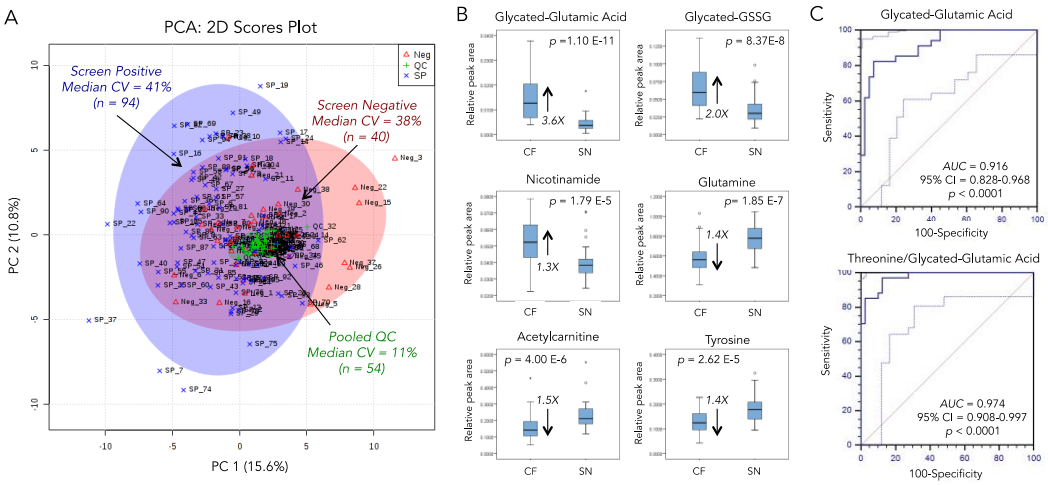

Figure 3.2. (A) A 2D PCA score plot provides an overview of the metabolic phenotype of neonates in terms of their biological variance (*CV* = 40%) relative to technical variance (*CV* = 11%) (based on repeated analysis of QC in every run) measured for 70 polar/ionic metabolites from DBS extracts in both screen-positive CF and screen-negative controls. (B) 29 different metabolites were significantly different in CF infants (confirmed with high sweat chloride, > 60 mM, *n*=34) as compared to healthy/screen-negative controls (*n*=40; refer to Table 1), including elevations in *N*-glycated amino acids, oxidized glutathione and nicotinamide, as well as lower amino acids and acetylcarnitine. Excellent classification of CF infants (*n*=34) from healthy controls (*n*=40) was demonstrated by *single or ratiometric* biomarkers of CF based on ROC curves as reflected by an *AUC* > 0.920

(*n*=40) reveal a greater extent of biological variability with a median *CV* of 41% and 38%, respectively. The first stage of this study focused on the identification of metabolites capable of differentiating between asymptomatic CF neonates relative to age/sex-matched healthy neonates based on their characteristic metabolic phenotype as measured from their DBS extracts. All confirmed CF infants without meconium ileus were detected based on a two-tiered IRT/DNA screening algorithm at NSO and later confirmed with a high sweat chloride (> 60 mM) with pancreatic insufficiency (with exception of one CF case) at regional pediatric hospitals in the province of Ontario. No pre-term/critically ill infants were included in this study and all neonates were of normal gestational age (38-42

weeks) range with birth weight (above a cutoff of 2,500 g). Since the relative ion responses for metabolites defined by their *m/z*:RMT and compound name (if identified) were not normally distributed even following a *log*-transformation (Shapiro-Wilk $p < 0.05$), non-parametric statistical analysis was largely performed on non-transformed data in this study. Overall, 29 metabolites (out of 70) were differentially expressed in CF neonates as compared to healthy controls using a Benjamini-Hochberg false discovery rate (FDR) correction ($q < 0.05$) as listed in **Table 3.2**. Also, **Fig. 3.2B** depicts box-whisker plots for some of the most discriminating metabolites associated with CF neonates, which included higher levels of *N*-glycated glutamic acid (Glc-Glu), a glycated oxidized glutathione (Glc-GSSG), and nicotinamide, as well as lower levels of glutamine (Gln), tyrosine (Tyr), and *O*-acetyl-*L*-carnitine (C2). The identification of *N*-glycated amino acids were confirmed by high resolution, accurate MS/MS.[54] **Fig. 3.3A** shows a full-scan TOF-MS spectra for Glc-GSSG, highlighting that the protonated molecule [MH_2^{2+}] had a charge state of $z = 2$. Also, the addition of the reducing agent dithiothreitol (DTT) to DBS extract led to complete attenuation of the signal for the protonated molecule, confirming the unknown ion was a mixed oxidized glutathione with the formation of reduced glutathione (GSH, *m/z* 308.091, MH^+) along with a new protonated molecule not present in original DBS extract (*m/z* 470.1438; MH^+) (**Fig. 3.3B**), while fragmentation of the precursor ion using MS/MS confirmed a neutral loss of a hexose (*m/z* 162.053) and a low signal

Table 3.2. Mann-Whitney *U* test to rank metabolites from DBS extracts that were significantly different ($q < 0.05$) in CF ($n = 34$) relative to screen-negative ($n = 40$) neonates by MSI-CE-MS.

Metabolite ID	*m/z*:RMT	Mass Error (ppm)	*p*-value	FDR *q*-value	Effect Size	FC (CF/Neg.)[c]
Glc-Glutamic acid[b]	310.115:1.430	3.39	1.10 E-11[a]	7.62 E-10	0.739	3.58
Glc-Glutamine[b]	309.129:1.421	-1.49	1.58 E-09[a]	5.46 E-08	0.674	3.00
Glc-Leucine[b]	294.155:1.283	-2.98	7.77 E-08[a]	1.44 E-06	0.611	3.92
Glc-GSSG[b]	388.109:1.300	-0.81	8.37 E-08[a]	1.44 E-06	0.610	1.99
Glutamine	147.076:0.960	-1.39	1.85 E-07[a]	2.56 E-06	0.595	0.74
Threonine	120.066:0.930	0.24	1.31 E-06[a]	1.51 E-05	0.558	0.70
Glc-Glycine[b]	238.092:1.175	1.14	2.17 E-06[a]	2.14 E-05	0.547	2.14
Acetylcarnitine	204.123:0.791	-1.05	4.00 E-06[a]	3.45 E-05	0.534	0.68
Oxidized Glutathione	307.083:1.109	-2.92	6.83 E-06[a]	5.23 E-05	0.522	0.76
Nicotinamide	123.055:0.650	0.31	1.79 E-05[a]	1.24 E-04	0.500	1.33
Tyrosine	182.081:1.015	-0.60	2.62 E-05[a]	1.64 E-04	0.491	0.72
Histidine	156.077:0.630	-0.58	3.42 E-05[a]	1.97 E-04	0.484	0.71
3-Methylhistidine	170.092:0.648	-0.17	2.83 E-04[a]	1.50 E-03	0.428	0.75
Glycine	76.039:0.720	0.13	3.71 E-04[a]	1.83 E-03	0.420	0.81
Ornithine	133.097:0.582	0.18	6.27 E-04[a]	2.88 E-03	0.405	0.77
Asparagine	133.061:0.930	0.82	8.08 E-04	3.49 E-03	0.397	0.83
Serine	106.050:0.880	0.45	1.04 E-03	4.21 E-03	0.389	0.74
Proline	116.071:0.952	0.25	1.96 E-03	7.52 E-03	0.368	0.86
Methionine	150.058:0.941	-0.1	2.47 E-03	8.96 E-03	0.360	0.84
Lysine	147.113:0.585	-0.74	5.12 E-03	1.74 E-02	0.395	0.85
Unknown $M+2H^{2+}$	521.798:0.970	1.78	5.30 E-03	1.74 E-02	0.333	1.17
Unknown	357.249:0.651	0.11	6.98 E-03	2.19 E-02	0.323	0.79
Unknown	162.076:0.795	-0.06	7.72 E-03	2.30 E-02	0.319	1.22
Homoarginine*	189.135:0.612	0.58	7.99 E-03	2.30 E-02	0.317	0.69
Ophthalmic Acid	290.135:1.225	0.41	8.82 E-03	2.43 E-02	0.313	0.78
Unknown $M+3H^{3+}$	438.258:0.833	-0.03	1.30 E-02	3.45 E-02	0.298	1.15
Unknown	123.594:0.577	0.73	1.72 E-02	4.36 E-02	0.286	0.84
Unknown	161.129:0.603	1.83	1.77 E-02	4.36 E-02	0.285	0.72
Kynurenine	209.092:0.919	0.80	2.05 E-02	4.89 E-02	0.278	0.99

[a] *These metabolites were significant after a Bonferroni correction ($p < 0.000725$)*
[b] *Identification based on accurate mass match and MS/MS fragmentation patterns (DiBattista et al, Anal. Chem. 2017, 89, 8112)*
[c] *Fold-change (FC) was calculated as the ratio of the median of CF-affected to screen-negative neonates*
** Tentative identification based on accurate mass match from Human Metabolome Database within 5 ppm mass error*

for GSSG (*m/z* 307.0833) as a product ion. Collectively, MS and MS/MS spectral assignments and chemical reactivity studies indicate that the unknown divalent ion was an *N*-glycated glycine mixed oxidized glutathione (Glc-GSSG) as shown in **Fig. 3.3C**. Overall, 15 of the 29 top-ranked metabolites ($q < 0.05$) associated with CF neonates also satisfied a Bonferroni adjustment ($p < 7.25$ E-5) with moderate (> 0.400) to strong (> 0.600) effect sizes as summarized in **Table 3.2**. Additionally, **Fig. 3.2C** depicts receiver operating characteristic (ROC) curves for the top performing single marker (Glc-Glu) and ratiometric marker (Thr/Glc-Glu) demonstrating excellent discrimination of CF neonates from healthy controls ($p <$ 0.0001) with an area under the curve (*AUC*) > 0.900.

3.4.3 Differentiation of Affected Neonates from Likely Unaffected CF Screen-Positive Cases

Given that CF affected neonates have measurable metabolic phenotype differences relative to healthy neonates, the second stage of this study explored the ability of a metabolite panel from DBS extracts to differentiate true CF (category A) from SP/non-CF. The latter group of neonates comprised likely unaffected carriers (category B) and hypertrypsinogenemic (category C) cases, who were all identified as presumptive CF when using a two-tiered IRT/DNA algorithm at NSO. **Fig. S3.2** depicts a 2D scores plot from a partial least squares-

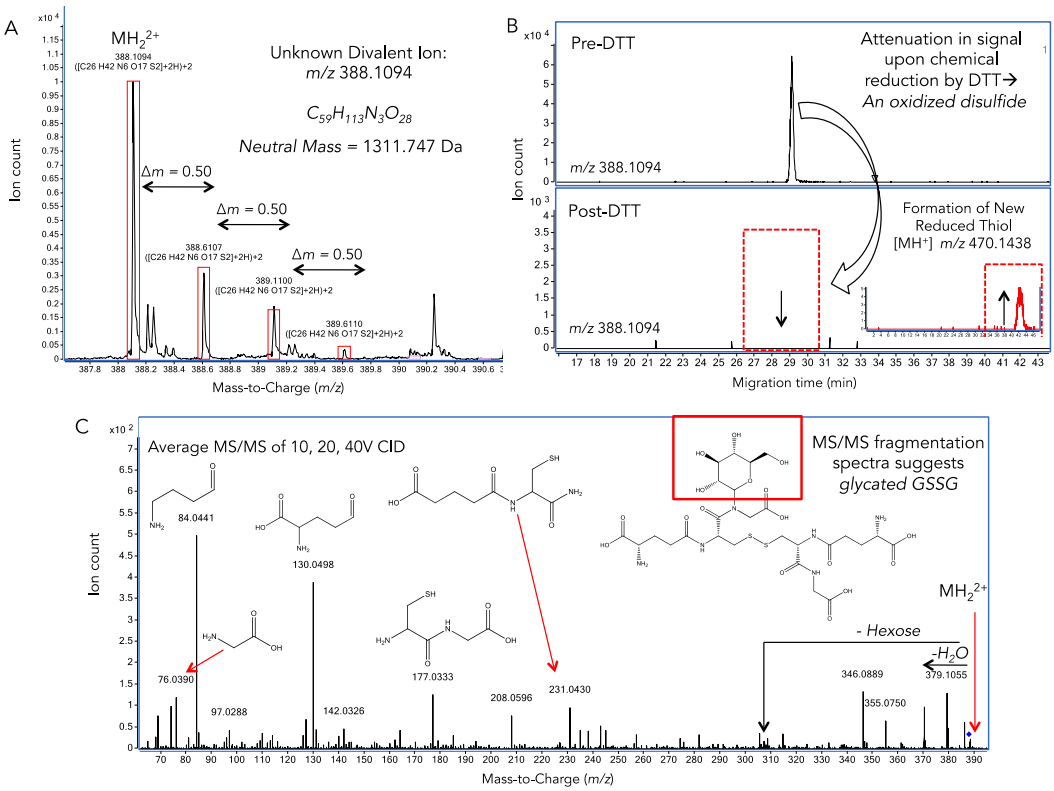

Figure 3.3. Structural elucidation of an unknown modified glutathione analog in DBS extracts based on (A) its most likely molecular formula for the divalent protonated molecule (MH_2^{2+}) based on its accurate mass, charge state and isotopic pattern, (B) specific chemical reactivity to excess DTT, confirming it as a mixed oxidized disulfide that resulted in complete attenuation of its signal together with formation of reduced glutathione (GSH, *m/z* 308.091, MH^+) and a late migrating reduced thiol analog (*m/z* 470.144, MH^+) not originally detected in DBS extract, and (C) collision-induced dissociation of the precursor ion generating a MS/MS fragmentation spectrum that is consistent with a mixed oxidized glutathione disulfide with a modified *N*-glycated glycine residue.

discriminate analysis (PLS-DA) together with VIP score ranking for the top 10 ranked metabolites (VIP scores > 1.5) associated with CF neonates as reflected by their box-whisker plots and ROC curves. Similarly, **Table 3.3** summarizes the results from a Mann-Whitney *U* test (without data transformation) demonstrating that 16 metabolites from DBS extracts were differentially expressed ($q < 0.05$, FDR) in CF neonates (n=34) as compared to unaffected screen-positives (n=60), including 6 metabolites that satisfied a Bonferroni adjustment ($p < 7.25$ E-5) with

Table 3.3. Mann-Whitney U test to rank metabolites from DBS extracts that were significantly different ($q < 0.05$) in CF infants ($n = 34$) relative to screen-positive CF yet unaffected neonates ($n = 60$) when using non-targeted metabolite profiling by MSI-CE-MS.

Metabolite ID	*m/z*:RMT	Mass Error (ppm)	*p*-value	FDR *q*-value	Effect Size	FC [b] (CF/ nonCF)
Unknown M+3H^{3+} [c]	438.258:0.833	-0.03	5.89 E-05 [a]	2.58 E-03	0.484	1.22
Ophthalmic Acid [c]	290.135:1.225	0.41	2.27 E-04 [a]	5.79E-03	0.444	0.81
Threonine [c]	120.066:0.930	0.24	3.93 E-04 [a]	6.03E-03	0.427	0.80
Proline [c]	116.071:0.952	0.25	5.76 E-04 [a]	6.03 E-03	0.415	0.91
Serine [c]	106.050:0.880	0.45	6.11 E-04 [a]	6.03 E-03	0.413	0.76
Tyrosine [c]	182.081:1.015	-0.60	6.47 E-04 [a]	6.03 E-03	0.411	0.77
Alanine	90.055:0.782	0.32	1.42 E-03	1.20 E-02	0.384	0.81
Asparagine [c]	133.061:0.930	0.82	1.67 E-03	1.25 E-02	0.379	0.90
Glutamine [c]	147.076:0.960	-1.39	2.55 E-03	1.74 E-02	0.364	0.83
3-Methylhistidine [c]	170.092:0.648	-0.17	4.13 E-03	2.60 E-02	0.346	0.83
Lysine [c]	146.118:0.700	0.03	6.71 E-03	3.42 E-02	0.327	0.97
Arginine	175.119:0.608	-0.14	6.71 E-03	3.42 E-02	0.327	0.70
Glycine [c]	76.039:0.720	0.13	6.87 E-03	3.42 E-02	0.326	0.85
Aminoisobutyric acid*	104.071:0.834	-0.46	8.68 E-03	4.05 E-02	0.316	0.86
Unknown M+2H^{2+}	179.129:0.651	3.99	9.74 E-03	4.26 E-02	0.312	0.88
Creatine	132.077:0.768	-1.69	1.04 E-02	4.49 E-02	0.307	0.89

[a] *These p-values are significant after a Bonferroni correction ($p < 0.000725$).*
[b] *Fold-change (FC) is calculated as the ratio of the median of CF relative to likely unaffected neonate.*
[c] *These metabolites are also significantly different between CF infants and screen-negative controls.*
** Tentative identification based on accurate mass match in Human Metabolome Database.*

moderate effect sizes (> 0.400). These CF-specific metabolites corresponded primarily to amino acids that were consistently lower in CF neonates (*e.g.*, Thr, Ser, Pro, Tyr, Gln) similar to results measured in healthy neonates (**Table 3.2**). However, the two most significant CF-specific biomarkers were ophthalmic acid, which is a tripeptide and glutathione analog, where the cysteine is substituted with 2-aminobutyric acid that was lower in CF affected infants (fold-change, $FC = 0.81$; $p = 2.27$ E-4), whereas an unknown ion (*m/z* 438.258) was significantly

elevated in CF neonates (*FC* = 1.22; *p* = 5.89 E-5). **Fig. 3.4** confirms that this CF-specific unknown metabolite was detected as a trivalent protonated molecule [MH_3^{3+}] that was not reactive to DTT, and its MS/MS fragmentation spectra was largely consistent with a polypeptide with neutral mass of 1311.75 Da. However, its exact molecular structure remains unclear following an extensive database search in open access metabolomic spectral libraries (*e.g.,* Metlin, HMDB). Ophthalmic acid (OPA) was putatively identified based on high resolution, accurate MS, a lack of signal attenuation upon DTT addition, confirming that the ion did not correspond to an oxidized disulfide, whereas its MS/MS fragmentation was consistent with three diagnostic product ions reported for ophthalmic acid by Soga *et al.*[62] (**Fig. 3.1C**). **Table S3.1** summarizes the results of the Kruskal-Wallis test and pair-wise Mann-Whitney *U* tests when comparing true CF neonates with both SP/non-CF and screen-negative/healthy controls, including 31 significant metabolites ($q < 0.05$) detected in DBS extracts by MSI-CE-MS, as well as IRT (ng/mL) concentrations measured independently by standard fluorescence-based immunoassays at NSO. Interestingly, all *N*-glycated amino acids (*e.g.*, Glc-Glu, Glc-Gln, Glc-Leu/Ile, Glc-GSSG, Glc-Gly) and aminoadipic acid were significantly elevated in both CF and SP/Non-CF cases relative to healthy neonates, whereas certain amino acids (Orn, His, Gln, Lys), nicotinamide, GSSG and acetylcarnitine were significantly depleted in all presumptive CF cases relative to screen-negatives, though Gln was also depleted in CF relative to SP/non-CF cases. All metabolites are annotated by their characteristic *m/z*:RMT,

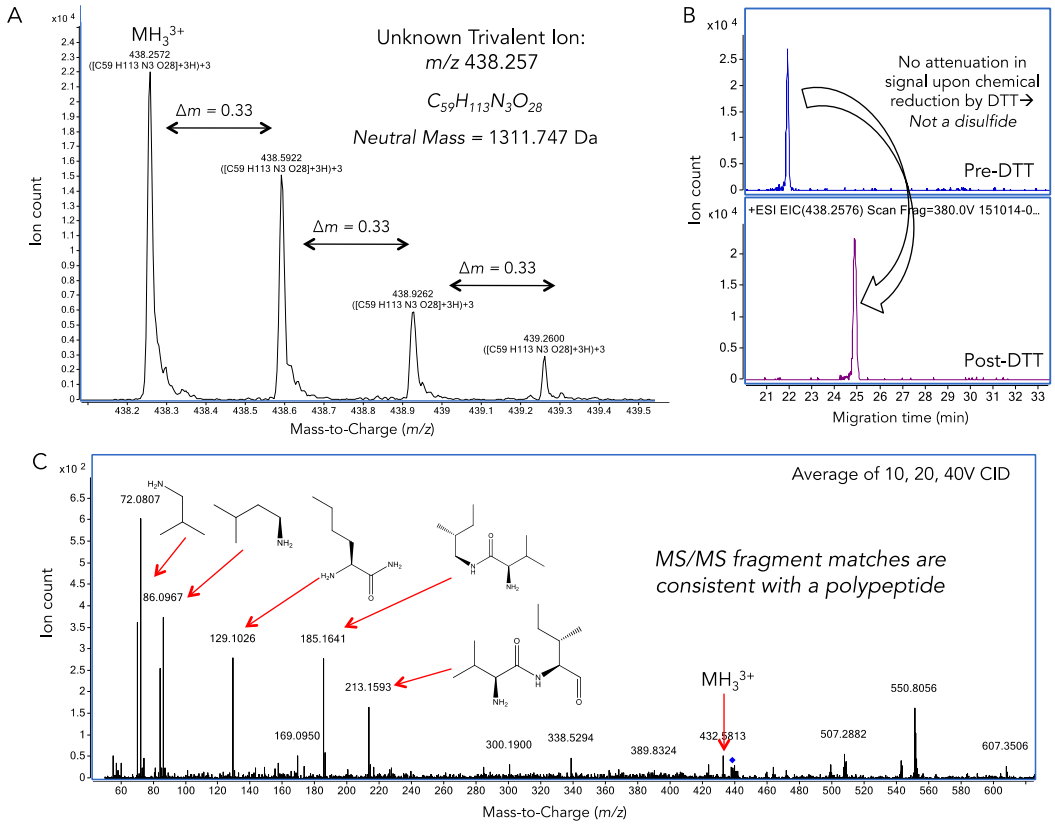

Figure 3.4. Structural elucidation of an unknown trivalent cation based on its most likely molecular formula as derived from accurate mass, charge state and isotopic pattern, its lack of chemical reactivity to DTT (not a disulfide) and its characteristic MS/MS fragmentation spectrum that has yet to be fully solved, but is indicative of a polypeptide. This unknown cation was the only metabolite that was positively correlated with IRT suggesting that it may be a by-product of trypsinogen activation.

as well as a confirmed or tentative compound ID (where applicable), together with a mass error (in ppm). Exact two-tailed *p*-values and FDR corrected *p*-values are listed for the Kruskal-Wallis test, with metabolites whose *p*-values satisfied a FDR correction ($q < 0.05$) in the Mann-Whitney *U* test denoted in bold. Similar to **Table 3.3**, thirteen metabolites and IRT (*FC* = 1.60; *p* = 7.00 E-7) were found to be differentially expressed in true CF neonates relative to SP/Non-CF cases with the unknown trivalent peptide (*FC* = 1.22; *p* = 5.24 E-4) and OPA (*FC* = 0.81; *p* =

1.68 E-4) among the most significant. **Fig. 3.5A-C** depicts box-whisker plots for the unknown trivalent peptide ion (*m/z* 438.258)**,** OPA and Tyr (similar to other CF-specific amino acids, such as Thr, Pro, and Ser), including a ROC curve based on the unknown peptide/OPA ratio (**Fig. 3.5D**) that shows good discriminating ability to distinguish CF neonates relative to likely unaffected SP/non-CF cases with an *AUC* = 0.831 ($p < 0.001$). Intriguingly, the unknown peptide was the only metabolite measured in DBS extracts that was directly correlated with IRT based on a Spearman-rank correlation ($\rho = 0.420$, p = 2.57 E-5) as shown in **Fig. 3.5E**.

3.4.4 Metabolic Differentiation of CF from Targeted Panel of Biomarkers by MS/MS at NSO

Several amino acids and acylcarnitines measured by MSI-CE-MS when using a non-targeted metabolite profiling in fact overlapped with a targeted 44 panel of biomarkers for NBS of IEM already measured by a validated method based on stable-isotope dilution, direct infusion (DI)-MS/MS at NSO. As a result, we retrospectively analyzed this data that was acquired by a separate 3.2 mm diameter DBS cut-out specimen within days of original specimen collection from neonates as compared to retrospective analysis of stored DBS specimens (> 2 years at -80°C) in this work. **Table S3.2** revealed that ten (out of 44) metabolites were consistently lower in CF relative to SN/healthy neonates ($q < 0.05$) as measured by DI-MS/MS, including three metabolites independently measured by MSI-CE-MS, namely Tyr, Gly and Arg (**Table S3.1**). The other short/medium-chain acylcarnitines (C12, C3DC, C4DC) were not detected by MSI-CE-MS from DBS extracts as they were below the concentration detection limits when using

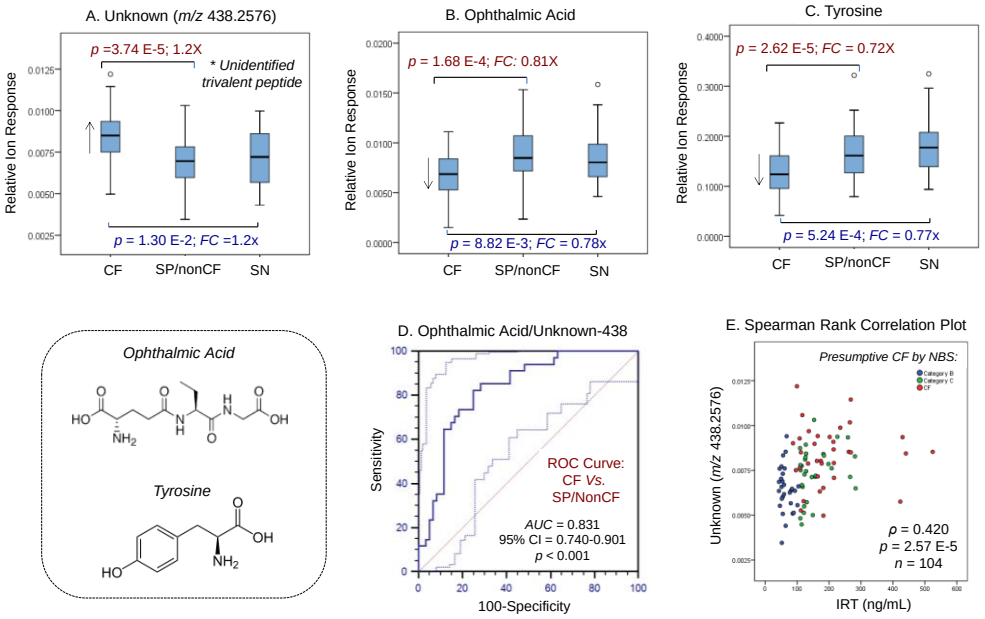

Figure 3.5. (A-C) Three of the most significant metabolites identified from an initial DBS cutout collected shortly after birth that may serve as promising CF-specific biomarkers for differentiation of CF affected neonates from unaffected carriers, transient neonatal IRT cases and healthy controls when using existing DI-MS/MS infrastructure. In addition to lower levels of Tyr in CF neonates, ophthalmic acid was also found to be significantly depleted in CF infants, whereas an unknown trivalent polypeptide (*m/z* 438.2576) was significantly elevated in CF neonates. (D) Receiver operating characteristic (ROC) curve highlighting that the measured ratio of "ophthalmic acid/unknown" provided excellent predictive accuracy (*AUC* = 0.831) to differentiate asymptomatic CF neonates from unaffected carriers/false positives. (E) Also the unknown peptide was found to be the only metabolite that was directly correlated with IRT levels, which indicated that it may be a likely by-product of trypsinogen activation.

full-scan data acquisition, whereas total leucines (Leu + Ile) and phenylalanine (Phe) were not found to be significant in MSI-CE-MS. Importantly, **Table S3.3** also demonstrates that only 3 (out of 44) metabolites from original DI-MS/MS data were found to be significantly lower ($q < 0.05$) in CF affected infants as compared to SP/unaffected controls, including Gly, Tyr and Phe. The former two amino acids also satisfied a Bonferroni adjustment ($p < 0.00114$) when correcting for multiple hypothesis testing with moderate effect sizes (0.500), including

average fold-changes (*FC* ≈ 0.80) consistent with outcomes measured independently by MSI-CE-MS on separate DBS cut-out specimens. Furthermore, **Fig. S3.3A** and **B** depict inter-laboratory method comparisons for measured Tyr and Gly concentrations from independent DBS extracts based on a Bland-Altman % difference plots and Passing-Bablok regression highlighting that there was no evidence of systematic bias between the two MS-based methods with good mutual agreement in data overall, as reflected by a mean bias of +11.8% and -1.2% for Tyr and Gly, respectively, and slopes not deviating from linearity ($p > 0.05$) ranging from 0.91 to 1.09. Importantly, a large fraction of metabolites measured by MSI-CE-MS are not included within current targeted biomarker panels by DI-MS/MS for NBS, such as OPA.

3.5 Discussion

Despite conclusive data supporting the economic, social and long-term health benefits of universal NBS for CF as compared to non-screened populations,[7–9] the implementation of optimal neonatal screening strategies for CF have presented unique ethical and technical challenges to public health programs.[63] While there is no evidence of long-term psychosocial harm from false-positive results, provided that delays are minimized from initial notification and confirmatory testing to reach a conclusive CF diagnosis, many parents report transient anxiety/distress.[64,65] In this context, CF NBS programs worldwide largely apply a 3-stage model for screening based on IRT, DNA and sweat chloride. Recently, the state of California evaluated a 4 year pilot study involving

next-generation sequencing for comprehensive screening of *CFTR* mutations from all hypertrypsinogenemic neonates in order to achieve 100% sensitivity, notably for non-Caucasian ethnic groups in the population.[66] While a PPV of 34% was achieved, a significant number of screen-negative cases were identified (28 out of 345), and only about 10-20% of all *CFTR* mutations have known or probable clinical consequence. Furthermore, extended genetic sequencing also identified a large fraction of CF-SPID/CRMS (≈ 5.8%) with an inconclusive diagnosis, resulting in a growing burden of follow-up monitoring and genetic counseling for families who have an uncertain prognosis given that a small fraction of such infants may have delayed CF. However, the main goal of NBS is early detection and disease prevention of affected neonates in the population, not carrier identification, thus current IRT/DNA screening algorithms are not optimal for this purpose as they may contribute to potential healthcare disparities that impact ethnic and racial communities differently.[67] Carrier identification also raises ethical issues, precluding the right for the parents and the child to choose to learn their carrier status; this is especially problematic as NBS is mandatory, but carrier detection screens require informed consent. In this work, we hypothesize that metabolite phenotyping of screen-positive CF infants following an elevated IRT from an original DBS specimen offers a more effective and ethical strategy to reduce the high rate of false positives, as well as diagnostic dilemmas for CF (*i.e.*, unaffected carrier or CF-SPID/CRMS identification) by more accurately identifying neonates affected with CF. To the best of our knowledge, this is first

comprehensive metabolomics study of retrospective DBS specimens for the improved screening of asymptomatic CF neonates.

Due to the challenges in interpreting the clinical significance from exclusively molecular genetic results, NBS for CF was only made possible by the discovery that neonates with elevated IRT in their DBS specimens were subsequently diagnosed with CF.[17–19,68] However, low birth weight and sick neonates also exhibit high IRT levels as a result of incidental neonatal stress (*e.g.*, low Apgar scores), respiratory distress, hypoglycemia, infections, bowel atresia or certain trisomies,[69] reflecting the poor specificity of IRT for detection of CF particularly in the absence of a detected *CFTR* mutation.[68] Also, most commercial DELFIA immunoassay kits do not distinguish between the specific IRT isoforms and can suffer from batch to batch variability when relying on polyclonal antibody reagents that may impact screening performance.[70] In our work, we demonstrated that 29 metabolites ($q < 0.05$, FDR) derived from a single 3.2 mm diameter DBS cut-out were differentially expressed in CF neonates (without meconium ileus) relative to healthy controls when using MSI-CE-MS (**Table 3.2**), which included elevations in a series of *N*-glycated amino acid adducts, as well as lower levels of several amino acids, GSSG and nicotinamide. The *N*-glycated amino acids likely represent markers of hyperglycemia formed by non-enzymatic glycation of free amino acids with elevated glucose via the Maillard reaction, which is commonly associated with chronic diseases and advanced glycation end-products.[71] Our recent study also revealed that *N*-galactated amino acids represent

pathognomonic markers of galactosemia caused by deleterious accumulation in galactose as measured in DBS extracts [54] Although CF-related diabetes often does not develop until later in childhood/adolescence following progressive pancreatic fibrosis, earlier presentations have been reported in CF patients during infancy[72] with growing recommendations to screen and treat for impaired glucose tolerance early in life.[73] Notably, we identified for the first time a novel modified mixed oxidized glutathione comprising a *N*-glycated Gly moiety when using MS/MS together with selective chemical reduction by excess DTT (**Fig. 3.3**) that was significantly elevated in CF infants relative to healthy neonates similar to other *N*-glycated amino acids (*e.g.,* Glc-Glu, Glc-Gln), including free *N*-glycated Gly. Additionally, CF infants were found to have much lower oxidized glutathione (GSSG), nicotinamide, and acetylcarnitine, as well as a depletion in a wide range of (conditionally) essential amino acids, including modified amino acids/intermediates, such as 3-methylhistidine, ornithine, adipic acid and homoarginine. All DBS extracts were found to have no consistently detected levels of reduced glutathione (GSH) despite its high abundance in erythrocytes suggesting that GSH is largely oxidized to GSSG during specimen collection and storage. These results are consistent with previous studies demonstrating that CFTR dysfunction in exocrine epithelial cells not only impacts chloride transport, but also nucleotide-regulated glutathione efflux[74,75] contributing to oxidative/redox stress with reduced mucolytic activity that plays a key role in CF pathophysiology.[76] Similarly, serum metabolomic studies of CF children

compared to non-CF lung disease subjects demonstrated elevations in oxidative stress markers and lower medium-chain acylcarnitines as indicators of mitochondrial dysfunction.[47] Although not detected by MSI-CE-MS due to inadequate sensitivity, retrospective analysis of DBS specimens by a targeted panel of biomarkers for IEM using DI-MS/MS at NSO confirmed that several short- and medium-chain acylcarnitines, as well as a number of amino acids, were also depleted in CF neonates as compared to healthy controls (**Table S3.2**). Recently, a plasma metabolomics study of the vitamin D status of adult CF patients relative to healthy subjects reported elevated glucose and a depletion in amino acids reflective of a catabolic state that may be modulated by high-dose vitamin D interventions during acute pulmonary exacerbations[77] while low bioavailability of circulating glutamine and arginine has been frequently associated with pulmonary disease in CF as related to neutrophil-associated inflammation of lung tissue[78] and nitric oxide deficiency[79] in children, respectively. Interestingly, both CF neonates and SP/non-CF cases (*i.e.*, unaffected carriers or transient hypertrypsinogenemic cases unrelated to CF) had similar elevations in *N*-glycated amino acids, as well as lower levels of GSSG and nicotinamide as compared to healthy controls (**Table S3.1**) suggesting that these metabolites most likely represent non-specific markers of metabolic or physiological stress in neonates.

In order to elucidate CF-specific biomarkers in asymptomatic neonates, a comparison of metabolic phenotypes was performed for true CF neonates and

screen-positive/presumptive CF cases as defined by two-tiered IRT/DNA algorithm, that were subsequently determined as likely unaffected with CF based on a low sweat chloride test (< 29 mM). Several amino acids were found to be significantly and consistently depleted (ranging from 10-30%) in CF-affected neonates relative to unaffected carriers and hypertrypsinogenemic cases as summarized in **Table 3.3**. However, Tyr, Thr, Ser, Pro, Gly, Asn, Arg, Ala, Gln and 3-MeHis were found to be selectively depleted in CF neonates after adjustment for FDR (q < 0.05) relative to both healthy controls and SP/non-CF cases as shown in **Table S3.1**. This is in contrast to higher levels of free amino acids reported in BALF specimens from CF patients that were associated with greater protein turn-over/catabolism with severe neutrophil-dependent lung inflammation due to elevated protease activity in CF airways.[51] As a result, our neonatal metabolomics data likely signifies maldigestion/malabsorption of dietary protein due to exocrine pancreatic insufficiency with lower prandial enzyme secretion.[80] Indeed, earlier studies have reported altered Tyr metabolism was likely attributed to unabsorbed Tyr in the lumen of large intestine of CF children,[81,82] which is consistent with lower circulating Tyr in DBS extracts of CF neonates. It is noteworthy, therefore, that Tyr is already included within a panel of targeted amino acids used for NBS of tyrosinemia and phenylketonuria by MS/MS at NSO, but it is not applied for CF screening. In fact, Tyr and Gly were the two most significant amino acids that were measured as being depleted in CF as compared to SP/non-CF neonates after correction for Bonferroni adjustment by

DI-MS/MS, which was also independently replicated by MSI-CE-MS on a separate DBS cut-out specimen (**Table S3.3**). However, the current metabolite panel screened by DI-MS/MS at NSO does not include several other amino acids demonstrated to be selectively lower in CF neonates in our study, including Thr, Ser, Asn, Arg, Pro, Ala, Gln and 3-MeHis. Overall, the two most significant biomarkers associated with CF were OPA, and an unknown putative polypeptide elevated in CF that was the only metabolite directly correlated with IRT (ρ = 0.420, p = 2.57 E-5) as highlighted in **Fig. 3.5**, **Table 3.3** and **Fig. S3.2**. OPA was conclusively identified by high resolution accurate MS/MS since access to authentic standard was not available (**Fig. 3.3**), and is a non-thiol/glutathione analog and marker of oxidative stress caused by severe GSH depletion.[62] Furthermore, OPA (and GSSG) is a chemically stable metabolite that is reliably measured from DBS extracts and thus may serve as a proxy for assessment of GSH deficiency that is prevalent in CF.[83] In fact, both OPA and GSSG were reported to be depleted in airway epithelial cells of CF patients relative to non-CF donors representing an important mechanism in the pathogenesis of CF cells.[48] The unknown trivalent CF-specific metabolite (*m/z*:RMT, 438.258:0.833) was tentatively assigned as a large polypeptide based on its high neutral mass (1311.747 Da) after interpretation of isotopic pattern and MS/MS spectra with certain product ions matching fragments from peptides typically containing Ile, Leu, and Val residues, included in the Metlin online database (**Fig. 3.4**). Unambiguous structural elucidation of the CF-specific polypeptide remains

incomplete, however we hypothesize that it may represent a by-product of trypsinogen activation due to its correlation with IRT, which may be linked to underlying pancreatic insufficiency in CF. In fact, small pancreatic duct blockage begins *in utero*, eventually leading to post-natal large duct obstruction and the subsequent secretion of proteins, including IRT, from the pancreas into the bloodstream in CF patients early in life.[84] Further work is needed to sequence the peptide and identify the protein origin and its exact biochemical role. Importantly, **Fig. 3.5D** demonstrated that a ROC curve based on the measured ratio of OPA/unknown peptide was able to serve as a promising biomarker for discriminating between affected CF from unaffected carriers or hypertrypsinogenemic cases, as required for more accurate NBS screening performance for CF as a "third-tier" MS/MS screen following IRT, which may reduce the need for widespread genetic testing and improving overall *PPV* by reducing false positives.

The present study is not without limitations. Samples were analyzed using a method optimized for the separation of polar/cationic metabolites and only detected using positive ion-mode electrospray ionization (ESI+). NBS is performed exclusively using DI-MS/MS with ESI+ and, as a result, our biomarker panel can be easily translated to the current NBS infrastructure and methodology with minimal, incremental cost.[85] However, this precludes the inclusion of acidic metabolites that are optimally detected in negative-ion mode (*e.g.* organic acids, sugar phosphates, nucleotides and metabolites derived from microflora)[86] which

may provide deeper insight into the neonatal pathophysiology of CF. Furthermore, the aqueous CE-MS method used in this study is ideal for only for polar/ionic compounds and thus limits metabolome coverage, such as neutral and/or lipophilic compounds. The pancreatic insufficiency that is present in almost 90% of CF cases also leads to fat malabsorption, steatorrhea and difficulties gaining and maintaining weight.[76] Indeed, the presence of steatorrhea remains a crucial part of symptomatic CF diagnosis,[27] particularly for those born prior to the advent of NBS programs, thus the analysis of phospholipids and fatty acids may provide additional clinically relevant CF-specific biomarkers. This study also lacks an independent holdout or validation set that is necessary for more rigorous biomarker qualification. Given the average birthrate in Ontario (~ 145,000 infants/year), obtaining an adequate number of CF-positive samples in the training set was challenging. Immediate future work includes the validation of these results on an independent cohort, including a blinded/hold-out set of DBS specimens from multiple NBS centres, whereas longer-term studies will involve a prospective study for assessment of the clinical utility of CF-specific biomarkers measured by DI-MS/MS relative to the current IRT/DNA and sweat algorithm.

3.6 Conclusion

In summary, this study presents the first nontargeted metabolomics study for the discovery of biomarkers for presymptomatic CF detection in neonatal DBS. A rigorously validated analytical method was applied in the context of a nontargeted metabolomic workflow with built-in quality assurance[54] while batch

correction reduced instrumental drift and permitted the analysis of independent batches of samples with acceptable QC precision. A total of 70 cationic metabolites were detected after data filtering to ensure only authentic and non-redundant features were analyzed and a subset of those were independently validated by DI-MS/MS at NSO. Preliminary data suggest that CF neonates are already encountering protein maldigestion/malabsorption resulting from exocrine pancreatic insufficiency as evidenced by lower levels of circulating amino acids while a depletion in ophthalmic acid (OPA) may be indicative of the early onset of oxidative stress. Furthermore, the ratio of OPA to an unknown peptide shows promise in discriminating between CF neonates and unaffected carriers and hypertrypsinogenemic cases suggesting that a third screening step may provide additional specificity while exploiting the existing NBS infrastructure. This work has the potential to alter current CF screening practices by reducing the number unaffected individuals (*e.g.* carriers) or individuals with inconclusive diagnoses (*i.e.* CF-SPID) that are sent for follow-up analyses, a direct result of screening for *CFTR* mutations of unclear or variable consequence. However, these "diagnostic dilemmas" are real infants who must endure lengthy and stressful testing with non-trivial costs to both the family and the broader healthcare system. Reducing costly and unnecessary testing can alleviate familial anxiety and direct healthcare resources to those truly affected by CF.

3.7 Acknowledgments

P.B.M. wishes to acknowledge funding support from the Natural Sciences and Engineering Research Council of Canada, Canada Foundation for Innovation, and Cystic Fibrosis Canada. Further thanks are directed to Marcus Kim at Agilent Technologies Inc. and to CDC's Newborn Screening Quality Assurance Program.

3.8 References

(1) Tsui, L.-C.; Dorfman, R. *Cold Spring Harb. Perspect. Med.* **2013**, *3*, 1–16.

(2) Sosnay, P. R.; Siklosi, K. R.; Van Goor, F.; Kaniecki, K.; Yu, H.; Sharma, N.; Ramalho, A. S.; Amaral, M. D.; Dorfman, R.; Zielenski, J.; Masica, D. L.; Karchin, R.; Millen, L.; Thomas, P. J.; Patrinos, G. P.; Corey, M.; Lewis, M. H.; Rommens, J. M.; Castellani, C.; Penland, C. M.; Cutting, G. R. *Nat. Genet.* **2013**, *45*, 1160–1167.

(3) Garland, A. L.; Walton, W. G.; Coakley, R. D.; Tan, C. D.; Gilmore, R. C.; Hobbs, C. a; Tripathy, A.; Clunes, L. a; Bencharit, S.; Stutts, M. J.; Betts, L.; Redinbo, M. R.; Tarran, R. *Proc. Natl. Acad. Sci. U. S. A.* **2013**, *110*, 15973–15978.

(4) Elborn, J. S. *Lancet* **2016**, *388*, 2519–2531.

(5) Li, W.; Soave, D.; Miller, M. R.; Keenan, K.; Lin, F.; Gong, J.; Chiang, T.; Stephenson, A. L.; Durie, P.; Rommens, J.; Sun, L.; Strug, L. J. *Hum. Genet.* **2014**, *133*, 151–161.

(6) Collawn, J. F.; Matalon, S. *AJP Lung Cell. Mol. Physiol.* **2014**, *307*, L917–L923.

(7) Dijk, F. N.; McKay, K.; Barzi, F.; Gaskin, K. J.; Fitzgerald, D. A. *Arch. Dis. Child.* **2011**, *96*, 1118–1123.

(8) Farrell, P. M.; Lai, H. J.; Li, Z.; Kosorok, M. R.; Laxova, A.; Green, C. G.; Collins, J.; Hoffman, G.; Laessig, R.; Rock, M. J.; Splaingard, M. L. *J. Pediatr.* **2005**, *147*, S30–S36.

(9) Sims, E. J.; Clark, A.; McCormick, J.; Mehta, G.; Connett, G.; Mehta, A. *Pediatrics* **2007**, *119*, 19–28.

(10) Kalnins, D.; Wilschanski, M. *Drug Des. Devel. Ther.* **2012**, *6*, 151–161.

(11) De Boeck, K.; Munck, A.; Walker, S.; Faro, A.; Hiatt, P.; Gilmartin, G.;

Higgins, M. *J. Cyst. Fibros.* **2014**, *13*, 674–680.

(12) Wainwright, C. E.; Elborn, J. S.; Ramsey, B. W.; Marigowda, G.; Huang, X.; Cipolli, M.; Colombo, C.; Davies, J. C.; De Boeck, K.; Flume, P. A.; Konstan, M. W.; McColley, S. A.; McCoy, K.; McKone, E. F.; Munck, A.; Ratjen, F.; Rowe, S. M.; Waltz, D.; Boyle, M. P. *N. Engl. J. Med.* **2015**, *373*, 220–231.

(13) Stephenson, A. L.; Sykes, J.; Stanojevic, S.; Quon, B. S.; Marshall, B. C.; Petren, K.; Ostrenga, J.; Fink, A. K.; Elbert, A.; Goss, C. H. *Ann. Intern. Med.* **2017**, *166*, 537–546.

(14) Farrell, P. M.; White, T. B.; Ren, C. L.; Hempstead, S. E.; Accurso, F.; Derichs, N.; Howenstine, M.; McColley, S. A.; Rock, M.; Rosenfeld, M.; Sermet-Gaudelus, I.; Southern, K. W.; Marshall, B. C.; Sosnay, P. R. *J. Pediatr.* **2017**, *181*, S4–S15.e1.

(15) Massie, R. J. H.; Curnow, L.; Glazner, J.; Armstrong, D. S.; Francis, I. *Med. J. Aust.* **2011**, *196*, 67–70.

(16) Baker, M. W.; Groose, M.; Hoffman, G.; Rock, M.; Levy, H.; Farrell, P. M. *J. Cyst. Fibros.* **2011**, *10*, 278–281.

(17) Crossley, J. R.; Elliott, R. B.; Smith, P. A. *Lancet* **1979**, *313*, 472–474.

(18) Ryley, H. C.; Robinson, P. G.; Yamashiro, Y.; Bradley, D. M. *J. Clin. Pathol.* **1981**, *34*, 906–910.

(19) Pederzini, F.; Faraguna, D.; Giglio, L.; Pedrotti, D.; Perobelli, L.; Mastella, G. *Acta Paediatr Scand* **1990**, *79*, 935–942.

(20) Ranieri, E.; Lewis, B.; Gerace, R.; Ryall, R. G.; Morris, C. P.; Nelson, P. V; Carey, W. F.; Robertson, E. F. *BMJ* **1994**, *308*, 1469–1472.

(21) Ranieri, E.; Ryall, R. G.; Morris, C. P.; Nelson, P. V; Carey, W. F.; Pollard, A. C.; Robertson, E. F. *BMJ* **1991**, *302* , 1237–1240.

(22) Riordan, J. R.; Rommens, J. M.; Kererm, B.-S.; Alon, N.; Rozmahel, R.; Grzelczak, Z.; Zielenski, J.; Lok, S.; Plavsic, N.; Chou, J.-L.; Drumm, M. L.; Iannuzzi, M. C.; Collins, F.; Tsui. *Science* **1989**, *245*, 1066–1073.

(23) Ioannou, L.; McClaren, B. J.; Massie, J.; Lewis, S.; Metcalfe, S. A; Forrest, L.; Delatycki, M. B. *Genet. Med.* **2014**, *16*, 207–216.

(24) Watson, M. S.; Cutting, G. R.; Desnick, R. J.; Driscoll, D. A.; Klinger, K.; Mennuti, M.; Palomaki, G. E.; Popovich, B. W.; Pratt, V. M.; Rohlfs, E. M.; Strom, C. M.; Richards, C. S.; Witt, D. R.; Grody, W. W. *Genet. Med.* **2004**, *6*, 387–391.

(25) Kay, D. M.; Maloney, B.; Hamel, R.; Pearce, M.; DeMartino, L.; McMahon, R.; McGrath, E.; Krein, L.; Vogel, B.; Saavedra-Matiz, C. A.; Caggana, M.; Tavakoli, N. P. *Eur. J. Pediatr.* **2016**, *175*, 181–193.

(26) Frazier, D. M.; Millington, D. S.; McCandless, S. E.; Koeberl, D. D.; Weavil, S. D.; Chaing, S. H.; Muenzer, J. *J. Inherit. Metab. Dis.* **2006**, *29*, 76–85.

(27) Rosenfeld, M.; Sontag, M. K.; Ren, C. L. *Pediatr. Clin. North Am.* **2016**, *63*, 599–615.

(28) Levy, H.; Farrell, P. M. *J. Pediatr.* **2015**, *166*, 1337–1341.

(29) Sontag, M. K.; Lee, R.; Wright, D.; Freedenberg, D.; Sagel, S. D. *J. Pediatr.* **2016**, *175*, 150–158.e1.

(30) Price, J. F. *Arch. Dis. Child.* **2006**, *91*, 209–210.

(31) Sommerburg, O.; Krulisova, V.; Hammermann, J.; Lindner, M.; Stahl, M.; Muckenthaler, M.; Kohlmueller, D.; Happich, M.; Kulozik, A. E.; Votava, F.; Balascakova, M.; Skalicka, V.; Stopsack, M.; Gahr, M.; Macek, M.; Mall, M. A.; Hoffmann, G. F. *J. Cyst. Fibros.* **2014**, *13*, 15–23.

(32) Seror, V.; Cao, C.; Roussey, M.; Giorgi, R. *J. Med. Screen.* **2016**, *23*, 62–69.

(33) Sommerburg, O.; Lindner, M.; Muckenthaler, M.; Kohlmueller, D.; Leible, S.; Feneberg, R.; Kulozik, A. E.; Mall, M. A.; Hoffmann, G. F. *J. Inherit. Metab. Dis.* **2010**, *33*, S263-271.

(34) Quinton, P. M. *Nature* **1983**, *301*, 421–422.

(35) Kirk, J. M. *Clin. Biochem.* **2011**, *44*, 487–488.

(36) Collie, J. T. B.; Massie, R. J.; Jones, O. A. H.; Legrys, V. A.; Greaves, R. F. *Pediatr. Pulmonol.* **2014**, *49*, 106–117.

(37) Ooi, C. Y.; Castellani, C.; Keenan, K.; Avolio, J.; Volpi, S.; Boland, M.; Kovesi, T.; Bjornson, C.; Chilvers, M. A.; Morgan, L.; van Wylick, R.; Kent, S.; Price, A.; Solomon, M.; Tam, K.; Taylor, L.; Malitt, K.-A.; Ratjen, F.; Durie, P. R.; Gonska, T. *Pediatrics* **2015**, *135*, e1377–e1385.

(38) Lefterova, M. I.; Shen, P.; Odegaard, J. I.; Fung, E.; Chiang, T.; Peng, G.; Davis, R. W.; Wang, W.; Kharrazi, M.; Schrijver, I.; Scharfe, C. *J. Mol. Diagnostics* **2016**, *18*, 267–282.

(39) Barben, J.; Southern, K. W. *Curr. Opin. Pulm. Med.* **2016**, *22* (6), 617–622.

(40) Beger, R. D.; Dunn, W.; Schmidt, M. A.; Gross, S. S.; Kirwan, J. A.; Cascante, M.; Brennan, L.; Wishart, D. S.; Oresic, M.; Hankemeier, T.; Broadhurst, D. I.; Lane, A. N.; Suhre, K.; Kastenmüller, G.; Sumner, S. J.; Thiele, I.; Fiehn, O.; Kaddurah-Daouk, R. *Metabolomics* **2016**, *12* (10.

(41) Xia, J.; Broadhurst, D. I.; Wilson, M.; Wishart, D. S. *Metabolomics* **2013**, *9*, 280–299.

(42) Fogelman, A. M. *Circ. Res.* **2015**, *116*, 396–397.

(43) Johnson, C. H.; Ivanisevic, J.; Siuzdak, G. *Nat. Rev. Mol. Cell Biol.* **2016**, *17*, 451–459.

(44) Langley, R. J.; Tsalik, E. L.; Velkinburgh, J. C. v.; Glickman, S. W.; Rice, B. J.; Wang, C.; Chen, B.; *et al*. *Sci. Transl. Med.* **2013**, *5*, 1-17.

(45) Raamsdonk, L. M.; Teusink, B.; Broadhurst, D.; Zhang, N.; Hayes, A.; Walsh, M. C.; Berden, J. A.; Brindle, K. M.; Kell, D. B.; Rowland, J. J.; Westerhoff, H. V; van Dam, K.; Oliver, S. G. *Nat Biotechnol* **2001**, *19*, 45–50.

(46) Muhlebach, M. S.; Sha, W. *Mol. Cell. Pediatr.* **2015**, *2*, 1-7.

(47) Joseloff, E.; Sha, W.; Bell, S. C.; Wetmore, D. R.; Lawton, K. a; Milburn, M. V; Ryals, J. a; Guo, L.; Muhlebach, M. S. *Pediatr. Pulmonol.* **2014**, *49*, 463–472.

(48) Wetmore, D. R.; Joseloff, E.; Pilewski, J.; Lee, D. P.; Lawton, K. a; Mitchell, M. W.; Milburn, M. V; Ryals, J. a; Guo, L. *J. Biol. Chem.* **2010**, *285*, 30516–30522.

(49) Robroeks, C. M. H. H. T.; van Berkel, J. J. B. N.; Dallinga, J. W.; Jobsis, Q.; Zimmermann, L. J. I.; Hendriks, H. J. E.; Wouters, M. F. M.; van der Grinten, C. P. M.; van de Kant, K. D. G.; van Schooten, F.-J. J.; Dompeling, E. *Pediatr. Res.* **2010**, *68*, 75–80.

(50) Wolak, J. E.; Esther, C. R.; O'Connell, T. M. *Biomarkers* **2009**, *14*, 55–60.

(51) Esther, C. R.; Coakley, R. D.; Henderson, A. G.; Zhou, Y. H.; Wright, F. A.; Boucher, R. C. *Chest* **2015**, *148*, 507–515.

(52) Esther, C. R.; Turkovic, L.; Rosenow, T.; Muhlebach, M. S.; Boucher, R. C.; Ranganathan, S.; Stick, S. M. *Eur. Respir. J.* **2016**, *48*, 1612–1621.

(53) Quinn, R. A.; Lim, Y. W.; Mak, T. D.; Whiteson, K.; Furlan, M.; Conrad, D.; Rohwer, F.; Dorrestein, P. *PeerJ* **2016**, *4*, 1-21.

(54) DiBattista, A.; McIntosh, N.; Lamoureux, M.; Al-Dirbashi, O. Y.;

Chakraborty, P.; Britz-McKibbin, P. *Anal. Chem.* **2017**, *89*, 8112–8121.

(55) Macedo, A. N.; Mathiaparanam, S.; Brick, L.; Keenan, K.; Gonska, T.; Pedder, L.; Hill, S.; Britz-McKibbin, P. *ACS Cent. Sci.* **2017**, *3*, 904–913.

(56) Chace, D. H.; Kalas, T. a; Naylor, E. W. *Clin. Chem.* **2003**, *49*, 1797–1817.

(57) Kuehnbaum, N. L.; Kormendi, A.; Britz-McKibbin, P. *Anal. Chem.* **2013**, *85*, 10664–10669.

(58) Wehrens, R.; Hageman, J. A.; van Eeuwijk, F.; Kooke, R.; Flood, P. J.; Wijnker, E.; Keurentjes, J. J. B.; Lommen, A.; van Eekelen, H. D. L. M.; Hall, R. D.; Mumm, R.; de Vos, R. C. H. *Metabolomics* **2016**, *12*, 1-12.

(59) Xia, J.; Sinelnikov, I. V.; Han, B.; Wishart, D. S. *Nucleic Acids Res.* **2015**, *43*, W251–W257.

(60) Mak, D. Y. F.; Sykes, J.; Stephenson, A. L.; Lands, L. C. *J. Cyst. Fibros.* **2016**, *15*, 302–308.

(61) Kuehnbaum, N. L.; Gillen, J. B.; Kormendi, A.; Lam, K. P.; DiBattista, A.; Gibala, M. J.; Britz-Mckibbin, P. *Electrophoresis* **2015**, *36* , 2226–2236.

(62) Soga, T.; Baran, R.; Suematsu, M.; Ueno, Y.; Ikeda, S.; Sakurakawa, T.; Kakazu, Y.; Ishikawa, T.; Robert, M.; Nishioka, T.; Tomita, M. *J. Biol. Chem.* **2006**, *281*, 16768–16776.

(63) Sosnay, P. R.; Farrell, P. *Pediatrics* **2015**, *136*, 1181–1184.

(64) Schmidt, J. L.; Castellanos-Brown, K.; Childress, S.; Bonhomme, N.; Oktay, J. S.; Terry, S. F.; Kyler, P.; Davidoff, A.; Greene, C. *Genet. Med.* **2012**, *14*, 76–80.

(65) Hayeems, R. Z.; Miller, F. A.; Barg, C. J.; Bombard, Y.; Kerr, E. *Pediatrics* **2016**, *138*, 1-10.

(66) Kharrazi, M.; Yang, J.; Bishop, T.; Lessing, S.; Young, S.; Graham, S.; Pearl, M.; Chow, H.; Ho, T.; Currier, R.; Gaffney, L.; Feuchtbaum, L. *Pediatrics* **2015**, *136*, 1062–1072.

(67) Ross, L. F. *J. Pediatr.* **2009**, *153*, 308–313.

(68) Crossley, J. R.; Smith, P. A.; Edgar, B. W.; Gluckman, P. D.; Elliott, R. B. *Clin. Chim. Acta* **1981**, *113*, 111–121.

(69) Ravine, D.; Francis, R. I.; Danks, D. M. *Eur. J. Pediatr.* **1993**, *152*, 348–349.

(70) Lindau-Shepard, B. A.; Pass, K. A. *Clin. Che* **2010**, *56*, 445–450.

(71) Zhang, Q.; Ames, J. M.; Smith, R. D.; Baynes, J. W.; Metz, T. O. *J. Proteome Res.* **2008**, *8*, 754–769.

(72) Gelfand, I. M.; Eugster, E. A.; Haddad, N. G. *Diabetes Care* **2005**, *28*, 2693–2594.

(73) Mainguy, C.; Bellon, G.; Delaup, V.; Ginoux, T.; Kassai-Koupai, B.; Mazur, S.; Rabilloud, M.; Remontet, L.; Reix, P. *J. Pediatr. Endocrinol. Metab.* **2017**, *30*, 27–35.

(74) Hudson, V. M. *Free Radic. Biol. Med.* **2001**, *30*, 1440–1461.

(75) Kogan, I.; Ramjeesingh, M.; Li, C.; Kidd, J. F.; Wang, Y.; Leslie, E. M.; Cole, S. P. C.; Bear, C. E. *EMBO J.* **2003**, *22*, 1981–1989.

(76) Ntimbane, T.; Comte, B.; Mailhot, G.; Berthiaume, Y.; Poitout, V.; Prentki, M.; Rabasa-Lhoret, R.; Levy, E. *Clin. Biochem. Rev.* **2009**, *30*, 153–177.

(77) Alvarez, J. A.; Chong, E. Y.; Walker, D. I.; Chandler, J. D.; Michalski, E. S.; Grossmann, R. E.; Uppal, K.; Li, S.; Frediani, J. K.; Tirouvanziam, R.; Tran, V. L. T.; Tangpricha, V.; Jones, D. P.; Ziegler, T. R. *Metabolism.* **2017**, *70*, 31–41.

(78) D'Eufemia, P.; Finocchiaro, R.; Celli, M.; Tote, J.; Ferrucci, V.; Zambrano, A.; Troiani, P.; Quattrucci, S. *Pediatr. Res.* **2006**, *59*, 13–16.

(79) Engelen, M. P. K. J.; Com, G.; Luiking, Y. C.; Deutz, N. E. P. *J. Pediatr.* **2013**, *163*, 369–376.

(80) Li, L.; Somerset, S. *Dig. Liver Dis.* **2014**, *46*, 865–874.

(81) Robinson, R. *Clin. Chim. Acta* **1966**, *14*, 166–170.

(82) Gibbons, I. S. E.; Seakins, J. W. T.; Ersser, R. S. *Lancet* **1967**, *289*, 877–878.

(83) Hudson, V. M. *Treat.Respir Med* **2004**, *3*, 353–363.

(84) Wilschanski, M.; Novak, I. *Cold Spring Harb. Perspect. Med.* **2013**, *3*, 1–17.

(85) Wilcken, B.; Wiley, V.; Hammond, J.; Carpenter, K. *N. Engl. J. Med.* **2003**, *348*, 2304–2312.

(86) Yamamoto, M; Ly, R.; Gill, B.; Zhu. Z.; Moran-Mirabal, J.; Britz-McKibbin, P. *Anal. Chem.* **2016**, *88*, 10710-19.

3.9 Supplemental Information

Table S3.1. Results from a Kruskal-Wallis test on QC-corrected data showing compounds that are significantly different between CF-positive, SP and screen-negative samples. Bolded *p*-values are significant at an FDR ($q < 0.05$)

***m/z*:RMT**	**Compound Identification**	**Mass Error**	**Kruskal-Wallis**	**FDR-corrected**	***Post hoc* Mann-Whitney *p*-value**					
		(ppm)	***p*-value**	***q*-value**	**CF *vs* Neg**	**FC (CF/Neg)**	**CF *vs* SP**	**FC (CF/SP)**	**SP *vs* Neg**	**FC (SP/Neg)**
--	IRT	--	2.64E-21	1.82E-19	**1.46E-21**	10.4	**7.00E-07**	1.60	**1.45E-28**	6.52
310.115:1.430	Glycated Glutamic acid	3.39	7.50E-14	2.59E-12	**1.10E-11**	3.58	6.36E-01		**3.08E-16**	3.10
309.130:1.421	Glycated Glutamine	-1.49	1.29E-12	2.97E-11	**1.58E-09**	3.00	6.30E-01		**4.37E-15**	3.04
123.055:0.650	Nicotinamide	0.31	8.13E-11	1.40E-09	**1.79E-05**	1.33	4.83E-02		**1.24E-13**	1.53
294.155:1.283	Glycated Leucine	-2.98	3.72E-10	5.14E-09	**7.77E-08**	3.92	2.64E-01		**2.89E-11**	2.71
388.109:1.300	Glycated GSSG	-0.81	5.25E-10	6.03E-09	**8.37E-08**	1.99	9.16E-01		**3.47E-11**	2.15
307.083:1.109	Oxidized Glutathione	-2.92	1.29E-08	1.27E-07	**6.83E-06**	0.76	4.08E-01		**6.07E-10**	0.72
238.092:1.175	Glycated Glycine	1.14	3.12E-08	2.69E-07	**2.17E-06**	2.14	7.69E-01		**4.59E-09**	1.92
147.076:0.960	Glutamine	-1.39	9.75E-07	7.48E-06	**1.85E-07**	0.74	**2.27E-03**	0.83	**1.12E-03**	0.87
120.0656:0.930	Threonine	0.24	5.97E-06	4.12E-05	**1.31E-06**	0.70	**3.05E-04**	0.80	3.47E-02	
156.077:0.630	Histidine	-0.58	8.92E-06	5.59E-05	**3.42E-05**	0.71	2.28E-01		**1.44E-05**	0.80
133.097:0.582	Ornithine	0.18	1.58E-05	9.11E-05	**6.27E-04**	0.77	7.63E-01		**2.11E-06**	0.70
204.123:0.791	Acetylcarnitine	-1.05	3.46E-05	1.83E-04	**4.00E-06**	0.68	1.40E-02		**6.87E-03**	0.84
162.076:0.795	Aminoadipic Acid*	-0.06	1.00E-04	4.31E-04	**7.72E-03**	1.22	5.49E-01		**7.05E-06**	1.37
182.081:1.015	Tyrosine	-0.6	1.00E-04	4.31E-04	**2.62E-05**	0.72	**5.24E-04**	0.77	2.03E-01	
278.572:1.088	*Unknown*, $M+2H^{2+}$	-1.52	1.00E-04	4.31E-04	1.17E-01		5.11E-02		**2.98E-06**	0.71
438.258:0.833	*Unknown*, $M+3H^{3+}$	-0.03	2.00E-04	8.12E-04	**1.30E-02**	1.15	**3.74E-05**	1.22	3.35E-01	
106.050:0.880	Serine	0.45	5.00E-04	1.82E-03	**1.04E-03**	0.74	**4.92E-04**	0.76	5.26E-01	
290.135:1.225	Ophthalmic Acid*	0.41	5.00E-04	1.82E-03	**8.82E-03**	0.78	**1.68E-04**	0.81	2.51E-01	
170.092:0.648	3-Methylhistidine	-0.17	7.00E-04	2.42E-03	**2.83E-04**	0.75	**3.77E-03**	0.83	1.68E-01	
76.039:0.720	Glycine	0.13	9.00E-04	2.82E-03	**3.71E-04**	0.81	**6.43E-03**	0.85	1.04E-01	
133.061:0.930	Asparagine	0.82	9.00E-04	2.82E-03	**8.08E-04**	0.83	**1.45E-03**	0.90	2.34E-01	
116.071:0.952	Proline	0.25	1.10E-03	3.16E-03	**1.96E-03**	0.86	**4.62E-04**	0.91	9.41E-01	
129.066:0.756	*Unknown, MH^+*	-0.11	1.10E-03	3.16E-03	4.86E-01		1.31E-02		**4.85E-04**	1.21
90.055:0.782	Alanine	0.32	2.20E-03	5.84E-03	1.42E-01		**1.22E-03**	0.81	2.74E-02	
147.113:0.585	Lysine	-0.74	2.20E-03	5.84E-03	**5.12E-03**	0.85	3.86E-01		**1.72E-03**	0.85
136.062:0.667	Adenine	-0.66	1.08E-02	2.76E-02	8.50E-01		1.60E-02		**1.10E-02**	0.82
189.135:0.612	Homoarginine*	0.58	1.55E-02	3.82E-02	**7.99E-03**	0.69	2.62E-02		3.01E-01	
150.058:0.941	Methionine	-0.1	1.62E-02	3.85E-02	**2.47E-03**	0.84	1.59E-01		1.35E-01	
123.594:0.577	*Unknown, MH^+*	0.73	1.87E-02	4.30E-02	**1.72E-02**	1.33	3.86E-01		1.92E-02	
175.119:0.608	Arginine	-0.14	1.94E-02	4.32E-02	3.63E-02		**6.28E-03**	0.70	8.53E-01	
146.118:0.700	Deoxycarnitine	-0.03	2.09E-02	4.51E-02	2.45E-01		**6.28E-03**	0.97	1.55E-01	

** Tentative identification based on accurate mass match in Human Metabolome Database with a consistent electrophoretic mobility.*

Table S3.2. Mann-Whitney *U* test to rank metabolites from NBS panel at NSO that were different ($q < 0.05$) in CF ($n = 34$) relative to screen-negative neonates ($n = 40$) by DI-MS/MS.

Metabolite ID	*p* value	FDR *q* value	Effect Size	FC (CF/Neg.) [b]
Total Leu/Ile	1.32 E-04 [a]	5.81 E-03	0.563	0.72
Phenylalanine	4.01 E-04 [a]	7.71 E-03	0.523	0.86
C12	5.26 E-04 [a]	7.71 E-03	0.513	0.63
C3DC	7.75 E-04 [a]	8.52 E-03	0.498	0.89
Tyrosine [c]	2.02 E-03	1.51 E-02	0.460	0.83
Arginine [c]	2.06 E-03	1.51 E-02	0.459	0.67
C4DC	3.33 E-03	2.10 E-02	0.438	0.76
Glycine [c]	6.24 E-03	3.43 E-02	0.409	0.86
C12.1	7.70 E-03	3.76 E-02	0.399	0.70
C4OH	1.06 E-02	4.65 E-02	0.383	0.73

[a] *These metabolites were significant after a Bonferroni correction ($p < 0.00114$)*
[b] *Fold-change (FC) was calculated as the ratio of the median of CF-affected to screen-negative neonates*
[c] *These metabolites were also significantly different as measured independently by MSI-CE-MS*

Table S3.3. Mann Whitney *U* test for ranking metabolites from NBS panel that were different ($q < 0.05$) between CF ($n = 34$) and SP/non-CF and likely unaffected neonates ($n = 60$) by DI-MS/MS at NSO.

Compound	*p* value	FDR *q* value	Effect Size	FC (CF/NonCF) [b]
Glycine [c,d]	5.36 E-04 [a]	2.10 E-02	0.514	0.83
Tyrosine [c,d]	9.56 E-03 [a]	2.10 E-02	0.491	0.80
Phenylalanine [c]	3.12 E-03	4.57 E-02	0.441	0.86

[a] *These metabolites were significant after a Bonferroni correction ($p < 0.00114$)*
[b] *Fold-change was calculated as the ratio of the median of CF to SP yet unaffected neonates*
[c] *These metabolites were also different between CF and screen-negative neonates by MSI-CE-MS*
[d] *These metabolites were also different between CF and screen-positive/unaffected neonates by MSI-CE-MS*

Table S3.4. Metabolites quantified by stable-isotope dilution FIA-MS/MS at NSO as part of expanded NBS for 20 different amino acid, fatty acid and organic acid-related IEM

Metabolite (Symbol)	Primary Marker for IEM	Secondary Marker for IEM
Alanine (Ala)		MSUD
Arginine (Arg)		CIT; ASA
Argininosuccinic Acid (ASA)	ASA	CIT
Citrulline (Cit)	CIT; ASA	CUD
Glycine (Gly)		NKHG[b]
Total Leucine (Leu)	MSUD	
Methionine (Met)	HCY	
Ornithine (Orn)		CIT; ASA
Phenylalanine (Phe)	PKU	HCY
Succinylacetone (SUAC)	TYR I	
Tyrosine (Tyr)	TYR I	PKU
Valine (Val)		MSUD, PKU, TYRI[a]
Carnitine (C0)	CUD; CPT 1	IVA
Acetylcarnitine (C2)	PA/MMA	MCADD; CUD; IVA; GA I
Propionylcarnitine (C3)	CblA/B; MMA; PA; MCD	CUD; IVA
Methylcitric acid (MCA)		PA; MMA
Malonylcarnitine (C3DC)		GA1[a]
Butyrylcarnitine (C4)		IVA
Hydroxybutyrylcarnitine (C4OH)		HMG; BKT, MCD, 3-MCC[a]
Methylmalonylcarnitine (C4DC)		PA; MMA[a]
Isovalerylcarnitine (C5)	IVA	
Tiglylcarnitine (C5:1)	BKT	
Glutarylcarnitine (C5DC)	GA I	IVA
3-OH-isovalerylcarnitine (C5OH)	3-MCC; BKT; HMG; MCD	GA I
Hexanoylcarnitine (C6)		MCADD
Methylglutarylcarnitine (C6DC)	HMG	
Octanoylcarnitine (C8)	MCADD	GA I
Octenoylcarnitine (C8:1)		IVA[a]
Decanoylcarnitine (C10)		MCADD
Decenoylcarnitine (C10:1)		MCADD
Dodecanoylcarnitine (C12)		GA I[a]
Dodecenoylcarnitine (C12:1)		VLCADD

Tetradecanoylcarnitine (C14)		VLCADD
Tetradecenoylcarnitine (C14:1)	VLCADD	VLCADD
Tetradecadienoylcarnitine (C14:2)		VLCADD
Palmitylcarnitine (C16)	CPT 1	LCHADD; VLCADD; CUD; IVA; GA I
3-OH-palmitoleylcanitine (C16:1OH)		LCHADD
3-OH-palmitylcarnitine (C16OH)	LCHADD; TPD	LCHADD
Stearoylcarnitine (C18)	CPT 1	CUD
Oleylcarnitine (C18:1)		GA I; CPT I; CUD; VLCADD[a]
3-OH-oleylcarnitine(C18:1OH)		LCHADD
Linoleylcarnitine (C18:2)		CPT I[a]
3-OH-stearoylcarnitine (C18OH)		LCHADD
Hydroxyltetradecanoylcarnitine (C14OH)		LCHADD

[a]*These metabolites are or were reported on "risk" letters that are sent out following a positive screen result*

[b]*Glycine can be used to screen for NKHG, though it is not currently used as part of any disorder logic*

**IEM acronyms: 3-MCC-3-methylcrotonyl coA carboxylase deficiency; ASA- argininosuccinic acidemia; BKT- beta-ketothiolase deficiency; CblA/B- cobalamin A and B defects; CIT-citrullinemia; CPT I-carnitine palmitoyltransferase I deficiency; CUD- carnitine uptake deficiency; GAI- glutaric aciduria type I; HMG-HMG coA lyase deficiency; HCY-homocystinuria; IVA- isovaleric acidemia; LCHADD- long chain 3-hydroxyl coA dehydrogenase deficiency; MCADD- medium chain acyl coA dehydrogenase deficiency; MCD- multiple carboxylase deficiency; MMA-methylmalonic acidemia; MSUD- maple syrup urine disease; NKHG- nonketotic hyperglycemia; PA- propionic acidemia; PKU-phenylketonuria; TYR I-tyrosinemia type I; TPD-trifunctional protein deficiency; VLCADD- very long chain acyl coA dehydrogenase deficiency*

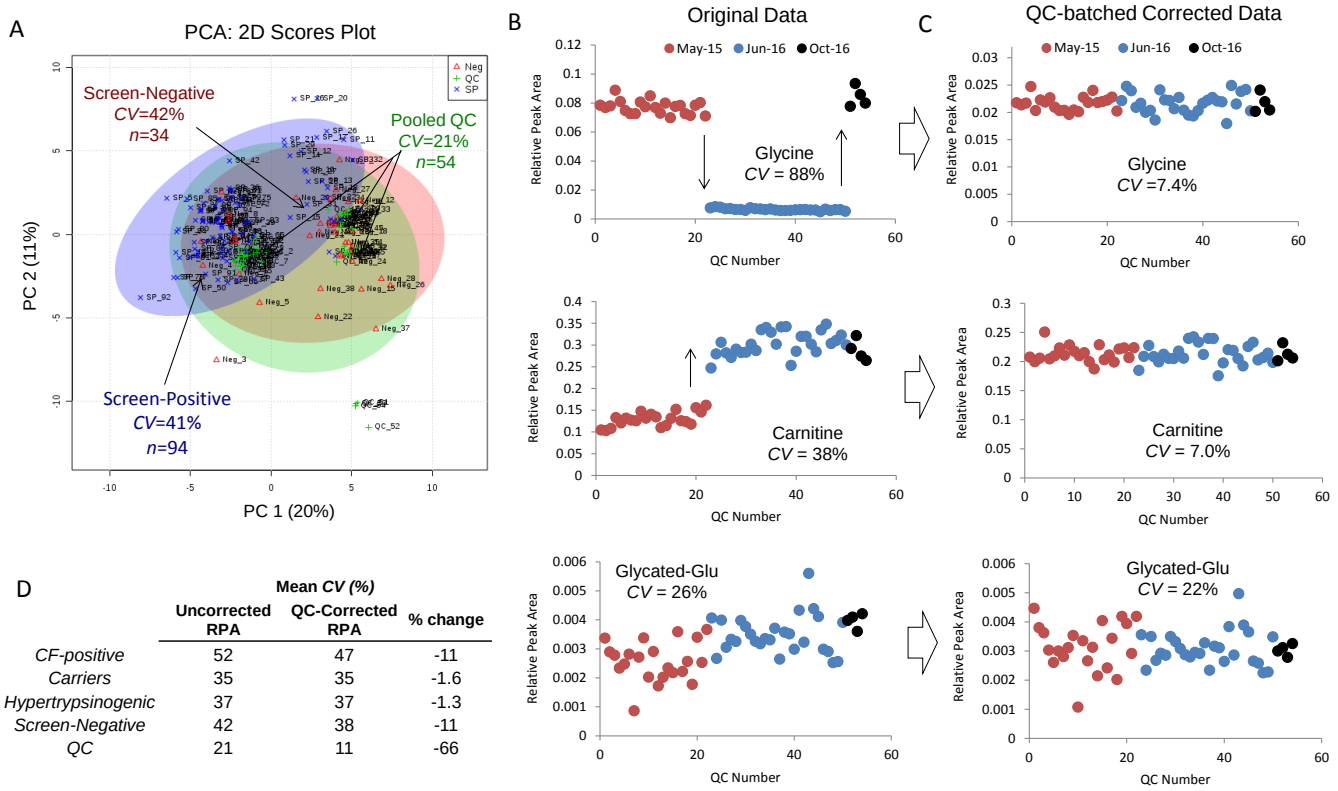

D

	Mean *CV (%)*		
	Uncorrected RPA	QC-Corrected RPA	% change
CF-positive	52	47	-11
Carriers	35	35	-1.6
Hypertrypsinogenic	37	37	-1.3
Screen-Negative	42	38	-11
QC	21	11	-66

Figure S3.1. (A) A 2D scores plot using PCA which provides an overview of the metabolomics data following *log*-transformation and autoscaling of the relative peak area (RPA) response measured for 70 cationic metabolites normalized to an internal standard. Three distinct clusters of QC (*i.e.*, pooled healthy neonate samples) are evident in this case suggestive of bias/system drift throughout the period of analysis with poor technical precision (median *CV* = 21%) as compared to overall biological variance (median *CV* = 42%). (B) Representative control charts for three metabolites measured by MSI-CE-MS demonstrate that the extent of temporal system drift throughout the data acquisition period was compound dependent with the greatest bias evident for glycine as compared to carnitine or glycated-Glu. (D) Overall, all metabolite control charts are significantly improved after applying a QC-batched correction algorithm to the original data, resulting in a much lower technical variance (median *CV* = 11%) without effecting overall biological variance in different sub-groups of neonatal DBS extracts analyzed.

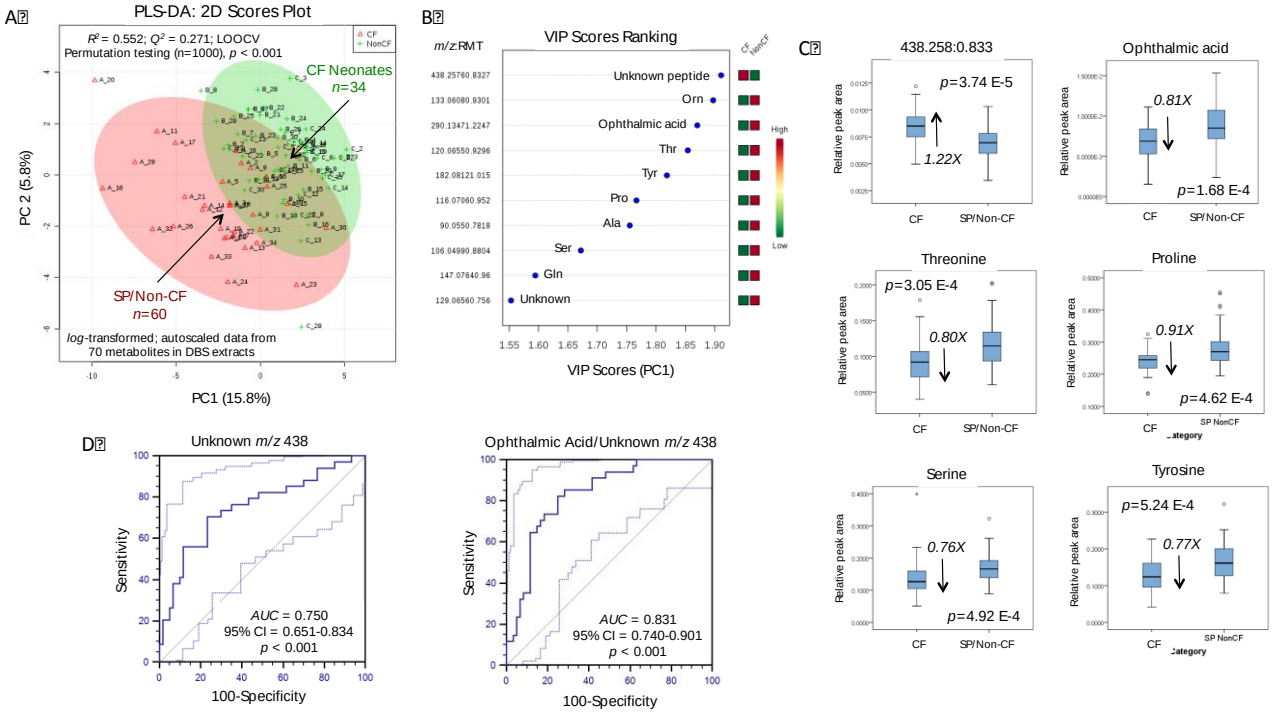

Figure S3.2. (A) A 2D scores plot using PLS-DA together with (B) VIP scores ranking for selection of top-ranked metabolites associated with CF neonates as compared to screen-positive/likely unaffected CF (SP/Non-CF) identified by two-tiered IRT/DNA algorithm based on 70 cationic metabolites reliably measured in retrospective DBS specimens. (C) Representative box-whisker plots for a panel of the most significant metabolites associated with true CF neonates as compared to unaffected SP/Non-CF neonates who are presumptive CF cases, including unknown peptide, ophthalmic acid and a series of amino acids (Thr, Ser, Pro, Tyr). (D) Two receiver operating characteristic (ROC) curves for single (unknown peptide, *m/z* 438.258; RMT = 0.833) or ratiometric (ophthalmic acid/unknown peptide) metabolites demonstrating good discrimination potential for CF neonates from an original 3.2 mm diameter DBS specimen (*AUC* > 0.750; $p < 0.001$). These metabolites can be readily measured using existing DI-MS/MS infrastructure available at NBS facilities.

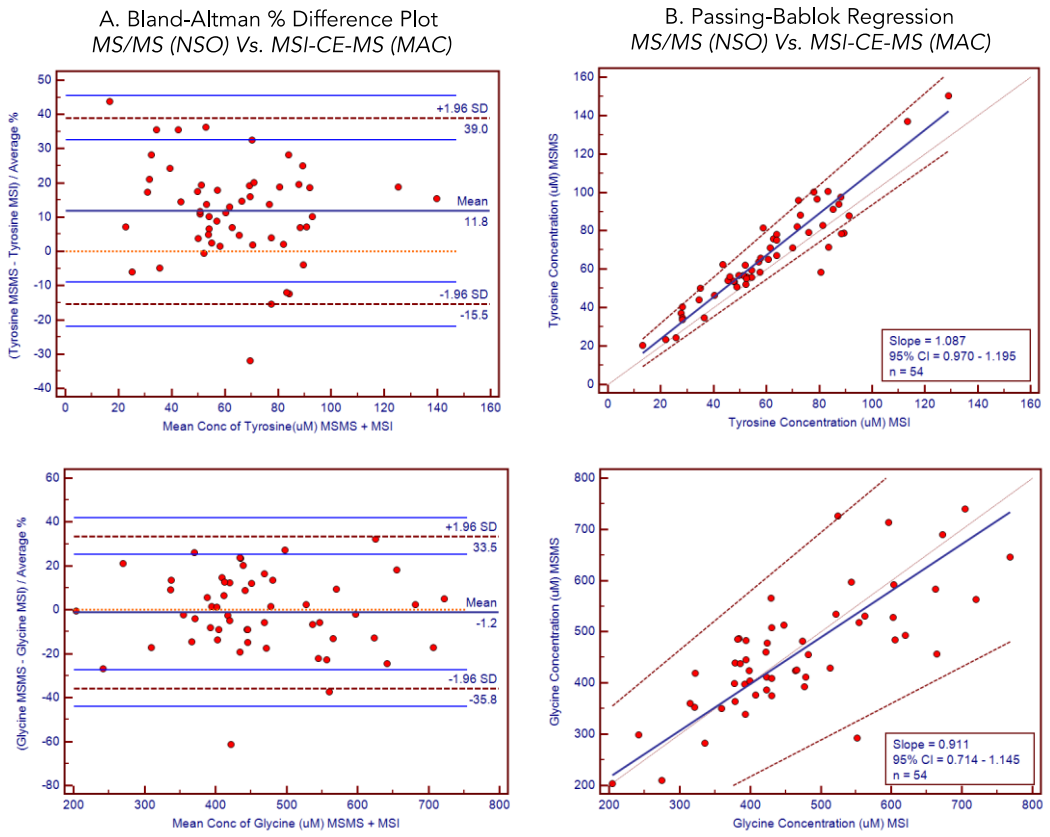

Figure S3.3. Inter-laboratory method comparison of MSI-CE-MS (MAC) and DI-MS/MS (NSO/CHEO) for quantification of tyrosine (Tyr) and glycine (Gly) from two independent 3.2-mm DBS specimens from our first batch of specimens, including CF (*n*=14) and screen-negatives/healthy infants (*n*=40). (A) A Bland-Altman % difference plot highlights good mutual agreement between the two methods when analyzing two different DBS cut-out samples with an average bias of 11.8% (Tyr) and -1.2% (Gly) with only 1 extreme outlier beyond agreement limits, and (B) Passing-Bablok regression similarly confirm good mutual agreement for measured Tyr and Gly concentrations when using two independent methods and DBS specimens as reflected by a slope close to linearity.

Chapter IV

High Throughput and Nontargeted Screening by Multisegment Injection-Capillary Electrophoresis-Mass Spectrometry for Systematic Drugs of Abuse Surveillance

Authors of this work are Alicia DiBattista, Dianne Rampersaud, Howard Lee, Marcus Kim and Philip Britz-McKibbin

Anal. Chem. **2017** *89,* 11853-11861

A.D conducted all of the optimization and validation experiments and MS/MS analyses, did most of the data analysis and wrote the initial draft for publication. Other co-authors prepared all calibrator and internal standard materials and provided feedback and improvements on the manuscript drafts.

Chapter IV: High Throughput and Nontargeted Screening by Multisegment Injection-Capillary Electrophoresis-Mass Spectrometry for Systematic Drugs of Abuse Surveillance

4.1 Abstract

New technologies are urgently required for reliable drug screening given a worldwide epidemic of prescription drug abuse and its devastating socioeconomic impacts on public health. Primary screening of drugs of abuse (DoA) currently relies on immunoassays that are prone to bias, and are not applicable to detect an alarming array of psychoactive stimulants, tranquilizers and synthetic opioids. These limitations impact patient safety when monitoring for medication compliance, drug substitution or misuse/abuse, and require follow-up confirmatory testing by more specific yet lower throughput instrumental methods. Herein, we introduce a high throughput platform for nontargeted screening of a broad spectrum of DoA and their metabolites based on multisegment injection-capillary electrophoresis-mass spectrometry (MSI-CE-MS). We demonstrate that MSI-CE-MS enables serial injections of ten samples within a single run (< 3 min/sample), where multiplexed electrophoretic separations are coupled to high resolution MS with full-scan data acquisition. Unambiguous drug identification was achieved by four or more independent parameters, including co-migration with a deuterated internal standard or *in silico* prediction of electromigration behavior together with accurate mass, most likely molecular formula, as well as MS/MS as required for confirmation testing. Acceptable precision was demonstrated for over 50 DoA at three concentration levels over four days

(median CV = 13%, *n*=117) with minimal ion suppression, isobaric interferences and sample carry-over (<1%). This approach offers a rapid yet accurate screening method for simultaneous detection and identification of DoA at their recommended cut-off levels in human urine while allowing for systematic surveillance, specimen verification and retrospective testing of designer drugs that elude conventional drug tests.

4.2 Introduction

Urine screening for illicit, prescription and over-the-counter drugs is widely performed in a variety of settings, including pre-employment screening and workplace testing, chronic pain management, substance abuse monitoring and sexual assault cases, as well as clinical and forensic toxicology.[1] However, the abuse of and addiction to opioids and other classes of prescription medications to treat common medical and psychiatric illnesses has become a global health crisis with over 36 million people addicted to pain relief opioids alone.[2] The worsening US epidemic has resulted in a 200% increase in the rate of opioid overdose since 2000 with 52,404 total fatalities reported from 1999-2015. These alarming trends have been attributed to natural (*i.e.*, heroin) and increasingly, synthetic opioids due to the availability of inexpensive drugs (*e.g.*, fentanyl) in the illegal market.[3] Indeed, the abuse of prescription medications has inflicted a devastating toll on rural and urban communities in the US with an estimated total economic burden of $78.5 billion in 2013, including costs related to substance abuse treatment, health care, criminal justice and lost productivity.[4] As a result, new analytical

platforms are needed for systematic surveillance of drugs of abuse (DoA) to ensure medical compliance, prevent diversion or trafficking, and reduce illicit drug use, including a plethora of veterinary medications and designer drugs that are not currently part of targeted drug panels.[5]

Currently, a "two-tiered" strategy for urine drug screening is performed by immunoassays using automated laboratory analyzers, with follow-up testing and drug quantification by GC-MS and, increasingly, LC-MS/MS with multiple reaction monitoring.[6-8] Although fast and inexpensive, particularly for point-of-care testing applications, immunoassays are prone to false-positives due to antibody cross-reactivity for commonly prescribed opioids, illicit drugs and certain foods,[9-12] while also suffering from high false negative rates for specific drug classes, such as benzodiazepines.[12,13] Consequently, urinary test results using immunoassays are considered presumptive until confirmed independently by a chemically-specific laboratory test for drug quantification while also taking into account a patient's prescription history.[14] In this context, there is growing interest in developing more accurate screens that allow for broad spectrum urine drug testing when using LC with high resolution MS in conjunction with full-scan[15,16] and/or data-independent MS/MS acquisition.[17-20] This strategy enables the identification of unknown drug metabolites or emerging classes of synthetic opioids when antibody reagents, reference standards and/or spectral libraries do not exist,[21] while enabling retrospective data analysis.[22] However, sample throughput is limited in LC due to optimum gradient elution programs (> 7-10

min/sample) required to resolve chemically diverse classes of DoA and their isomers together with adequate post-run column equilibration times to reduce sample carry-over.[15-20] Alternatively, CE-MS offers a high efficiency separation platform that is ideal for resolving complex mixtures of drugs that vary widely in their polarity from small volumes of biological specimens.[23-27]

Herein, we demonstrate that multisegment injection-capillary electrophoresis-mass spectrometry (MSI-CE-MS)[28] offers a high throughput platform for nontargeted screening of DoA that takes advantage of serial sample injections and novel data workflows in metabolomics with quality assurance.[29-33] Acceptable precision and accuracy was achieved for screening a broad spectrum of DoA and their metabolites with minimal sample carry-over, matrix effects and isobaric interferences when comparing analysis in a synthetic urine matrix relative to human urine. This offers a cost-effective yet rapid method for reliable detection and unambiguous identification of over 50 DoA at their recommended screening cutoff limits, while also allowing for urine specimen verification, creatinine normalization, and retrospective testing for emerging drugs of major concern to public health.

4.3 Experimental

4.3.1 CE-MS Instrumentation

An Agilent 6550 quadrupole-time-of-flight (QTOF) mass spectrometer with a dual Agilent JetStream electrospray (dual AJS ESI) ionization source

equipped with an Agilent 7100 capillary electrophoresis (CE) unit was used for drug screening and confirmatory testing. An Agilent 1260 Infinity Isocratic pump and a 1260 Infinity degasser were used to deliver a 60:40 methanol:water with 0.1% *v/v* formic acid at a rate of 10 µL/min when using a coaxial sheath liquid interface. In this case, the nebulizer was set at 8 psi and the drying gas was delivered at 16 L/min at 200°C with a sheath gas flow of 3.5 L/min at 200°C. Instrument control and data acquisition was performed using Agilent MassHunter Workstation LC/MS Data Acquisition Software (B.06.01). Separations were performed on 120 cm bare fused-silica capillaries with an internal diameter of 50 µm (Polymicro Technologies Inc., AZ, USA). Approximately 7 mm of the polyimide coating was removed from both the capillary inlet and the outlet using a capillary window maker (MicroSolv, Leland, NC, USA) in order to reduce sample carry-over, as well as polymer swelling or degradation when in contact with organic solvent or buffer solutions containing ammonia, respectively.[31] An applied voltage of 30 kV at 25°C was used for all runs in conjunction with a pressure gradient of 2 mbar/min to allow for elution of slow migrating benzodiazepenes prior to the electroosomotic flow (EOF) within about 30 min. The background electrolyte (BGE) was 1 M formic acid with 13% *v/v* acetonitrile as organic modifier with a pH 1.8. Samples were injected hydrodynamically at 50 mbar (5 kPa), alternating between 5 s for each sample and 40 s for the BGE that serves as a buffer spacer plug to encode mass spectral information temporally within a separation,[32] for a total of 10 discrete samples analyzed within a single

run. Customized serial injection configurations using drug calibrants, blanks and quality controls (QC) were implemented depending on study design requirements, such as interday precision, sample carry-over, or external calibration. Previous studies using MSI-CE-MS[29-33] have used a 7-sample plug injection format in order to maximize metabolome coverage without overlap of involatile salts (*e.g.*, Na^+, K^+) with fast migrating small cations (*e.g.*, glycine, choline), which was not a constraint for the panel of DoA examined in this work. Prior to first use, each bare fused-silica capillary was conditioned by flushing for 20 min at 950 mbar (95 kPa), sequentially, with methanol, 1 M sodium hydroxide, water and BGE. Between runs, the capillary was flushed with BGE for 15 min at 950 mbar (95 kPa). At the start of each day, the spray chamber of ion source and CE electrode at the inlet were cleaned with isopropanol:water (50:50) to prevent sample carryover and salt build up, whereas mass calibration was performed daily as part of routine maintenance of QTOF-MS system. Reference ions purine and hexakis(2,2,3,3-tetrafluoropropoxy)phosphazine (HP-921) were spiked into the sheath liquid at 0.02% *v/v* to provide constant mass signals at *m/z* 121.05087 and *m/z* 922.00979 to enable real-time reference mass correction, which also allows for monitoring for potential ion suppression/enhancement effects during separation. The instrument was operated in 4GHz Hi res mode with the slicer in high resolution position. The Vcap and nozzle voltage were both 2,000V, while the fragmentor was 380 V, the skimmer was 65 V and the Octopole RF was 750 V. The QTOF scan range was 50-1,700 *m/z* that was configured with full-scan data acquisition

mode for broad spectrum screening of DoA at a rate of 1 spectra/s. This allowed for a broad spectrum of DoA and their metabolites to be detected in a targeted or nontargeted manner, including a wide range of endogenous urinary metabolites. All drug calibrator solutions were prepared in a pooled 24 h human urine sample derived from the Prospective Urban-Rural Epidemiological study,[34] or a certified synthetic urine matrix, Surine™ Negative Urine Control (Cerilliant, Round Rock, TX, USA), followed by enzyme deconjugation using IMCSzyme β-glucuronidase solution and rapid hydrolysis buffer solution under standard conditions (IMCS, Irmo, SC, USA). Processed multidrug calibrants were then diluted five-fold in deionized water including a common internal standard (IS), 4-fluoro-*L*-phenylalalnine (10 μM, F-Phe), as well as a mixture of deuterated internal standards (D-IS) for specific DoA prior to MSI-CE-MS. Confirmatory drug identification was also performed using targeted MS/MS with collisional-induced dissociation at an optimal collisional energy (10, 20 or 40V) when performing a single injection in CE-MS with on-line sample preconcentration[35,36] in order to improve sensitivity for high quality MS/MS acquisition. Correction for changes in migration time was performed by normalization to 10 μM F-Phe as IS (*i.e.*, relative migration time), whereas data normalization for peak integration used either F-Phe or a suitable D-IS. Other experimental information, including materials and methods, sample preparation and method validation are described in the Supporting Information section.

4.4. Results and Discussion

4.4.1 Multiplexed Separations for Rapid and Nontargeted Screening of DoA

Since zonal separation and ionization of solutes in CE-MS occur under homogenous/isocratic conditions, serial sample injections can be implemented to enhance sample throughput while maximizing duty cycle during mass spectral data acquisition without additional infrastructure costs. **Figure 4.1A** depicts a total ion electropherogram (TIE) derived from a serial injection sequence of 10 discrete sample plugs by MSI-CE-MS within a single run, where each sample was comprised of a multi-drug panel mixture prepared in a commercial synthetic urine matrix (Surine™) following enzyme deconjugation (*i.e.,* drug glucuronides). This resulted in a series of ten time-resolved signals detected for each drug species, which were annotated based on their characteristic accurate mass (*m/z*) and relative migration time (RMT). CE separations were performed under strongly acidic conditions (pH 1.8) with a coaxial sheath liquid interface to ensure stable spray formation under steady-state ionization conditions. Overall, there were three major migration time windows noted for the DoA panel, including a major group of fast migrating/fully ionized (pK_a > 8.0) alkaloids (*e.g.,* amphetamines, opioids, tricyclic antidepressants etc.) followed by a sub-group of slower migrating/weakly basic (pK_a < 2) benzodiazapene analogs, and neutral compounds/acidic drugs (*e.g.,* carbamates, barbituates) that co-migrate with the electroosmotic flow (EOF). Importantly, high efficiency separations were critical for resolution of low abundance DoA (*e.g.,* ketamine) from involatile salts (*i.e.,* Na^+, K^+) and other

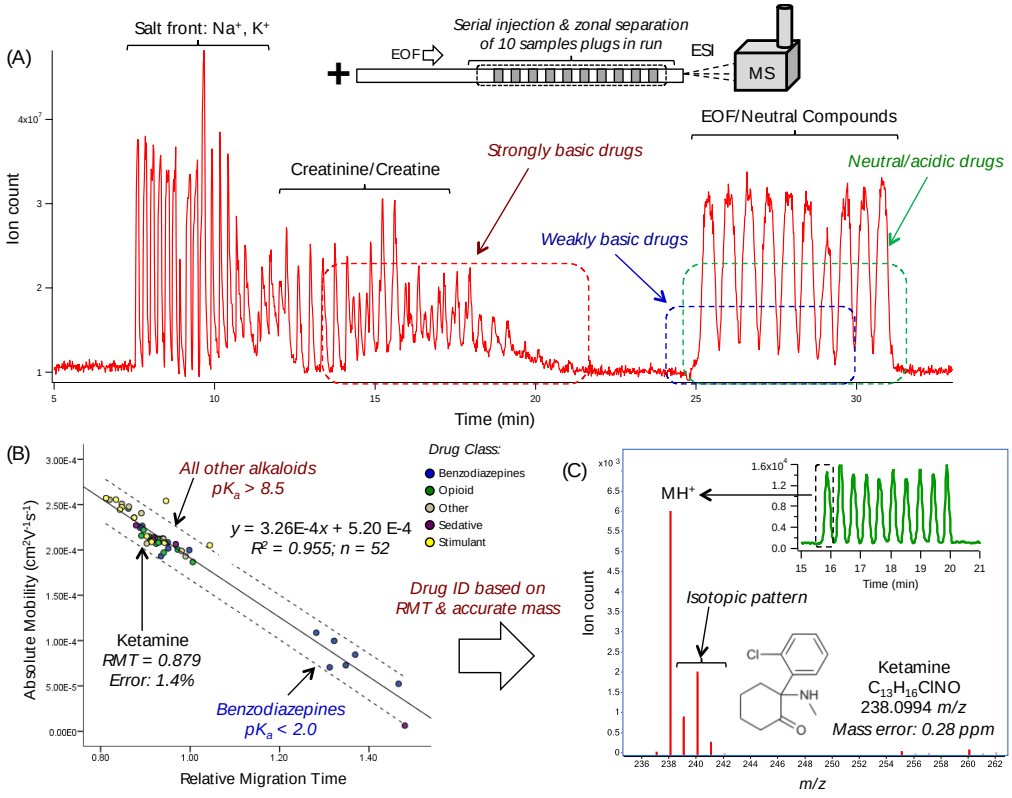

Figure 4.1. (A) Multiplexed separations for high throughput and nontargeted screening of a broad spectrum of DoA and their metabolites when using MSI-CE-MS under acidic conditions (pH 1.8) with full-scan data acquisition and positive ion mode detection, where 10 discrete sample plugs are analyzed within a single run. A total ion electropherogram (TIE) depicts resolution of major electrolytes/solutes in a synthetic urine matrix from two distinct classes of DoA, namely a large fraction of fully ionized (*e.g.*, opioids) and weakly basic compounds (*e.g.*, certain benzodiazepine analogs) from neutral/acidic drugs (*e.g.* barbituates) that co-migrate with the EOF. (B) A linear regression model with 95% confidence interval (dashed line) that demonstrates accurate prediction of the relative migration time (RMT) of a panel of DoA (n=52) based on their characteristic absolute electrophoretic mobility (pK_a and molecular volume) that facilitates identification of ketamine (m/z 238.0994; RMT = 0.879) when coupled to (C) high resolution MS for determination of the most likely molecular formula for its protonated molecule (MH^+) with low mass error (< 1 ppm). Note that electrolytes in synthetic urine were detected as their salt formate clusters for sodium and potassium that migrate prior to DoA and their metabolites.

major metabolites (*e.g.*, creatinine, creatine) in urine to reduce ion suppression especially when matching deuterated internal standards (D-IS) were not available for many drugs. The inherent desalting feature of CE was confirmed by

monitoring the internal reference mass calibrant signal over time since it was included in the sheath liquid solution for real-time mass calibration. In this case, ion suppression for MSI-CE-MS occurred primarily in the region of the salt front and EOF as shown in **Figure S4.1** of the Supporting Information. An overlay of extracted ion electropherograms (EIE) for various classes of DoA are also depicted in **Figures S4.2-S4.4** in the Supporting Information, including opioids, stimulants, and benzodiazepenes, whose migration behavior is dependent on their effective charge density in free solution. Out of the 86 drug panel originally examined in this work, 52 DoA were reliably measured by MSI-CE-MS at their recommended screening cut-off levels as shown in **Table S4.1** of the Supporting Information, which ranged from 10 to 2,500 ng/mL for norfentanyl and acetaminophen, respectively. Additionally, 6 DoA were not detectable due to inadequate sensitivity as a result of their lower cut-off limits following a 5-fold dilution in synthetic urine, whereas 8 other compounds were detectable, but had isobaric interferences from other drugs (*e.g.*, methylphenidate is isobaric and comigrates with normeperidine) or D-IS in mixture (*e.g.*, cocaine-D3 is isobaric with zolpidem). The latter cross-interference problem thus requires careful selection of optimal D-IS when performing broad spectrum drug screening by MS with full-scan data acquisition.[37] The remaining 19 drugs from panel were primarily acidic (*e.g.*, barbituates, cannabinoids) or neutral (*e.g.*, carbamates) classes of DoA that co-migrate with the EOF and thus were poorly ionizable in positive ion mode as summarized in **Table S4.2-S4.5** of the Supporting

Information. In this case, weakly acidic DoA are preferably analyzed by MSI-CE-MS under alkaline BGE conditions with negative ion mode detection, which offers a robust platform for large-scale profiling of anionic metabolites in urine.[31]

4.4.2 Confident Detection and Identification of DoA Above Cutoff Levels

Overall, there were two groups of cationic drugs resolved by MSI-CE-MS as shown in **Figure 4.1B**, whose migration behavior can be accurately predicted *in silico* when using a Hubbard-Onsager model for absolute mobility based on two intrinsic molecular parameters for an ion, namely effective charge and molecular volume.[35,36] Due to variations in EOF between runs in CE when using bare fused-silica capillaries without covalent neutral coatings,[38] the apparent migration times for all drugs were normalized to a single non-deuterated IS (F-Phe) for determination of their relative migration times (RMT). Overall, there was excellent linearity ($R^2 > 0.955$) for the regression model for a diverse array of DoA (n=52), which is useful for identification of unknown synthetic drug analogs and is complementary to high resolution MS.[39] For instance, the dissociative anesthetic, ketamine (m/z 238.0994), which is increasingly used recreationally despite concerns that chronic usage contributes to neurocognitive impairment, memory loss and ulcerative cystitis,[40] was accurately predicted within 1.4% error of its average RMT. **Figure 4.1C** shows an EIE inset with all ten resolved peaks for ketamine together with a full-scan TOF-MS mass spectrum for its protonated molecule (MH^+, mass error = 0.28 ppm), and isotope pattern for determination of its most likely molecular formula ($C_{13}H_{16}ClNO$). The average mass error for

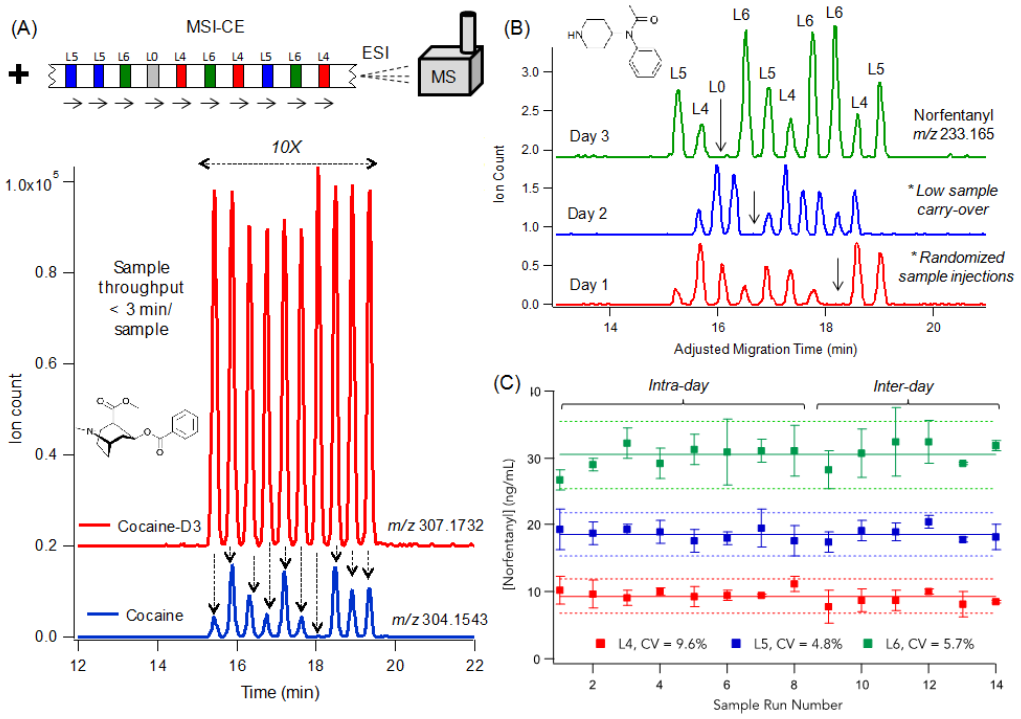

Figure 4.2. (A) Schematic of a 10-sample injection sequence in MSI-CE-MS used for evaluation of intraday precision by triplicate analysis of a multi-drug calibrator in synthetic urine matrix at three different concentration levels (L4: 1.0 X cut-off, L5: 2.0 X cut-off, L6: 3.0 X cut-off). A blank calibrator (L0) is also included to confirm lack of sample carryover together with a co-migrating D-IS that corrects for differences in injection volume between samples, as well as potential matrix effects. (B) An overlay of extracted ion electropherograms (EIE) for norfentanyl (*m/z* 233.1648) shows unique signal pattern when using randomized injection sequences for each run over 3 days together with new capillaries and buffer/sheath liquid solutions, where apparent migration times are adjusted for changes in EOF. (C) A control chart highlighting robust and reliable performance for screening norfentanyl at (L4) or above (L5, L6) screening cutoff limits at three concentration levels (n=117) with good precision (CV < 10%), where each data represents average concentration (n=3) per run with standard deviation (error bars) and 95% confidence intervals (dashed lines).

all 52 detectable DoA and their metabolites was 1.6 ppm, whereas the average error for RMT prediction was 0.40% as summarized in **Table S4.1** of the Supporting Information. As a result, MSI-CE-MS is anticipated to provide greater positive predictive value than immunoassays[41] due to its greater specificity for both drug detection and identification, which is provided by complementary

molecular information, including RMT, *m/z*, isotopic pattern and most likely molecular formula.

4.4.3 Long-term Precision and Assay Robustness

Next, both intraday and interday precision were evaluated when using MSI-CE-MS by analyzing repeated injections (n = 117 over 4 days) of DoA from processed Surine™ calibrators following enzyme deconjugation at three concentrations at recommended screening cutoff levels. In this case, new calibrant solutions/blanks, buffers and sheath liquid solutions, as well as fused-silica capillaries were prepared each day while performing preventative maintenance/mass calibration protocols. **Figure 4.2A** illustrates a serial injection format used for precision studies by MSI-CE-MS, where triplicate injections of each drug calibrator (where, L4, L5 and L6, correspond to 1X, 2X and 3X of screening cutoff level, respectively) were injected alongside a blank (L0) within a randomized sequence for each run. For instance, an EIE for cocaine (*m/z* 304.1543) together with its co-migrating D-IS (cocaine-D3, 188 ng/mL) highlights baseline resolution of all ten samples analyzed at three different concentration levels (< 3 min/sample) with no measurable signal for blank. In contrast, consistent ion responses were measured for cocaine-D3 reflecting minor differences in on-column injection volume between samples. As a result, integration of the measured ion response ratio for each drug relative to its corresponding D-IS from the same plug in MSI-CE-MS corrects for variations in sample injection volume between samples, as well as for potential matrix-induced

ion suppression effects in human urine. Consequently, detection of a drug and/or its metabolite above screening cutoff levels together with qualitative identification based on its accurate mass (*m/z*) and co-migration with a matching D-IS constitutes a reliable screen-positive urine test. **Figure 4.2B** shows an EIE overlay for norfentanyl (*m/z* 233.1648) over four days, a major urinary metabolite of the synthetic opioid, fentanyl that is up to 100-fold more potent than heroin, when using a randomized injection sequence for each run in MSI-CE-MS. While there were significant drifts in absolute migration times between days (≈ 2-5 min) due to variations in EOF as a result of changes in buffer/solution conditions and capillary wall surface properties (*i.e.*, zeta potential), the average RMT was under 0.50% when normalized to F-Phe. Thus, changes in the apparent migration time for F-Phe between runs was subsequently used as a simple way to adjust for migration time drift in CE. Additionally, **Figure 4.2C** depicts a control chart for norfentanyl demonstrating robust and reliable quantification over four days of analysis (total injections, n = 117) with a coefficient of variance (CV) ranging from 4.8% to 9.6% at three concentration levels at and above screening cut-off limits (10 ng/mL). Similarly, **Figure S4.5** in the Supplemental Information depicts representative control charts and long-term precision results for other classes of DoA by MSI-CE-MS, including illicit yet addictive stimulants (methamphetamine), a hypnotic benzodiazepine analog for treating anxiety and insomnia (nitrazepam), as well as over-the-counter medications prone to overdose (acetaminophen).

In this work, DoA were either normalized to a matching D-IS, a closely migrating D-IS from a similar drug class, or when the latter two options were not available, nor feasible due to cross-interferences, F-Phe was used as a non-deuterated IS. Optimal interday precision (n=15 over 3 days for each drug at each level) was achieved for all detectable DoA following selection of an optimal IS for each drug with a median CV = 13.8% ranging from 17.1% (L4), 13.5% (L5) and 11.6% (L6). As expected, these results were better than using F-Phe as a common IS for all 52 DoA with a median CV = 15.0% ranging from 19% (L4), 15% (L5), and 14% (L6). Similar trends were also observed for intraday precision studies (n=24 for each drug at each level in a single day) in MSI-CE-MS as shown in histograms of precision distribution in **Figure S4.6** of the Supporting Information. By choosing an IS that migrates near the analyte of interest, matrix effects from co-migrating compounds and salts can be mitigated and precision further improved. For example, acetaminophen is neutral at pH 1.8 and co-migrates with the EOF, a region of ion suppression (**Figure S4.1** of Supporting Information); thus normalization of measured ion responses to acetaminophen-D4 significantly improves overall precision to CV = 5.7% as compared to 13.8% when using F-Phe. However, D-IS are expensive and often not commercially available for many DoA and may contribute to potential cross interferences. Our work demonstrates that adequate reproducibility was still achieved in the context of broad spectrum drug screening when using F-Phe as a common IS since it

migrates close to the majority of DoA as reflected by an overall median CV = 14.4% as compared to CV = 13.0% following optimal selection of D-IS or F-Phe.

4.4.4 Sample Carryover, Matrix Effects and Isobaric Interferences in Urine

Sample carryover studies were also examined by MSI-CE-MS for method validation when performing an alternating series of injections comprising a blank (L0, *n*=8) and the highest level calibrator (L6, 3X cutoff level, *n*=12) over two separate runs. In this case, residual sample carryover effects were measured by the ratio of the mean ion response of the blank relative to L6 calibrator for each DoA. Removal of a section of the polyimide coating at the capillary inlet (*i.e.*, site of injection in contact with sample solution) was found to be important to reduce solute adsorption during repeated serial injections in MSI-CE-MS (data not shown) as required for high throughput drug screening of complex biological samples, such as human urine.[31] **Figure S4.7** of the Supporting Information depicts a schematic of the serial injection sequence used for sample carry-over studies together with an overlay of EIE for representative DoA. The median residual sample carryover across all DoA was only 0.62% (ranging from 0.1 to 9.1%), whereas 26 DoA had no detectable signals measured in the blank. Sample carryover > 4% were associated with certain hydrophobic drugs within the panel, including nortriptyline, fluoxetine, and tramadol. Increasing the organic solvent content (*i.e.,* acetonitrile) in the BGE or use of non-aqueous separation conditions[42] may further help reduce residual sample carry-over when performing serial injections from different samples. However, sample carryover overall was

not a significant concern for the vast majority of DoA examined. A unique advantage of MSI-CE-MS is that blank/screen-negative and QC/screen-positive controls can be introduced within the serial sample injection sequence for quality assurance as required within an accredited laboratory setting.[32] In this case, multiplexed separations that incorporate pooled QC samples (*e.g.*, DoA spiked in a reference urine) not only allow for assessment of technical precision between runs via control charts in order to detect for outliers/bias, but also permit batch-correction of long-term signal drift during large-scale metabolite screening studies.[33] This is in contrast to intermittent analysis of QC samples between blocks of runs (every 5-10) as part of quality assurance protocols in LC-MS when using conventional single sample injections.[43]

Synthetic urine is widely used for preparing matrix-matching calibrants/blank solutions for drug testing, however it does not comprise a large fraction of the human urine metabolome,[44] including exogenous metabolites from diet, environmental exposures and gut microflora. As a result, a comparison of the measured ion response for DoA (L6; 3X cutoff level) when spiked in Surine™ relative to authentic human urine (*i.e.*, pooled 24 h urine)[34] was performed as a way evaluate for potential matrix effects and unanticipated isobaric interferences. For instance, a base peak electropherogram of the synthetic urine matrix by MSI-CE-MS demonstrated that it was composed primarily of major electrolytes detected as various "salt-formate" cluster ions, such as *m/z* 90.9770, $(HCOONa)Na^+$ and *m/z* 206.8868, $(HCOOK)_2K^+$), as well as creatine, creatinine

and urea (co-migrated with EOF) as shown in **Figure S4.8** in the Supporting Information. In contrast, human urine contains a large number of other abundant cationic solutes that migrate after creatine, including proline betaine (*m/z* 144.1025) that is a robust biomarker of dietary citrus intake.[45] Indeed, drug screens implement several tests for specimen verification in order to detect fraudulent sample submission (*i.e.,* fake urine) or adulteration (*i.e.,* oxidation), including urine temperature upon collection, as well as pH, specific gravity and/or creatinine values within normal reference ranges. **Figure 4.3A** depicts a Passing-Bablok regression analysis that was used to evaluate for urine matrix effects as compared to measuring the same DoA panel in synthetic urine when using precision-optimized D-IS or F-Phe selected for data normalization. Overall, there was only modest ion suppression in human urine as reflected by a slope less than unity (slope = 0.953, n=52). However, this effect was not significantly different from the line of unity ($p > 0.05$) at a 95% confidence level with a mean bias of about 17% when performing a Bland-Altman %difference plot (data not shown). As anticipated, **Figure S4.9** in the Supporting Information demonstrates that urine-induced matrix effects were more evident when using F-Phe as a single non-deuterated IS for data normalization of all DoA as reflected by a slope significantly less than unity (slope = 0.735, $p < 0.05$) and a mean bias of 29%.

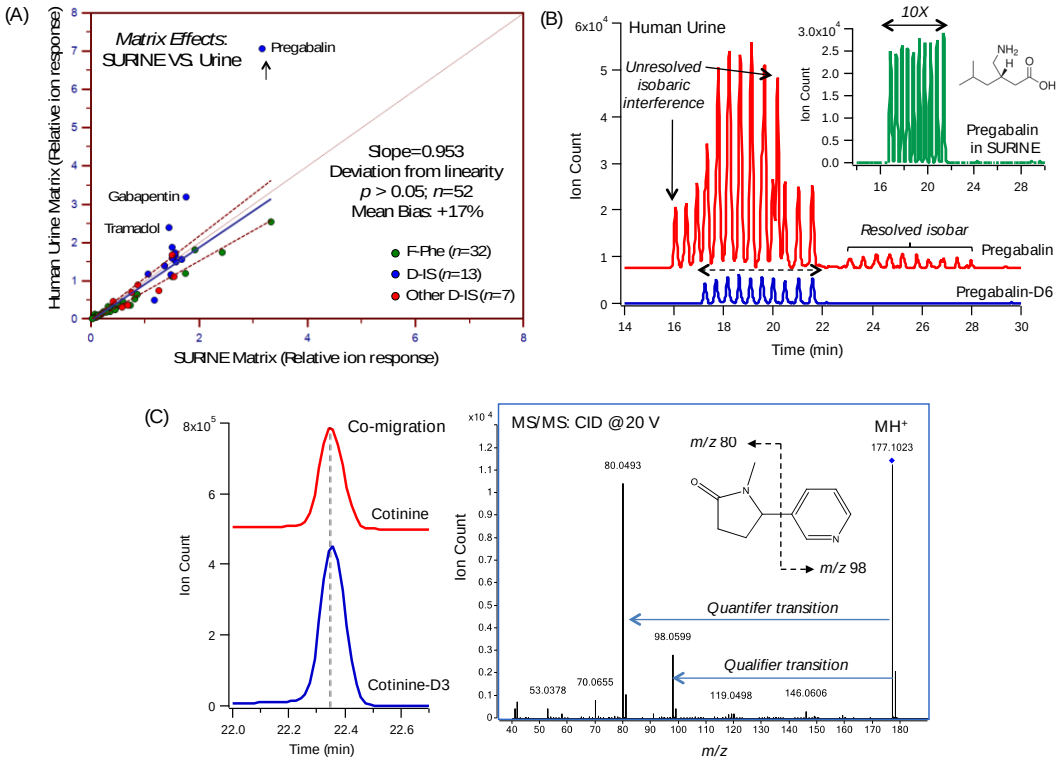

Figure 4.3. (A) Passing-Bablok regression analysis comparing the average ion response ratio for 52 DoA at L6 (3.0X cut-off level) spiked in a synthetic urine matrix (Surine™) relative to pooled human urine when normalized to matching D-IS, a closely migrating class-matched D-IS, or F-Phe that was optimized for assay precision. Overall, reliable screening by MSI-CE-MS was achieved for most drugs within the 95% confidence interval (dashed line) with minimal matrix effects and few isobaric interferences in human urine as reflected by a slope close to unity (0.953, $p > 0.05$) and an overall bias of 17%; (B) The positive bias for the extreme outlier (pregabalin) was the result of an unexpected co-migrating urinary isobar since Surine™ lacks a majority of metabolites in human urine. (C) Unambiguous identification of a screen-positive urine specimen was demonstrated by repeat analysis using a single injection by CE-MS with on-line sample preconcentration in order to acquire a high quality MS/MS product ion spectra with improved separation resolution. For instance, the confirmation of cotinine was derived from four criteria, namely co-migration with a D-IS, accurate mass of the protonated molecule (*m/z* 177.1023) and two characteristic product ions (*m/z* 80.0492; *m/z* 98.0599) at an optimal collisional voltage (20 V).

Nevertheless, these results are still acceptable in the context of MS-based screening of DoA without matching D-IS given other sources of variation that impact apparent concentration levels of drugs and their metabolites in human urine, including dosage, genetics, hydration status, and gut microbiome.[46] As

shown in **Figure 4.1**, MSI-CE-MS with full-scan mass spectral acquisition allows for broad spectrum drug screening together with creatinine normalization, as well as authentication of human urine based on a panel of common "host-microbe" co-metabolites[47] measured within a single run.

Unexpectedly, there were three drugs that displayed a large positive bias in human urine relative to Surine™ despite using matching D-IS (*i.e.*, not caused by matrix-induced ionization enhancement) that was attributed to unknown isobaric interferences, including pregabalin, gabapentin, and tramadol. For instance, **Figure 4.3B** shows that there were two urinary isobaric interferences detected for the outlier, pregabalin when performing full-scan data acquisition under positive ion mode detection in MSI-CE-MS. There was a fully resolved late migrating minor isobar, however an unknown early migrating second isobar (*m/z* 160.1332) partially overlapped with pregabalin. Indeed, both isobaric interferences were not detected in pregabalin when analyzed in Surine™ (inset), nor were problematic for pregabalin-D6 (*m/z* 166.1709) in human urine (blue trace). Similarly, the positive bias detected for tramadol in **Figure 4.3A** was also attributed to a partially overlapping unknown isobaric interference in urine (*m/z* 264.1958) as shown in **Figure S4.10** of the Supporting Information. One way to overcome these urinary interferences is to monitor an alternative ion for drug screening instead of the intact molecular ion (MH^+), such as the in-source product ion (*i.e.*, pseudo MS/MS) for pregabalin that is formed via loss of water (*m/z* 144.1228) during spray formation. In this case, improved specificity was achieved for

detection of pregabalin as highlighted in **Figure S4.11** of the Supporting Information.

4.4.5 Confirmatory Testing, External Calibration, and Detection Limits

Confirmatory testing can also be performed by MSI-CE-MS for unambiguous identification and quantification of presumptive/screen-positive urine specimens. In this case, repeat analysis using the same CE-QTOF-MS platform was ideally performed when using on-line sample preconcentration based on transient isotachophoresis via electrokinetic focusing of a single long injection plug on-capillary.[35] This provides three major benefits, namely greater concentration sensitivity for confirmatory testing of DoA misuse/abuse typically set at lower cutoff levels to reduce false positives, while also acquiring a higher quality product ion scan for drug identification when using high resolution MS/MS with spectral library matching under standardized conditions.[49] Additionally, improved separation performance was achieved with a single injection plug in CE as demonstrated by full resolution of all isobaric interferences described previously for pregabalin and tramadol as highlighted in **Figure S4.12** of the Supporting Information. For example, **Figure 4.3C** highlights that four characteristic parameters were used to confirm the identity of cotinine as a marker of recent nicotine exposure, including co-migration with its D-IS, as well as its molecular ion (MH^+) and two diagnostic product ions measured with high mass accuracy (< 2 ppm). Thus, the same instrumental platform can be used for rapid and multiplexed drug screening (*i.e.*, high throughput MSI-CE-MS mode with full

data acquisition) with follow-up confirmatory testing of screen-positive cases (*i.e.*, high selectivity CE-MS mode with targeted MS/MS analysis). For example, pre-operative drug testing for nicotine and other tobacco metabolites (*e.g.*, cotinine) in urine is often performed in high risk patients prone to substance abuse to prevent complications following surgery or while under anesthesia.[49] Similarly, **Figure S4.13** of the Supporting Information demonstrates confirmatory testing of the fast-acting benzenoid class opioid, tapentadol based on its characteristic qualifier and quantifier transitions, which has shown to have significantly lower abuse potential than prescribed opioid medications used for pain management, such as oxycodone.[50]

Although primary screening by immunoassays does not require absolute quantification, MSI-CE-MS still allows for reliable measurement of drug concentrations even when D-IS are lacking due to the modest extent of matrix effects in human urine. As a result, external calibration curves were prepared in synthetic urine matrix over a 25-fold concentration range with data normalized to a suitable IS (*i.e.*, F-Phe, or compound/class specific D-IS) using drug calibrators corresponding to 0.13X to 3.0X of recommended screening cut-off levels for a panel of 52 DoA. As shown in **Figure S4.14** and **Table S4.1** of the Supporting Information, good linearity (R^2 > 0.990) was achieved for measurement of drug concentrations both below and above recommended cut-off limits with a median LOD of 2.1 ng/mL ($S/N \approx 3$) that was dependent on solute ionization efficiency in positive ion mode detection[36] ranging from 0.4 ng/mL (benzoylecgonine) to 9.6

ng/mL (lorazepam) when using MSI-CE-MS with an on-column injection volume ≈ 5 nL. These LOD are adequate for screening the majority of cationic DoA at even lower cutoff thresholds to reduce false negatives with the exception of a subset of opioids with cut-off concentrations below 5 ng/mL, such as fentanyl and buprenorphine (**Table S4.2** of Supporting Information). In this case, MSI-CE-MS when coupled to new low flow/sheathless ion source designs[52, 53] can further boost concentration sensitivity for low abundance DoA without comprising sample throughput for systematic drug surveillance. Future work will also integrate MSI-CE-MS with automated search algorithms using customized MS/MS forensic spectral libraries allowing for the identification of over 1,200 DoA and toxic compounds.[51] Moreover, a simple "dilute-and-shoot" strategy will be examined for simultaneous screening and confirmation of DoA and their intact urinary glucuronide conjugates without enzymatic hydrolysis.[54] This strategy will offer considerable cost savings when using MSI-CE-MS as compared to conventional immunoassays by expanding drug coverage with improved accuracy that will ultimately reduce confirmatory activity in the laboratory currently performed by second-tier LC-MS/MS methods. Nontargeted drug screening is particularly relevant when identifying novel psychoactive substances not included within known drug panels,[55] as well as drug surveillance for suicide prevention as non-medical prescription drug users are at higher risk of death by suicide.[56] Future work will include a rigorous validation of MSI-CE-MS for large-scale drug screening and confirmatory testing as compared to immunoassays and LC-

MS/MS, while expanding drug coverage by using more sensitive ion source interfaces and alternative biospecimens, such as dried blood spots.[32]

4.5 Conclusion

This work introduces a rapid and nontargeted platform for drug screening based on multiplexed CE separations in conjunction with high resolution MS that is applicable to diverse classes of DoA prone to bias when using targeted colorimetric-based immunoassays. Simultaneous analysis of 10 independent samples within a single run was achieved by MSI-CE-MS with minimal sample carry-over, matrix effects and isobaric interferences in human urine, which allows for reliable detection and identification of more than 50 DoA at or above their recommended screening cut-off limits. In addition to the increase in sample throughput (< 3 min/sample) without added infrastructure costs, MSI-CE-MS provides excellent long-term precision with adequate accuracy for screening a broad spectrum of DoA even when matching D-IS are lacking. Moreover, novel serial injection sequences together with temporal signal pattern recognition in MS can be designed to include a calibrant, blank and/or QC together with randomized urine specimens within each run for quality assurance within an accredited laboratory facility. Confirmatory testing of screen-positive cases can also be performed by the same platform when using CE-MS with on-line sample preconcentration together with MS/MS product ion scanning that allows for unambiguous drug confirmation and absolute quantification. Importantly, MSI-CE-MS with full-scan data acquisition allows for *a posteriori* testing to detect

concurrent polydrug usage beyond known illicit drugs and prescribed medications. This approach also offers a promising way to screen for commercial adulterants and synthetic urine products by simultaneous measurement of a panel of common dietary and microflora-derived metabolites, while also correcting for hydration status using creatinine, without the need to use stand-alone urine verification tests.

4.7 Acknowledgements

P.B.M. wishes to acknowledge funding support from the Natural Sciences and Engineering Research Council of Canada, the Canada Foundation for Innovation, Genome Canada and McMaster University.

4.8 References

(1) Rentsch, K. M. *TrAC - Trends Anal. Chem.* **2016**, *84*, 88–93.

(2) Degenhardt, L.; Hall, W. *Lancet* **2012**, *379*, 55–70.

(3) Rudd R. A.; Aleshire N.; Zibbell J. E.; Gladden R.M. *MMWR Morb. Mortal. Wkly Rep.* **2016**, *64*, 1378–82.

(4) Florence, C.S.; Zhou, C.; Luo, F.; Xu, L. *Medical Care*, **2016**, *54*, 901-6.

(5) Meyer M. R.; Maurer H. H. *Curr. Drug Metab.* **2010**, *11*, 468-82.

(6) Standridge, J. B.; Adams, S. M.; Zotos, A. P. *Am. Fam. Physician* **2010**, *81*, 635–40.

(7) Peters, F.T. *Clin. Biochem.* **2011**, *44*, 54-65

(8) Milone, M. C. *J. Med. Toxicol.* **2012**, *8*, 408–16.

(9) Brahm, N. C.; Yeager, L.Y Y.; Fox, M. D.; Farmer, K.C.; Palmer, T.A. *Am. J. Health Syst. Pharm.* **2010**, *67*, 1344-50.

(10) Saitman, A.; Park, H. D.; Fitzgerald R. L. *J. Anal. Toxicol.* **2014**, *38*, 387-96.

(11) Marin, S. J.; Doyle, K.; Chang, A.; Concheiro-Guisan, M.; Huestis, M. A; Johnson-Davis, K. L. *J. Anal. Toxicol.* **2016**, *40*, 37–42

(12) Lachenmeier, D. W.; Sproll, C.; Musshoff, F. *Ther. Drug Monitor.* **2010**, *32*, 11-8.

(13) Mikel, C.; Pesce, A. J.; Rosenthal, M.; West, C. *Clin. Chem. Acta* **2012**, *413*, 1199-202.

(14) Reisfeld, G. M.; Goldberger, B.A.; Bertholf, R. L. Bioanalysis **2009**, *1*, 937-52.

(15) Marin, S. J.; Hughes, J. M.; Lawlor, B. G.; Clark, C. J.; McMillin, G. A. *J. Anal. Toxicol.* **2012**, *36*, 477–86.

(16) Chindarkar, N. S.; Wakefield, M. R.; Stone, J. A.; Fitzgerald, R. L. *Clin. Chem.* **2014**, *60*, 1115-25.

(17) Tsai, I. L.; Weng, T. I.; Tseng, Y. J.; Tan, H. K. L.; Sun, H. J.; Kuo, C. H. *J. Anal. Toxicol.* **2013**, *37*, 642–51.

(18) Kinyua, J.; Negreira, N.; Ibanez, M.; Bijlisma, L.; Hernandez, F., Covaci, A.; van Nuijs A. L. *Anal. Bioanal. Chem.* **2015**, *407*, 8773-85.

(19) Gao, Y.; Zhang, R.; Bai, J.; Xia, X.; Chen, Y.; Luo, Z.; Xu, J.; Gao, Y.; Liu, Y.; He, J.; Abliz, Z. *Anal. Chem.* **2015**, *87*, 7535-39.

(20) Thoren, K. L.; Colby, J. M.; Shugarts, S. B.; Wu, A. H. B.; Lynch, K. L. *Clin. Chem.* **2016**, *62*, 170–78.

(21) Schneir, A.; Metushi, I. G.; Sloane, C.; Barnaron, D. J.; Fitzgerald, R. L. *Clin. Toxicol.* **2017**, *55*, 51-54.

(22) Wu, A. H.; Colby J. *Methods Mol. Biol.* **2016**, *1383*, 153-66.

(23) Lazar, I. M; Naisbitt, G.; Lee, M. L. *Analyst* **1998**, *123*, 1449-54.

(24) Gottardo, R.; Fanigliulo, A.; Bortolotti, F., De Paoli, J. P.; Tagliaro, F. *J. Chromatogr. A* **2007**, *1159*, 190-7.

(25) Gottardo, R.; Polettini, A.; Sorio, D.; Pascali, J. P.; Bortolotti, F.; Liottra, E.; Tagliaro, F. *Electrophoresis* **2008**, *29*, 4078–87.

(26) Botello, I.; Borrull, F.; Calull, M.; Aguilar, C.; Somsen G. W.; de Jong, G. J. *Anal. Bioanal. Chem.* **2012**, *403*, 777–84.

(27) Kohler I., Schappler J., Rudaz S. *Anal. Chim. Acta* **2013**, *780*, 101-9.

(28) Kuehnbaum, N. L.; Kormendi, A.; Britz-McKibbin, P. *Anal. Chem.* **2013**, *85*, 10664–69.

(29) Kuehnbaum, N. L.; Gillen, J. B.; Gibala, M. J.; Britz-McKibbin, P. *Sci. Reports* **2014**, *4*, 6166.

(30) Kuehnbaum, N. L.; Gillen, J. B.; Kormendi, A.; Lam, K. P.; DiBattista, A.; Gibala, M. J.; Britz-McKibbin, P. *Electrophoresis* **2015**, *36*, 2226-36.

(31) Yamamoto, M; Ly, R.; Gill, B.; Zhu. Z.; Moran-Mirabal, J.; Britz-McKibbin, P. *Anal. Chem.* **2016**, *88*, 10710-19.

(32) DiBattista, A.; McIntosh, N.; Lamoureux, M.; Al-Dirbashi, O.; Chakraborty, P.; Britz-McKibbin, P. *Anal. Chem.* **2017**, *89*, 8112-21.

(33) Nori de Macedo, A.; Mathiaparanam, S.; Brick. L.; Keenan, K.; Gonska, T.; Pedder, T.; Hill, S.; Britz-McKibbin, P. *ACS Cent. Sci.* **2017**, doi:10.1021/acscentsci.7b00299.

(34) Nori de Macedo, A.; Teo, K.; Mente, A.; McQueen, M; Zeidler, J.; Poirier, P.; Lear, S.; Wielgosz A.; Britz-McKibbin, P. *Anal. Chem.* **2014**, *86*, 10010-15.

(35) Lee, R.; Ptolemy, A. S.; Niewczas, L.; Britz-McKibbin, P. *Anal. Chem.* **2007**, *79*, 403–15.

(36) Chalcraft, K. R.; Lee, R.; Mills, C.; Britz-McKibbin, P. *Anal. Chem.* **2009**, *81*, 2506–15.

(37) Wang, S.M; Chen, B.G.; Wu, M.Y.; Liu, R.H.; Lewis, R.J.; Ritter, R.M.; Canfield, D.V. *Forensic Sci. Rev.* **2009**, *21*, 69-144.

(38) Zhu, G.; Sun, L.; Dovichi N. J. *Talanta* **2016**, *146*, 839-43.

(39) D'Agostino, L.A.; Lam, K.P; Lee, R.; Britz-McKibbin, P. *J. Proteome Res.* **2011**, *10*, 592-603.

(40) Morgan, C. J.; Curran, H. V. *Addiction* **2012**, *107*, 27-38.

(41) Bertholf, R. L.; Sharma, R.; Reisfield, G. M. *J. Anal. Toxicol.* **2016**, *40*, 726-31.

(42) Roscher, J., Faber, H.; Stoffels, M.; Hachmöller, O.; Happe, J.; Karst, U. *Electrophoresis* **2014**, *35*, 2386-91.

(43) Kamleh, M.A; Ebbels, T.M.D; Spagou, K.; Masson, P.; Want, E.J. *Anal. Chem.* **2012**, *84*, 2670-77.

(44) Bouatra, S.; Aziat, F.; Mandal, R.; Guo, A.C.; Wilson, M.R.; Knox, C.; Bjorndahl, T.C.; Krishnamurthy, R.; Saleem, F.; Liu, P.; Dame, Z.T.; Poelzer. J.; Huynh, J.; Yallou, F.S.; Psychogios, N.; Dong, E.; Bogumil, R.; Roehring, C.; Wishart, D.S. *PLoS One* **2013**, *8*, e73076.

(45) Lang, R.; Lang, T.; Bader, M.; Beusch, A.; Schlagbauer, V.; Hofmann, T. *J. Agric. Food Chem.* **2017** *65*,1613-19.

(46) Swanson, H.I. *Drug Metab. Dispos*. **2015**, *43*, 1499-1504.

(47) Palau-Rodriguez, M.; Tupliani, S.; Queipo-Ortuño, M.I.; Urpi-Sarda, M.; Tinahones, F.J.; Andres-Lacueva C. *Front. Microbiol.* **2015**, *6*, 1151.

(48) Concheiro, M.; Castaneto, M.; Kronstrand, R.; Huestis, M.A. *J. Chromatogr. A* **2015**, *1397*, 32-42.

(49) Kork, F.; Neumann, T.; Spies, C. *Curr. Opin. Anaesthesiol.* **2010**, *23*, 384-90.

(50) Butler, S.F.; McNaughton, E.C.; Black, R.A. *Pain Med.* **2015**, *16*, 119-30.

(51) Sun, L.; Zhu, G.; Zhang, Z.; Mou, S.; Dovichi, N.J. *J. Proteome. Res.* **2015**, *14*, 2312-21.

(52) Zhang, W.; Hankemeier, T.; Ramataur, R. *Curr. Opin. Biotechnol.* **2017**, *43*, 1-7.

(53) Liu, H.-C.; Yang, C.-A., Liu, R.H.; Dong-Liang, L. *J. Anal. Toxicol.* **2017**, *41*, 421-30.

(54) Cao, Z.; Kaleta, E.; Wang, P. *J. Anal. Toxicol.* **2015**, *39*, 335-46.

(55) Heikman, P.; Sundstrom, M.; Pelander, A.; Ojanpera, I. *Hum. Psychopharmacol.* **2016**, *31*, 44-52.

(56) Wong, S.S.; Zhou, B.; Goebert, D.; Hishinuma, E.S. *Soc. Psychiatry Psychiatr. Epidemiol.* **2013**, *48*, 1611–20.

4.9 Supporting Experimental

4.9.1 Materials and Methods

All drug standards and their deuterated internal standards (D-IS) were purchased from Cerilliant (Round Rock, TX, USA) at a purity of 99% or better. All other chemicals, including 4-fluoro-*L*-phenylalanine (F-Phe) were purchased from Sigma-Aldrich (St. Louis, MO, USA). All drug stock solutions and calibrators were prepared in methanol and subsequently diluted in acetonitrile, respectively, whereas F-Phe was prepared in ultra LC-MS water (Caledon, Georgetown, ON, Canada). All standards were stored at 4°C. Multidrug calibrator solutions were made by diluting drug stock solutions into a synthetic urine matrix (Surine™ Negative Urine Control) from Cerilliant, whereas IMCSzyme β-glucuronidase solution, rapid hydrolysis buffer and standard solutions were obtained from IMCS (Irmo, SC, USA).

4.9.2 Sample Preparation

Multidrug calibrator solutions consisting of 86 drugs and their metabolites/isomers at various cutoff levels were prepared in 90:10 Surine™:acetonitrile, which were used as unextracted calibrators for external calibration curves. Extracted calibrators were prepared by adding 50 µL of calibrator to 60 µL of a 1:1:1 mixture of IMCSzyme β-glucuronidase solution, IMCSzyme Rapid Hydrolysis Buffer and internal standard solution, which were

used for precision, matrix effects and sample carry-over studies at concentrations at or above recommended cut-off levels for drug screening. This was to mimic conditions widely used in drug testing for selectively hydrolyzing drug-glucuronide conjugates excreted as secondary metabolites in human urine. The mixture was shaken for 30 min at 55°C to complete enzyme hydrolysis. A 10 µL aliquot of 10% *v/v* trichloroacetic acid was then added to quench the reaction and the resulting mixture was centrifuged for 10 min at 2,200 rpm (480 *x g*). Finally, 150 µL of 90:10 Surine™:acetonitrile was added before centrifuging for 10 min at 2,200 rpm (480 *x g*). Prior to analysis by MSI-CE-MS, each processed drug calibrator (5 µL) was diluted 5-fold with equal volumes of a deuterated internal standard (D-IS) mix, 10 µM F-Phe as IS and deionized water. Processed drug calibrators were also spiked into pooled 24 h human urine samples collected from the Prospective Urban-Rural Epidemiological Study[1] in order to evaluate for potential matrix effects not accounted by the synthetic urine.

4.9.3 Method Validation

Repeatability (intraday precision, *n*=24 for each drug at each level in a single day) was evaluated for a 86-drug panel mixture at three different concentrations corresponding to 1.0X (L4), 2.0X (L5) and 3.0X (L6) of screening cutoff levels (ng/mL) following a five-fold dilution in deionized water together with a Surine™ blank (L0). The recommended initial screening cut-off levels vary widely for different DoA depending on their pharmacokinetics, toxicity and background interferences in order to reduce false positives and false negatives

based on guidelines from the Substance Abuse and Mental Health Services Administration (SAMHSA).[2] Drug calibrators were prepared fresh and a new BGE was used for each run for precision studies. Eight runs were performed in total within a single day, and the injection position for each calibrant and blank was randomized in each run when using multisegment injection-capillary electrophoresis-mass spectrometry (MSI-CE-MS).[3] Similarly, reproducibility (interday precision, n=15 for each drug at each level over three days) was determined for a 86-drug panel by analyzing calibrators at three concentration levels (L4, L5, L6) and blank/L0 in two runs over three days, for a total of six runs. Overall, 117 sample injections were performed for each drug over four different days (intraday and interday precision) at three concentration levels by MSI-CE-MS, which were depicted in control charts to demonstrate method robustness and long-term precision. For long-term precision studies, new capillaries, sheath liquid and BGE solutions and drug calibrators were prepared each day while performing daily preventative maintenance and mass calibration. Data normalization for peak integration was optimized during precision studies by measuring the ratio of signal for the molecular ion (as MH^+) of drug relative to a matching IS (if available), D-IS from the same drug class (if close migrating) or F-Phe as a common non-deuterated IS that has a similar mobility to the majority of drugs and their metabolites within panel. Also, correction for changes in migration time was performed by normalization to F-Phe (*i.e.*, relative migration time or RMT), whereas adjusted migration times used a correction factor derived

from average migration time for F-Phe within each run to scale electropherograms accordingly. Additionally, sample carryover was evaluated by analyzing 12 injections by alternating injections of the highest calibrator (L6) drug mixture with a blank (L0) when performing two independent runs by MSI-CE-MS. External calibration curves were performed in duplicate for a series of unprocessed calibrators in Surine™ over a 25-fold linear dynamic range, including blank (L0), 0.13X cutoff (L1), 0.25X cutoff (L2), 0.33X cutoff (L3), 1.0X cutoff (L4), 2.0X cutoff (L5), 3.0 X cutoff (L6), as well quality controls (QC) at three different concentration levels. Method detection limits were determined by the minimum drug concentration that generated a signal to noise ratio (S/N) ≈ 3 for the molecular ion (MH^+) under positive ion mode detection.

4.9.4 Data Analysis

MSI-CE-MS data was analyzed by Agilent MassHunter Qualitative Analysis (B.06.00) software. All electropherograms were processed using Igor Pro 5.0 software (Wavemetric Inc., Lake Oswego, OR, USA). Statistical analyses including linear regression for relative migration time (RMT) prediction were performed using PASW Statistics 18 (SPSS Inc., Chicago, IL, USA). Chem 3D Professional software, version 12, (CambridgeSoft Inc., Cambridge, MA, USA) was used to calculate the Connolly solvent-excluded molecular volume (MV) after energy minimization using molecular mechanisms 2 (MM2) algorithm with molecular dynamics with 10,000 iterations as described previously.[4,5] The effective charge (z_{eff}) was estimated based on pK_a calculations using

chemicalize.org (ChemAxon, http://chemaxon.com). Passing-Bablok regression and Bland Altman % difference plots for evaluation of matrix effects when comparing drug quantification in Surine™ (synthetic urine matrix) relative to pooled human urine were performed in MedCalc version 12.5.0.0 (MedCalc Software, Ostend, Belgium).

4.10 Supporting References

(1) Nori de Macedo, A.; Teo, K.; Mente, A.; McQueen, M; Zeidler, J.; Poirier, P.; Lear, S.; Wielgosz A.; Britz-McKibbin, P. *Anal. Chem.* **2014**, *86*, 10010-10015.

(2) Substance Abuse and Mental Health Services Administration. "Analytes and Their Cutoffs." www.samhsa.com https://www.samhsa.gov/sites/default/files/workplace/2010GuidelinesAnalytesCutoffs.pdf (Accessed August 8, 2017).

(3) Kuehnbaum, N. L.; Kormendi, A.; Britz-McKibbin, P. *Anal. Chem.* **2013**, *85*, 10664–10669.

(4) Lee, R.; Ptolemy, A. S.; Niewczas, L.; Britz-McKibbin, P. *Anal. Chem.* **2007**, *79*, 403–415.

(5) Chalcraft, K. R.; Lee, R.; Mills, C.; Britz-McKibbin, P. *Anal. Chem.* **2009**, *81*, 2506–2515.

Table S4.1a. Summary of validation results for 52 DoA and their metabolites for high throughput yet reliable screening by MSI-CE-MS, including interday precision with optimal IS at three concentration levels, matrix effects/bias, sample carryover, as well as linearity, sensitivity and detection limits.

Drug Class	Drug of Abuse	Optimal IS for Precision	Precision[a] 1X Cutoff (CV, %)	Precision[a] 2X Cutoff (CV, %)	Precision[a] 3X Cutoff (CV, %)	Sample Carryover[b] (% of L6)
Benzodiazepine	Nordiazepam	F-Phe	13.0	6.4	7.6	0.71
Benzodiazepine	Nitrazepam	F-Phe	20.2	7.5	7.7	<LOD
Benzodiazepine	7-Aminoflunitrazepam	Meperidine-D4	24.3	9.8	13.0	0.10
Benzodiazepine	Diazepam	O-Desmethyl-cis-tramadol-D6	19.3	17.1	9.1	<LOD
Benzodiazepine	7-Aminoclonazepam	F-Phe	18.5	12.3	14.0	<LOD
Benzodiazepine	Oxazepam	F-Phe	27.0	20.7	14.3	<LOD
Benzodiazepine	Temazepam	F-Phe	29.9	19.2	15.2	<LOD
Benzodiazepine	Flunitrazepam	F-Phe	34.3	21.3	23.9	<LOD
Benzodiazepine	Clonazepam	F-Phe	30.9	20.3	16.6	<LOD
Benzodiazepine	Lorazepam	Diazepam-D5	31.5	17.5	12.1	<LOD
Benzodiazepine	Citalopram	Citalopram-D6	10.5	10.8	4.2	0.54
Benzodiazepine	Triazolam	F-Phe	23.0	19.8	19.2	<LOD
Benzodiazepine	Flurazepam	F-Phe	13.6	9.5	9.4	<LOD
Opioid	Gabapentin	Gabapentin-D10	14.5	11.3	9.6	0.72
Opioid	Tapentadol	F-Phe	10.4	12.6	9.6	<LOD
Opioid	Norfentanyl	F-Phe	17.2	8.1	10.0	<LOD
Opioid	Meperidine	Meperidine-D4	7.5	7.1	4.9	0.40
Opioid	Desmethyltramadol	O-Desmethyl-cis-tramadol-D6	6.7	6.5	4.7	0.51
Opioid	Tramadol	Tramadol-D3	5.2	7.4	5.8	4.61
Opioid	Hydrocodone	F-Phe	16.9	16.8	16.9	<LOD
Opioid	Codeine	F-Phe	14.8	11.6	12.2	<LOD
Opioid	Noroxycodone+ Oxymorphone	F-Phe	25.0	12.4	12.4	0.16
Opioid	Dihydrocodeine	F-Phe	15.1	16.1	14.4	<LOD
Opioid	Methadone	F-Phe	19.3	18.7	18.6	1.65
Opioid	Oxycodone	Oxycodone-D3	11.5	7.9	5.9	0.15
Opioid	Naltrexone	F-Phe	46.6	37.2	16.5	<LOD

[a] *Interday precision was assessed by analyzing five injections of each calibrator level (L4 or 1X cutoff level; L5 or 2X cutoff level; L6 or 3X cutoff level) each day over different 3 days (n = 15 for each drug at each level).*

[b] *Sample carryover was determined by alternating injections of highest calibrant (L6 or 3X cutoff level) for each drug and synthetic urine blank (L0) in two sets of runs (n=12 for L6).*

[c] *Matrix effects were assessed by Bland-Altman % difference plots by comparing average ion response (n=10) for L6 drug calibrant drug mixture spiked in synthetic urine matrix (Surine™) relative to pooled human urine when using optimal IS derived from inter-day precision studies.*

Table S4.1b. Summary of validation results for 52 DoA and their metabolites for high throughput yet reliable screening by MSI-CE-MS, including interday precision with optimal IS at three concentration levels, matrix effects/bias, sample carryover, as well as linearity, sensitivity and detection limits.

Drug Class	Drug of Abuse	Molecular Formula	Screening Cutoff (ng/mL)	*m/z* [MH^+]	Mass Error (ppm)	RMT (F-Phe)	Matrix Effects[c] (%Bias)	Sensitivity[d] $(ng/mL)^{-1}$	Linearity[d] (R^2)	LOD[e] (ng/mL)
Benzodiazepine	Nordiazepam	$C_{15}H_{11}ClN_2O$	50	271.0633	0.0	0.940	+21	0.0023	0.9990	4.12
Benzodiazepine	Nitrazepam	$C_{15}H_{11}N_3O_3$	50	282.0873	0.24	0.998	-66	0.0013	0.9952	2.96
Benzodiazepine	7-Aminoflunitrazepam	$C_{16}H_{14}FN_3O$	50	284.1194	0.12	0.997	-11	0.0051	0.9988	1.25
Benzodiazepine	Diazepam	$C_{16}H_{13}ClN_2O$	50	285.0789	2.22	1.014	+5.2	0.0035	0.9999	1.66
Benzodiazepine	7-Aminoclonazepam	$C_{15}H_{12}ClN_3O$	50	286.0742	0.35	0.893	+23	0.0024	0.9995	2.00
Benzodiazepine	Oxazepam	$C_{15}H_{11}ClN_2O_2$	50	287.0582	3.83	1.322	+34	0.0007	0.9261	4.08
Benzodiazepine	Temazepam	$C_{16}H_{13}ClN_2O_2$	50	301.0738	4.98	1.369	+27	0.0008	0.9845	3.92
Benzodiazepine	Flunitrazepam	$C_{16}H_{12}FN_3O_3$	50	314.0935	0.32	1.282	+45	0.0008	0.9774	11
Benzodiazepine	Clonazepam	$C_{15}H_{10}ClN_3O_3$	50	316.0483	2.64	1.348	+8.9	0.0008	0.9903	5.88
Benzodiazepine	Lorazepam	$C_{15}H_{10}Cl_2N_2O_2$	50	321.0192	3.63	1.545	+58	0.0008	0.9943	9.62
Benzodiazepine	Citalopram	$C_{20}H_{21}FN_2O$	100	325.1711	0.41	1.000	-5.9	0.0081	0.9997	1.58
Benzodiazepine	Triazolam	$C_{17}H_{12}C_{l2}N_4$	50	343.0512	0.19	1.312	+29	0.0010	0.9853	8.00
Benzodiazepine	Flurazepam	$C_{21}H_{23}ClFN_3O$	50	388.1586	1.12	0.935	+5.9	0.0032	0.9964	2.82
Opioid	Gabapentin	$C_9H_{17}NO_2$	50	172.1332	0.39	1.000	-58	0.0012	0.9965	2.34
Opioid	Tapentadol	$C_{14}H_{23}NO$	50	223.1852	0.9	0.908	+37	0.0113	0.9985	1.24
Opioid	Norfentanyl	$C_{14}H_{20}N_2O$	10	233.1648	0.57	0.896	+45	0.0033	0.9962	1.31
Opioid	Meperidine	$C_{15}H_{21}NO_2$	50	248.1645	0.94	1.000	-6.7	0.0108	0.9990	1.19
Opioid	Desmethyltramadol	$C_{15}H_{23}NO_2$	100	250.1802	0.53	1.000	--	--	--	--
Opioid	Tramadol	$C_{16}H_{25}NO_2$	50	264.1958	1.39	1.000	-50	0.0077	0.9996	0.83
Opioid	Hydrocodone	$C_{18}H_{21}NO_3$	50	300.1594	0.22	0.910	+43	0.0040	0.9973	1.82
Opioid	Codeine	$C_{18}H_{21}NO_3$	50	300.1594	2.11	0.918	+32	0.0040	0.9990	2.63
Opioid	Noroxycodone+ Oxymorphone	$C_{17}H_{19}NO_4$	50/50	302.1387	1.54	0.930	+21	0.0018	0.9984	1.69
Opioid	Dihydrocodeine	$C_{18}H_{23}NO_3$	50	302.1751	2.21	0.924	+65	0.0053	0.9969	0.731
Opioid	Methadone	$C_{21}H_{27}NO$	100	310.2165	0.54	0.941	+33	0.0086	0.9998	1.28
Opioid	Oxycodone	$C_{18}H_{21}NO_4$	50	316.1543	2.21	1.000	+23	0.0048	0.9999	1.18
Opioid	Naltrexone	$C_{20}H_{23}NO_4$	50	342.17	0.10	0.972	+39	0.0033	0.9998	1.99

[c] *Matrix effects were assessed by Bland-Altman % difference plots by comparing average ion response (n=10) for L6 drug calibrant drug mixture spiked in synthetic urine matrix (Surine™) relative to pooled human urine when using optimal IS derived from inter-day precision studies.*

[d] *External calibration data was calculated from duplicate analysis of six calibrants in synthetic urine matrix over a 25-fold linear dynamic range from 0.13X (L1) below to 3X (L6) above recommended screening cutoff (L4) limits when using full-scan data acquisition in positive ion mode.*

[e] *Method detection limit was estimated as the lowest drug concentration that generated a signal-to-noise ratio ≈ 3.*

Table S4.1c. Summary of validation results for 52 DoA and their metabolites for high throughput yet reliable screening by MSI-CE-MS, including interday precision with optimal IS at three concentration levels, matrix effects/bias, sample carryover, as well as linearity, sensitivity and detection limits.

Drug Class	Drug of Abuse	Optimal IS for Precision	Precision[a] 1X Cutoff (CV, %)	Precision[a] 2X Cutoff (CV, %)	Precision[a] 3X Cutoff (CV, %)	Sample Carryover[b] (% of L6)
Other/Hypotensive	Clonidine	Meperidine-D4	13.4	17.4	11.2	0.41
Other/Analgesic	Acetaminophen	Acetaminophen-D4	4.3	6.2	4.9	1.80
Other/Anticonvulsant	Pregabalin	Pregabalin-D6	9.3	9.6	8.2	0.58
Other/Stimulant	Cotinine	Cotinine-D3	5.3	6.7	4.1	0.52
Other/Antidepressant	Trazodone	Trazodone-D6	20.0	14.2	9.7	<LOD
Other/Antidepressant	Nortriptyline	Imipramine-D3	25.5	14.2	12.1	9.06
Other/Muscle relaxer	Baclofen	F-Phe	27.0	24.8	21.3	<LOD
Other/Antidepressant	Fluoxetine	Tramadol-D3	30.5	29.2	26.6	5.79
Other/Antidepressant	Amitriptyline	F-Phe	18.0	15.4	14.5	3.86
Other/Sedative	Norketamine	F-Phe	30.5	22.7	23.5	<LOD
Other/Sedative	Ketamine	Ketamine-D4	5.6	8.7	4.7	0.56
Other/Sedative	Desipramine	F-Phe	23.0	25.5	19.2	<LOD
Other/Sedative	Zaleplon	F-Phe	48.0	23.4	18.0	<LOD
Other/Muscle relaxant	Cyclobenzaprine	Tramadol-D3	27.1	24.1	12.1	2.87
Stimulant	Methamphetamine + Phentermine	F-Phe	12.1	14.2	7.7	1.28
Stimulant	Mephedrone	F-Phe	11.9	12.8	10.1	<LOD
Stimulant	MDA	F-Phe	27.4	32.2	21.7	0.62
Stimulant	MDMA	F-Phe	15.8	17.7	17.0	<LOD
Stimulant	MDEA	F-Phe	8.7	7.1	9.9	0.24
Stimulant	Ritalinic Acid	F-Phe	11.4	7.8	6.4	1.95
Stimulant	Diphenhydramine	F-Phe	16.4	9.8	9.6	<LOD
Stimulant	Naphyrone	Naphyrone-D5	39.6	26.4	14.0	<LOD
Stimulant	Benzoylecgonine	F-Phe	12.3	12.3	8.0	1.04
Stimulant	Cocaine	F-Phe	7.5	10.0	10.6	0.35

[a] *Interday precision was assessed by analyzing five injections of each calibrator level (L4 or 1X cutoff level; L5 or 2X cutoff level; L6 or 3X cutoff level) each day over different 3 days (n = 15 for each drug at each level).*

[b] *Sample carryover was determined by alternating injections of highest calibrant (L6 or 3X cutoff level) for each drug and synthetic urine blank (L0) in two sets of runs (n=12 for L6).*

[c] *Matrix effects were assessed by Bland-Altman % difference plots by comparing average ion response (n=10) for L6 drug calibrant drug mixture spiked in synthetic urine matrix (Surine™) relative to pooled human urine when using optimal IS derived from inter-day precision studies.*

Table S4.1d. Summary of validation results for 52 DoA and their metabolites for high throughput yet reliable screening by MSI-CE-MS, including interday precision with optimal IS at three concentration levels, matrix effects/bias, sample carryover, as well as linearity, sensitivity and detection limits.

Drug Class	Drug of Abuse	Molecular Formula	Screening Cutoff (ng/mL)	*m/z* [MH^+]	Mass Error (ppm)	RMT (F-Phe)	Matrix Effects[c] (% Bias)	Sensitivity[d] $(ng/mL)^{-1}$	Linearity[d] (R^2)	LOD[e] (ng/mL)
Other/Hypotensive	Clonidine	$C_9H_9Cl_2N_3$	25	230.0246	0.14	0.951	--	--	--	--
Other/Analgesic	Acetaminophen	$C_8H_9NO_2$	2500	152.0706	0.22	1.000	-23	0.0004	0.9987	16.8
Other/Anticonvulsant	Pregabalin	$C_8H_{17}NO_2$	150	160.1332	0.21	1.000	-76	0.0009	0.9981	4.23
Other/Stimulant	Cotinine	$C_{10}H_{12}N_2O$	250	177.1022	1.32	0.986	-2.6	0.0028	0.9971	1.87
Other/Antidepressant	Trazodone	$C_{24}H_{21}NO_3$	25	372.1594	3.49	1.000	+5.6	0.0067	0.9999	0.98
Other/Antidepressant	Nortriptyline	$C_{19}H_{21}N$	25	264.1747	1.26	1.001	+51	0.0056	0.9954	0.893
Other/Muscle relaxer	Baclofen	$C_{10}H_{12}ClNO_2$	25	214.0629	8.1	0.891	--	--	--	--
Other/Antidepressant	Fluoxetine	$C_{17}H_{18}F_3NO$	100	310.1413	2.04	1.007	+59	0.0022	0.9949	4.06
Other/Antidepressant	Amitriptyline	$C_{20}H_{23}N$	25	278.1903	0.6	0.903	+27	0.0115	0.9982	0.907
Other/Sedative	Norketamine	$C_{12}H_{14}ClNO$	20	224.0837	1.64	0.875	--	--	--	--
Other/Sedative	Ketamine	$C_{13}H_{16}ClNO$	100	238.0993	0.28	0.986	+7.2	0.0046	0.9994	1.12
Other/Sedative	Desipramine	$C_{18}H_{22}N_2$	25	267.1856	1.62	0.918	+55	0.0055	0.9995	2.56
Other/Sedative	Zaleplon	$C_{17}H_{15}N_5O$	20	306.1349	4.68	1.480	--	--	--	--
Other/Muscle relaxer	Cyclobenzaprine	$C_{20}H_{21}N$	25	276.1747	3.14	0.985	+5.7	0.0096	0.9990	2.11
Stimulant	Methamphetamine + Phentermine	$C_{10}H_{15}N$	100/50	150.1277	1.11	0.811	+42	0.0021	0.9701	3.01
Stimulant	Mephedrone	$C_{11}H_{15}NO$	100	178.1226	0.75	0.847	--	--	--	--
Stimulant	MDA	$C_{10}H_{13}NO_2$	100	180.1019	3.7	0.834	--	0.0004	0.9992	--
Stimulant	MDMA	$C_{11}H_{15}NO_2$	100	194.1176	0.17	0.843	+26	0.0028	0.9923	8.33
Stimulant	MDEA	$C_{12}H_{17}NO_2$	100	208.1332	0.96	0.875	+29	0.0053	0.9982	9.2
Stimulant	Ritalinic Acid	$C_{13}H_{17}NO_2$	50	220.1332	1.21	0.946	-8.0	0.0017	0.9948	5.97
Stimulant	Diphenhydramine	$C_{17}H_{21}NO$	100	256.1696	0.39	0.903	+25	0.0021	0.9981	2.45
Stimulant	Naphyrone	$C_{19}H_{23}NO$	20	282.1852	0.35	1.000	--	--	--	--
Stimulant	Benzoylecgonine	$C_{16}H_{19}NO_4$	25	290.1387	2.87	1.044	+28	0.0070	0.9981	0.475
Stimulant	Cocaine	$C_{17}H_{21}NO_4$	50	304.1543	0.88	0.914	+56	0.0028	0.9712	0.98

[c] *Matrix effects were assessed by Bland-Altman % difference plots by comparing average ion response (n=10) for L6 drug calibrant drug mixture spiked in synthetic urine matrix (Surine™) relative to pooled human urine when using optimal IS derived from inter-day precision studies.*

[d] *External calibration data was calculated from duplicate analysis of six calibrants in synthetic urine matrix over a 25-fold linear dynamic range from 0.13X (L1) below to 3X (L6) above recommended screening cutoff (L4) limits when using full-scan data acquisition in positive ion mode.*

[e] *Method detection limit was estimated as the lowest drug concentration that generated a signal-to-noise ratio ≈ 3.*

Table S4.2. Calibration data for 5 DoA that were not reliably detected at cut-off levels (L4) during inter-day precision studies by MSI-CE-MS due to their low cutoff levels or neutral (carisoprodol).

Drug Class	Drug of Abuse	Molecular Formula	Cutoff (ng/mL)	*m/z* [MH^+]	Mass Error (ppm)	RMT (F-Phe)	Sensitivity $(ng/mL)^{-1}$	Linearity (R^2)	LOD (ng/mL)[a]
Other	Carisoprodol	$C_{12}H_{24}N_2O_4$	50	261.1809	5.87	1.766	0.0002	0.9852	51.7
Opioid	6-Acetylmorphine+ Naloxone	$C_{19}H_{21}NO_4$	10/20	328.1543	0.61	0.927	0.0033	0.9942	0.816
Opioid	Fentanyl	$C_{22}H_{28}N_2O$	2	337.2274	2.57	0.967	0.0075	0.9985	1.54
Opioid	Norbuprenorphine	$C_{25}H_{35}NO_4$	5	414.2639	6.76	0.996	0.0029	0.9887	1.97
Opioid	Buprenorphine	$C_{29}H_{41}NO_4$	5	468.3018	0.0	1.043	0.0021	0.9788	3.41

[a]*Method detection limit was estimated as the lowest drug concentration that generated a signal-to-noise ratio ≈ 3.*

Table S4.3. List of 8 DoA and their metabolites that were detectable by MSI-CE-MS, but were not integrated due to the stated interferences.

Drug Class	Drug of Abuse	Molecular Formula	Cutoff Level (ng/mL)	*m/z* [MH^+]	Notes
Stimulant	Methylphenidate	$C_{14}H_{19}NO_2$	50	234.1489	Unresolved isomers
Opioid	Normeperidine	$C_{14}H_{19}NO_2$	50	234.1489	
Opioid	EDDP	$C_{20}H_{23}N$	100	278.1903	Partially Resolved
Other/TCA	Imipramine	$C_{19}H_{24}N_2$	25	281.2012	Interference with EDDP-D3
Opioid	Hydromorphone	$C_{17}H_{19}NO_3$	50	286.1438	Unresolved isomers
Opioid	Morphine	$C_{17}H_{19}NO_3$	50	286.1438	
Opioid	Norhydrocodone	$C_{17}H_{19}NO_3$	50	286.1438	
Sedative/hypnotic	Zolpidem	$C_{19}H_{21}N_3O$	10	308.1757	Interference with Cocaine-D3
Stimulant	Amphetamine	$C_9H_{13}N$	100	136.1121	Suppression by creatinine

Table S4.4. List of 19 DoA and their metabolites that were not detectable by MSI-CE-MS under positive ion mode with full-scan acquisition.

Drug Class	Drug of Abuse	Molecular Formula	Cutoff Level (ng/mL)	*m/z* [MH^+]	Notes
Benzodiazepine	Hydroxyalprazolam	$C_{17}H_{13}ClN_4O$	50	325.0851	Not detectable
Benzodiazepine	Alprazolam	$C_{17}H_{13}ClN_4$	50	309.0902	Not detectable
Barbituate/Sedative	Butalbital	$C_{11}H_{16}N_2O_3$	200	225.1234	Acidic/Not detectable
Other/Opioid	Desmethyltapentadol	$C_{13}H_{21}NO$	20	208.1696	Not detectable
Other/SNRI	Duloxetine	$C_{18}H_{19}NOS$	100	298.1260	Not detectable
Synthetic cannabinoid	JWH-018 Pentanoic	$C_{24}H_{21}NO_3$	5	372.1594	Acidic/Not detectable
Synthetic cannabinoid	JWH-073 Butanoic	$C_{23}H_{19}NO_3$	5	358.1438	Acidic/Not detectable
Synthetic cannabinoid	JWH-073 Hydroxybutyl	$C_{23}H_{21}NO_2$	5	344.1645	Acidic/Not detectable
Synthetic cannabinoid	JWH-200	$C_{25}H_{24}N_2O_2$	20	385.1911	Neutral/Not detectable
Barbituate/sedative	Meprobamate	$C_9H_{18}N_2O_4$	50	219.1339	Neutral/not detectable
Other/Muscle relaxant	Metaxalone	$C_{12}H_{15}NO_3$	10	222.1125	Neutral/Not detectable
Other/Opioid	Mitragynine	$C_{23}H_{30}N_2O_4$	4	399.2278	Neutral/Not detectable
Other/Anaesthetic	Phencyclidine	$C_{17}H_{25}N$	5	244.2060	Not detectable
Barbituate/Sedative	Phenobarbital	$C_{12}H_{12}N_2O_3$	200	233.0921	Acidic/Not detectable
Other/Opioid	Propoxyphene	$C_{22}H_{29}NO_2$	60	340.2271	Not detectable
Barbituate/Sedative	Secobarbital	$C_{12}H_{18}N_2O_3$	200	239.1390	Acidic/Not detectable
Other/Cannabinoid	THC-COOH	$C_{21}H_{28}O_4$	10	245.2060	Acidic/Not detectable
Other/Muscle relaxant	Tizanidine	$C_9H_8ClN_5S$	25	254.0262	Not detectable
Other/Sedative	Zopiclone	$C_{17}H_{17}ClN_6O_3$	100	389.1123	Not detectable

Table S4.5. Working concentrations of 41 deuterated internal standards.

Deuterated Internal Standard	*m/z* [MH^+]	Concentration (ng/mL)
O-Desmethyl-cis-Tramadol-D6	256.2178	3750
6-Acetylmorphine-D3	331.1732	375
Acetaminophen-D4	156.0957	18750
Amphetamine-D5	141.1435	3750
Benzoylecgonine-D3	293.1575	937.5
Butalbital-D5	230.1548	7500
Carisoprodol-D7	268.2248	1875
Citalopram-D6	331.2087	3750
Cocaine-D3	307.1732	937.5
Codeine-D6	306.1971	1875
Cotinine-D3	180.1211	1875
Diazepam-D5	290.1103	750
Diphenhydramine-D3	259.1884	3750
Duloxetine-D3	301.1448	3750
EDDP-D3	281.2092	3750
Fentanyl-D5	342.2588	75
Fluoxetine-D6	316.179	3750
Gabapentin-D10	182.196	937.5
Hydromorphone-D6	292.1814	1875
Imipramine-D3	284.2201	937.5
JWH-073-3-Hydroxybutyl metabolite-D5	349.1959	187.50
Ketamine-D4	242.1244	750
Meperidine-D4	252.1896	1875
Metaxalone -D6	228.1501	375
Morphine-D3	289.1626	150
Naltrexone-D3	345.1888	1875
Naphyrone-D5	287.2166	750
Norbuprenorphine-D3	417.2827	187.5
Norfentanyl-D5	238.1962	375
Oxycodone-D3	319.1732	1875
Oxymorphone-D3	305.1575	1875
Phencyclidine-D5	249.2374	187.5
Phenobarbital-D5	238.1235	7500
Pregabalin-D6	166.1709	1125
Secobarbital-D5	244.1704	7500
THC-COOH-D9	354.2625	375
Tramadol-D3	268.218	1875
Trazadone-D6	378.1962	937.5
Zaleplon-d4	310.16	750
Zolpidem-D7	315.2197	937.5
Zopiclone-D4	393.1374	3750

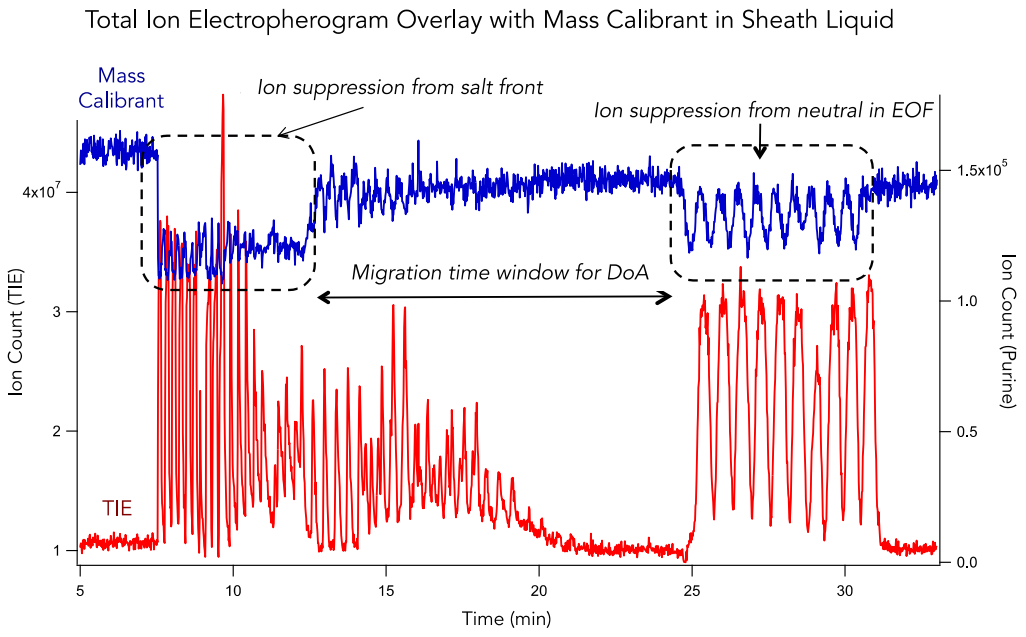

Figure S4.1. Total ion electropherogram (TIE) of 10 injections of an L6 calibrator (red trace) when using MSI-CE-MS as compared to an extracted ion electropherogram (EIE, blue trace) of the internal reference mass, purine (*m/z* 121.0509) that is added to sheath liquid solution highlighting two major regions of ion suppression in the synthetic urine matrix (Surine™). The first migrating zone is associated with migration of involatile electrolytes (*i.e.*, salt front comprising Na^+ and K^+) and a late eluting zone associated with neutral compounds in matrix (*e.g.*, urea, *m/z* 61.0393; unknown disaccharide, *m/z* 365.1072) that co-migrate with the electroosmotic flow (EOF). The majority of DoA migrate within the migration time window that extends from the salt front to the EOF allowing for their reliable quantification without significant ion suppression or enhancement effects even when matching deuterated internal standards (D-IS) are unavailable.

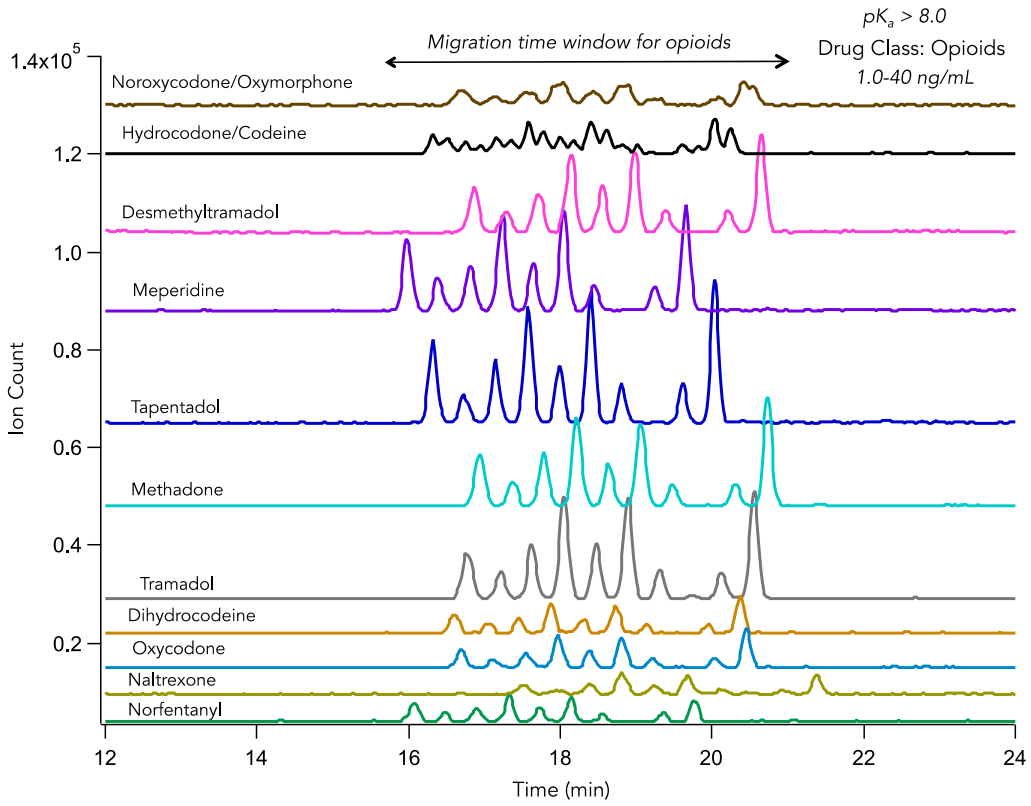

Figure S4.2. Extracted ion electropherograms (EIE) overlay from an intraday precision run (*i.e.*, randomized L4, L5, L6 calibrants in synthetic urine matrix injected in triplicate with single L0/blank within run) using MSI-CE-MS showing the migration of representative opioids and related DoA, including anticonvulsants, muscle relaxants and antidepressants. Most opioids migrate within a narrow separation window since they are fully ionized (pK_a > 8.0), where small difference in electrophoretic mobility (or RMT) are related to molecular volume of ion.

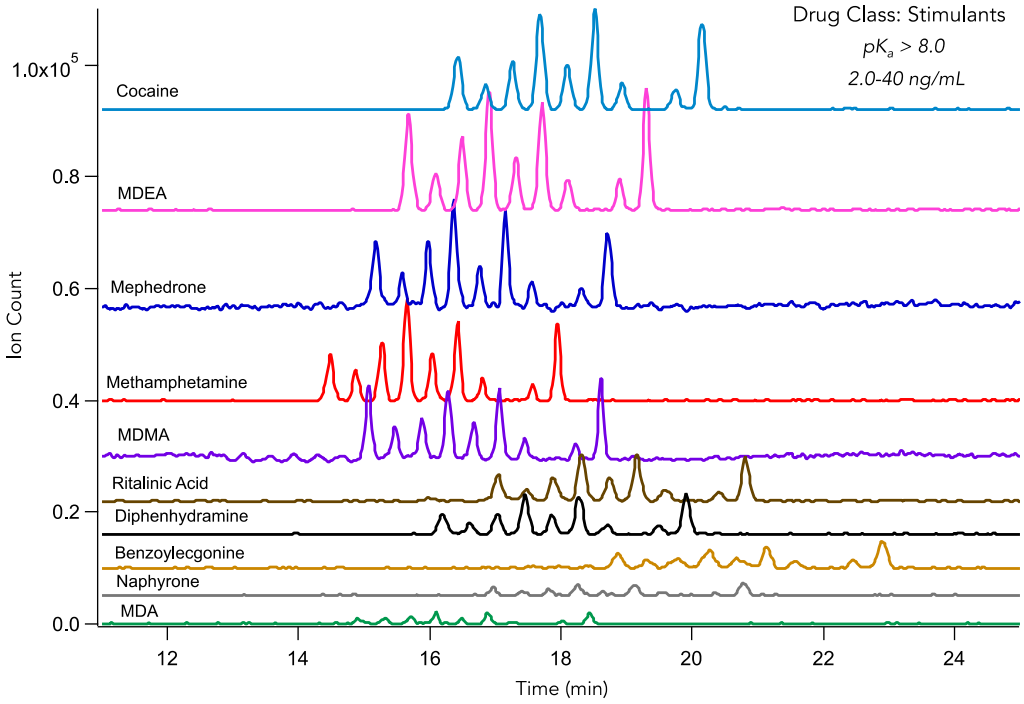

Figure S4.3. Extracted ion electropherograms (EIE) overlay from an intraday precision run (*i.e.*, randomized L4, L5, L6 calibrants in synthetic urine matrix injected in triplicate with single L0/blank within run) using MSI-CE-MS showing the migration of representative stimulants and amphetamines, including anticonvulsants, muscle relaxants and antidepressants. Most stimulants migrate within a wider separation window since they have more variable chemical structures despite being fully ionized (pK_a > 8.0), where differences in electrophoretic mobility (or RMT) are related to molecular volume of ion.

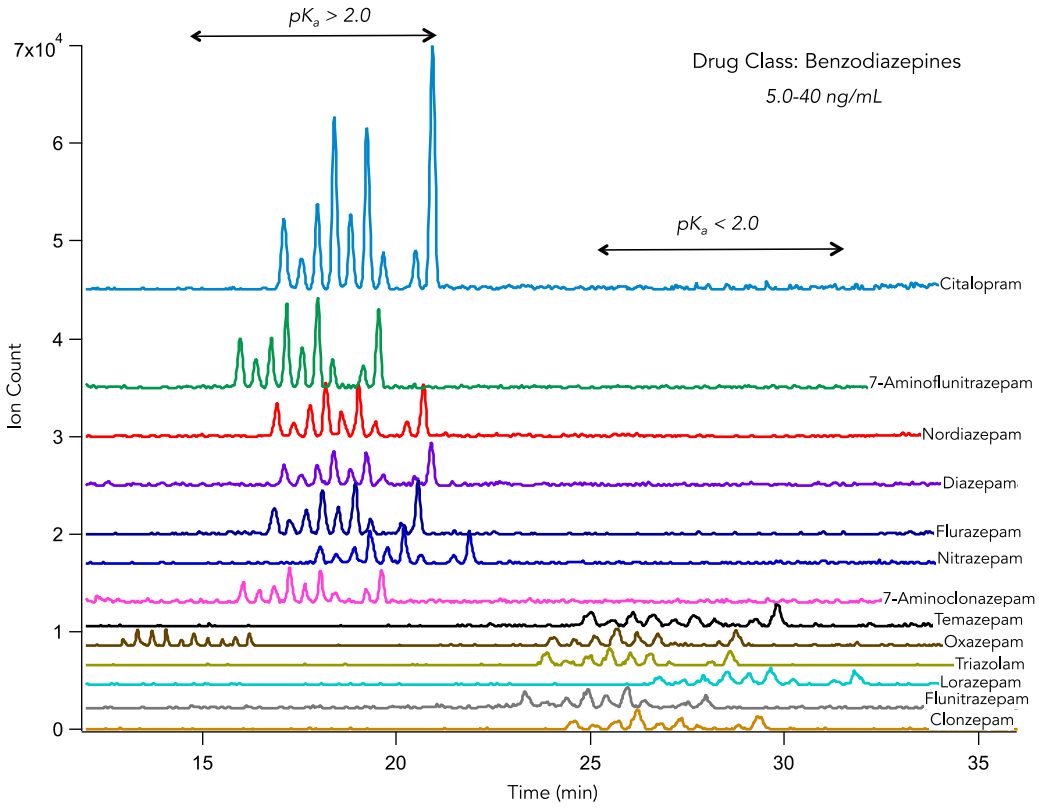

Figure S4.4. Extracted ion electropherograms (EIE) overlay from an intraday precision run (*i.e.*, randomized L4, L5, L6 calibrants in synthetic urine matrix injected in triplicate with single L0/blank within run) using MSI-CE-MS showing the migration of representative benzodiazapenes and their synthetic analogs. Most benzodiazapenes migrate within two discrete separation windows depending on their ionization state and molecular volume with less basic compounds (pK_a > 2.0, such as diazepam, pK_a = 3.3) migrating faster than less basic analogs (pK_a < 2.0, such as lorazepam, pK_a = 1.3) that are only partially ionized and thus elute prior to the EOF.

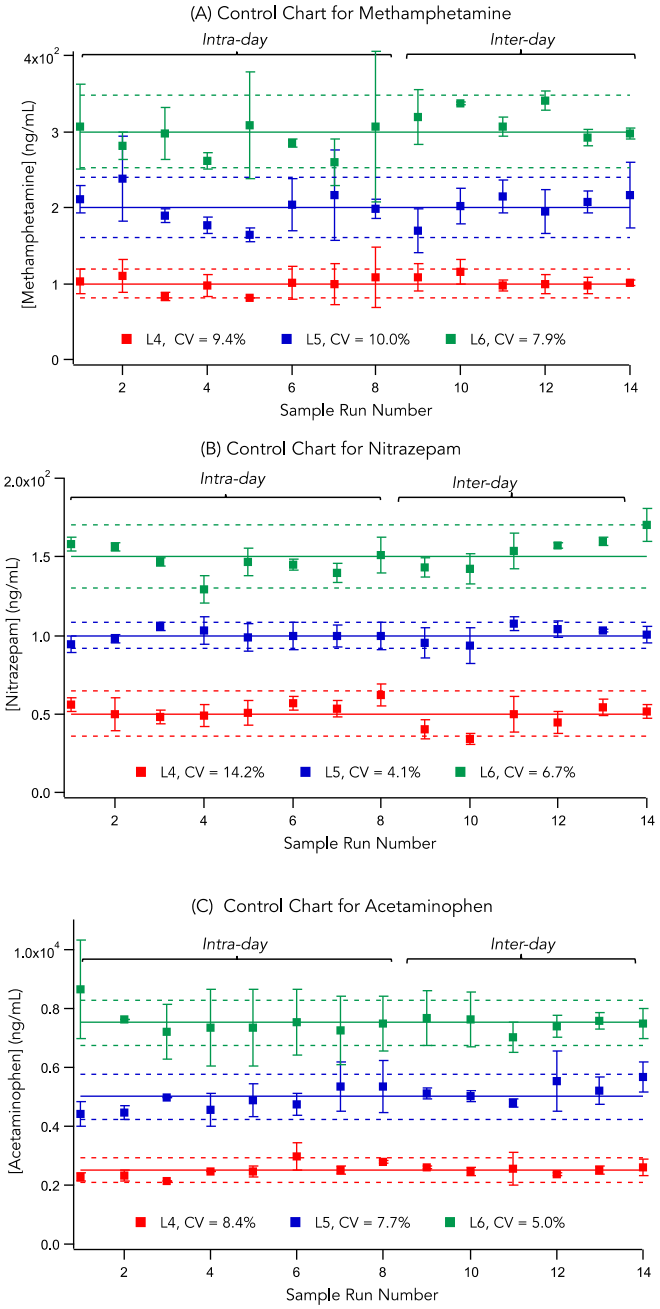

Figure S4.5. Representative control charts highlighting robust and reliable performance for screening diverse classes of DoA at (L4) or above (L5, L6) cutoff limits (*n*=117 total injections over 4 days) with good precision (CV < 15%) when using MSI-CE-MS, where each data represents average drug concentrations with standard deviation (error bars) and 95% confidence intervals (dashed lines). Overall, both intraday (8 runs in one day) and interday (2 runs per day over 3 days) precision studies demonstrate reliable screening of illegal stimulants (methamphetamine), benzodiazepine antidepressants (nitrazepam), and over-the-counter drugs prone to overdose (acetaminophen).

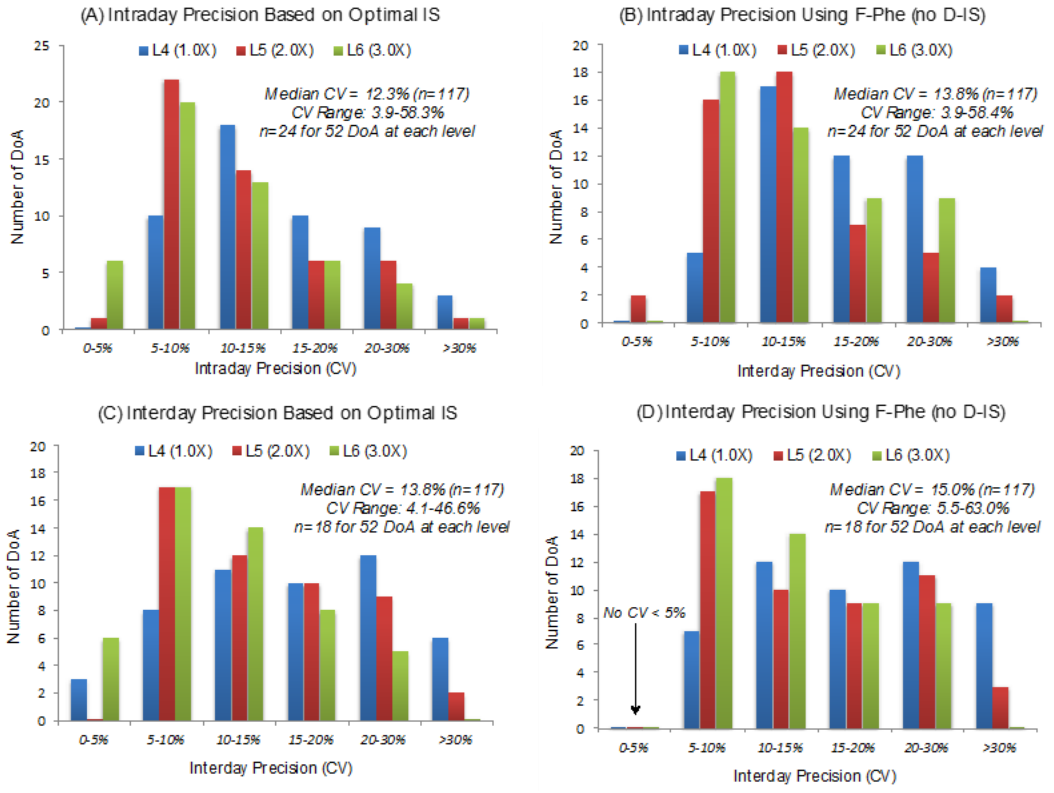

Figure S4.6. Histograms comparing the intraday and interday precision (*n*=117 for each drug at 3 levels over 4 days in total) for screening a broad spectrum of 52 DoA at 3 concentration levels at or above recommended cut-off limits in synthetic urine matrix (Surine™). For intraday precision studies, 8 runs were performed by MSI-CE-MS within a single day for a total of 24 repeated injections per drug at 3 concentration levels (*n*=72). For interday precision studies, 2 runs were performed each day over 3 different days for a total of 15 repeated injections per drug at 3 concentration levels (*n*=45). Overall, optimal precision was realized when using appropriate matching D-IS, D-IS from same drug class or F-Phe when the latter two options were not available, nor feasible due to isobaric interferences (*e.g.,* D-IS with other drugs in panel). However, acceptable precision for DoA screening was still achieved when using a single non-deuterated IS for data normalization, F-Phe that introduced only a slightly larger variance for DoA in terms of their median CV and range. This is important since matching D-IS are both expensive and not widely available for designer drugs or emerging synthetic drug analogs.

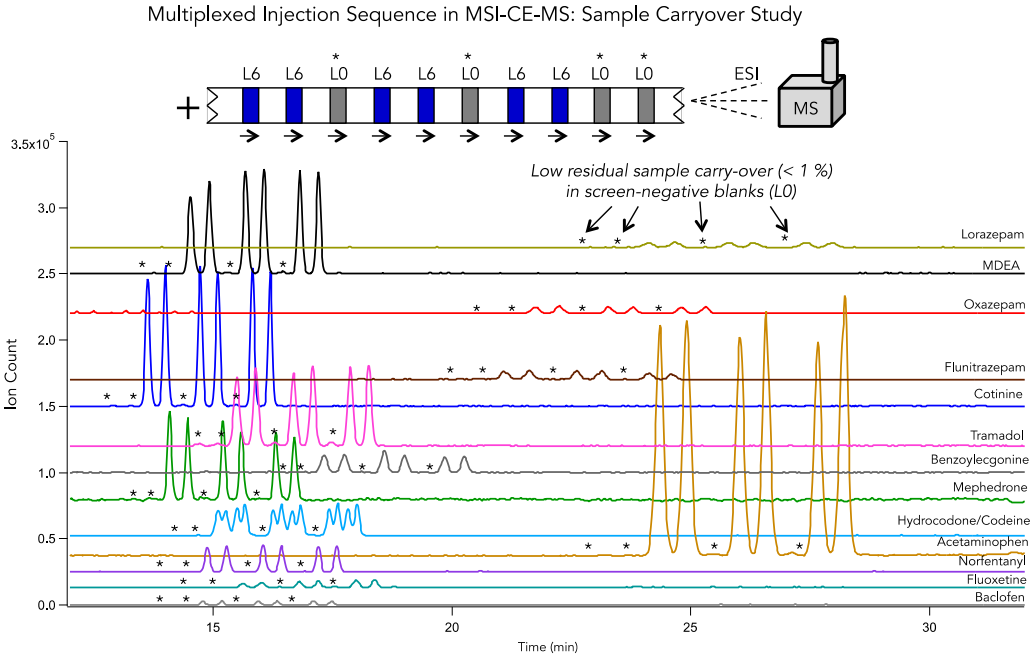

Figure S4.7. Schematic of the serial injection sequence used in MSI-CE-MS for assessment of sample carryover effects (n=12) by alternating six replicate injections of the highest calibrant mixture (L6 equivalent to 3X cutoff levels for DoA) in synthetic urine matrix with four replicate injections of sample blank (L0) within a single run performed twice within the same day. Extracted ion electropherograms (EIE) for representative classes of DoA highlighting that there was low residual median sample carry-over in blank of 0.62% with the exception of certain hydrophobic drugs, such as nortriptyline, amitriptyline, tramadol and fluoxetine. Removal of polyimide coating at inlet side of capillary, as well as inclusion of organic solvent modifier in BGE (13% *v/v* ACN) were critical to reduce sample carry-over effects notably when performing repeated serial sample injections in MSI-CE-MS.

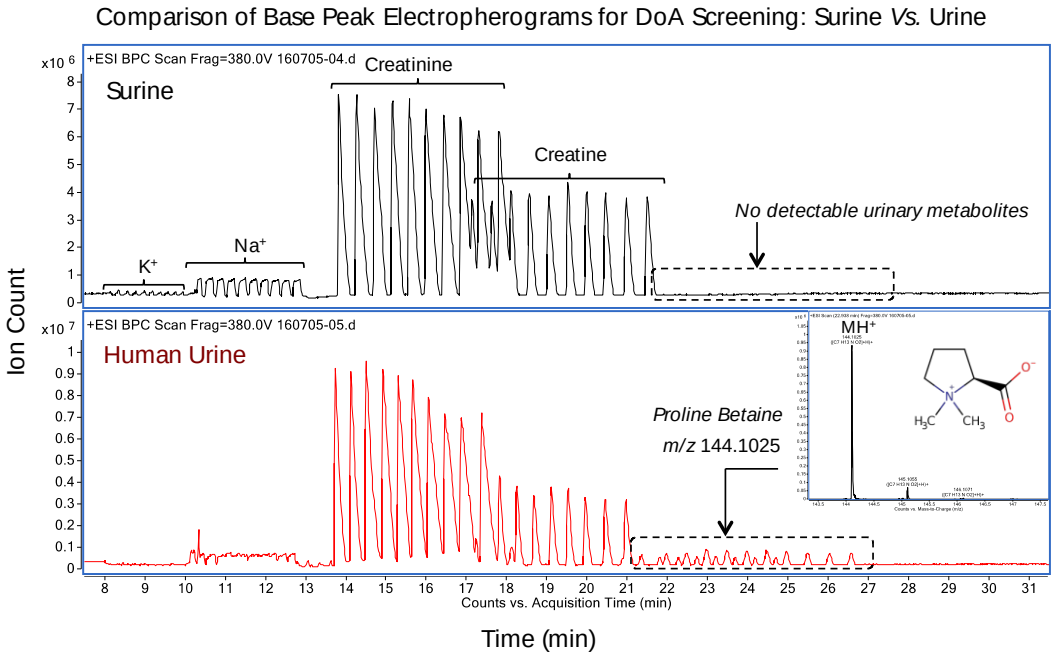

Figure S4.8. Overlay of base peak electropherograms when performing high throughput and nontargeted drug screening by MSI-CE-MS with full-scan data acquisition of a synthetic urine matrix (Surine™) relative to pooled human urine. Surine™ is largely comprised of major electrolytes (K+, Na+), creatinine and creatine, but lacks a majority of other urinary metabolites derived from diet, environmental exposures and gut microflora. For instance, the base peak electropherogram for human urine reveals a series of late migrating cations not present in Surine™, such as the major osmolyte and marker of dietary citrus intake, proline betaine (*m/z* 144.1025).

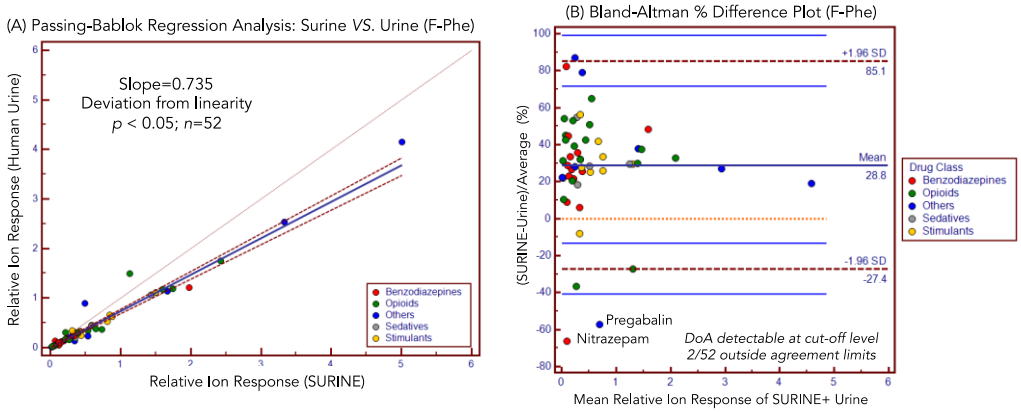

Figure S4.9. Passing-Bablok regression and Bland-Altman %difference plot for evaluation of matrix effects when screening for DoA by MSI-CE-MS when using F-Phe as common non-deuterated IS for data normalization for each drug (L6; 3X cut-off limit) spiked in synthetic urine matrix (Surine™) as compared to pooled 24 human urine. Since Surine™ lacks the majority of urinary metabolites that contribute to both isobaric interferences for certain drugs (positive bias), and ionization suppression (negative bias) notably when matching D-IS were lacking for many drugs on panel. Overall, ion suppression was evident from the urine matrix that was not accounted for by synthetic urine as reflected by a slope significantly less than unity (0.735, $p < 0.05$). However, there was still deemed acceptable in the context of primary drug screening as it contributes to only about 29% overall bias. Improved accuracy for absolute quantification during confirmatory testing can be realized by using matching D-IS and/or increased dilution of urine samples in deionized water in conjunction with targeted MS/MS via multiple reaction monitoring.

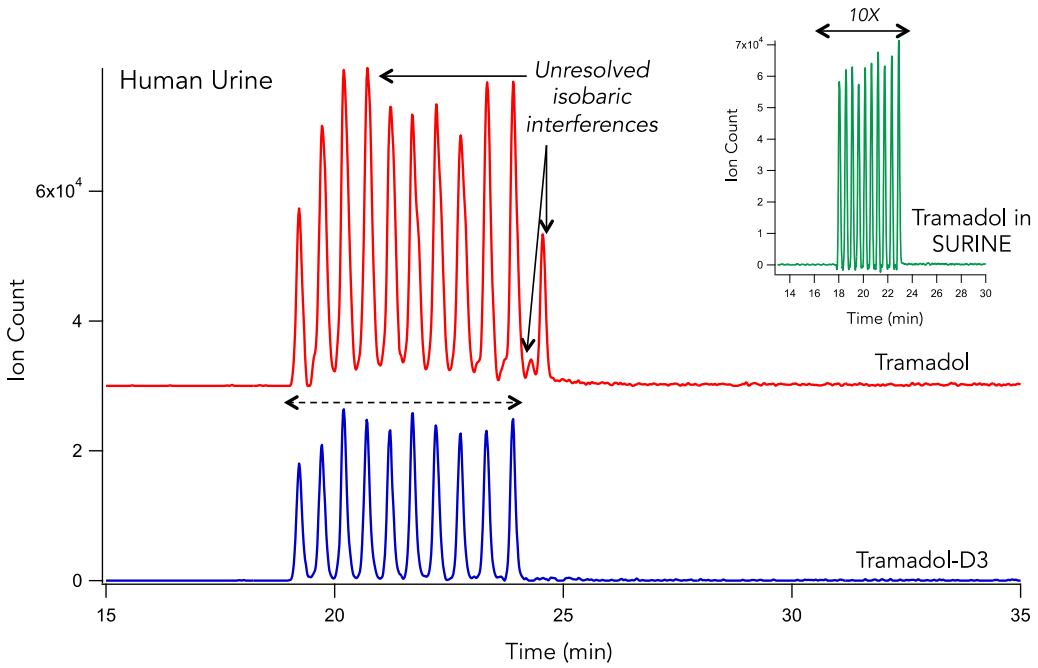

Figure S4.10. Unknown isobaric interferences in human urine for tramadol (*m/z* 264.1958) resulting in a significant positive bias when comparing mean ion response ratios for drug relative to tramadol-D3 measured in synthetic urine matrix (Surine™) and human urine as detected in a Passing-Bablok regression analysis. Resolution of interferences was achieved by performing a single injection in CE-MS in conjunction with on-line sample preconcentration as shown in **Fig. S12**.

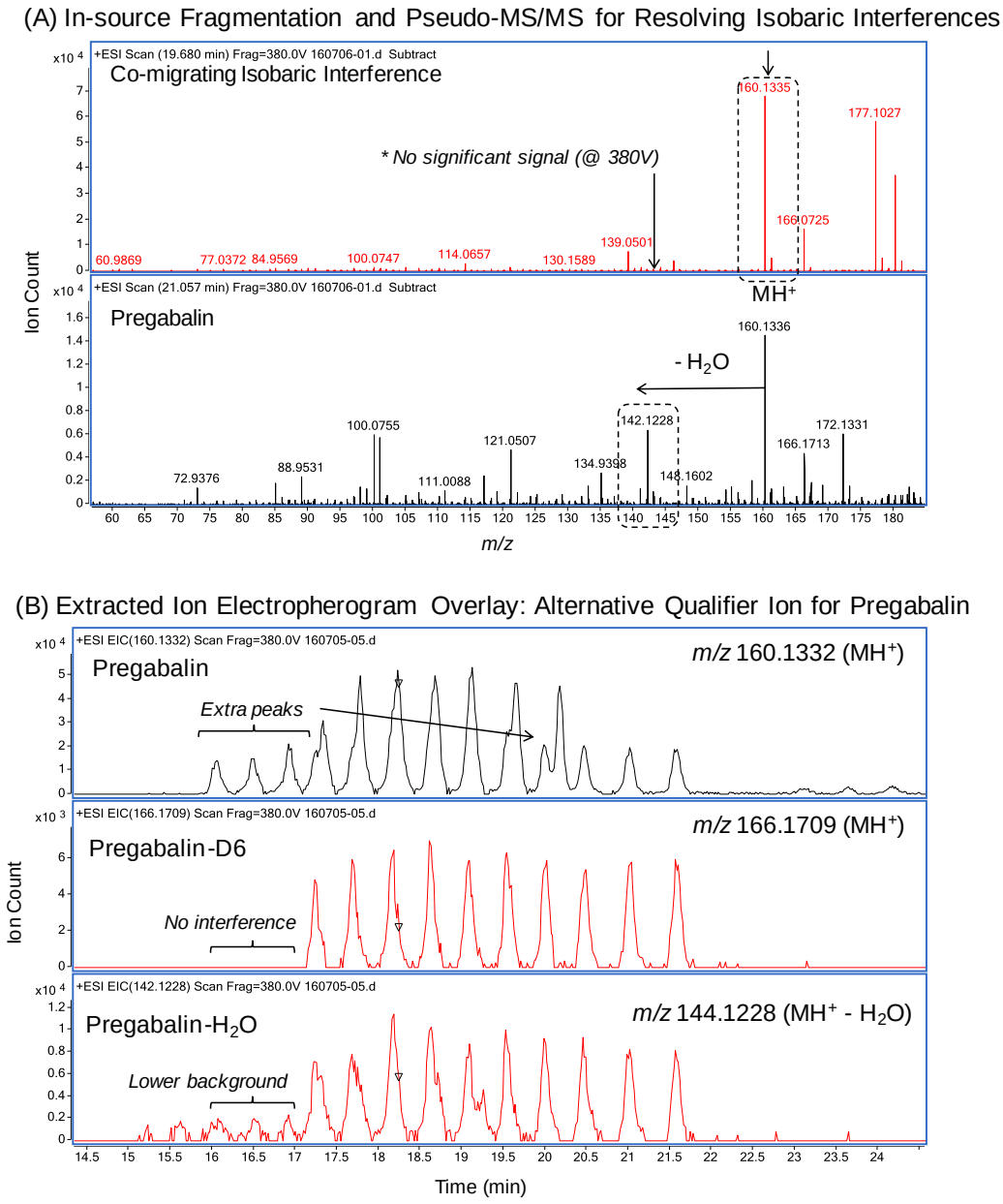

Figure S4.11. (A) Overlay of full-scan TOF-MS spectra for pregabalin relative to an isobaric urinary interference when using a fragmentor voltage at 380V during electrospray formation highlighting in-source fragmentation of pregabalin (via a water loss). (B) This process improves selectivity (but with lower sensitivity) to reduce the extent of spectral overlap for pregabalin by monitoring an alternative molecular ion (product ion, *m/z* 144.1228) as shown in extracted ion electropherogram overlays as compared to pregabalin-D6, which does have any detectable isobaric interferences in urine.

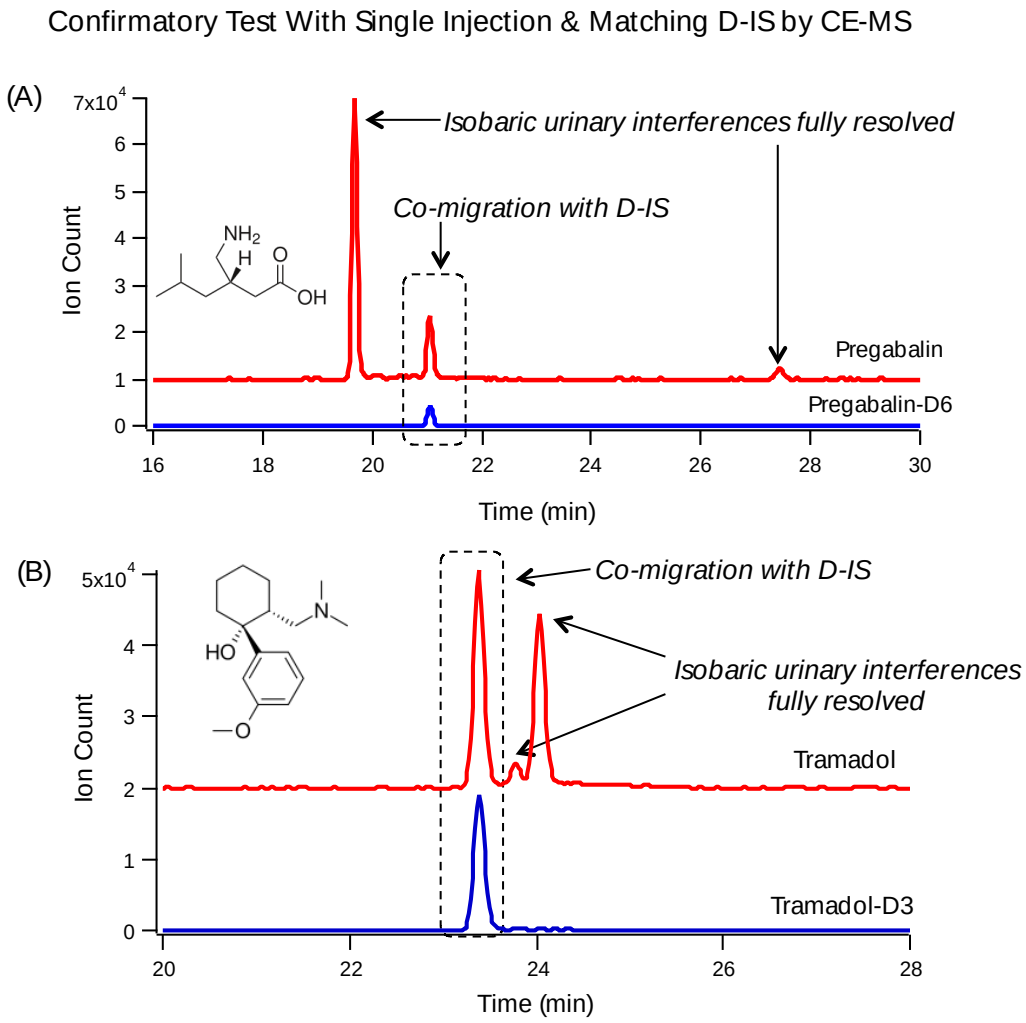

Figure S4.12. Confirmatory testing of screen-positive urine specimens following MSI-CE-MS can be performed by repeated analysis of sample when using a single injection in CE-MS with on-line sample preconcentration. This is important for improving concentration sensitivity as required for acquiring high quality MS/MS spectra for unambiguous identification with two or more diagnostic product ions while also improving separation resolution without isobaric interferences in human urine as shown for (A) pregabalin (*m/z* 160.1332) that is resolved from two other isobaric ions, and (B) tramadol (*m/z* 264.1958) that is resolved from two unknown isobaric ions from human urine. Co-migration with matching D-IS also facilitates identification of DoA in screen-positive urine samples especially when certain isobaric ions may generate similar MS/MS product ion spectra.

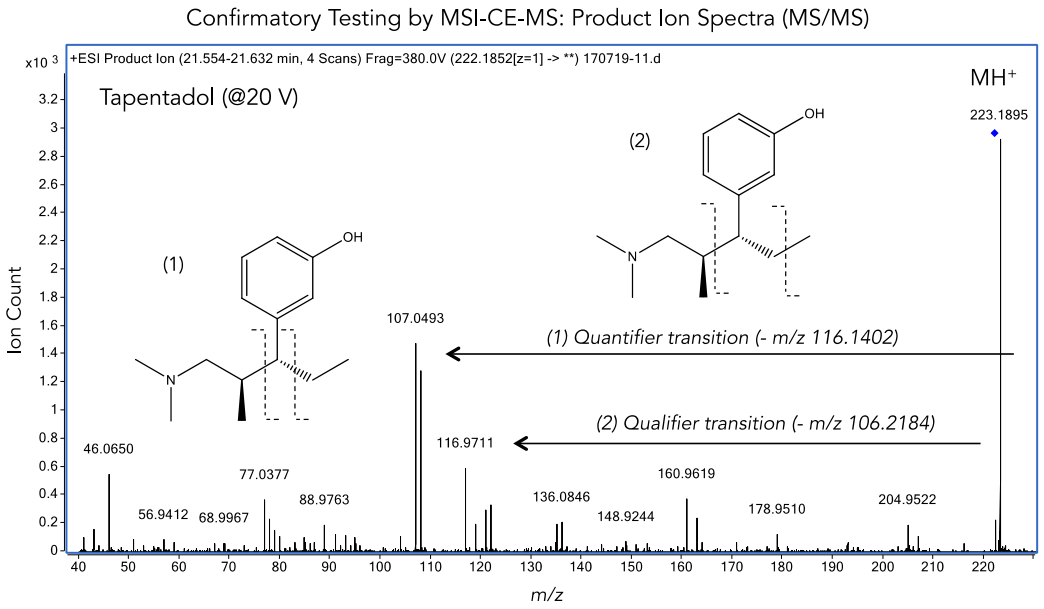

Figure S4.13. Product ion spectra (Q-TOF) for confirmatory testing and unambiguous identification of the benzenoid class of opioid analgesics, tapentadol following its detection in urine samples above recommended screening cut-off limits when using CE-MS with on-line sample preconcentration that allows for detection of its molecular ion (MH^+) and two diagnostic product ions, which can also serve as quantifier and qualifier transitions when using CE-MS/MS with collisional-induced dissociation.

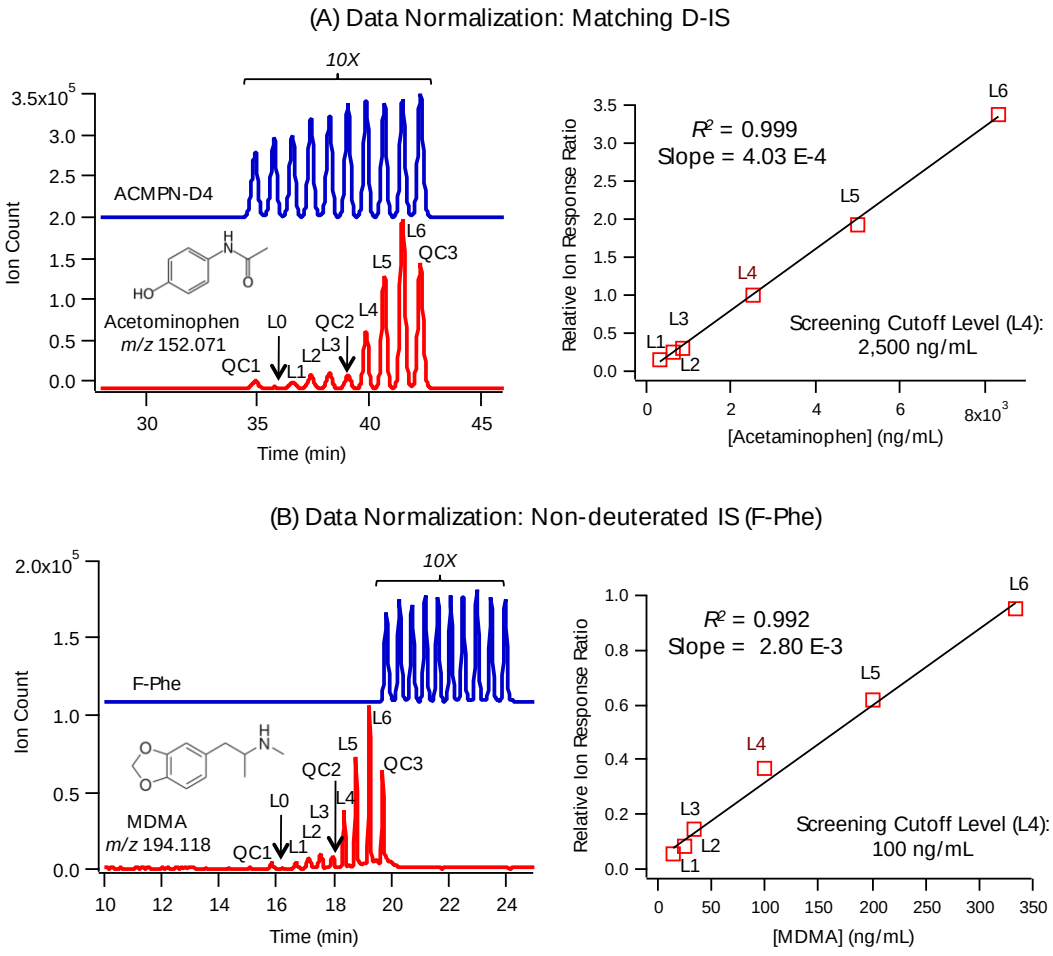

Figure S4.14. Representative extracted ion electropherograms (EIE) and external calibration curves (where, L1-L6 ranges from 0.13X to 3.0X of recommended screening cut-off levels for specific drug classes, L0 is blank, and QC1-3 are quality control samples at three different concentration levels) of DoA in synthetic urine matrix when using MSI-CE-MS. In this case, optimal assay precision was achieved by measuring the integrated peak area ratio for each drug relative to (A) a suitable D-IS (acetaminophen-D3) notably for regions that are prone to ion suppression, such as EOF, or (B) F-Phe as a single non-deuterated IS as required for correction for differences in injection volume between samples. Thus, rapid detection of a broad panel of DoA above their recommended cutoff limits together with their reliable identification and quantification can be realized by MSI-CE-MS.

Chapter V

Future Directions in Metabolomics for Biomarker Discovery and Improved Population-based Screening

Chapter V: Future Directions in Metabolomics for Biomarker Discovery and Improved Population-based Screening

5.1 Overview of major thesis contributions

The work presented in this thesis has contributed novel analytical tools to the fields of newborn screening (NBS) and drug surveillance both of which are relevant to public health. This thesis has demonstrated the advantages of multiplexed separation methods coupled to high resolution, accurate mass spectrometry for the targeted analysis of known biomarkers for confirmatory testing of inborn errors of metabolism (IEM), as well as high-throughput screening and unambiguous identification of drugs of abuse (DoA) with quality assurance. Furthermore, these methods have demonstrated the benefits of nontargeted metabolite profiling for the discovery of new biomarkers for galactosemia and cystic fibrosis (CF) relevant to pre-symptomatic detection of affected neonates, which have the potential to transform current newborn screening practice. Unlike NBS for other IEM based on multi-analyte MS/MS technology, both galactosemia and CF continue to rely on conventional bioassays and genetic screens that are prone to false positives and unaffected carrier identification. Additionally, broad-spectrum screening of known prescription and/or illicit drugs, as well as emerging designer drugs not included in standard panels, is critical to ensure optimal treatment efficacy and patient safety given the alarming usage of potentially toxic and addictive medications, including opioids and anti-anxiety drugs. This work was motivated by the desire to explore and develop underused analytical techniques to improve and streamline essential

clinical health practices. NBS represents one of the finest contributions to public health in the past century and it is easy to overlook the simple truth that population-based screening initiatives save lives, prevent morbidity, and improve quality of life well into adulthood. Developing robust and reliable analytical methods and validating new biomarkers that have proven clinical utility supports further innovation in clinical medicine and NBS initiatives especially if implemented to improve screening performance and directly impact patient care at lower healthcare expenditures. Metabolomics is uniquely capable of uncovering new biomarkers closely associated with phenotype while also providing deeper insights into the pathophysiology of complex disease processes, such as those in CF, that are not well described by molecular (*CFTR* mutation) and physiological (sweat chloride) tests alone. An increasing number of metabolomic studies have demonstrated discrimination of CF *vs.* non-CF controls in a variety of biological samples, including serum, sputum, bronchoalveolar lavage fluid and exhaled breath condensate. However, these studies have focused on understanding the underlying pathophysiology or disease severity/progression in CF patients with a definitive diagnosis. Until now, there have been no reports of MS-based metabolomics for detection of asymptomatic CF neonates in the context of NBS. The CF phenotype is considered a complex disease spectrum of variable symptoms given its heterogeneous clinical presentation. This is mainly due to the overreliance of extended genetic analysis of *CFTR* mutations of unknown or variable clinical consequences, and the weak genotype-phenotype correlation as

modulated by modifier genes and environment.[1,2] Metabolomics studies on neonates can therefore shed light on measurable metabolic changes prior to the onset of symptoms that provide new insights into the function of poorly characterized *CFTR* mutations and other genetic and non-genetic factors that impact disease severity and treatment responses to therapy.

Chapter I of this thesis provided an overview of the role of biomarkers in clinical science and summarized the challenges of biomarker discovery. The importance of rigorous study design and care during the pre-analytical, analytical and post-analytical stages of a metabolomics workflow, as well as the need for careful analytical and clinical validation were highlighted in the context of population-based screening initiatives. *Chapter II* introduced a novel metabolomics platform based on multisegment injection-capillary electrophoresis-mass spectrometry (MSI-CE-MS) method for second-tier or confirmatory testing of various IEM from a single 3.2 mm diameter neonatal dried blood spot (DBS) extracts.[3] The limitations of confirmatory testing when using conventional liquid chromatography-tandem mass spectrometry (LC-MS/MS) were overcome by using a multiplexed MSI-CE-MS method with temporal pattern recognition which injects three samples in uniquely diluted pairs to encode information about sample identity within the separation alongside a pooled quality control (QC) for system drift monitoring, reference control and batch correction. Metabolite extraction conditions were first optimized and a targeted analysis of amino acids, acylcarnitines and nucleosides as primary or secondary biomarkers for diverse

classes of IEM was successfully performed. Rigorous method validation demonstrated acceptable analytical performance of this method on both proficiency testing (PT) samples provided by the Newborn Screening Quality Assurance Program (NSQAP) from Centres for Disease Control and Prevention (CDC) and authentic neonatal DBS specimens from Newborn Screening Ontario (NSO). Furthermore, the multiplexed platform provided an accelerated data workflow for the identification of novel biomarkers grossly elevated in galactosemia as compared to healthy neonates and disease controls. Fragmentation by MS/MS revealed for the first time that a series of *N*-galactated amino acids detected in positive ion mode conditions were elevated alongside galactose-1-phosphate (Gal-1-P) and galactonic acid (GA) when using negative ion mode conditions in MSI-CE-MS. This is consistent with studies that report galactation of lysine residues of human serum albumin (HSA) in the presence of elevated galactose in patients with galactosemia.[4,5] This work offers the potential to screen for galactosemia with greater specificity, accuracy and cost-effectiveness using existing MS/MS infrastructure at NBS facilities as compared to stand-alone enzyme kinetic assays that are prone to false-positives.

Chapter III details the application of the rigorously validated MSI-CE-MS protocol for metabolomic studies of DBS extracts applied to known biomarkers for IEM currently screened by MS/MS in *Chapter II* to the discovery of new and largely unanticipated biomarkers for CF using retrospective DBS specimens from NSO. In this case, DBS specimens were derived from confirmed yet

asymptomatic CF neonates, CF-screen positive but likely unaffected (*i.e.* false-positives or unaffected carriers) and screen-negative samples (*i.e.* healthy controls). For the first time, we demonstrated that there exists CF-specific metabolites from DBS extracts that allow for differentiation of CF neonates from both screen-negatives and, importantly, screen-positive/presumptive CF cases who later are confirmed to not be affected (< 29 mM sweat chloride) as a result of the lack of specificity of two-tiered IRT/DNA screening algorithms for CF. Depletions in circulating amino acids such as tyrosine, asparagine, glycine and threonine were highly suggestive of protein maldigestion and malabsorption, which have been shown to result from the pancreatic dysfunction that is characteristic of CF and begins *in utero*.[6,7] Decreases specifically in glutamine are consistent with reports that this conditionally essential amino acid is involved in an inflammatory response, as systemic reductions in glutamine have been reported in the plasma of patients with inflammatory conditons.[8] Furthermore, reductions in neutrophilic levels of glutamine have been reported in children with a confirmed diagnosis of CF and the depletions seen in this thesis may reflect the fact that DBS extracts represent whole blood, and includes cellular components. A unique strength of the study design was the ability to independently confirm the significance of certain commonly measured biomarkers originally measured on a different DBS cut-out by MS/MS at NSO, which conclusively demonstrated that tyrosine and glycine were indeed depleted in CF neonates as compared to carriers/hypertryspsinogenemic cases. Additionally, there were also CF-specific

decreases in ophthalmic acid (*i.e.*, a non-thiol glutathione analog and biomarker of severe glutathione depletion) which is highly suggestive of the initiation of oxidative stress and inflammation, which are characteristic of CF in childhood and adulthood. Finally, we report the CF-specific increase of an unknown trivalent peptide as denoted by its characteristic MS/MS fragmentation. Remarkably, this compound was the only metabolite directly correlated with immunoreactive trypsinogen (IRT), suggesting that they may be biochemically or causally related. Further work is needed to identify the origin of this unknown peptide that may be a by-product of proteolysis from the trypsinogen activation pathway. When taken together, the results from *Chapter IV* suggest that asymptomatic CF neonates have a distinctive metabolic phenotype reflecting sub-clinical molecular signatures of inflammation, oxidative stress and malnutrition that will come to define many of their symptoms later in life if left untreated.

Chapter IV of this thesis contributed to the development and validation of a high throughput MSI-CE-MS method for broad-spectrum screening of DoA that is a crucial part of routine employment screening, toxicological/forensic studies, therapeutic drug monitoring and medication compliance testing (*e.g.* pain management). This method was proposed as an alternative to the traditional immunoassay-based methods which lack sensitivity and specificity as they are prone to both false-positive results due to antibody cross-reactivity for prescribed drugs and/or false-negative results due to poor affinity of antibodies for certain drug classes, such as benzodiazapenes and semi-synthetic opioids.[9,10] In this case,

sample throughput in MSI-CE-MS was expanded to allow for ten serial sample injections of urine simultaneously with high resolution, full scan MS acquisition. This method demonstrated acceptable precision, accuracy and sample carryover for a wide range of DoA and their metabolites/isomers at recommended screening cut-off concentration levels in commercial synthetic urine. Additionally, minimal matrix effects and isobaric interferences in human urine were also demonstrated. Drugs and their metabolites were confidently and unambiguously identified based on four independent parameters, including accurate mass, most likely molecular formula, co-migration with a deuterated internal standard or *in silico* prediction of relative migration times, as well as MS/MS fragmentation spectra at different collisional energies. Furthermore, this method permits re-interrogation of the data to detect synthetic and emerging drugs (*e.g.*, the designer cannabinoids "Spice" and "K2") that may be relevant in forensic toxicology investigations or emergency medicine.[11] Finally, MSI-CE-MS is capable of detecting metabolite signatures as required for specimen verification beyond pH, specific gravity or creatinine, such as proline-betaine, a commonly detected dietary marker of citrus fruit consumption that can aid in the detection of commercial "fake pee" products designed to simulate a screen-negative urine test result (*e.g.* "Quick Fix").

5.2 Analysis of additional IEM by MSI-CE-MS

The MSI-CE-MS method with temporal signal pattern recognition described in *Chapter II* should be applied to a larger set of authentic IEM to assay the applicability of this method to confirm a diagnosis in a range of diverse

diseases. While a total of 14 samples were processed and analyzed, this only represented 11 unique diseases which accounts for about half of the 21 IEM (out of 29 genetic diseases overall) NSO currently screens using MS/MS infrastructure. Furthermore, only 9 of those IEM were analyzed in authentic neonatal DBS. For example, citrullinemia type I (CIT I) and maple syrup urine disease (MSUD) were both validated only in standardized quality assurance materials. While PT materials from the CDC NSQAP program provide an invaluable service to ensure laboratory compliance with strict quality assurance criteria through the Clinical Laboratory Improvement Amendments (CLIA), the vast majority of these samples are created from pooled adult donor blood that has been enriched for relevant analytes.[12] It has been reported that various amino acids show age-related differences in distribution[13] and that children and adults have significantly different fasting plasma references ranges for many of these compounds.[14] As a result, these NSQAP samples may not represent a true neonatal metabolic background and could underestimate matrix effects that may interfere with the analysis of clinically relevant metabolites. Therefore, a pertinent next step is the expansion of the study to encompass additional IEM from authentic DBS to provide confidence that this method is suitable for rapid and reliable confirmatory tests. This is especially pertinent for IEM with low PPV caused by isomeric or isobaric interferences (*i.e.* MSUD which requires the separation and detection of isomeric and pathognomonic *allo*-isoleucine from benign hydroxyproline and isovaleric acidemia which has an interference from the

common antibiotic pivalic acid), or if this method is to be widely used for confirmatory testing with high sample throughput.

This method should also be further validated on a larger sample of affected individuals; with the exception of two independent tyrosinemia type I (TYR I) patients, all IEM were represented by only a single individual. IEM are thought to represent extreme cases of variation in human metabolism[15] and individual differences in genetic background, lifestyle and environment can lead to a wide range of metabolite concentrations. This leads so-called monogenic diseases such as phenylketonuria (PKU) to show variable metabolic phenotypes, even in the presence of identical mutant alleles.[16] As a result, MSI-CE-MS requires further validation on a larger number of IEM cases to ensure that it is appropriate for a large and diverse screening population. Longer term future work must include the collection of prospective evidence of the confirmatory performance of this method. A direct comparison of the results from MSI-CE-MS and LC-MS/MS methods at NSO should be performed for confirmatory testing of presumptive IEM cases, including an evaluation of its clinical utility, cost-effectiveness and analytical performance (*e.g.*, intermediate precision, robustness, cost-effectiveness). Results must be in agreement with the established methods and Bland-Altman comparisons should be used to quantify the agreement between the methods and detect potential method bias.[17] A major advantage of MSI-CE-MS is implementation of QC samples alongside each individual sample which is

strongly recommended to ensure adequate performance of all follow-up testing methodologies and long-term system performance can be determined.[18]

5.3 Confirmation of putative biomarkers of galactosemia

Chapter II also revealed the presence of a correlated group of *N*-galactated amino acids that were consistently elevated in an infant with "classic" galactosemia. The discovery of potential MS-compatible biomarkers for routine screening of galactosemia by MS/MS is extremely exciting, as current screening relies on bioassays which are prone to seasonal variability and false-positive results as the galactose-1-phosphate uridylyltransferase (GALT) enzyme is susceptible to denaturation when samples are mailed during hot or humid weather.[19] A robust, specific yet chemically stable biomarker for galactosemia measured with existing MS/MS infrastructure would provide significant clinical value to NBS programs. At the time of writing, additional DBS punches corresponding to 10 neonates confirmed with classic galactosemia and related variants have been received from NSO. These samples will be extracted and analyzed alongside additional negative controls to determine if a series of *N*-galactated amino acids remain consistently elevated in classic galactosemia (type 1, severe GALT deficiency) cases, as well as milder variants (*i.e.,* Duarte galactosemia having about 25% or less residual GALT activity) in affected infants relative to healthy/screen-negative neonates. If these biomarkers prove to be consistently elevated in these samples relative to galactose-phosphate and galactonate, synthesis of reference standards and quantification of their

concentrations in DBS extracts will be conducted in order to establish reference ranges and optimal screening cut-off values relative to healthy neonates (99th percentile).[20] These markers must then be validated on a much larger, independent cohort which, given the rarity of classical galactosemia (*i.e.* 1 in 60,000 in Ontario), will likely require a national or international collaboration of NBS centres to ensure adequate sample sizes with performance outcomes compared to classic enzyme kinetic assays. Merit indicators of stable-isotope dilution MS/MS-assay for primary screening of galactosemia include precision, accuracy, limits of detection, linear range and stability (*i.e.* for short term drying, shipping and preparation and for longer-term storage). Prospective data collection using MS/MS as compared to bioassays can determine an optimal panel of biomarkers and screening cut-off ranges to maximize sensitivity and specificity to determine if these compounds have clinical utility for improved neonatal screening, including the detection of milder variants of the disease (Duarte galactosemia – some of whom may not be affected during infancy), as well as other more rarer forms of galactosemia (type II, type III) not detected by conventional GALT enzyme assays that represent potentially concerning false-negatives.

5.4 Validation of preliminary findings of CF-specific metabolic differences in neonatal dried blood spots

Chapter III reported, for the first time, metabolic differences in neonates with CF relative to those who are screen-negative, as well as screen-positive/presumptive CF but who are ultimately diagnosed as likely unaffected

following sweat chloride testing; neonates who carry one *CFTR*-disease causing mutation or have elevated immunoreactive trypsinogen (IRT) in the absence of any mutations, are collectively referred to SP/non-CF. Immediate next steps in this study are to identify the unknown peptide and understand its biochemical relationship to IRT, while ensuring there is no analytical bias for the lead CF-specific biomarkers (ophthalmic acid, Tyr, Thr, Ser, Pro, Gly) by re-extracting a stored duplicate DBS punch to be analyzed on a different analytical platform, such as DI-MS/MS or LC-MS/MS.[21] While these DBS samples have been stored for an additional 1-2 years at -80°C, an aliquot of the extract can be set aside and re-analyzed by MSI-CE-MS to ensure there are no artifacts related to storage. The unknown trivalent peptide at *m/z* 438.2576 must be identified to provide biochemical context to the study by potentially revealing pathophysiological information about CF.[22,23] A simple, initial approach is to enzymatically digest the peptide to its amino acid constituents using a mixture of proteases (*i.e.* pronase) and separate the digest by CE-MS. Attenuation of the peak corresponding to the intact putative peptide will confirm the presence of peptide. The amino acid monomers may be identified by increases in free amino acid levels. While sequence information will not be known, knowing the amino acid constituents may provide some biochemical information to rule out certain peptide possibilities. A bottom-up mapping approach may also be used, which also enzymatically digests and separates peptides, however the samples are then analyzed by fragmentation using data-dependent acquisition.[24] Fragments can

then be matched or mapped to peptide databases using mapping software to identify the peptide sequence.

It is imperative that this study be repeated on a larger independent set of samples to confirm these preliminary findings. Using area under the curve (AUC) of receiver operating characteristic (ROC) curves as a measure of the diagnostic performance of the metabolites, the best outcome was derived from the ratio of ophthalmic acid to unknown peptide ($AUC > 0.830$). Replication of this study with greater study power, including testing on a blinded hold-out/validation set, may require coordination and collaboration with other newborn screening facilities across Canada to ensure adequate sample sizes. Samples should be analyzed together in a single batch to avoid drastic changes in instrument performance and reduce the need for batch-correction procedures. The collection of prospective data and the ability of these metabolite(s) to predict which samples are more likely to receive a diagnosis of CF is absolutely necessary to determine the clinical performance of these biomarkers on a real, screening population, such as assessment of positive predictive value. The top-ranked biomarker candidates for CF, confirmed in an independent cohort training/validation study, should be quantified and used to determine if a sample with elevated IRT is likely to be CF-positive and should therefore proceed to *CFTR* mutational analysis and sweat testing. The results can be compared to the IRT/DNA screening algorithm to determine if there is a significant reduction in the number of false-positives that require unnecessary sweat chloride testing and genetic counselling at regional CF

clinics, since more than 90% of presumptive CF cases currently have low sweat chloride (< 29 mM) and unlikely to have CF. A reduction in the number of false-positive screening results can have profound impacts on NBS in Ontario. The cost of the IRT/DNA screen is estimated to be approximately $318CAD, while the sweat test and genetic counselling, required for carriers and hypertrypsinogenics, are around $342CAD for a total of $660CAD per analysis.[25] Given that a recent study has indicated only 5.6% of screen positives in Ontario will receive a diagnosis of CF and a further 3.7%[26] will have an inconclusive diagnosis requiring extensive follow-up testing, this represents over $270,000CAD/year in lost healthcare costs. If the specificity of our most promising biomarkers (ophthalmic acid/putative peptide) is indeed close to 75-85%, this represents a reduction in the false positive rate from over 90% to only 15-25%, which could save close to $200,000/year. However, the intangible, emotional costs of a false-positive result cannot be overlooked. Follow-up genetic counselling for carriers is challenging and a significant minority of parents remain unsure of what carrier status implies for themselves or their child.[27] Furthermore, those screen-positive infants with an indeterminate diagnosis (*i.e.* intermediate sweat chloride and ≥1 mutation or normal sweat and 2 mutations in the absence of clinical presentation) are classified as cystic fibrosis-screen positive-inconclusive diagnosis (CF-SPID) may be at risk for delayed CF onset with follow-up monitoring, although most infants remain asymptomatic with an unknown natural history.[26] Uncertainty about a child's diagnosis or disease status can cause many parents and caregivers

fear and anxiety, particularly during the vulnerable newborn period.[28] These represent some of the major "diagnostic dilemmas" caused by widespread genetic screening of *CFTR* mutations of unknown or variable consequence in the population, which research discoveries described in this thesis may overcome by introducing an inexpensive "third-tier" confirmatory MS/MS screen following an initial high IRT result that has poor specificity.

5.5 Analytical validation of DoA screening on authentic/blinded samples

Chapter IV introduced a high throughput screening method based on MSI-CE-MS for the rapid, sensitive yet selective screening of a potentially an unlimited panel of drugs of abuse (DoA) in a synthetic urine matrix, as well as human urine. This method was rigorously validated and demonstrated acceptable inter-day precision for accurate quantification of more than 50 DoA and their metabolites relative to an optimal internal standard at recommended screening cut-off concentration levels. Adequate LOD were achieved for most cationic DoA with minimal sample carryover between injections. However, certain low abundance DoA with low cut-off limits ($\leq$ 5 ng/mL) could benefit from improved concentration sensitivity in MSI-CE-MS when using a sheathless interfaces which can enhance ionization responses by up to two orders of magnitude.[29] While relative migration times showed good reproducibility, absolute migration times were variable over 4 days of analysis due to changes in electroosomtic flow. In this case, covalent coating of the inner surface of the capillary with polyvinyl alcohol would suppress the EOF while minimizing solute adsorption to the

capillary wall to stabilize apparent migration times in CE.[30] This would enable automated data processing when coupled to a laboratory information management system (LIMS) as required for high throughput drug screening applications. Furthermore, for those isomeric compounds that were not fully resolvable by this method, suppressing the EOF can improve the separation performance as ion migration is now solely dependent on small differences in electrophoretic mobility (*i.e.* charge and hydrodynamic radius) that can potentially allow for better resolution in CE with less variability (*e.g.* morphine and hydromorphone).[31]

This method can also be modified to directly analyse intact glucuronide conjugates of many DoA, eliminating the need for a time-consuming hydrolysis with a glucuronidase enzyme. This can produce a streamlined "dilute and shoot" method for those drugs that undergo phase II metabolism. An anionic buffer system such as ammonium acetate at a high pH (~ pH 8.5) would allow for separation while the addition of ammonia to the sheath liquid would enhance deprotonation for detection of these acidic drug conjugates when using MSI-CE-MS under negative ion mode ionization conditions.[32] Additionally, this method would also be conducive to screening acidic cannabinoids, as well as barbituates, particularly relevant given plans for legalization of cannabis in Ontario in 2018.

Finally, the performance of this method must be validated on authentic, blinded clinical samples. At the time of writing, a set of 218 fasted morning urine samples from individuals receiving in-patient psychiatric care were transferred into the lab. These patients have known prescriptions for a wide variety of anti-

anxiety and anti-depressants, but are also suspected of abusing illict drugs and are at risk for polydrug usage. These urine samples will be split into aliquots and screened by conventional immunoassays for five major drug classes (including opioids, amphetamines, benzodiazepenes, cannibinoids and nicotine), as well as targeted screening for a 86-drug panel using LC-MS/MS in a CLIA certified laboratory. A third aliquot will be analyzed independently using a non-targeted and targeted broad-spectrum drug screen by MSI-CE-MS. The results from MSI-CE-MS will be compared to data from the acceptable "gold standard" methods to determine if the screening results are in agreement (*i.e.* if they identify the same drugs as being present or absent) while also revealing unanticipated DoA or designer drugs not included within standard panels. Moreover, MSI-CE-MS will also allow for direct specimen verification and identify commercial "fake-pee" specimens (included in cohort in blinded manner) that otherwise would pass conventional screens for creatinine, specificity gravity and pH. Overall, this work may allow for rapid yet comprehensive drug surveillance for psychiatric patients at risk for self-harm who may not be compliant with prescribed medications and/or involved with illicit and highly toxic synthetic opioid analogs, such as fentanyl.

5.6 Overall Conclusion

In summary, this thesis presents the development and thorough validation of a multiplexed CE-MS method for routine analyses in IEM confirmation and DoA screening. Moreover, this thesis identified blood-based, MS-compatible

metabolites that show significant differences in asymptomatic neonates with galactosemia and CF, which currently utilize low throughput and error-prone bioassays for newborn screening. This work sets the stage for future studies wherein these lead candidate biomarkers can be further validated and evaluated for their clinical utility to improve current NBS practices in order to more accurately identify affected infants for early treatment intervention at reduced healthcare expenditures. Furthermore, this work has the potential to drastically change the way drug surveillance is routinely performed with far greater specificity and certainty as a way to reduce the number of costly and unnecessary confirmatory LC-MS/MS tests. This screening approach is critical for new advances in public health and safety by ensuring timely yet accurate results are used to make the most informed clinical and/or legal decisions that benefit patients who may be at risk for self-harm.

5.7 References

(1) De Boeck, K.; Wilschanski, M.; Castellani, C.; Taylor, C.; Cuppens, H.; Dodge, J.; Sinaasappel, M. *Thorax* **2006**, *61*, 627–635.

(2) Tsui, L.-C.; Dorfman, R. *Cold Spring Harb. Perspect. Med.* **2013**, *3*, 1–16.

(3) DiBattista, A.; McIntosh, N.; Lamoureux, M.; Al-Dirbashi, O.; Chakraborty, P.; Britz-McKibbin, P. *Anal. Chem.* **2017**, *89*, 8112–8121.

(4) Urbanowski, J. C.; Cohenford, M. A.; Levy, H. L.; Crawford, J. D.; Dain, J. A. *Med. Intell.* **1982**, *306*, 84–86.

(5) Frost, L.; Chaudhry, M.; Bell, T.; Cohenford, M. *Anal. Biochem.* **2011**, *410*, 248–256.

(6) Li, L.; Somerset, S. *Dig. Liver Dis.* **2014**, *46*, 865–874.

(7) Wilschanski, M.; Novak, I. *Cold Spring Harb. Perspect. Med.* **2013**, *3*, 1–17.

(8) Hulsewé, K. W. E.; van der Hulst, R. W. W. J.; van Acker, B. A. C.; von Meyenfeldt, M. F.; Soeters, P. B. *Clin. Nutr.* **2004**, *23*, 1209–1216.

(9) Pesce, A.; Rosenthal, M.; West, R.; West, C.; Crews, B.; Mikel, C.; Almazan, P.; Latyshev, S. *Pain Physician* **2010**, *13*, 273–281.

(10) Archer, J. R. H.; Wood, D. M.; Dargan, P. I. *Arch. Dis. Child. Educ. Pract. Ed.* **2012**, *97*, 194–199.

(11) Rentsch, K. M. *TrAC - Trends Anal. Chem.* **2016**, *84*, 88–93.

(12) De Jesús, V.; Mei, J.; Cordovado, S.; Cuthbert, C. *Int. J. Neonatal Screen.* **2015**, *1*, 13–26.

(13) Lepage, N.; McDonald, N.; Dallaire, L.; Lambert, M. *Clin. Chem.* **1997**, *43*, 2397–2402.

(14) Armstrong, M. D.; Stave, U. *Metabolism* **1973**, *22*, 561–569.

(15) Shin, S.-Y.; Fauman, E. B.; Petersen, A.-K.; Krumsiek, J.; Santos, R.; *et al*. *Nat. Genet.* **2014**, *46*, 543–550.

(16) Scriver, C. R.; Waters, P. J. *Trends Genet.* **1999**, *15*, 267–272.

(17) Giavarina, D. *Biochem. Medica* **2015**, *25*, 141–151.

(18) Whitley, R. J.; Hannon, W. H.; Dietzen, D. J.; Rinaldo, P. In *Follow-up Testing for Metabolic Diseases Identified by Expanded Newborn Screening Using Tandem Mass Spectrometry*; 2009; pp 9–29.

(19) Frazier, D.M.; Clemons, E.H.; Kirkman, H.N. *Biochem. Med. Metab. Biol.* **1992**, 48, 199–211.

(20) McHugh, D. M. S.; Cameron, C. A.; Abdenur, J. E.; Abdulrahman, M.; Adair, O.; *et al.Genet. Med.* **2011**, *13*, 230–254.

(21) Koulman, A.; Lane, G. A.; Harrison, S. J.; Volmer, D. A. *Anal. Bioanal. Chem.* **2009**, *394*, 663–670.

(22) Sumner, L. W.; Amberg, A.; Barrett, D.; Beale, M. H.; Beger, R.; Daykin, C. A.; Fan, T. W.-M.; Fiehn, O.; Goodacre, R.; Griffin, J. L.; Hankemeier, T.; Hardy, N.; Harnly, J. *Metabolomics* **2007**, *3*, 211–221.

(23) Creek, D. J.; Dunn, W. B.; Fiehn, O.; Griffin, J. L.; Hall, R. D.; Lei, Z.; Mistrik, R.; Neumann, S.; Schymanski, E. L.; Sumner, L. W.; Trengove, R.; Wolfender, J. L. *Metabolomics* **2014**, *10* , 350–353.

(24) Aebersold, R.; Mann, M. *Nature* **2016**, *537*, 347–355.

(25) Nshimyumukiza, L.; Bois, A.; Daigneault, P.; Lands, L.; Laberge, A. M.; Fournier, D.; Duplantie, J.; Giguère, Y.; Gekas, J.; Gagn, C.; Rousseau, F.; Reinharz, D. *J. Cyst. Fibros.* **2014**, *13*, 267–274.

(26) Ooi, C. Y.; Castellani, C.; Keenan, K.; Avolio, J.; Volpi, S.; Boland, M.; Kovesi, T.; Bjornson, C.; Chilvers, M. A.; Morgan, L.; van Wylick, R.; Kent, S.; Price, A.; Solomon, M.; Tam, K.; Taylor, L.; Malitt, K.-A.; Ratjen, F.; Durie, P. R.; Gonska, T. *Pediatrics* **2015**, *135*, e1377–e1385.

(27) Ciske, D. J.; Haavisto, A.; Laxova, A.; Rock, L. Z. M.; Farrell, P. M. *Pediatrics* **2001**, *107*, 699 LP-705.

(28) Schmidt, J. L.; Castellanos-Brown, K.; Childress, S.; Bonhomme, N.; Oktay, J. S.; Terry, S. F.; Kyler, P.; Davidoff, A.; Greene, C. *Genet. Med.* **2012**, *14*, 76–80.

(29) Zhang, W.; Hankemeier, T.; Ramautar, R. *Curr. Opin. Biotechnol.* **2017**, *43*, 1–7.

(30) Daniel, D.; dos Santos, V. B.; Vidal, D. T. R.; do Lago, C. L. *J. Chromatogr. A* **2015**, *1416*, 121–128.

(31) dos Santos, V. B.; Daniel, D.; Singh, M.; do Lago, C. L. *J. Chromatogr. B Anal. Technol. Biomed. Life Sci.* **2016**, *1038*, 19–25.

(32) Heitmeier, S.; Blaschke, G. *J. Chromatogr. B. Biomed. Sci. Appl.* **1999**, *721*, 93–108.